

University of Southampton Research Repository  
ePrints Soton

Copyright © and Moral Rights for this thesis are retained by the author and/or other copyright owners. A copy can be downloaded for personal non-commercial research or study, without prior permission or charge. This thesis cannot be reproduced or quoted extensively from without first obtaining permission in writing from the copyright holder/s. The content must not be changed in any way or sold commercially in any format or medium without the formal permission of the copyright holders.

When referring to this work, full bibliographic details including the author, title, awarding institution and date of the thesis must be given e.g.

AUTHOR (year of submission) "Full thesis title", University of Southampton, name of the University School or Department, PhD Thesis, pagination

**UNIVERSITY OF SOUTHAMPTON**  
FACULTY OF ENGINEERING, SCIENCE AND MATHEMATICS  
School of Civil Engineering and the Environment

**Evaluation of the vertical and horizontal hydraulic conductivities  
of household wastes**

by

**Andrew Philip Hudson**

Thesis for the degree of Doctor of Philosophy

December 2007

UNIVERSITY OF SOUTHAMPTON

ABSTRACT

FACULTY OF ENGINEERING, SCIENCE & MATHEMATICS

SCHOOL OF CIVIL ENGINEERING AND THE ENVIRONMENT

Doctor of Philosophy

EVALUATION OF THE VERTICAL AND HORIZONTAL HYDRAULIC CONDUCTIVITIES OF HOUSEHOLD WASTES

by Andrew Philip Hudson

Hydraulic conductivity is a measurement of the ease of movement of a fluid through a medium and is therefore a key parameter in the design of landfill leachate management systems. Hydraulic conductivity of landfilled wastes may be affected by several factors such as overburden stress from the weight of overlying waste, water content, the type, age and pre-processing of the waste, and the presence of landfill gas. A further factor that may affect leachate movement through wastes is the predominantly horizontal orientated structure of compacted wastes. This anisotropic structure may result in hydraulic conductivity in the horizontal direction being greater than that in the vertical direction. However existing research has been effectively limited to evaluating hydraulic conductivity in a single plane and so the presence of anisotropic flow in waste remains unproven. Consequently, modelling of leachate and contaminant movement in landfills may be compromised by the use of isotropic, or assumed anisotropic, hydraulic conductivity values.

The object of this research has been to assess for the first time the inherent anisotropy of two different waste samples by measuring and comparing the vertical and horizontal hydraulic conductivities over a range of stresses typical of landfill conditions. In this thesis, factors affecting the measurement of hydraulic conductivity of wastes are discussed, and details of the samples tested and test methodology are given. The results of the tests are shown and alternative test methods are discussed. The effects of gas accumulation and pore water pressure on waste hydraulic conductivity encountered during testing are also reported as further research has developed from this important finding.

## Table of Contents

<b>1. Introduction</b>	<b>1</b>
<b>2. Background: Measurement of hydraulic conductivity of soils and wastes</b>	<b>7</b>
<b>2.1 Introduction</b>	<b>7</b>
<b>2.2 Hydraulic conductivity</b>	<b>8</b>
<b>2.3 Published waste hydraulic conductivity values</b>	<b>10</b>
<b>2.4 Factors influencing hydraulic conductivity of wastes</b>	<b>10</b>
<b>2.4.1 Introduction</b>	<b>10</b>
<b>2.4.2 Density and viscosity of permeant</b>	<b>11</b>
<b>2.4.3 Leaching effect of permeant</b>	<b>13</b>
<b>2.4.4 Density and effective stress</b>	<b>13</b>
<b>2.4.5 Waste type and pre-processing</b>	<b>15</b>
<b>2.4.6 Water content and gas accumulation</b>	<b>15</b>
<b>2.4.7 Pore water pressure</b>	<b>18</b>
<b>2.4.8 Turbulent Flow</b>	<b>19</b>
<b>2.4.9 Heterogeneity</b>	<b>20</b>
<b>2.4.10 Sampling</b>	<b>21</b>
<b>2.5 Anisotropic hydraulic conductivity in soils and wastes</b>	<b>22</b>
<b>2.6 Summary</b>	<b>28</b>
<b>3. Test apparatus</b>	<b>29</b>
<b>3.1 Introduction</b>	<b>29</b>
<b>3.2 The Pitsea compression cell</b>	<b>30</b>
<b>3.3 Modifications required to seal samples in the         compression cell cylinder</b>	<b>32</b>
<b>3.4 Modifications required to provide a horizontal leachate         flow across a sample in the compression cell cylinder</b>	<b>34</b>
<b>3.5 Horizontal flow header tanks</b>	<b>36</b>
<b>3.6 Summary</b>	<b>37</b>

<b>4. Samples tested</b>	<b>38</b>
<b>4.1 Waste sample analysis</b>	<b>38</b>
<b>4.2 Discussion</b>	<b>41</b>
<b>5. Sample loading, compression, water content and density</b>	<b>42</b>
<b>5.1 Introduction</b>	<b>42</b>
<b>5.2 Sample loading</b>	<b>43</b>
<b>5.2.1 Methodology</b>	<b>43</b>
<b>5.2.2 Discussion</b>	<b>46</b>
<b>5.3 Sample compression</b>	<b>48</b>
<b>5.3.1 Compression methodology</b>	<b>48</b>
<b>5.3.2 Compression results and discussion</b>	<b>50</b>
<b>5.4 Water content</b>	<b>54</b>
<b>5.4.1 Methodology to assess water content</b>	<b>54</b>
<b>5.4.2 Water content results</b>	<b>56</b>
<b>5.5 Waste density</b>	<b>57</b>
<b>5.5.1 Density definitions and methodology</b>	<b>57</b>
<b>5.5.2 Density results</b>	<b>58</b>
<b>5.6 Summary</b>	<b>60</b>
<b>6. Drainable porosity</b>	<b>62</b>
<b>6.1 Introduction</b>	<b>62</b>
<b>6.2 Drainable porosity methodology</b>	<b>63</b>
<b>6.3 Results and discussion</b>	<b>67</b>
<b>6.4 Summary</b>	<b>70</b>
<b>7. Vertical hydraulic conductivity</b>	<b>71</b>
<b>7.1 Introduction</b>	<b>71</b>
<b>7.2 Vertical hydraulic conductivity methodology</b>	<b>71</b>
<b>7.3 Potential errors in hydraulic conductivity measurement</b>	<b>77</b>
<b>7.4 Results</b>	<b>79</b>

<b>7.5 Discussion</b>	<b>86</b>
<b>7.5.1 Comparison of hydraulic conductivity results with previous research</b>	<b>86</b>
<b>7.5.2 The effects of pore water pressure on hydraulic conductivity</b>	<b>88</b>
<b>7.6 Summary of physical and hydraulic property results</b>	<b>89</b>
<b>7.7 Summary</b>	<b>91</b>
<b>8. Horizontal hydraulic conductivity</b>	<b>92</b>
<b>8.1 Introduction</b>	<b>92</b>
<b>8.2 Methodology to induce horizontal flow across samples</b>	<b>93</b>
<b>8.3 Numerical analysis methodology</b>	<b>96</b>
<b>8.4 MODFLOW validation</b>	<b>101</b>
<b>8.4.1 Validation using simple vertical flow analysis</b>	<b>101</b>
<b>8.4.2 Validation using well drawdown analysis</b>	<b>103</b>
<b>8.4.3 Observations of the validation results</b>	<b>106</b>
<b>8.5 Results</b>	<b>107</b>
<b>8.6 Discussion</b>	<b>112</b>
<b>8.6.1 Results overview</b>	<b>112</b>
<b>8.6.2 Application of results</b>	<b>113</b>
<b>8.6.3 Accuracy of results</b>	<b>115</b>
<b>8.7 Recommendations</b>	<b>116</b>
<b>8.7.1 Suggested improvements to the compression cell design</b>	<b>116</b>
<b>8.7.2 Alternative methods of obtaining waste samples</b>	<b>120</b>
<b>8.7.3 Alternative laboratory testing design</b>	<b>121</b>
<b>8.8 Summary</b>	<b>124</b>
<b>9. Summary and conclusion</b>	<b>125</b>
<b>Appendices</b>	
<b>References</b>	

## List of Appendices

<b>Appendix A</b>	<b>Laboratory methods of testing hydraulic conductivity</b>	<b>i</b>
<b>Appendix B</b>	<b>Determination of horizontal flow port sizes</b>	<b>xxv</b>
<b>Appendix C</b>	<b>Relationship between hydraulic ram pressure and applied stress</b>	<b>xxix</b>
<b>Appendix D</b>	<b>Assessment of stress transmission losses arising from friction between the waste sample and cylinder wall</b>	<b>xxxi</b>
<b>Appendix E</b>	<b>Effective stress</b>	<b>xliv</b>
<b>Appendix F</b>	<b>Potential head loss in horizontal hydraulic conductivity assessments</b>	<b>1</b>
<b>Appendix G</b>	<b>Application of results to pumping of vertical wells</b>	<b>lii</b>
<b>Appendix H</b>	<b>Sensitivity of numerical analyses</b>	<b>lvi</b>
<b>Appendix I</b>	<b>Numerical analyses accuracy</b>	<b>lxii</b>
<b>Appendix J</b>	<b>Anomalous flow rates in horizontal hydraulic conductivity tests</b>	<b>lxiv</b>
<b>Appendix K</b>	<b>Details of test results</b>	<b>lxxiii</b>

# List of Figures

## 1. Introduction

Figure 1.1	The Loscoe explosion	2
Figure 1.2	Main features of current 'contained' landfill	3
Figure 1.3	Schematic diagram of isotropic and anisotropic flow	4
Figure 1.4	The Pitsea compression cell	6

## 2. Background: Measurement of hydraulic conductivity of soils and wastes

Figure 2.1	Decrease in hydraulic conductivity with effective stress for various household waste samples	14
Figure 2.2	Possible contributory factors of cross-anisotropy in municipal wastes	26
Figure 2.3	Ejection of compressed waste sample from the Pitsea compression cell	27

## 3. Test apparatus and procedure

Figure 3.1	Pitsea compression cell	31
Figure 3.2	Top platen showing the stack of three inflatable seals	33
Figure 3.3	Plan view of compression cell cylinder showing existing and new port positions	35
Figure 3.4	Close up view of horizontal flow ports	35
Figure 3.5	Individual Perspex header tanks	37

## 5. Sample loading, compression, water content and density

Figure 5.1	Gravel layer installed at the base of the compression cell	44
Figure 5.2	Sample loading using grab lorry	44
Figure 5.3	Pressure cell positioned on top of bottom gravel layer	45
Figure 5.4	Top gravel layer installed prior to lowering the top platen	46
Figure 5.5	Schematic cross-section of sample and gravel layer arrangement in the compression cell	47
Figure 5.6	Top platen in raised position showing graduated staff	49

Figure 5.7	Acrow props for preventing upward movement of top platen	49
Figure 5.8	Comparison of dry densities of different household wastes	60

## 6. Drainable porosity

Figure 6.1	DN1 drainable porosity test configurations	65
Figure 6.2	Compression of drainable porosities for samples DN1	68
Figure 6.3	Comparison of AG2 & DN1 drainable porosities with other wastes	69

## 7. Vertical hydraulic conductivity

Figure 7.1	Test arrangement for vertical hydraulic conductivity assessment	73
Figure 7.2	Inlet and outlet arrangement for upward flow vertical hydraulic conductivity tests	74
Figure 7.3	Outlet valves and pipes on the side of the compression cell	76
Figure 7.4	View of top of compression cell showing gas tanks	76
Figure 7.5	Vertical hydraulic conductivity with sample depth AG2 at 40 kPa	80
Figure 7.6	Vertical hydraulic conductivity with sample depth AG2 at 87 kPa	81
Figure 7.7	Vertical hydraulic conductivity with sample depth AG2 at 165 kPa	81
Figure 7.8	Vertical hydraulic conductivity with sample depth AG2 at 322 kPa	82
Figure 7.9	Vertical hydraulic conductivity with sample depth AG2 at 603 kPa	82
Figure 7.10	Vertical hydraulic conductivity with sample depth DN1 at 134 kPa	83
Figure 7.11	AG2 vertical hydraulic conductivity	84
Figure 7.12	DN1 vertical hydraulic conductivity	85
Figure 7.13	Hydraulic conductivity values measured for samples AG2 and DN1 compared with data from Beaven (2000)	87

## 8. Horizontal hydraulic conductivity assessment method

Figure 8.1	Arrangement of confined horizontal hydraulic conductivity test	94
Figure 8.2	Grid representation of the compression cell using MODFLOW	98
Figure 8.3	Cross sectional numerical analysis of an unconfined horizontal hydraulic conductivity test	100

Figure 8.4	Section of vertical flow validation analysis	103
Figure 8.5	Drawdown validation test simulating central well in compression cell with a pumping rate of 131 cm <sup>3</sup> /s	104
Figure 8.6	Drawdown validation test simulating central well in compression cell with a pumping rate of 1049 cm <sup>3</sup> /s	105
Figure 8.7	Comparison of MODFLOW and calculated drawdown for a pumping rate of 131 cm <sup>3</sup> /s	105
Figure 8.8	Comparison of MODFLOW and calculated drawdown for a pumping rate of 1049 cm <sup>3</sup> /s	106
Figure 8.9	Comparison of vertical and horizontal hydraulic conductivity for samples AG2 and DN1	110
Figure 8.10	$k_h$ ; $k_v$ assessments for sample AG2	111
Figure 8.11	$k_h$ ; $k_v$ assessments for sample DN1	112
Figure 8.12	Suggested modifications to the Pitsea compression cell	118
Figure 8.13	Sketch of suggested baffle plate arrangement on bottom platen	119
Figure 8.14	Compression cell bottom platen showing top surface normally covered by the bottom gravel layer	119
Figure 8.15	Cross section of lower portion of suggested modified arrangement showing baffle plates	120
Figure 8.16	Side view of horizontal flow permeameter	122
Figure 8.17	Outline of suggested design of rectangular section permeameter	123

## Appendix A

Figure A1	Constant head permeameter (upward flow)	iv
Figure A2	Falling head permeameter	iv
Figure A3	Cross section of a rigid walled compaction (Proctor) mould wall permeameter	viii
Figure A4	Double-ringed permeameter for detecting sidewall flow	x
Figure A5	Consolidation-cell permeameter (oedometer) – fixed ring type	xi
Figure A6	Schematic view of a flexible wall permeameter	xiii
Figure A7	Rowe cell	xviii
Figure A8	Rowe cell design using o-ring seal in top plate assembled	xix
Figure A9	Modified oedometer for horizontal hydraulic conductivity testing of kaolin samples	xxiii

## Appendix C

Figure C1	Additional weight of oil with extension of top platen rams	xxx
-----------	--	-----

## Appendix D

Figure D1	Cross-section of differential compression measurement string method used on sample AG2	xxxii
Figure D2 a) and b)	Displacement of magnets in sample DN1 at 40 kPa and 87 kPa applied stress	xxxiv
Figure D2 c) & d)	Displacement of magnets in sample DN1 at 134 kPa and 228 kPa applied stress	xxxv
Figure D2 e)	Displacement of magnets in sample DN1 at 334 kPa applied stress	xxxvi
Figure D3 a), b) & c)	Drainable porosity plots for sample AG2 at applied stresses of a) 40 kPa, b) 87 kPa and c) 165 kPa	xxxix
Figure D4 a) & b)	Drainable porosity plots for sample DN1 at applied stresses of a) 40 kPa, b) 87 kPa	xli
Figure D4 c) and d)	Drainable porosity plots for sample DN1 at applied stresses of c) 134 kPa and d) 228 kPa	xli
Figure D5	Drainable porosity plots for sample AG2 showing estimated minimum stress at base of the sample	xlii
Figure D6	Drainable porosity plots for sample DN1 showing estimated minimum stress at base of the sample	xlii
Figure D7	Plot of theoretical maximum and estimated transmission losses at base of sample AG2	xliii
Figure D8	Plot of theoretical maximum and estimated transmission losses at base of sample DN1	xliii

## Appendix E

Figure E1	Diagram of typical inlet and outlet pore water pressure for vertical hydraulic conductivity tests	xlvi
Figure E2	Variations in vertical hydraulic conductivity assessments with sample depth for sample DN1 at 134 kPa	xlviii

## **Appendix F**

Figure F1 Relationship between inlet flow rate and head loss

li

## **Appendix G**

Figure G1 Vertical drainage well pumping arrangement

liii

Figure G2 Vertical well spacings for isotropic and anisotropic conditions  
(unsaturated conditions)

liv

Figure G3 Vertical well spacings for isotropic and anisotropic conditions  
(saturated conditions)

lv

## **Appendix H**

Figure H1 Examples of changes in flow rate according to different  
 $k_h : k_v$  ratios used in numerical analyses

lviii

Figure H2 Examples of changes in flow rate in unconfined tests  
according to different  $k_h : k_v$  ratios used in numerical analyses

lix

Figure H3 Numerical analyses cross-sections for  $k_h : k_v$  ratios of  
2, 9.5 and 20 showing changes in pressure head

lxii

## **Appendix I**

Figure I1 Comparison of numerical analyses cross-sections using a  
gravel hydraulic conductivity of 10m/s and 0.1 m/s

lxiii

## **Appendix J**

Figure J1 Underside of top platen

lxvi

Figure J2 Plan and elevation of MODFLOW cross sections for Test 39

lxix

Figure J3 Plan and elevation of MODFLOW cross sections for Test 73

lxx

Figure J4 Plan and elevation of MODFLOW cross sections for Test 77

lxxi

## List of Tables

### **2. Background: Measurement of hydraulic conductivity of soils and wastes**

Table 2.1	Hydraulic conductivity temperature correction factors	12
Table 2.2	Results of early anisotropic hydraulic conductivity tests	23

### **4. Samples tested**

Table 4.1	Size and category analysis of waste AG2	39
Table 4.2	Size and category analysis of waste DN1	39

### **5. Sample loading, compression, water content and density**

Table 5.1	Sample AG2 compression	50
Table 5.2	Sample DN1 compression	50
Table 5.3	Range of possible stresses transmitted to base of sample AG2	53
Table 5.4	Range of possible stresses transmitted to base of sample DN1	54
Table 5.5	Water content (WC <sub>wet</sub> ) of sample DN1 for various test conditions	57
Table 5.6	Sample AG2 dry density	58
Table 5.7	Sample DN1 density	59

### **6. Drainable porosity**

Table 6.1	Sample AG2 drainable porosity	67
Table 6.2	Sample DN1 drainable porosity	67

## **7. Vertical hydraulic conductivity**

Table 7.1	Summary of AG2 test results	89
Table 7.2	Summary of DN1 test results	90

## **8. Horizontal hydraulic conductivity**

Table 8.1	Hydraulic conductivity values for DN1 at 134 kPa	102
Table 8.2	Summary of AG2 horizontal hydraulic conductivity tests	108
Table 8.3	Summary of DN1 horizontal hydraulic conductivity tests	109
Table 8.4	List of potential errors in the $k_h : k_v$ assessment process	116

## **Appendix B**

Table B1	Flow rates for 42mm diameter ports. No outflow through top and bottom of waste	xxvi
Table B2	Flow rates for 42mm diameter ports. Outflow via ports and top and bottom of waste	xxvi
Table B3	Flow rates for 9 x 72mm diameter ports. No outflow via top and bottom of waste	xxvii
Table B4	Flow rates for 9 off 72mm diameter ports with outflow also through top and bottom of waste	xxvii

AUTHOR'S DECLARATION

With the oversight of my main supervisor, editorial advice has been sought. No changes of intellectual content were made as a result of this advice.

## **Acknowledgements**

I wish to extend my gratitude to everyone who has helped make this research possible.

Many people have been involved at various stages. This includes contractors, researchers and staff at the University of Southampton and Veolia Environmental Services. In particular I wish to thank my supervisors William Powrie and Richard Beaven, and members of the University of Southampton Waste Management Research Group for their advice, guidance, and encouragement throughout this project.

I also wish to thank the staff at Veolia Environmental Services for their warm hospitality and assistance. A special mention goes to the workshop staff for their practical help on many occasions.

## ABBREVIATIONS

a.g.l.	distance above ground level
AG1	Aged household waste sample tested by Beaven (2000)
AG2	Aged household waste sample tested in this report
ASTM	American Society for Testing and Materials
BS	British Standards
Defra	Department for Environment, Food and Rural Affairs
DM3	Fresh crude household waste sample tested by Beaven (2000)
DN1	Dano treated household waste sample tested in this report
Fe	Ferrous metal fraction of a waste sample
MBT	Mechanical-biological treated wastes
Mc	Miscellaneous combustibles fraction of a waste sample
Mnc	Miscellaneous non combustibles fraction of a waste sample
nFe	Non ferrous metal fraction of a waste sample
PV1	Pulverised household waste sample tested by Beaven (2000)
UK	United Kingdom
USGS	United States Geological Survey

## NOTATIONS

$A$	cross sectional area
$A_1$	cross section area of sample (in falling head test), cross sectional area of hydraulic rams
$A_2$	cross section area of pipe (in falling head test), area of top platen
$B$	saturation coefficient
$d$	dry weight, diameter of central drain well (Rowe cell)
$D$	diameter of sample
$F$	applied force
$F_{plat}$	weight of cylinders and top platen
$F_{topgl}$	weight of top gravel layer
$F_{oil}$	weight of oil in rams
$g$	gravitational acceleration ( $9.81 \text{ m/s}^2$ )
$h$	head (sometimes denoted $h$ )
$h_1$	starting head (of water level in falling head test)
$h_2$	final head (of water level in falling head test)
$h_w$	depth of fluid / head in the well
$H$	depth of waste/sample (sometimes denoted $H$ ), maximum leachate head in landfill, inlet constant head (Agaki and Ishida, 1994)
$i$	hydraulic gradient (sometimes denoted $I$ )
$k$	hydraulic conductivity / coefficient of permeability
$k_h$	horizontal hydraulic conductivity (directional values in horizontal plane can be denoted $k_x$ and $k_y$ )
$k_t$	see $R_t$
$k_v$	vertical hydraulic conductivity (may also be denoted $k_z$ )
$K$	intrinsic permeability
$l$	flowpath length ( <i>i.e.</i> the sample depth) for Rowe cell
$L$	distance (between piezometers)
$M_s$	dry mass of solids
$M_w$	mass of water
$MC_{wet}$	wet moisture content of a sample
$n$	total porosity
$n_e$	drainable (or effective) porosity

$p_1$	inlet back pressure (Rowe cell)
$p_2$	outlet back pressure (Rowe cell)
$P_1$	hydraulic pressure (in rams)
$P_2$	stress applied to sample (in compression cell)
$q$	rate of discharge (Agaki and Ishida, 1994)
$Q$	steady state volumetric flow
$r, r_w$	radius of well
$r_v$	radius of capture (or influence) of well
$R$	radius of cell
$R_t$	Temperature correction factor (sometimes denoted $k_t$ )
$S_r$	saturation ratio
$T$	time
$u_w$	pore water pressure
$v$	recharge rate
$v_D$	superficial or Darcy seepage velocity
$V_d$	drainable volume
$V_s$	volume of solids
$V_T$	sample volume
$V_v$	volume of voids
$w$	wet weight
$WC_{dry}$	water content based on dry mass of waste
$WC_{wet}$	water content based on a wet mass of waste
$\alpha$	constant (Agaki and Ishida, 1994)
$\delta$	friction angle
$\phi'$	internal friction angle
$\gamma_w$	unit weight of permeating fluid
$\mu$	dynamic viscosity of fluid
$\rho$	density
$\rho_{DRY}$	dry density of sample
$\rho_{FC}$	density of sample at field capacity
$\sigma$	total stress, confining pressure
$\sigma'$	effective stress

## 1. Introduction

The aim of the research described in this thesis is to assess the hydraulic conductivities of landfilled wastes in both vertical and horizontal directions. Assessments have previously been made with fluid flow in a single direction, but there has been no systematic study comparing the flow characteristics of landfill waste in both vertical *and* horizontal planes. The purpose of the research is to further the understanding of leachate movement through landfilled wastes. This is fundamental to the control of leachate levels within landfills in order to prevent leakage into, and contamination of, surrounding ground and groundwater.

Historically landfill has been the predominant method used for UK waste disposal and currently nearly 70% of municipal waste is disposed in landfill sites (Environment Agency 2004/5 figures for England & Wales - [www.environment-agency.gov.uk](http://www.environment-agency.gov.uk)). In total about 100 million tonnes of municipal, commercial and industrial, and construction and demolition waste is landfilled each year (Defra 2002/3 data - [www.defra.gov.uk/environment/statistics/waste](http://www.defra.gov.uk/environment/statistics/waste)). In the future the volumes of waste disposed in landfill may be reduced as waste minimisation, recycling and alternative methods of waste treatment become established. However, alternative methods such as incineration and waste pre-treatment still require final disposal of significant volumes of residual wastes. The need for understanding the processes involved in managing new and existing landfill wastes will be with us for many decades both in the UK and internationally.

Understanding landfill processes is necessary as both gas and leachate generated by landfill sites can cause damage to the environment. Landfill gas arises from the decay of organic matter in the wastes. These gases may be released to the atmosphere (landfill gas is mainly methane and carbon dioxide which are greenhouse gases), or may migrate to the surrounding ground, killing vegetation or potentially creating a fire or explosion hazard. Probably the most notable case of this in the UK was the 1986 Loscoe landfill explosion (Figure 1.1) which destroyed a nearby bungalow and damaged several others (Sarsby, 2000). Internationally there have been several cases of fatalities arising from poor landfill practices.



Figure 1.1 The Loscoe explosion. Photograph from the Landfill Gas Web Site ([www.landfill-gas.com](http://www.landfill-gas.com))

Leachate is present in most landfills and arises from contaminants leached or squeezed (by the weight of overlying waste and/or landfill plant) from the wastes combined with infiltrating rainwater percolating downwards through the wastes. This can seep from landfills and contaminate the surrounding ground or groundwater. Until relatively recently (30 years ago) seepage of leachate from landfill sites was largely unregulated in ‘uncontrolled’ or ‘dilute and disperse’ landfills. This is now unacceptable and current ‘contained’ sites minimise leachate seepage by use of low permeability containment liners, assisted by drainage and pumping systems to maintain hydraulic heads at acceptable levels. Sites are now usually capped with a low permeability final layer to reduce rainwater infiltration and thereby abate leachate generation within wastes (Figure 1.2).

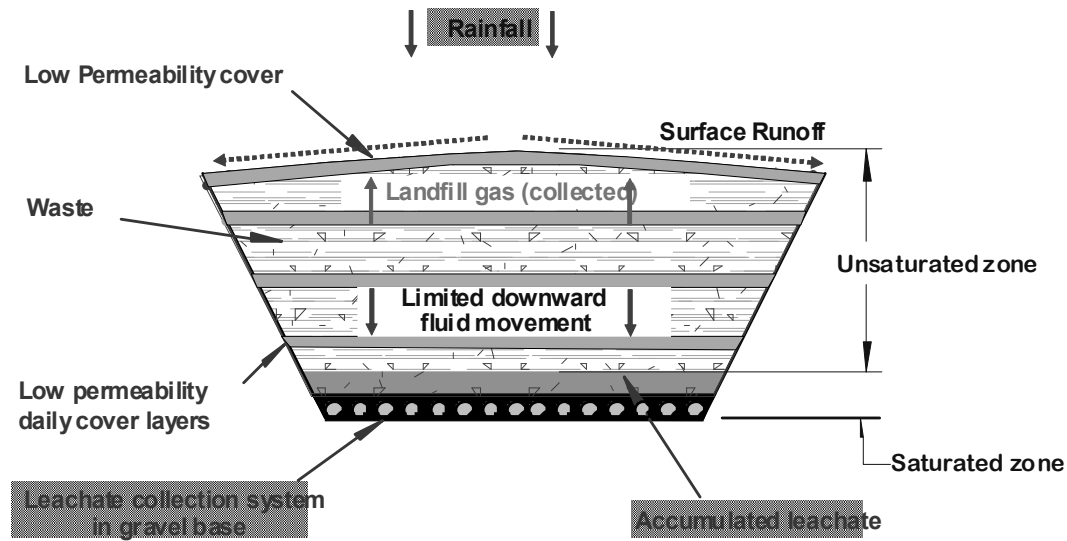


Figure 1.2 Main features of current 'contained' landfill

The research presented in this thesis concerns the control of leachate in landfill wastes. Fundamental to this is hydraulic conductivity (designated  $k$ ) which can also be referred to as the *permeability coefficient* or *coefficient of permeability* (section 2.2) which is an indication of the ease with which water (or other fluids) can move through a medium such as soil or waste (Wood, 1990, Cartwright and Hensel, 1995). Measurement of the hydraulic conductivity of soils has been established for a long time - for example the founding of Darcy's law, the basic tenet of hydraulic conductivity measurement, dates from 1856 (section 2.2). Many of the basic principles for assessing the properties of soils, such as Darcy's law, can be applied to wastes.

One of the most comprehensive research projects investigating the hydraulic conductivities of wastes has been that undertaken by Beaven (2000). Changes in hydraulic conductivity were evaluated for several different types of household waste subjected to a range of compressive stresses. Such stress will generally increase with depth of burial in a landfill due to the weight of overlying wastes. This is often referred to as overburden stress. A major finding of the work is that stress is the main controlling factor of hydraulic conductivity in wastes (section 2.4.4). Waste composition and pre-processing is of secondary importance.

A limitation to the laboratory based work by Beaven (2000) and that of other researchers (with the exception of some basic tests discussed in section 2.5) is that hydraulic conductivity was measured according to percolant flow in a single (usually vertical) plane. However it has been conjectured (Landva and Clark, 1990, Bendz and Flyhammar, 1999) that the deposition of waste and subsequent compression by plant and overburden stress may result in a predominantly horizontally layered structure that may favour horizontal rather than vertical flow. Consequently horizontal hydraulic conductivity ( $k_h$ ) may be greater than vertical hydraulic conductivity ( $k_v$ ). Such anisotropy is evident in many soils arising from the natural alignment or layering of elongated soil particles (Weeks, 1969, Craig, 1983, Cartwright and Hensel, 1995). Fluid flow in the direction perpendicular to the plane in which the particles are aligned is subject to longer and more tortuous paths than flow parallel with particle alignment. Consequently hydraulic conductivity is higher in the plane parallel with rather than perpendicular to particle alignment. A schematic diagram of isotropic and anisotropic flow through an ideal matrix is shown in Figure 1.3.

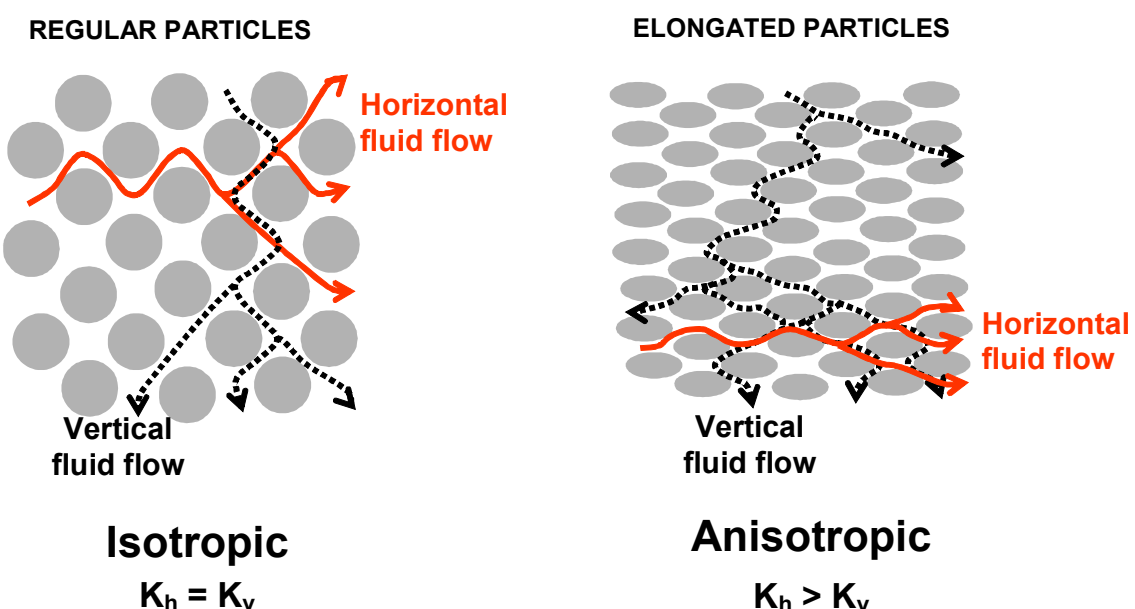


Figure 1.3 Schematic diagram of isotropic and anisotropic flow

In modelling leachate and contaminant movement in landfill wastes it has to be assumed, in the absence of any measured anisotropic values, that leachate movement is uniform in all directions. Alternatively an arbitrary  $k_h : k_v$  ratio could be used (e.g. McCleanor and Reinhart, 2000) but this potentially introduces significant error as no systematic assessment of waste anisotropy values has been undertaken. The aim of the research described in this thesis is to meet this outstanding research requirement by evaluating both the vertical and horizontal hydraulic conductivity of landfill wastes, thus providing the necessary data for more accurate assessment of modelling of fluid movement in landfilled wastes.

To perform the task of assessing waste anisotropy within given cost, time and practical limitations, it was necessary to use laboratory based rather than *in situ* methods. The equipment selected for the research was the Pitsea compression cell (section 3.2) shown in Figure 1.4. With modification (detailed in section 3.3 to 3.5) this facility fulfilled at reasonable cost the major requirements for assessing the horizontal and vertical hydraulic conductivities of wastes. These were that:

- samples could be tested that were of sufficient size to obtain representative results from heterogeneous wastes
- samples could be compressed to represent landfill overburden stresses of about 60 metres burial depth.
- both vertical and horizontal flow tests could be carried out without the need to modify or replace the sample

In this thesis a description is given of the test methodology used and results of tests undertaken for assessing vertical and horizontal hydraulic conductivity of two waste samples. However the results must be considered in their true context. Firstly it has to be recognised that the tests were limited to wastes in (nominally) saturated conditions. The findings are therefore not applicable to wastes in the unsaturated zone of a landfill through which drainage would be expected to be predominantly vertical. Secondly, the  $k_h : k_v$  ratios presented in the results are inherent in the waste and do not include the effect of other layering within the waste body such as low permeability



Figure 1.4 The Pitsea compression cell

daily cover layers. These features could totally alter the perceived flow regime in a waste body. As these are site specific each case would require individual examination. A third observation is that the results obtained from the samples tested may not necessarily be representative of all types of waste (section 4.2).

Providing the above conditions are recognised, the research described in this thesis represents a major step forward in the understanding of leachate movement in landfills. It is the first time that a systematic set of tests have been conducted on representative wastes subjected to a range of landfill overburden stresses. The research has advanced the understanding of laboratory testing methods for wastes and has led to new and original research investigating the influence of gas accumulation on waste permeability.

## **2. Background: Measurement of hydraulic conductivity of soils and wastes**

### **2.1 Introduction**

Assessment of waste hydrogeological properties is a relatively recent research area and no standardised testing methods exist for hydraulic conductivity tests on wastes even for single plane (*i.e.* just vertical or just horizontal) flow. Devising a suitable bi-planar flow testing method suitable for waste material was therefore a prerequisite for the research described in this thesis. In this chapter the background information relevant to the evaluation of the hydraulic conductivity of wastes is presented. This commences with a definition of the term *hydraulic conductivity* (section 2.2) followed by a summary of previously published waste hydraulic conductivity values (section 2.3). In the following sections (2.4.1 to 2.4.10) factors that may affect measurement of hydraulic conductivity are summarised.

Soil testing methods are referred to throughout the chapter as laboratory methods for testing the hydraulic conductivity of soils have been established for a long time and the basic principles may be applied to testing of wastes. However as discussed in the chapter, testing of waste can be more complex due to large variations in particle size, compressibility and the influence of landfill gas generated in the waste.

The key issue to this research, the anisotropic structure of wastes, is discussed in section 2.5. Reference is again made to soils as it has been long understood that the alignment of elongated soil particles in a particular plane is the underlying cause of directional differences of hydraulic conductivity. As highlighted in the section, it has been conjectured that a similar situation arises in landfilled wastes.

An important distinction is made in this section between anisotropy due purely to particle alignment (referred to as inherent anisotropy – the subject of this thesis) and that arising from the presence of low permeability layers (stratification) in a waste / soil formation.

The review in this chapter provides the background information for the method used to assess the hydraulic conductivity of wastes in two planes for this research described in the following chapters.

## 2.2 Hydraulic conductivity

Hydraulic conductivity ( $k$ ) is a measure of the capacity of a porous medium, such as soil or waste, to allow the flow of a liquid (usually water) into or through it under a unit hydraulic gradient without impairing its structure (Bell, 1992, Watkins, 1997). It is sometimes called the *permeability coefficient* or *coefficient of permeability* (these terms tend to be used by civil engineers, whereas soil scientists and hydrogeologists tend to use ‘hydraulic conductivity’- Daniel, 1994).

Hydraulic conductivity is calculated using Darcy’s law. This was proposed by Henri Darcy in 1856 based on a series of experiments in which water was passed through soil samples at a constant flow rate (a typical test arrangement is shown in Appendix A, Figure A1).

Hydraulic conductivity is given by:

$$k = \frac{Q}{Ai} \quad (2.1)$$

where:

$k$  is hydraulic conductivity / coefficient of permeability (m/s)

$A$  is the cross sectional area through which flow takes place ( $m^2$ )

$Q$  is the steady state volumetric flow rate of water ( $m^3/s$ )

$i$  is the hydraulic gradient – the rate of decrease of total head with distance in the direction of flow

It is sometimes written as:

$$v_D = ki \quad (2.2)$$

where:

$v_D$  = superficial or Darcy seepage velocity ( $Q$  divided by the cross-sectional area of particles and voids through which flow takes place)

*n.b.* true fluid velocity is obtained by dividing  $Q$  by the cross-sectional area of the voids alone

Soils and aggregates exhibit an extremely large range of hydraulic conductivity values: from  $1 \times 10^{-12}$  m/s for some unweathered marine clays (Freeze and Cherry, 1979) to more than 1 m/s for coarse gravel (Craig, 1983, Barnes, 2000). This is largely due to the huge range in particle size, ranging from less than  $2\mu\text{m}$  for clay to 60 mm for coarse gravel (Wood, 1990). In general, materials consisting of larger particles will exhibit larger hydraulic conductivity than small particles due to larger void openings between the particles (Craig, 1983, Fetter, 1988, Wood, 1990).

Other factors affecting hydraulic conductivity (Whitlow 1983, Beavis 1985) may be:

- the shape / orientation of particles
- the degree of saturation / presence of air or gas
- viscosity of the permeant
- stress
- the presence of cracks and fissures
- turbulent flow
- cations in clays
- presence of organic matter (Mitchell, 1976)

## 2.3 Published waste hydraulic conductivity values

Published waste hydraulic conductivity values (for flow in a single plane) can vary by several orders of magnitude. A review by Oweis *et al.* (1990) showed evaluations ranging from  $1.5 \times 10^{-6}$  to  $2 \times 10^{-4}$  m/s. A more recent review by Jain *et al.* (2006) gave laboratory measurements between  $1 \times 10^{-8}$  to  $1 \times 10^{-2}$  m/s and field measurements between  $3 \times 10^{-6}$  to 0.25 m/s. Hydraulic conductivities between  $3.9 \times 10^{-7}$  and  $6.7 \times 10^{-5}$  m/s were obtained from pumping tests by Burrows *et al.* (1997) at four different landfill sites in southern England. Bleiker *et al.* (1993) indicated that hydraulic conductivity at the bottom of a landfill could be as low as  $1 \times 10^{-9}$  m/s. Vertical hydraulic conductivity measurements on a number different types of waste using the Pitsea compression cell by Beaven (2000) indicated that values this low are only likely at landfill depths of about 100 m (Figure 2.1). Vertical hydraulic conductivity values as low as  $5 \times 10^{-9}$  m/s have since been recorded in compression cell tests by Hudson *et al.* (2000) at applied stresses of 600 kPa (equivalent to approximately 50 m + landfill depth).

In sections 2.4 the possible factors attributing to the large variation in measured waste hydraulic conductivity values are discussed.

## 2.4 Factors influencing hydraulic conductivity of wastes

### 2.4.1 Introduction

The published values summarised in section 2.3 demonstrate that measured waste hydraulic conductivity values can vary significantly. Several factors may influence hydraulic conductivity measurements and these had to be considered for the test method for this research. These factors are discussed in sections 2.4.2 to 2.4.10.

### 2.4.2 Density and viscosity of permeant

Hydraulic conductivity is dependent on both the *intrinsic permeability* (K) of the medium and the physical properties (fluid viscosity and density) of the permeant. The relationship is:

$$k = \frac{K \rho g}{\mu} \quad (2.3)$$

where:  $K$  = intrinsic permeability ( $\text{m}^2$ )  
 $k$  = hydraulic conductivity ( $\text{m/s}$ )  
 $\rho$  = density of fluid ( $\text{kg/m}^3$ )  
 $\mu$  = dynamic viscosity of fluid ( $\text{kg/ms}$ )  
 $g$  = gravitational acceleration ( $9.81 \text{ m/s}^2$ )

(Freeze and Cherry, 1979)

The density and viscosity of the permeant are functions of temperature. Viscosity of water, and hence hydraulic conductivity, changes by about 3% for every  $1^\circ\text{C}$  change in temperature (Daniel, 1994). Laboratory based soil hydraulic conductivity tests are normally conducted at a standard room temperature of  $20^\circ\text{C}$  (Bowles 1979, Barnes 2000), although  $15.6^\circ\text{C}$  is also quoted in some sources such as Fetter (1988).

Temperature effects may need to be considered when comparing laboratory and field results. For example, compared to measurements at the standard laboratory temperature of  $20^\circ\text{C}$ , hydraulic conductivity at a groundwater permeating temperature of  $10^\circ\text{C}$  will be reduced to 77% of that at the standard  $20^\circ\text{C}$  value. At  $0^\circ\text{C}$ , hydraulic conductivity is reduced to 56% of that at the standard  $20^\circ\text{C}$  value (Akroyd, 1957, Craig 1983).

The reverse situation may apply to landfill conditions as temperatures may be higher than standard laboratory temperatures. Campbell (1995) gave typical temperatures for landfills in anaerobic conditions between  $20^\circ\text{C}$  and  $40^\circ\text{C}$ , and  $60^\circ\text{C}$  to  $70^\circ\text{C}$  in aerobic conditions (although aerobic conditions are uncommon with the current practice of rapid waste disposal). Similar figures were given by Crawford and Smith (1985) of  $25^\circ\text{C}$  to  $45^\circ\text{C}$ , with temperatures of  $70^\circ\text{C}$  occasionally recorded. Burrows *et al.* (1997) found leachate temperatures in four different landfill sites in southern England to range from

18°C to 64°C. Oweis *et al.* (1990) recorded a temperature of 55°C in leachate discharged from a New Jersey landfill. Vapour temperatures in the wells were 60 to 65°C. Some differences can therefore be expected between hydraulic conductivity results from laboratory tests conducted at standard or ambient air temperature, and those within a landfill site. Temperature correction factors ( $R_t$  but sometimes denoted  $k_t$ ) for hydraulic conductivity values at permeant temperatures above and below the standard room temperature of 20°C are shown in Table 2.1 (reproduced from Whitlow, 1983):

Table 2.1 Hydraulic conductivity temperature correction factors (Whitlow, 1983)

Temperature	$R_t$	Temperature	$R_t$
0 °C	1.779	25 °C	0.906
4 °C	1.555	30 °C	0.808
10 °C	1.299	40 °C	0.670
15 °C	1.133	50 °C	0.550
20 °C	1.000	60 °C	0.468
		70 °C	0.410

The above temperature correction factors are for water rather than landfill leachate. The properties of leachate may differ: the viscosity of leachate can be 1% to 15% higher than water at the same temperature (Watkins, 1997), and leachate density (with typical dissolved solids concentrations of 20,000 mg/l) will be about 1% higher than that of water (Christensen, 1997). In the absence of published values for landfill leachates, the temperature correction factors for water may suffice as an approximate guide. The possible effects of leachate temperature on the results of the research undertaken for this thesis is discussed in sections 7.3 and 8.6.3.

A further temperature effect observed by Christiansen (1944) was that air (or other gases) entrapped in a soil (or waste) would increase in volume as temperature increased, thereby reducing permeability (see section 2.4.6). The effect however would be partly offset by the decrease in viscosity of the permeant.

### 2.4.3 Leaching effect of permeant

The use of distilled water as a permeant in soil hydraulic conductivity tests may leach a higher proportion of monovalent than divalent cations from the soil sample. As a result changes in hydraulic conductivity may occur in soils such as sodium bentonite that derive their low permeability from their abundance of monovalent cations (Yong, 1986 *cited in Oweis and Khera, 1990*). To prevent leaching the use of 0.01N CaSO<sub>4</sub> solution as a permeant is recommended as this is representative of salt concentrations found in soils. (Oweis and Khera, 1990).

### 2.4.4 Density and effective stress

Hydraulic conductivity may be reduced when a medium is compacted as flow paths become restricted or blocked. This is more likely to occur at depth due to the overburden stress arising from overlying material. Formations containing macropores, fractures and joints may be particularly affected by stress (Daniel, 1994). A general estimate of a reduction in hydraulic conductivity of an order of magnitude due to soil compression was given by Cedergren (1989 - *cited in Barnes, 2000*). Tests by Boynton and Daniel (1985) and Daniel *et al.* (1985) (*cited in Shackelford, 1994*) showed that the permeability of compacted clay specimens decreased from one to three orders of magnitude as the average effective stress in the samples were increased from 13.8 to 103.4 kPa.

In general wastes are much more compressible than soils and therefore hydraulic conductivity is much more likely to be affected by stress. Landfilled waste is likely to be subjected to stress from mechanical plant during tipping and burial, as well as the overburden weight of overlying waste. Typical overburden stress will be approximately 7 to 10 kPa per metre depth of waste - assuming a typical in place waste density of 0.65 to 1.0 tonne/m<sup>3</sup> (Beaven 2000, Sarsby, 2000, Vesilind *et al.*, 2002) depending on waste type, compaction and water content. The most comprehensive published waste stress/hydraulic conductivity data set is that by Beaven (2000).

Figure 2.1 shows vertical hydraulic conductivities in nominally saturated conditions

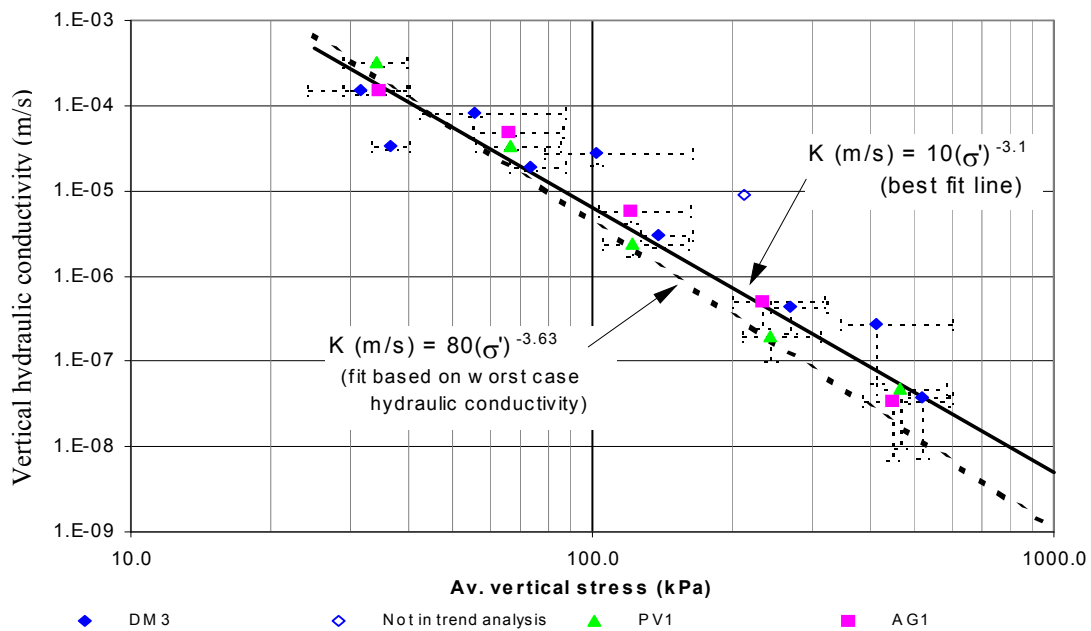


Figure 2.1 Decrease in saturated hydraulic conductivity with effective stress for various household waste samples (Beaven, 2000).

for three different waste types (a fresh crude household waste - DM3, a fresh pulverised waste - PV1 and a twenty year old decomposed waste - AG1) subjected to average vertical stresses between 30 kPa and 500 kPa. For all waste types, hydraulic conductivity reduced significantly as stress was increased. A reduction of about four orders of magnitude was apparent between waste hydraulic conductivity measured at low stress (about 30 kPa) and that measured at high stress (500 kPa) equivalent to a landfill depth of about 50 metres). Stress is the most influential factor governing hydraulic conductivity in saturated conditions. *n.b.* leachate temperature measurements and leachate analyses were not undertaken in these tests. Hydraulic conductivity in field conditions may vary according to leachate temperature and strength (section 2.4.2).

The effect of stress on the saturated hydraulic conductivity of waste was also demonstrated by Chen & Chynoweth (1995). A decrease in the average hydraulic conductivity of a saturated model municipal solid waste (MSW) from  $9.6 \times 10^{-4}$  to  $4.7 \times 10^{-7}$  m/s was recorded for simulated burial depths of 3 m and 15 m respectively.

#### 2.4.5 Waste type and pre-processing

In the UK in the last few decades the composition of municipal solid waste has changed. For example ash content has decreased as households have switched from coal fires to central heating, and plastics have become commonplace. Waste composition may vary seasonally, according to geographical location or local recycling initiatives. Waste may be deposited without further treatment or alternatively shredded or pulverised prior to tipping. Additionally, wastes settle and decompose according to prevailing conditions. Potentially all these factors could result in a large range of hydraulic conductivity values.

It may be expected that unprocessed wastes with a higher percentage of large particles and probable presence of larger void pathways would exhibit a higher hydraulic conductivity than shredded wastes of smaller particle size and higher bulk density. However Figure 2.1 gives no clear indication of a relationship between the hydraulic conductivity for different waste types. This unpredictability may be due to the compressive nature of some waste components or the blockage of some flow pathways by particulate matter/fines.

#### 2.4.6 Water content and gas accumulation

A saturated porous media is one in which all the void spaces are filled with water. It is a two-phase material consisting of solid particles and water. This is normally the situation for soils below the water table (Freeze and Cherry, 1979, Powrie, 1997). An unsaturated (or partly or partially saturated) medium also contains gas (usually air) within the void spaces and is therefore a three-phase material comprising solid, liquid and gas.

Gas in the void spaces of an otherwise saturated material results in a reduction in available flow paths and hence a reduction in hydraulic conductivity compared to fully saturated conditions. Reductions in soil permeability by a factor of four or five have been recorded for decreases in saturation from 98% to 85% (Mitchell *et al.*, 1965 *cited in Oweis and Khera, 1990*). Greater differences can occur if the soil moisture is

drained. For sands the difference between saturated and unsaturated hydraulic conductivities can be as high as nine orders of magnitude, and for clays about five orders of magnitude (Stephens, 1994). The larger difference for sand rather than clay may be due to the ease of drainage from the pore spaces of coarser grained materials. During drainage, water is more likely to be retained in some of the pore spaces in fine grained materials, and therefore hydraulic conductivity may not reduce as much as a coarser grained material under the same conditions (Fetter, 1988).

There appears to be no published research directly comparing the saturated and unsaturated hydraulic conductivities of wastes. Comparison of saturated and unsaturated values from different studies are unlikely to be valid due to differences between samples and conditions. For example, Zeiss and Major (1992) measured unsaturated vertical hydraulic conductivity values of  $1.2 \times 10^{-5}$  m/s in laboratory tests on fresh household waste subjected to low stress (as indicated by the very low sample densities which ranged from  $165 \text{ kg/m}^3$  and  $305 \text{ kg/m}^3$ ). The unsaturated hydraulic conductivity would be expected to be lower than that of a saturated waste subjected to similar stress. However the value is one and two orders of magnitude *higher* than the saturated hydraulic conductivity for household wastes subjected to low stress in Figure 2.1. Comparisons between saturated and unsaturated hydraulic conductivity should preferably be conducted on the same sample subjected to the same stress conditions.

One of the problems encountered in soil testing is creating and maintaining fully saturated conditions prior to and during testing. Laboratory investigations as long ago as the 1940's showed that unless natural soil cores were wetted under vacuum, they could not be completely saturated. For 200 different samples tested by Smith and Browning (1942), between 9% and 22% of the void space was occupied by air. Other considerations for attaining fully saturated conditions are the use of de-aired water as a permeant and using a high back pressure to compress any air in the sample and prevent dissolved gasses coming out of solution. However high back pressures cannot be used with some test arrangements such as the falling head test (Appendix A, section A1) and is not recommended for rigid wall permeameters as discussed in Appendix A, section A2).

If saturation cannot be maintained during testing then measured hydraulic conductivity may appear to be inconsistent. An example of this is given by Zimmie *et al.* (1981) (*cited in Oweis and Khera, 1990*) for which the hydraulic conductivity of a soil sample apparently reduced by more than 50% during testing due to dissolved gasses coming out of solution. A different situation was recorded by Christiansen (1944) of the permeability of soil samples *increasing* during downward flow tests by factors between 2 and 40 over periods ranging from several days to several months. This was attributed to air initially being present in the soil samples being gradually dissolved by the water flow - the time taken for this being dependent on the amount of air initially present, the permeability of the soil and the capacity of the water to absorb additional air.

In wastes the problem of maintaining fully saturated conditions is compounded by the generation of gas from degradation of some of the waste constituents. During the course of the research conducted for this thesis it was found that significant volumes of gas would accumulate in the void spaces of a nominally saturated waste sample even though the gas was free to vent to atmosphere. As a result hydraulic conductivity was up to 30 times lower than recorded in nominally saturated conditions (Figure 7.13, Hudson *et al.*, 2001, 2002). Similarly in borehole permeameter tests undertaken by Jain *et al.* (2006) in landfilled municipal solid waste, the low permeability of the waste was primarily attributed to entrapped gas. The accumulation of gas in pore spaces has also been observed in nominally saturated offshore soils (Sills *et al.*, 1991) and gravel drainage media (Nikolova *et al.*, 2001), although the effects on hydraulic conductivity are not known in these instances.

Although it is generally accepted that fully saturated conditions are suitable for the hydraulic conductivity assessment of soils, it should perhaps be questioned whether this is appropriate for wastes. Even highly processed mechanical biological pre-treated (MBP) waste wastes are anticipated to have an initial gas yield of about  $8 \text{ m}^3/\text{m}^3\text{.a}$  (Danhamer *et al.*, 1999). Fresh unprocessed municipal solid waste would be expected to produce much higher yields. It therefore follows that gas will be present in most nominally saturated wastes (as experienced in landfill pumping tests undertaken by Giardi, 1997). Hydraulic conductivity values obtained in gas accumulated, rather than nominally saturated conditions, are therefore likely to be more representative of the landfill situation.

The interaction between gas and water / leachate in soils and wastes appears to be complex. Not only does the presence of gas within a soil matrix appear to restrict water flow, but water also restricts or prevents the movement of gas. The restriction of landfill gas migration through saturated soils has been noted by a number of authors including Figueroa and Stegmann (1996), Kjeldsen (1996) and Boltze and de Freitas (1997). Lofy (1996) confirmed that gas movement is also restricted in waste with high water contents and corresponding elevated gas pressures within the waste have been observed. In comparison to typical gas pressures in landfills of 2.5 cm to 5.0 cm of water above atmospheric pressure (Crawford and Smith, 1985), Burrows *et al.* (1997) measured the pressure of unvented gas in saturated landfill waste equivalent to 70 cm of water. Several reported gas pressures in landfill are cited by Kjeldsen (1996). These generally range up to 20 to 30 cm H<sub>2</sub>O above barometric pressure, but pressures above 80 cm H<sub>2</sub>O were reported by Campbell (1989) and a maximum value of 250 cm H<sub>2</sub>O was recorded by Wittmann (1985). Other factors that may affect gas migration through landfill waste are the properties of the gas (diffusivity, solubility and viscosity), the properties / conditions of the waste (hydraulic conductivity, water content, temperature) and the degree of sorbtion onto waste particles. Ultimate release may depend on the permeability of, and methane oxidation in, the top soil covers and also barometric pressure changes, wind speed and air temperature. (Cernuschi and Giugliano, 1996, Kjeldsen, 1996).

#### 2.4.7 Pore water pressure

As hydraulic conductivity of a medium can be affected by the accumulation of gas in the void spaces (section 2.4.6), it follows that pressure changes that cause the gas to expand or contract may also result in a change in hydraulic conductivity. In unconfined hydrostatic conditions the pore water pressure ( $u_w$ ) at depth is given by:

$$u_w = \rho g h_w \quad (2.4)$$

where:

- $u_w$  is pore water pressure (kPa)
- $\rho$  is density of fluid (kg/m<sup>3</sup>)
- $g$  is gravitational acceleration (9.81 m/s<sup>2</sup>)
- $h_w$  is depth of fluid (m)

Atmospheric pressure may also affect the volume of accumulated gas within a saturated zone of a landfill, although the pressure differential is small in comparison to typical pore water pressures. Burrows *et al.*, (1997) observed variations in steady state landfill leachate levels by up to one metre in accordance with changes in atmospheric pressure. This was attributed to exchange of gas in solution in the leachate with gas bubbles in the pore spaces. Under falling head conditions it was envisaged that gas was released from solution, causing bubbles to expand and therefore resulting in a rise in leachate level.

Pore water pressure may affect hydraulic conductivity of a medium in other ways. It is possible that high pore water pressure may open up cracks and fissures, further increasing hydraulic conductivity. However the opposite effect, a *decrease* in hydraulic conductivity at elevated pore water pressure, has also been observed during the hydraulic conductivity testing of a clay sample (Agaki and Ishida, 1994). It was concluded that higher pore water pressure (above 80 kPa) resulted in silting of some of the fluid pathways as evidenced by the appearance of muddy outlet water in tests carried out at higher pressures.

A further potential effect of pore water pressure is the change in effective stress. This is discussed in section 7.5.2. and Appendix E.

#### 2.4.8 Turbulent Flow

Darcy's law is limited to laminar fluid flow through a medium. If flow velocities are high enough for turbulent flow to occur (as can occur in coarse gravels), the

relationship is not valid. It has also been questioned if Darcy's law is applicable at very low hydraulic gradients. Non-linear or no-flow thresholds have been suggested (Lancellotta, 1995). Research by Tavenas *et al.* (1983) concluded that Darcy's law is valid in natural soft clays for gradients as low (and probably lower than) 0.1.

#### 2.4.9 Heterogeneity

Variations in particle size or the presence of preferential flow channels within a soil/waste may result in large variations in hydraulic conductivity at different points in a sample. Rowe and Nadarajah (1996) noted that localised measurements of hydraulic conductivity in heterogeneous wastes could vary by a number of orders of magnitude.

For heterogeneous materials, large sample sizes are required to obtain hydraulic conductivity values representative of field conditions. Providing this is so, laboratory and field tests can give reasonably consistent results (Oweis and Khera, 1990). However if samples are of insufficient size to replicate the overall macropermeability of soil formations (*e.g.* features such as stratification, inhomogeneity, fissures and joints within the soil structure), it has been demonstrated that laboratory tests can yield hydraulic conductivity values 1000 times less than field assessments conducted on the same material (Day and Daniel, 1985).

For laboratory testing of soils, the American Society for Testing and Materials state that the minimum sample dimension should not be less than six times the maximum particle dimension (ASTM 1142, 1994, Daniel, 1994), although the standard test method for permeability of granular soils (constant head) ASTM D 2434 – 68 (2000) stipulates permeameter diameters of 8 or 12 times the maximum particle size. British Standards soil testing recommendations state that the maximum particle size should not exceed one twelfth the sample diameter (BS1377 part 1 & 5: 1990). However for some materials, this still may be insufficient to replicate features of the macrostructure such as fissures, bedding, laminations or root holes within a soil matrix and a minimum specimen size of 20 cm to 60 cm is recommended (Trautwein and Boutwell, 1994).

There are no standards governing minimum sample sizes for wastes. If soil testing standards are to be applied then samples may need to be several metres in height and diameter for waste containing particles measuring several hundred millimetres. This rules out the use of standard soil testing equipment for testing wastes.

#### 2.4.10 Sampling

It is recognised that truly undisturbed samples of unconsolidated materials for laboratory tests are almost impossible to obtain (Bouwer, 1978) as the structure of the soil / waste may be inadvertently altered during sampling. This may arise from compaction or smearing of the sample surfaces or loss of fine particles on sampling may lead to an overestimation of hydraulic conductivity, possibly by an order of magnitude or more (Powrie, 1997). Soil structure and fabric (such as fissures and anisotropy) which contribute significantly to the bulk permeability of a medium may be destroyed during sampling and not replicated in the laboratory (Powrie, 1997, Barnes, 2000). In some media it is possible to preserve the structure of the sample by using a Shelby sampling tube. Samples are taken by pushing the tube into the soil stratum using a piston sampler (Appendix A, section A2). The sample is often retained in the tube for testing in the laboratory. However during sampling smearing of the sample, or gouging of the tube wall by particles may occur. Both can affect hydraulic conductivity measurements.

## 2.5 Anisotropic hydraulic conductivity in soils and wastes

In a true isotropic medium hydraulic conductivity will be the same in any direction of permeant flow. However the structure of most natural soil deposits and clastic sedimentary rocks is anisotropic and consequently hydraulic conductivity may differ according to direction of flow (Weeks, 1969, Craig, 1983).

Anisotropy in soils arises from the original deposition process in which laminar, plate-like or columnar particles<sup>1</sup> tend to be deposited in a horizontal direction. This results in a pattern of micropores or macropores with a distinctly directional bias (Hillel, 1980, Trautwein and Boutwell, 1994). As a result, flow pathways in the plane perpendicular to the bedding / compaction plane (usually in the vertical direction) are more tortuous and possibly less numerous than those parallel to the bedding / compaction plane (usually horizontal direction). Consequently most soils exhibit a higher horizontal than vertical hydraulic conductivity.

The presence of preferential horizontal hydraulic conductivity in soils has several practical implications in civil engineering. For example, horizontal flow characteristics are required for the estimation of the dissipation of excess porewater pressure (and therefore settlement) beneath a structure, assessing underflow beneath dams, and in the design of cut-off structures to inhibit seepage. It can also be important in the design of drainage projects (*e.g.* Maasland, 1957) and groundwater investigations (Weeks, 1969).

Investigations into soil anisotropy were being made as early as 1907 with publications on fluid flow through anisotropic media appearing in 1915 (Maasland, 1957). Despite this, relatively few systematic studies appear to have been carried out to evaluate the differences in directional hydraulic conductivity in soils (Beavis, 1985, Al-Tabbaa and Wood, 1987). As a general guide, the ratio of the difference between hydraulic conductivity in the horizontal and vertical planes (the  $k_h : k_v$  ratio) for clays and shales is given as being less than 3:1, but occasionally may be as high as about 10:1 (Price,

---

<sup>1</sup> For example kaolin and bentonite have plate like particles, attapulgite clay has needle shaped particles (Shackelford, 1994)

1985).  $k_h : k_v$  ratios of between two and ten (but possibly up to 100) have been given for stratified sands and silts (Cartwright and Hensel, 1995) and  $k_h : k_v$  ratios between five and ten for imbricated gravel deposits (in which particles are lying on their flat sides, tilting slightly upwards and overlapping orientated in the direction of flow) (Bouwer, 1978). More specific results from early studies are listed in Table 2.2, some indicating higher  $k_h : k_v$  ratios than indicated above.

Table 2.2. Results of early anisotropic hydraulic conductivity tests  
(from Maasland, 1957)

Date	Researcher(s)	Soil type	Reported $k_h : k_v$ ratio(s)	Comments
1937	Muskat	Sand	7.3 (max)	2/3 of 65 samples exhibited preferential horizontal hydraulic conductivity
1947	Aronovici	Not stated	3.0 (max)	preferential horizontal hydraulic conductivity in all 15 samples
1949	Gould	Clay	37.5 (ave)	one sample
1951	Hvorslev	Clay	41.6	same clay as above
1951	Reeve & Kirkham	Not stated	9 to 40	discrepancies between different laboratory and field methods used

More recently, a  $k_h : k_v$  ratio of 7 was reported for sand deposits by Bouwer (1970). This result was unexpectedly high as the particles were seemingly uniform, but were confirmed using a second independent method. Tests on Narrabeen Group sandstones indicated a preferential hydraulic conductivity in the plane parallel to bedding of about twenty times that normal to the bedding plane (Pless, 1975 - *unpublished work cited by Beavis, 1985*). The effect of particle orientation on hydraulic conductivity of kaolin was demonstrated by Al-Tabbaa and Wood (1987). Hydraulic conductivity tests on the clay in slurry with random particle orientation indicated similar hydraulic conductivity in all directions. Preferential hydraulic conductivity developed as the clay was consolidated, and was about three times that of the vertical hydraulic conductivity at an effective stress of 500 kPa.

An observation that may be relevant to some of the above anisotropic values is that in some tests the hydraulic conductivity in the horizontal direction, and hence the magnitude of anisotropy, may be underestimated if the sample size is too small (Agaki and Ishida, 1994).

The anisotropic ratios shown so far relate (as far as it is known) to anisotropy inherent in media arising from particle orientation. However micro-stratification of soils (the structure consisting of very thin alternating layers with differing hydraulic conductivities) can also be a cause of preferential hydraulic conductivity parallel to the bedding plane (Maasland, 1957). Root systems, worm holes or vertical shrinkage planes within a soil can have the opposite effect and may in some cases result overall in a higher vertical than horizontal hydraulic conductivity (Maasland, 1957, Talsma, 1960).

Stratification can also occur on a larger scale, resulting in anisotropic hydraulic conductivity values within a geological formation. Tests conducted by Weeks (1969) on a glacial outwash with strata consisting of varying degrees of silts and gravel produced  $k_h : k_v$  ratios ranging from 2 to 20. In a deposit consisting of an irregular succession of layers of sand, gravel and some clay material, Bouwer (1970) measured the horizontal hydraulic conductivity to be sixteen times that of the vertical. The presence of high permeability horizontal layers within geological formations can result in the overall horizontal hydraulic conductivity being several orders of magnitude higher than vertical hydraulic conductivity (Freeze and Cherry, 1979, Sarsby, 2000).

Stratification can also arise in man-made structures as a result of construction techniques; for example the formation of earth embankments and dams in mechanically compacted layers may produce a stratified structure with horizontal hydraulic conductivity typically being between five and ten times that of the vertical hydraulic conductivity (Smith, 1974). The same situation can arise during the emplacement of landfill waste, with each layer of waste being subject to compaction prior to the emplacement of the next layer (greater compaction occurring at the top of the each layer).

From the above it is apparent that stratification will be fundamental to fluid movement in a geological formation. This may also be present in landfill sites. Vertical flow may be impeded or essentially prevented by the inclusion of low permeability daily cover material within the waste body (this is usually a soil or clay layer added at the end of each working day to minimise rainfall infiltration / prevent waste being blown away). The resultant anisotropic structure is referred to by a number of authors such as: Bendz *et al.* (1997), Bleiker *et al.* (1993), Blight (1996), Burrows *et al.* (1997), Chen and Chynoweth (1995), Kjeldsen (1996), McCreanor and Reinhart (2000), Oweis *et al.* (1990) and Rowe and Nadarajah (1996), but no research appears to have been undertaken to assess the overall directional differences in hydraulic conductivity of landfill formations. McCreanor and Reinhart (2000) used a  $k_h : k_v$  ratio of 10 in modelling leachate movement in unsaturated anisotropic conditions and Rowe and Nadarajah (1996) used  $k_h : k_v$  ratios between 1 and 20 in analyses of leachate pumping wells. In both cases no explanation was given for the anisotropic ratios used and it is assumed that the ratios were arbitrary. This appears to be confirmed by McCreanor and Reinhart (2000) as they highlight the need for evaluation of landfill anisotropies.

Fluid movement in landfills may also be affected by high permeability layers such as gas collection layers within the waste body. The research in this thesis is therefore limited to anisotropy inherent in the waste structure rather than that arising from stratification within a landfill formation as each situation would require individual examination. Anisotropy may be inherent in the waste structure from the tendency of elongated components of the waste to be deposited in the horizontal plane during tipping. Further alignment in the horizontal plane may occur subsequently from compaction by landfill plant or the weight of overburden waste. The high content of impermeable plastic items in modern wastes, particularly plastic sheeting, is also likely to be a contributory factor. Compressible items (Figure 2.2), such as plastic bottles, will tend to be flattened in the horizontal plane (perpendicular to applied stress). The resultant structure can be compared to particle layering in anisotropic soils but on a larger scale. Potential permeant flow is likely to be greater in the horizontal rather than vertical direction due to horizontal flow pathways being more direct and possibly more numerous than those in the vertical direction.



Figure 2.2. Possible contributory factors of cross-anisotropy in municipal wastes.  
Plastic film (left) and compressible items (right)

References to anisotropy inherent in the waste structure are few and are largely based on observation. Landva and Clark (1990) observed that fibrous and elongated particles in waste were aligned at right angles to the direction of consolidation stress (ie. aligned horizontally). Shear strength was found to be at a minimum parallel to (or within 10°) of this plane. Horizontally layered structures have been evident in some compressed waste samples ejected from the Pitsea compression cell (Figure 2.3) described in chapter 3. Furthermore it has been observed that the horizontal plane appears to be structurally weaker than the vertical plane as drilling into the waste is noticeably easier along the horizontal plane and samples tend to shear along the horizontal plane during ejection from the cylinder. Bendz and Flyhammar (1999) referred to plastic sheet as being a significant factor in horizontal leachate flow in landfills. The structure of landfilled waste was conceptualised to predominantly consist of horizontal flow paths linked by short vertical flow paths. Blight (1996) (cited in Rosqvist, 1999) also identified plastic sheet as a major cause of lateral flow in a tracer test in municipal waste.

The only research directly evaluating the horizontal and vertical hydraulic conductivities of waste appears to be by Buchanan & Clark (1997, 2001) who measured  $k_h : k_v$  ratios on fresh processed waste fines (<38 mm) between 1.24 and 2.25 for sample dry densities of  $0.55 \text{ t/m}^3$  and  $0.40 \text{ t/m}^3$  respectively. In addition to the conclusion that there was little significant difference between the vertical and horizontal permeabilities, Buchanan & Clark concluded that the

$k_h : k_v$  ratio *decreased* with waste density and therefore greater preferential horizontal hydraulic conductivity could be expected near the top of a landfill.



Figure 2.3. Ejection of compressed waste sample from the Pitsea compression cell.

The validity of the above results is questionable on the following basis:

- the fines fraction used in the tests is not likely to be representative of most landfilled wastes (this is acknowledged by Buchanan & Clark). It is probable that a significant proportion of larger items (such as plastic bottles and plastic film) were removed from the sample thereby altering the anisotropic structure of the sample
- the tests were only carried out at low stresses. Comparison of the maximum dry density ( $0.55 \text{ t/m}^3$ ) attained by Buchanan & Clark with household waste density data by Beaven (2000) indicate that the equivalent applied stress was limited to about 40 kPa. This is equivalent to a burial depth of about only 4 metres. The results cannot be regarded as conclusive evidence of decreasing

$k_h : k_v$  ratios with waste density in landfills with depths of the order of several tens of metres

- the cubic sample measured only 20 x 20 x 20 cm. Although the sample size was in borderline accordance with ASTM guidelines for soil testing (section 2.4.9) it is possible that the sample was of insufficient size to obtain representative results

The only other reference quantifying waste anisotropy appears to be by Lofy (1996). This refers to gas migration in waste rather than liquid movement, but as Darcy's law is also valid for air at low pressure gradients (Maasland, 1957) it is possible that both liquid and gas movement can be similarly influenced by the waste structure. Jain *et al.* (2006) reported air permeability values in landfilled municipal waste to be three orders of magnitude greater than that of water). Gas migration in the vicinity of gas extraction wells was found to be greater in the horizontal plane than in the vertical by a ratio between 2 : 1 and 3.8 : 1.

## 2.6 Summary

It is evident from the literature reviewed in this chapter that the hydraulic conductivity of soils and wastes can be affected by several factors. The problems are compounded for testing of wastes due to their compressible nature and the accumulation of gas within the sample arising from degradation of organic components. It has been established that stress is the main controlling factor of hydraulic conductivity of wastes, but waste type/processing, temperature, water content, gas accumulation, pore water pressure heterogeneity and anisotropy also have to be considered. Large differences are apparent between published waste hydraulic conductivity values.

The existence of anisotropic hydraulic conductivity in soils due to particle orientation has been long established. The indications are that such inherent anisotropy (as distinct from anisotropy due to the inclusion of layers of other material of different permeability within a landfill) could also be present in wastes. With one limited exception no published research has been undertaken to evaluate this.

## 3. Test apparatus

### 3.1 Introduction

From the discussions in chapter 2 it was considered that the most important requirements for assessing the vertical and horizontal hydraulic conductivity of wastes for this research were that:

- samples needed to be of sufficient size in order to obtain representative results from heterogeneous wastes
- tests would have to be carried out at a range of stresses representative of different landfill depths. This was necessary as the hydraulic conductivity of wastes is largely determined by overburden stress (section 2.4.4). It is also possible that anisotropy would increase with depth (section 2.5)
- the conditions for both the vertical and the horizontal hydraulic conductivity tests had to be as similar as possible in order to avoid pore water pressure and gas accumulation (section 2.4.6 and 2.4.7) affecting the comparison of hydraulic conductivities between the two flow planes

- the same waste sample should be used for both the vertical and horizontal flow tests to avoid the  $k_h : k_v$  ratios assessments being affected by variations in hydrogeological properties of different waste samples or areas of waste. The test method should preferably not require disturbing the sample between vertical and horizontal flow tests

Several laboratory methods have been devised to assess hydraulic conductivity in soils, including some for assessing hydraulic conductivity in two planes (Appendix A).

However there are no standard methods for assessing waste hydraulic conductivity and conventional soil laboratory equipment is far too small for testing wastes. To avoid the costs and time involved in design and construction of purpose built laboratory equipment, it was decided to modify the existing Pitsea compression cell to perform the tests for the research described in this thesis.

### **3.2 The Pitsea compression cell**

In modified form, the Pitsea compression cell (Figure 3.1) fulfilled the requirements listed at the start of this chapter within reasonable costs and timescales. This unique facility is owned by the University of Southampton and based at (then Cleanaway Ltd, now Veolia Environmental Services) landfill site at Pitsea, Essex, England. Built in 1989, it has been extensively used for assessing the hydrogeological properties of waste and tyre samples (Beaven 2000, Hudson *et al.* 2002, 2004) at a range of typical landfill overburden stresses.

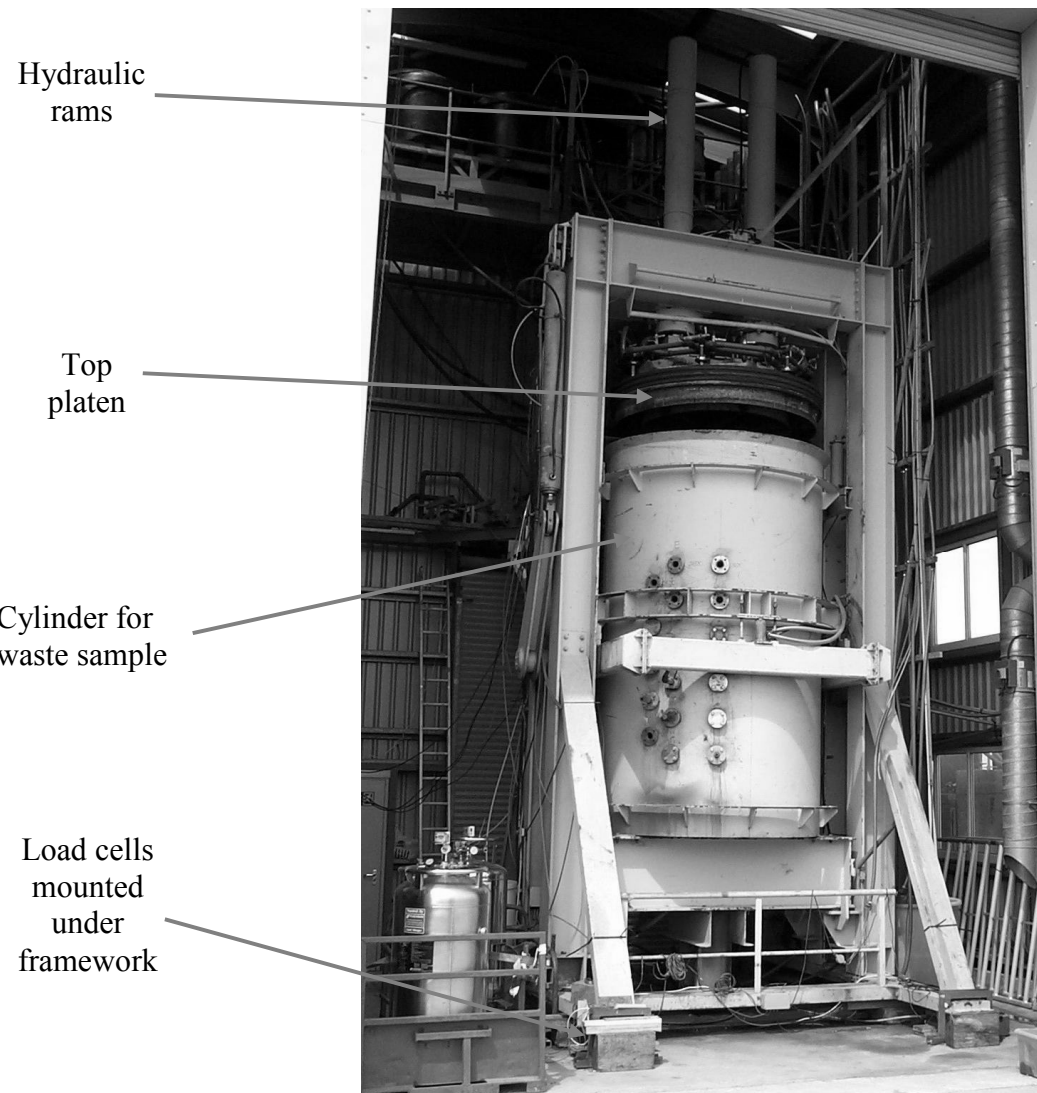


Figure 3.1. Pitsea compression cell

The compression cell cylinder and base (bottom platen) accommodates a sample of 2 metres in diameter with an initial uncompressed height of approximately 2.5 metres. During testing the compression cell cylinder is vertical but can be rotated using hydraulic cylinders and jacks to any position between vertical and horizontal to facilitate loading or unloading of the sample (section 5.2). The cylinder is mounted within a framework measuring approximately 8 metres high with a base of 4 metres x 3 metres. The framework rests on four load cells for monitoring the sample weight. These are sufficiently sensitive to record the volumes of leachate added or drained from the sample to the nearest 5 litres.

After loading (section 5.2), the top platen is lowered onto the sample. Sample compression is achieved by adjusting the pressure in the hydraulic rams attached to the top platen. Settlement, density, drainable porosity and hydraulic conductivity are evaluated at each compression stage as described in the following chapters. A detailed description of the compression cell in its original form is given by Beaven (2000). A general cross section diagram of the compression cell test arrangement is shown in Figures 7.1 (vertical flow) and 8.1 (horizontal flow)

The Pitsea compression cell was designed for vertical flow tests only. In order to induce horizontal flow across samples it was necessary to undertake modifications to:

- seal the sample in the cylinder
- allow a horizontal flow of leachate to be introduced across the sample through one side of the cylinder wall and discharged diametrically opposite
- measure the horizontal flow rate
- measure the piezometric heads at various locations in the sample

The required modifications are described in the following sections (3.3 to 3.5). A later modification to provide a range of inlet and outlet pressure heads is described in section 7.2.

### **3.3 Modifications required to seal samples in the compression cell cylinder**

In the existing compression cell arrangement the join between the base and cylinder was sealed during testing using an inflatable seal, but a join existed between the cylinder and top platen periphery with a clearance gap of about 10 mm. To allow horizontal flow tests to be run it was necessary to seal this gap to prevent leachate flowing out from the top of the sample.

The arrangement used to seal the join between the cylinder and top platen is shown in Figure 3.2. This comprised a stack of three 2 m (nominal) diameter inflatable seals located on a welded steel ring with 40 mm x 40 mm peripheral grooves. Three seals were required to ensure that, regardless of top platen position, at least one seal could be inflated without being breached by one or more of the ports in the cylinder wall. The seals could only be inflated when the top platen was static as there was a risk of puncturing the seals or dislocating them if the top platen was moved with the seals inflated. During sample compression they remained uninflated. When the final compressed position was reached, one or more of the seals that were not aligned with a port in the cylinder wall were inflated.



Figure 3.2. Top platen showing the stack of three inflatable seals added to allow horizontal flow tests to be carried out

After tests were completed at a given compression stage the seals were deflated before the top platen was moved. On deflation the seals would shrink back into their location grooves allowing the top platen to be moved without risk of damaging or dislocating the seals.

In service the design worked satisfactorily. It was found that greasing the seals assisted sealing and also helped reduce rusting of the grooves and cylinder wall. A

portable compressor was purchased for inflating the seals. Fitting the valves on long rubber tube extensions (visible in Figure 3.2) assisted inflation when the top platen was inside the cylinder wall. Seals were prone to damage and occasionally had to be replaced. This involved raising the platen to the position shown in Figure 3.2. Some problems were encountered with replacement seals due to a change in the rubber compound used by the manufacturer. This affected the fit of the seals on the grooves and required some trials before a satisfactory elastic fit was obtained.

### **3.4 Modifications required to provide a horizontal leachate flow across a sample in the compression cell cylinder**

A method of introducing a flow of leachate across the sample was required. Ideally two vertical slots positioned diametrically opposite in the cylinder wall would have been made to admit and discharge horizontal flow, but this would have structurally weakened the cylinder and created potential short-circuit routes for leachate during vertical flow tests. Instead two sets of diametrically opposite ports were added to the cylinder wall, effectively creating a large scale version of the Modified Shelby tube (Appendix A, section 1.3, Agaki and Ishida, 1994).

The new ports added were of similar design to the existing ‘A’ and ‘B’ sets of ports (used for installing piezometer tubes to measure the piezometric heads within the samples) with an effective port diameter of 72 mm (the method used for determining the size and number of ports is described in Appendix B). Flanges were made from stainless steel to prevent rusting from contact with leachate. The new sets were designated ‘D’ (inlet) and ‘E’ (outlet) ports. A further column of ports (‘C’ ports) was added to monitor the pore water pressure in the vicinity of the outlet ports (Figure 3.3). The ‘D’ and ‘E’ horizontal flow ports were each offset in two columns (by 200 mm) as arranging all the ports in a single column may have weakened the cylinder. Most ports had a vertical spacing of 150mm but some irregular spacing was necessary around the strengthening ring and framework at approximately mid-height of the cylinder.

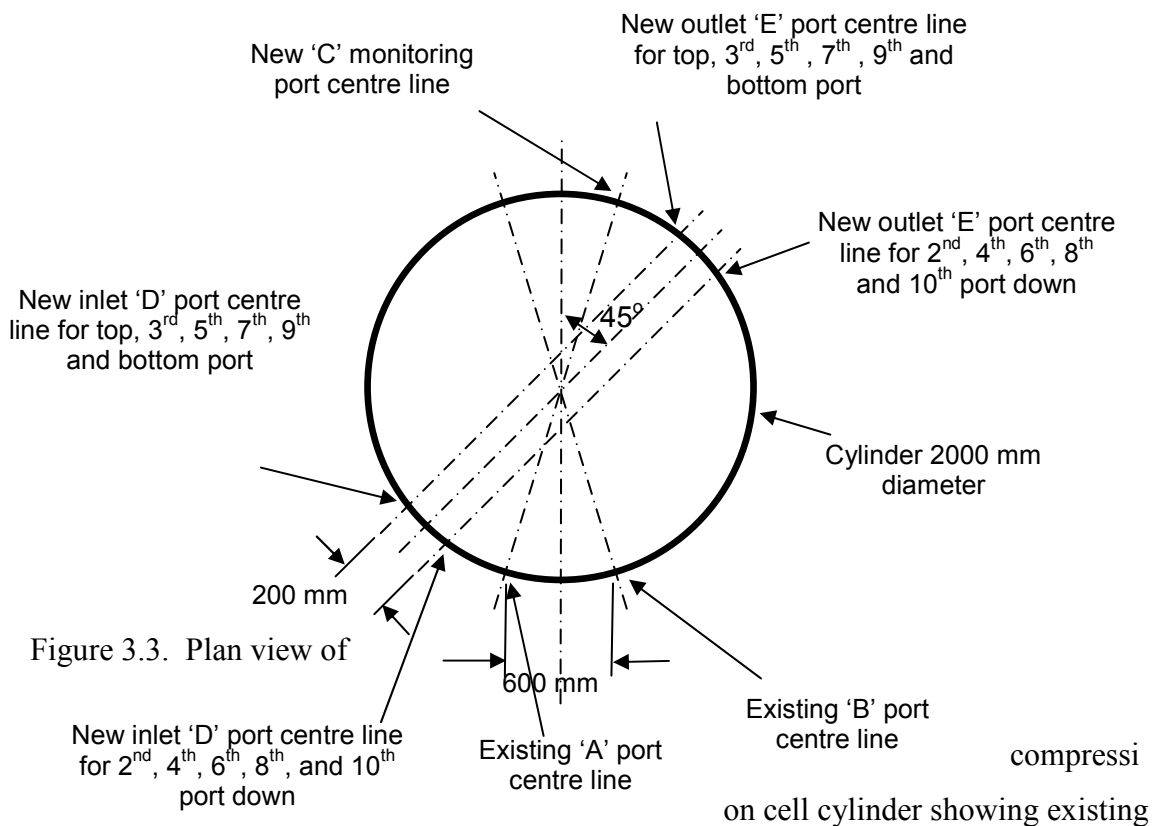


Figure 3.4. Close up view of horizontal flow outlet 'E' ports (two columns on left), and piezometer monitoring 'C' ports (right) for the outlet region

Ports not required during testing could be isolated either with a blanking plate or a valve. All horizontal flow ports were isolated during vertical flow tests. The vertical

flow was unaffected due to the relatively small area occupied by the ports (designs utilising large port areas or vertical slots in the cell wall introduce the possibility of vertical preferential flow paths). Thus the design fulfilled the requirement listed at the start of this chapter of being able to conduct hydraulic conductivity tests without replacing or modifying the sample between vertical and horizontal flow tests. This could not only result in errors in the overall  $k_h : k_v$  assessments but the additional loading and unloading of samples would have resulted in increased cost and time for the project.

### 3.5 Horizontal flow header tanks

In order to assess the horizontal hydraulic conductivity during tests it was necessary to measure both the inflow and outflow rates through each of the horizontal flow ports. This was relatively straightforward for the outlet ports as the outflows could be directed into a graduated containers and the volumes measured over time. Measuring inlet flow rates using flow meters for each port for the range of expected flow would have been prohibitively expensive (and not possible for extremely low flows). Instead eleven separate graduated clear perspex header tanks were mounted at height (about 9 m above ground level) (Figure 3.5) with a hose connection from each tank to a dedicated port (shown on Figure 8.1). The leachate common supply for the tanks was from the existing main header tanks with leachate levels maintained at a constant level by the header tank overflow, thus giving a constant pressure supply to each horizontal flow port.

The method for measuring flow rates through the horizontal flow ports using the header tanks is given in section 8.2. In brief, once stabilised conditions were established during tests, valves were used to cut off the inflow to the tanks, and the drop in water level in each tank was timed to obtain the flow rate through the port to which each tank is connected. When measurements were complete, the inlet valves were re-opened and the process repeated if required.



Figure 3.5. Individual Perspex header tanks (left background) for leachate supply for horizontal flow connected to main header tanks (right foreground)

### 3.6 Summary

The apparatus chosen for the research, the modified Pitsea compression cell, represented a viable method for assessing the vertical and horizontal hydraulic conductivities of wastes within the required time-span and cost of the project. In modified form it fulfilled the main requirements of testing samples of representative size at a range of applied stresses without the need to modify samples between tests.

Modifications were required to the compression cell to seal samples in the cylinder and induce and monitor horizontal flow across samples.

## 4. Samples tested

### 4.1 Waste sample analysis

Two different waste samples were tested. The first set of tests were carried out on a 20 year old degraded household waste (denoted AG2), excavated from Rainham landfill site, Essex. The second set of tests were on a recent Dano-processed household waste denoted DN1 (the Dano process is described below).

Categorisation and analysis of the samples was undertaken by M.E.L. Research, Birmingham on six sub-samples obtained using coning and quartering (Vesilind *et al.*, 2002) 500 kg samples of each waste. The moisture content was determined from the loss in weight of samples dried at 105 °C as below:

$$MC_{wet} = \frac{w - d}{w} \times 100 \quad (4.1)$$

where:

$MC_{wet}$  = moisture content on a wet basis (see section 4.5)

$w$  = initial (wet) weight of the sample

$d$  = final (dry) weight of the sample

(Vesilind *et al.*, 2002)

The particle size, category and water content analyses for AG2 are shown in Table 4.1. A large proportion (68% by weight) of the sample consisted of fines and this may have been due to the possible inclusion of soil in the sample. Paper/cardboard content was low (0.9% by weight compared to about 40% weight of typical 1980's and 1990's UK household wastes – Sarsby, 2000) possibly due to degradation.

Table 4.1 Size and category analysis of waste AG2

CATEGORY ASSAY%												
Size mm	Weight %	Paper cardb'd	Plastic film	Dense Plastic	Tex-tiles	Mc	Mnc	Glass	Fe	nFe	Soil	<10 Mm
120-80	3.1	-	4.5	4.7	1.5	21.2	0.3	-	55.8	-	12.0	-
80-40	11.1	5.7	7.5	3.1	5.5	24.1	15.7	3.4	30.6	0.4	4.0	-
40-20	11.3	2.6	9.6	4.9	4.0	29.7	26.7	7.4	10.3	-	5.0	-
20-10	6.5	-	4.1	5.2	-	12.4	58.8	15.5	4.1	-	-	-
<10	68.0	-	-	-	-	-	-	-	-	-	-	100
Total	100.0	0.9	2.3	1.4	1.1	7.5	8.6	2.2	6.6	0.1	1.4	68.0
Water content ( $W_{Cwet}$ ) of refuse = 40.1% Density as delivered = 0.58 t/m <sup>3</sup>												

Mc = Miscellaneous combustibles

Fe = Ferrous metal

Mnc = Misc. non combustibles

nFe = Non ferrous metal

The particle size, category and water content analyses for Dano treated sample DN1 are shown in Table 4.2.

Table 4.2 Size and category analysis of waste DN1

CATEGORY ASSAY%												
Size mm	Weight %	Paper/ cardb'd	P'stc film	Dense plastic	Tex-tiles	Mc	Mnc	Glass	Fe	nFe	Putres-cible	< 10mm
165+	9.1	70.7	10.1	5.1	9.1	-	-	3.0	1.5	0.5	-	-
165-80	39.4	62.1	12.3	8.9	4.5	6.6	0.1	0.6	3.4	0.9	0.7	-
80-40	16.4	49.0	9.8	5.8	3.2	11.7	5.6	7.1	3.7	1.8	2.3	-
40-20	8.2	36.2	5.8	4.2	2.1	4.9	6.1	26.2	1.3	0.9	12.4	-
20-10	2.1	16.7	-	-	8.3	-	25.0	33.3	-	-	16.7	-
<10	24.7	-	-	-	-	-	-	-	-	-	-	100
Total	100.0	42.3	7.9	5.3	3.5	4.9	2.0	4.5	2.2	0.8	2.0	24.7
Water content ( $W_{Cwet}$ ) of refuse = 32.5% Density as delivered = 0.40 t/m <sup>3</sup>												

Mc = Miscellaneous combustibles

Fe = Ferrous metal

Mnc = Misc. non combustibles

nFe = Non ferrous metal

In the Dano process (Motherwell Bridge Envirotec, 1998), fresh waste is fed into a rotating cylinder (25 m long x 3.7 m diameter). Water is added (approximately 200 litres per tonne) to soften paper and vegetable matter in the waste. The organic fraction is pulverised into a relatively homogeneous biomass by the tumbling action of the rotating cylinder, assisted by hard materials in the waste and steel spikes inside the drum. The inert fraction is largely unaffected but steel cans are removed from the waste using an electro-magnetic drum.

As delivered sample DN1 was less dense ( $0.40 \text{ t/m}^3$ ) than AG2 ( $0.58 \text{ t/m}^3$ ). Such differences in density were evident throughout subsequent compression stages (chapter 5) indicating that this was not just a result of the higher initial water content of AG2. The paper/cardboard content in sample DN1 was much higher (42.3%) than in AG2 (0.9%). The recorded putrescible waste content of DN1 was low for a recent household sample as the estimated putrescible content of current UK household waste is approximately 17% (Sarsby, 2000) to 23% (Barry *et al.*, 2001). It is possible that putrescible material may have been rendered unrecognisable by processing and categorised as fines or combustible material. Plastic film was visually prominent in sample DN1 and accounted for 7.9% of the weight.

The maximum particle size in sample AG2 was 120 mm. Larger items were present in sample DN1 with 9% (by weight) of the sample consisting of items larger than 165 mm. For a typical compression cell sample size of 2 metres diameter and similar height<sup>2</sup>, sample AG2 conformed with the ASTM recommended 6 : 1 ratio of maximum particle dimension to minimum sample dimension referred to in section 2.4.9 (Daniel, 1994). The maximum particle size of sample DN1 was not recorded, but would need to have exceeded 330 mm to breach the ASTM recommendations.

---

<sup>2</sup> Initial sample height was about 2.5 m – this reduced after the sample was compressed

## 4.2 Discussion

The research was limited to the testing of household wastes (*i.e.* waste collected from domestic sources). Time restricted testing to the two samples described above. These were selected to investigate if the  $k_h : k_v$  ratios of typical fresh and degraded household wastes differed significantly.

Ideally testing would have been undertaken on other household wastes with a different range of particle shape and size as these may exhibit different anisotropic values. A highly processed wastes such as relatively fine biodegraded mechanical-biological treated wastes (MBT) may have provided interesting comparative results, although at the time (1998) when the tests were being considered widespread adoption of the costly MBT process appeared unlikely in the UK. Recently several trial MBT plants have been commissioned in the UK and testing of such waste would now be a higher priority. In contrast, fresh unprocessed household wastes may exhibit high  $k_h : k_v$  ratios due to the high content of largely intact but compressed plastic bags / bin liners that are likely to impede vertical rather than horizontal flow. This type of waste is now a diminishing stream due to the increased recycling and processing of wastes.

It can be concluded that the waste types chosen for the research are probably broadly representative of most UK household waste streams providing they are not highly processed or coarse unprocessed wastes mentioned above.

## 5. Sample loading, compression, water content and density

### 5.1 Introduction

As discussed in section 2.4.4, stress is the main factor controlling the hydraulic conductivity of household wastes. The overburden stress acting on landfill waste at depth is replicated in the Pitsea compression cell by applying a compressive load, referred to as applied stress, to the samples. This is performed in several stages. At each compression stage the hydrogeological properties of the sample are determined (chapters 6 – 8) in order to evaluate changes in these properties throughout the depth of a landfill.

In this chapter the sample loading (section 5.2) and compression (section 5.3) methodologies are described, and the settlement results for the two samples tested are given for each compression stage. The terms water content (section 5.4) and density are defined (section 5.5.1) and the results presented. The compression and density values for the two samples tested are compared with those for other wastes (section 5.5.2). Potential errors such as the effects of sidewall friction are discussed.

## 5.2 Sample loading

### 5.2.1 Methodology

All tests were carried out in the Pitsea compression cell described in chapter 3. Prior to loading the compression cell sides and base were cleaned. Grease was liberally applied to the inside walls of the cylinder to prevent rusting and possibly reduce sidewall friction during sample compression. The bottom platen of the compression cell was bolted in position and the O-ring type seal inflated to create a watertight joint between the platen and cylinder wall.

A layer of gravel (particle size 10 to 20 mm) was installed at the bottom of the cylinder and raked level (Figure 5.1). The purpose of the gravel was to evenly distribute inflowing leachate across the sample (introduced through twelve holes in the bottom platen) during the following drainable porosity and hydraulic conductivity tests (chapters 6 and 7). The gravel was usually temporarily flooded before the waste sample was loaded to measure the drainable porosity of the layer - flow meter counters and / or the load cells were used to measure the amount of water admitted. The surface of the water also provided a useful guide for levelling the gravel layer. The thickness of the gravel layer was less than the 150 mm height of the dividing ring (shown on Figure 5.1 and 5.5) on the bottom platen to allow the ring to penetrate into the base of the waste sample. The same arrangement was used for the top gravel layer and top platen dividing ring. In vertical flow tests this permitted leachate flow rates through the inner core of the waste to be measured independently to that through the outer region. Comparison of these flow rates was used to assess if peripheral flow was occurring between the periphery of the waste and cylinder wall (section 7.3).



Figure 5.1 Gravel layer installed at the base of the compression cell ready for waste sample to be loaded. The tube on the left hand side of the photo is the extensometer tube for mounting magnets to assess differential settlement

Waste samples were loaded into the cylinder using a lorry-mounted hydraulic grab (Figure 5.2). The cylinder was tilted approximately 30° from the vertical position to provide sufficient clearance for the grab during loading and yet prevent the bottom gravel layer shifting. After each loading (of approximately 30 to 50 cm depth of waste) the cylinder was returned to the vertical position and the waste raked level. During loading, records were made of the sample depth and weight indicated by the load cells (the load cells had a resolution of 5 kg) under the compression cell framework.



Figure 5.2 Sample loading using grab lorry

Total earth pressure cells were installed in the sample (Figure 5.3). These were vibrating wire type cells manufactured by Soil Instruments and were calibrated by the manufacturer before installation. The purpose of these pressure cells was to measure the transmitted vertical stress at various depths in the sample as some reduction in stress (and compression) with sample depth was expected during compression due to friction between the sample and cylinder wall. In sample AG2 pressure cells were positioned at the top, mid-height and base of the sample. This was revised for sample DN1 to two pressure cells only, installed at the base of the sample. The pressure cells were packed in sand (if within the gravel layer) or vermiculite (if within the waste sample) to avoid direct contact with waste or gravel which may have affected readings.

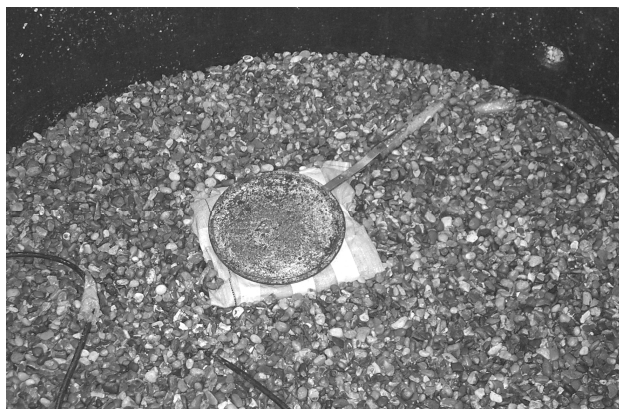


Figure 5.3. Pressure cell positioned on top of bottom gravel layer

For sample DN1, a magnetic extensometer tube (Soil Instruments) was mounted vertically throughout the depth of the sample (Figure 5.1). The vertical positions of sliding ring-magnets spaced on this tube (Figure 5.5) were located with an extensometer inserted in the tube, allowing settlement to be monitored throughout the sample depth (in addition to total settlement measured by the staff on the top platen – section 5.3.1).

The top gravel layer (6 to 7 cm thick) was installed on top of the sample and raked level (Figure 5.4). The sample was allowed to settle overnight and the settled sample depth recorded prior to testing. A diagrammatic view of a waste sample installed in the compression cell is shown in Figure 5.5.



Figure 5.4. Top gravel layer installed prior to lowering the top platen

### 5.2.2 Discussion

In section 2.4.10 it was observed that soil test results can be erroneous if the structure of the sample is not preserved during sampling. The situation may not be so critical for testing fresh wastes as they are artificially laid rather than occurring from natural processes. The method used of releasing large grab loads of waste into the compression cell cylinder is considered to reasonably replicate the process of waste being deposited off the back of a lorry. Raking the waste level at regular intervals during loading should have minimised ‘edge effects’ near the cylinder wall. However it is difficult to prove or disprove whether a true landfilled waste structure (which may vary from site to site) has been achieved.

The structure of the aged waste is probably more difficult to reproduce as during degradation it would have undergone a degree of natural settlement. The resultant structure would have been totally destroyed during excavation. There is uncertainty whether recompressing a degraded waste (as performed for these tests) would have given a reasonable replication of the original structure. An alternative method of

sampling is suggested in section 8.7.2, but there was insufficient time and funding for this to be used for this research.

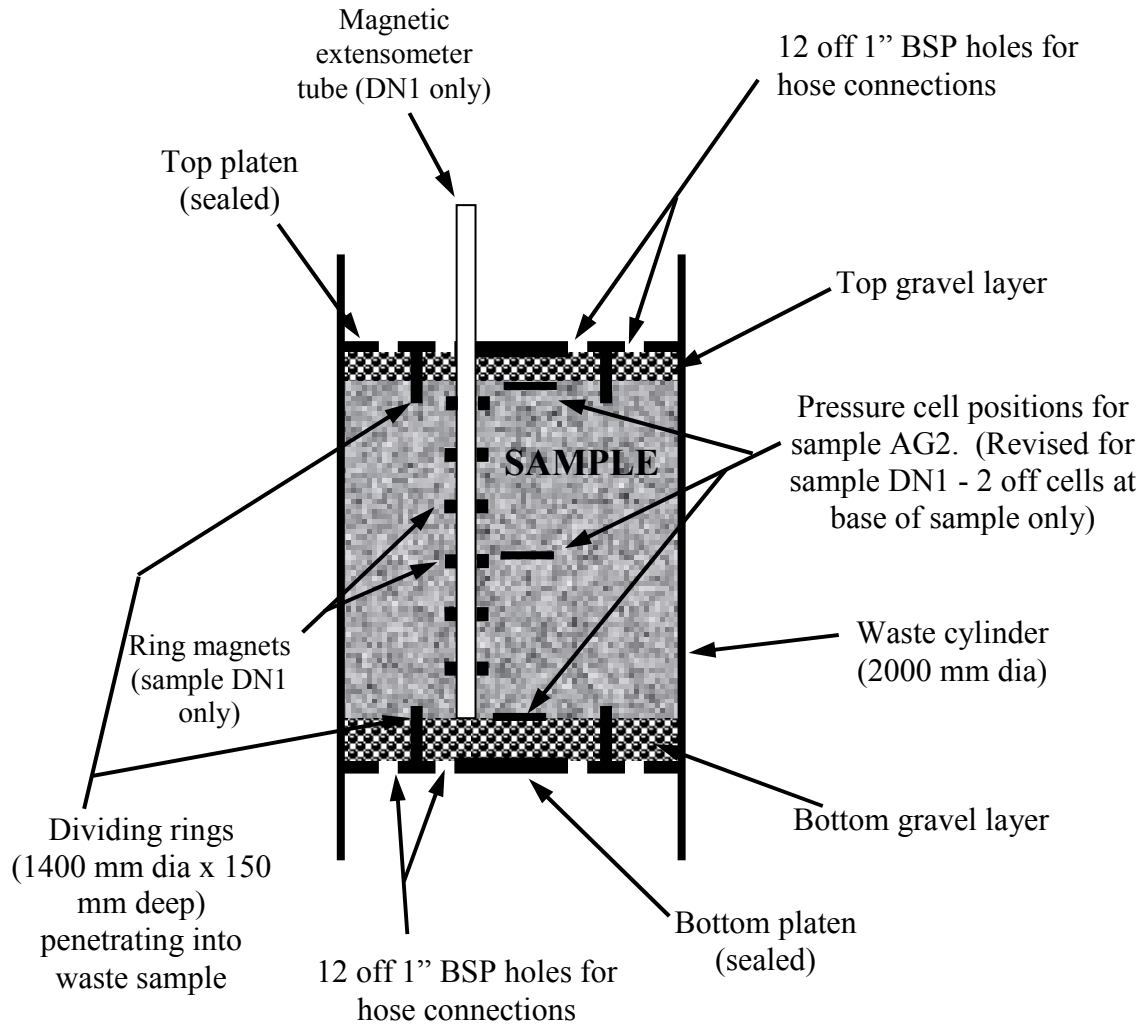


Figure 5.5. Schematic cross-section of sample and gravel layer arrangement in the compression cell

## 5.3 Sample compression

### 5.3.1 Compression methodology

After loading, the first compression stage was carried out by lightly compressing samples (applied stress of 40 kPa) to simulate overburden stress at shallow landfill depths (approximately 4 m unless subjected to additional compression by plant equipment). This was achieved by increasing the hydraulic pressure in the rams connected to the top platen (Figure 3.1) - the relationship between the hydraulic pressure in the rams and applied stress is shown in Appendix C. Sample compression throughout each compression stage was monitored by the movement of a graduated staff bolted to the top platen (shown in Figure 5.6) relative to a fixed pointer on the framework. For practical purposes, compression was considered complete when the rate of change of sample depth had fallen to less than 1% in 24 hours. After compression had effectively ceased, drainable porosity (chapter 6) and hydraulic conductivity (chapters 7 and 8) were assessed.

Following completion of tests at the first compression stage, applied stress was then increased (to replicate the overburden stress at greater burial depth) and the test procedure repeated. The applied stress was increased in five stages to 40, 87, 165, 322 and 603 kPa for sample AG2. Six compression stages of 40, 87, 134, 228, 334 and 603 kPa were used for sample DN1 in order to obtain more data at mid-range stresses. The maximum applied stress of 603 kPa represents an approximate landfill depth of 60 metres (based on a waste density of 1 tonne/m<sup>3</sup>).

Compression was completed normally within a week. However it was found that further compression could occur during subsequent testing. This was particularly evident after leachate was introduced into the sample (this occurred over a relatively short time period and so is thought to be due to a reduction in inter-particle friction rather than decomposition of the sample). Consequently conditions for drainable porosity and hydraulic conductivity tests were inconsistent and there was also a risk of dislocation of the top platen seals (sections 3.3). For these reasons, further top platen movement was prevented during tests on sample DN1 by reducing the applied stress to

a level that ensured no further compression. Acrow props were then inserted between the top platen and compression cell framework (Figure 5.7) to prevent any upward movement of the top platen from elastic recovery of the sample.

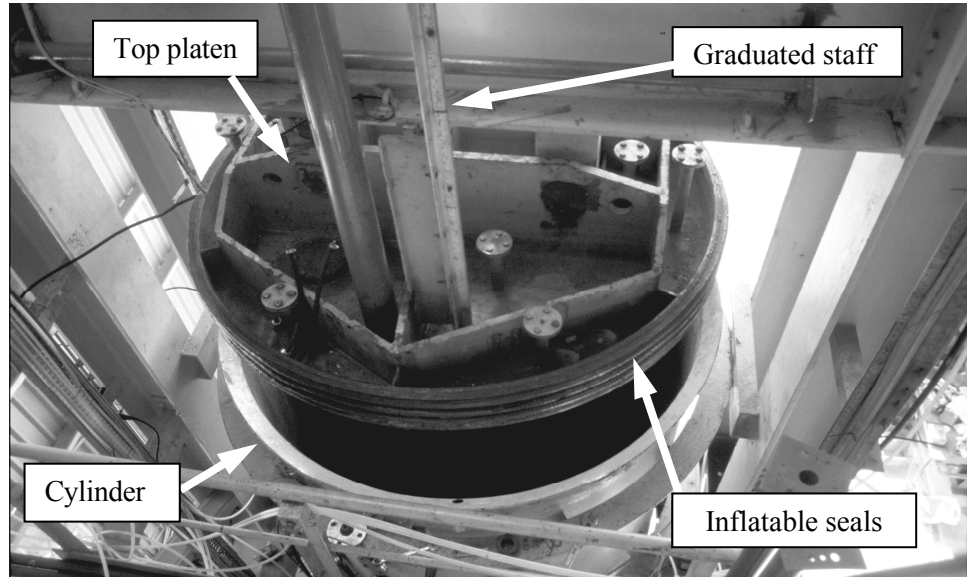


Figure 5.6. Top platen in raised position showing graduated staff

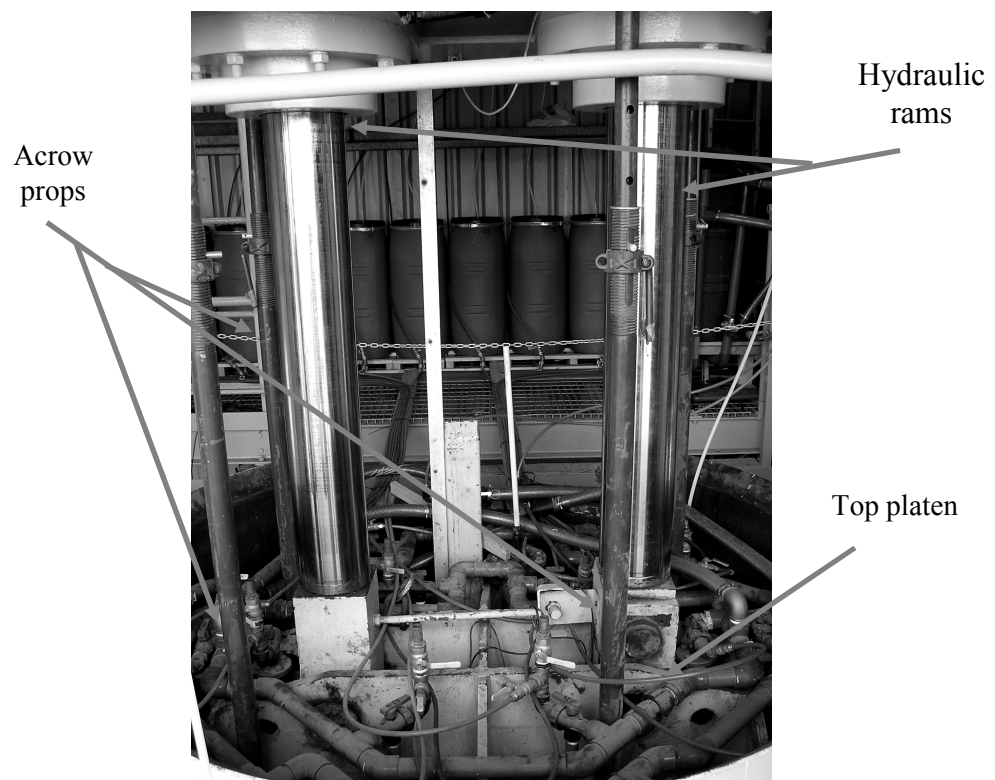


Figure 5.7 Acrow props for preventing upward movement of top platen

### 5.3.2 Compression results and discussion

Tables 5.1 and 5.2 respectively show the amount of compression of samples AG2 and DN1 at each compression stage. In Table 5.1 a separate entry is made for additional settlement of sample AG2 during “wet” testing mentioned above.

Table 5.1 Sample AG2 compression

Applied stress (kPa)	0	40	87	165	322	603
<b>After completion of compression stage</b>						
Sample height (mm)	2329	2037	1818	1654	1491	1377
% of original sample height	100%	87.5%	78.1%	71.0%	64.0%	59.1%
<b>after completion of wet testing</b>						
Sample height (mm)	-	1945	1778	1623	1480	1372
% of original sample height		83.5%	76.3%	69.7%	63.5%	58.9%

Table 5.2 Sample DN1 compression

Applied stress (kPa)	0	40	87	134	228	334	603
Sample height (mm)	2239	1663	1437	1313	1120	1029	933
% of original sample height	100%	74.3%	64.2%	58.6%	50.0%	46.0%	41.7%

The results show that sample AG2 was less compressible than DN1 (AG2 compressed to 59 % of the original sample height at an applied stress of 603 kPa whereas DN1 compressed to just under 42 % of original height at 603 kPa). The comparatively low

compressibility of AG2 was probably due to it having previously undergone secondary settlement during degradation.

In Tables 5.1 and 5.2, applied stresses are shown. Additional stress may arise from the self-weight of the sample. This would be negligible at the top of the waste (the top gravel layer exerts a stress of approximately 1 kPa on the sample) but could increase with sample depth to typically between 10 and 20 kPa at the base of the sample (Table 5.3 and 5.4). This could result in an increase of sample density and therefore a decrease in drainable porosity and hydraulic conductivity throughout sample - particularly at low applied stress as the stress exerted by the weight of the sample is significant in comparison with applied stress.

However the weight induced stress may be partly compensated by, or exceeded by, stress transmission losses arising from friction between the sample and the cylinder sidewall. The problem of transmission losses is more likely to increase with sample depth and so is a particular problem when testing deep samples. For this reason sample height (length) to diameter ratios of 0.25 or less are recommended for permeameters with loading pistons for testing soil samples (Daniel, 1994). The height to diameter ratio of uncompressed samples in the Pitsea compression cell exceeds 1.0 and is therefore much higher than that recommended for soil permeameters.

Consequently stress transmission losses could potentially be significant. However these are difficult to assess with certainty. Beaven (2000) stated that the magnitude of stress loss is dependent on the sample depth, the friction angle ( $\delta$ ) between the sample and cylinder wall and the internal friction angle ( $\phi'$ ). The sidewall friction angle for loose household waste against a smooth steel surface was estimated by Beaven (2000) to be about  $25^\circ$ . Estimates for the internal friction angle of wastes vary between  $20^\circ$  and  $40^\circ$  (Jessberger and Kockel, 1991). Lower values may be expected in decomposed wastes or wastes with high water contents. Higher internal friction angles are likely to occur in waste subjected to high strains. The range of possible values is limited by the sidewall friction angle being less than the internal friction angle of the waste and from this and the above estimated sidewall friction angle and range of internal friction angles, the maximum theoretical stress transmission losses at the base of samples in the compression cell can be calculated (Beaven, 2000). According to these calculations the

stress loss at the base of the sample of samples AG2 and DN1, could exceed 50 %. Stress transmission losses of similar magnitude (up to 60 %) have been recorded at the base of compressible tyre shred samples in smaller scale (300 mm diameter) permeameters (Benson *et al.*, 2002, Warith *et al.*, 2004) of similar height : diameter ratios to the Pitsea compression cell. Stress losses of this magnitude would be likely to have a significantly effect on density and hydraulic properties throughout the depth of the sample.

However it is possible that actual stress transmission losses may be significantly less than the theoretical maximum. Several methods were adopted in order to evaluate stress transmissions losses for the two samples tested. These were:

- the use of pressure cells installed in the waste sample (section 5.2) to directly measure transmitted stress – these failed to give reliable data
- the installation of a magnetic extensometer (section 5.2) in sample DN1 to directly measure differential settlement throughout the depth of the sample
- the use of drainable porosity data to detect changes in porosity throughout sample depth
- the examination of hydraulic conductivity data throughout sample depth

The drainable porosity data for both samples (the plots are shown in Appendix D, section D4) were fairly consistent throughout sample depth at all compression stages. Within the data variations present in the plots, it was possible to conclude that stress transmission losses were significantly less than the theoretical maximum (in excess of 50% - above). The minimum stresses at the base of the samples according to the drainable porosity data are shown in Figure 5.3 and 5.4. It is probable that stress transmission losses are much less and possibly negligible. This is largely supported by the magnetic extensometer data (Appendix D, section D3) which mainly indicates uniform compression and the hydraulic conductivity data (section 7.4) which although is not consistent sample depth, does not indicate overall that hydraulic conductivity is

lower at the top of the samples (as would be expected if samples were preferentially compressed). However this cannot be stated categorically as all methods exhibit some inconsistencies. Consequently minimum and maximum error bars are shown in the presentation of hydraulic conductivity measurements in Figures 7.12.

Table 5.3 Range of possible stresses transmitted to the base of sample AG2

Applied stress (kPa)	0	40	87	165	322	603
Sample height (mm) drained	2329	2037	1818	1654	1491	1377
Stress due to weight of sample (assuming no frictional losses)	20.8	21.8	21.6	20.8	19.6	19.2
<b>Maximum stress at base of sample (applied + sample weight stress) kPa</b>	<b>21</b>	<b>62</b>	<b>109</b>	<b>186</b>	<b>342</b>	<b>622</b>
<b>Minimum stress at base of sample (from drainable porosity data) kPa</b>	-	<b>28</b>	<b>68</b>	<b>131</b>	<b>232</b>	<b>435</b>

Table 5.4. Range of possible stresses transmitted to the base of sample DN1

Applied stress (kPa)	0	40	87	134	228	334	603
Sample height (mm) drained	2239	1663	1437	1313	1120	1029	933
Stress due to weight of sample (assuming no frictional losses)	8.8	14.2	13.5	13.1	11.4	11.2	10.2
<b>Maximum stress at base of sample (applied + sample weight stress) kPa</b>	<b>8.8</b>	<b>54</b>	<b>100.5</b>	<b>147</b>	<b>239</b>	<b>345</b>	<b>613</b>
<b>Minimum stress at base of sample (from drainable porosity data) kPa</b>	-	<b>22</b>	<b>66</b>	<b>107</b>	<b>177</b>	<b>270</b>	<b>490</b>

It should be noted that the sample compression is essentially primary; the duration of each compression stage (about one week) is insufficient to take into account of 'secondary compression' arising from waste degradation. Prolonged measurements of waste settlement have shown (e.g. Sarsby, 2000, Watts *et al.*, 2001, 2002, 2006) that secondary compression, although of a much smaller magnitude than primary compression, will continue on a timescale lasting several months and possibly years (and therefore is impractical to replicate in these tests). This may be of little consequence for the aged AG2 waste sample as it would already have undergone secondary settlement, but in the field situation fresh waste would be expected to undergo further settlement.

## 5.4 Water content

### 5.4.1 Methodology to assess water content

The dry mass of each sample was calculated from the initial mass of the sample (measured by the load cells) minus the weight of water in the sample (calculated from the initial water contents shown in Tables 4.1 and 4.2). Subsequent changes in water content during testing were deduced from the change in total sample weight (the dry

weight was assumed to remain unchanged) indicated by the load cell readings. These readings were compensated to account for the increased weight of oil arising from extension of the top platen cylinders during sample compression (Appendix C).

There are two ways normally used to express water content. In soil mechanics the water content is defined as the ratio of mass of water ( $M_W$ ) to the dry sample mass ( $M_S$ ). Following the notation used by Beaven (2000), this is designated as  $WC_{dry}$ :

$$WC_{dry} = \frac{M_W}{M_S} \quad (5.1)$$

In landfill science the water content is expressed as the ratio of the mass of water ( $M_W$ ) to the total mass of water and solids ( $M_W + M_S$ ). This is designated  $WC_{wet}$ :

$$WC_{wet} = \frac{M_W}{M_W + M_S} \quad (5.2)$$

The relationship between the two expressions is:

$$WC_{dry} = \frac{WC_{wet}}{1 - WC_{wet}} \quad (5.3)$$

$$WC_{wet} = \frac{WC_{dry}}{1 + WC_{dry}} \quad (5.4)$$

During tests the water content of a sample was dependent on the condition of the sample which could be either drained, at field capacity or saturated. When stating the water content the prevailing condition should be specified (as in Table 5.5). However it is unlikely that fully saturated conditions were ever achieved due to residual gas in the waste (as mentioned in section 2.4.6 and discussed further in Chapter 6 and 7) and the term ‘nominally saturated’ is used in this thesis. The term ‘gas accumulated conditions’ is used to describe partly saturated samples in which gas had been allowed to accumulate to what appeared to be a maximum threshold condition (section 6.2).

### 5.4.2 Water content results

Due to problems with the load cells it was not possible to monitor the water content of sample AG2 throughout the range of different applied stresses (its original water content  $WC_{wet}$  was 40.1 %) and so no results are shown. Table 5.5 shows the water content of DN1 for various test conditions. Both  $WC_{wet}$  and  $WC_{dry}$  conditions are shown (definitions given in section 5.4.1). No data are available at the highest compression stages due to problems with draining liquids from highly compressed waste. It will be noted that in nominally saturated conditions the water contents at high pore water pressure are greater than those for lower pore water pressure conditions. The only obvious mechanism for an increase in water content would appear to be compression of residual gas in the waste arising from an increase in pore water pressure (although it is possible that some compression of the waste also occurred under increased pore water pressure). This indicates that the samples were not fully saturated.

The field capacity water contents shown in Table 5.5 are generally lower than those published by Beaven (2000) for several household wastes of different age and pre-processing. At the lowest applied stress the  $WC_{wet}$  value of 38.5 % for DN1 is typical of those recorded by Beaven (2000) which ranged from about 30 % to 50 %. However the DN1 water contents decrease significantly with stress whereas those recorded by Beaven remained generally unchanged. An explanation for this may be that at higher stresses during the prolonged DN1 tests water contents were affected by residual gas accumulation in the sample.

Table 5.5 Water content ( $WC_{wet}$ ) of sample DN1 for various test conditions ( $WC_{dry}$  values are shown in brackets)

Applied stress (kPa)	40	87	134	228	334	603
Water content at field capacity (drained)	38.5% (62.5%)	35.5% (55.0%)	32.8% (48.7%)	24.0% (31.6%)	20.8% (26.3%)	13.5% (15.6%)
Water content in nominally saturated conditions (pore water pressure 0 to 20 kPa)	47.5% (90.6%)	41.7% (71.5%)	37.0% (58.8%)	25.5% (34.1%)	-	-
Water content in gas accumulated conditions (pore water pressure 30 to 40 kPa)	41.9% (72.2%)	39.8% (66.1%)	34.8% (53.4%)	24.7% (32.8%)	-	-
Water content in nominally saturated conditions (pore water pressure 60 to 70 kPa)	-	46.0% (85.1%)	42.3% (73.3%)	32.8% (48.8%)	-	-
Water content in gas accumulated conditions (pore water pressure 60 to 70 kPa)	-	42.4% (73.6%)	37.5% (60.0%)	27.2% (37.4%)	-	-

## 5.5 Waste density

### 5.5.1 Density definitions and methodology

The bulk density of the sample was monitored throughout the testing procedure. This was calculated from the sample weight shown by the load cell readings and the total sample volume ( $V_T$ ) (calculated from the sample depth). The values shown represent an average density throughout the sample, disregarding variations arising from heterogeneity or possible differential compression (section 5.3.2).

The actual density ( $\rho$ ) is the mass of solids and water within a unit volume of waste. If all the voids are full of water or leachate, this will be the saturated density:

$$\rho = \frac{M_S + M_W}{V_T} \quad (5.5)$$

Dry density ( $\rho_{DRY}$ ) is the mass of dry solids within a unit volume of waste:

$$\rho_{DRY} = \frac{M_S}{V_T} \quad (5.6)$$

Density at field capacity ( $\rho_{FC}$ ) is the mass of solids and water within a unit volume of waste when a saturated sample is fully drained under gravity to field capacity:

$$\rho_{FC} = \frac{M_S + M_{W(fc)}}{V_T} \quad (5.7)$$

### 5.5.2 Density results

The changes in density with stress are shown in Tables 5.6 and 5.7 for the two samples tested. Only dry density data are available for sample AG2; density in saturated or field capacity conditions could not be calculated as faults with the load cells resulted in a loss of sample weight data. The DN1 results in Table 5.7 show that density depends on the water content, the presence of gas, and the pore water pressure.

Table 5.6 Sample AG2 dry density

Applied stress (kPa)	0	40	87	165	322	603
Dry density (t/m <sup>3</sup> )	0.58	0.69	0.75	0.83	0.91	0.98

Table 5.7 Sample DN1 density

Applied stress (kPa)	0	40	87	134	228	334	603
Dry density (t/m <sup>3</sup> )	0.30	0.41	0.47	0.52	0.61	0.66	0.73
Density at field capacity (t/m <sup>3</sup> )	-	0.87	0.96	1.00	1.04	1.09	1.10
Density (t/m <sup>3</sup> ) in nominally gas purged conditions and low pore water pressure (30 to 40 kPa)	-	1.02	1.06	1.07	1.08	1.13	-
Density (t/m <sup>3</sup> ) in gas accumulated conditions and low pore water pressure (30 to 40 kPa)	-	0.92	1.03	1.04	1.05	-	-
Density (t/m <sup>3</sup> ) in nominally gas purged conditions and high pore water pressure (60 to 70 kPa)	-	-	1.14	1.17	1.18	-	-
Density (t/m <sup>3</sup> ) in gas accumulated conditions and high pore water pressure (60 to 70 kPa)	-	-	1.07	1.08	1.09	-	-

Figure 5.8 shows a comparison of the dry densities of the waste samples AG2 and DN1 with three different household samples tested by Beaven (2000) using the Pitsea compression cell. This data is used as it is the most comprehensive data available. The density of the aged samples AG1 and AG2 was significantly higher than the three fresh waste samples (DN1, DM3 and PV1). Both aged samples came from the same landfill but AG1 was excavated several years earlier. The higher density of the aged samples is expected due to the degradation of the waste but also may be due in part to soil mixed with the waste. The density data for sample AG2 is higher than AG1. This may be due to the additional compression of sample AG2 following 'wet' testing (section 5.3.1). The density of the Dano processed is generally higher than the unprocessed waste (DM3). This would be expected as pre-processing of a particular waste would generally reduce component size thus allowing tighter packing. Following this reasoning, the density of the pulverised sample PV1 should also be high but Figure 5.8 shows that this had the lowest density of all of the samples tested.

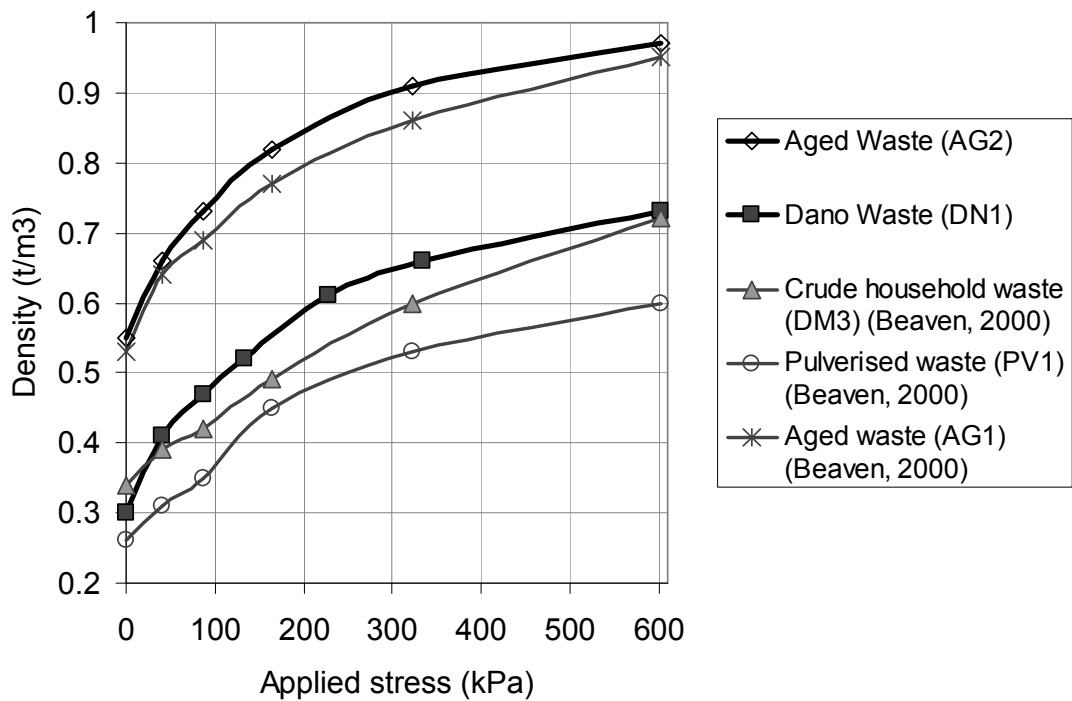


Figure 5.8 Comparison of dry densities of different household wastes

## 5.6 Summary

The waste samples were compressed at several applied stress stages up to a maximum applied stress of 603 kPa. Stress was applied until primary compression had effectively ceased but was of insufficient duration to fully include secondary settlement.

Additional settlement occurred in sample AG2 following ‘wet’ testing. In the later DN1 tests this was prevented by holding the top platen in position during ‘wet’ testing after initial compression was complete.

The methodology used during the loading and compression stages is important to the outcome of the later drainable porosity and hydraulic conductivity tests. The problem

of representative sampling is probably not as critical as that for natural soil deposits but the question of whether the structure of the samples is representative of landfilled wastes is not fully resolved. During compression there was the potential for sidewall friction to cause differential compression of the sample resulting in changes in hydraulic properties throughout the depth of the sample. Examination of the compression, drainable porosity and hydraulic conductivity data indicates that this was not the case.

Water content of a waste and therefore its density depends on the degree of saturation. Full saturation of household wastes is unlikely due to gas accumulating in the wastes.

Compression, water content and densities for the two samples at different applied stresses have been presented. At low applied stresses, the water content of sample DN1 was similar to previously tested wastes but was lower at higher stresses. This was possibly caused by gas accumulation in the sample. The density data for the two samples tested were similar but marginally higher than similar wastes tested by Beaven (2000).

## 6. Drainable porosity

### 6.1 Introduction

Drainable porosity is a useful parameter as it is directly related to the leachate level and the volume of leachate in the saturated zone of a landfill.

Total porosity  $n$  is defined as the volume of voids per unit total volume:

$$n = \frac{V_v}{V_v + V_s} \quad (6.1)$$

where:

$V_v$  = volume of voids

$V_s$  = volume of solids

In the field situation void spaces are unlikely to be fully occupied by leachate due to trapped air or pockets of landfill gas in the voids. A more practical measurement is drainable (or effective) porosity  $n_e$  which is the volume of fluid released per unit total volume when the waste is drained from nominally saturated to field capacity conditions:

$$n_e = \frac{V_d}{V_v + V_s} \quad (6.2)$$

where:

$V_v$  = volume of voids

$V_s$  = volume of solids

$V_d$  = drainable volume

In this chapter the methodology for assessing drainable porosity for samples AG2 and DN1 at each compression stage are described. The results are presented and compared with previous data. The additional tests that were carried out on sample DN1 to evaluate the drainable porosity in gas accumulated conditions (section 2.4.6) and at different pore water pressures (section 2.4.7) are described and illustrated. The implications of this original research are discussed.

## 6.2 Drainable porosity methodology

Commencing with the sample under test being drained to field capacity conditions, leachate was admitted in stages to raise the free standing water level in the sample. The rise in water level at each stage was plotted against the volume of water admitted and the drainable porosity calculated from the resulting gradient. The results were checked by draining the saturated sample in stages back to field capacity, measuring the water level and the volume of water drained at each stage.

For assessing drainable porosity in gas accumulated conditions the following procedure (illustrated in Figure 6.1) was used:

- water was admitted into the (nominally purged) sample to raise the free standing water level to that of an overflow port positioned just above the top of the waste. The distance between the top of the waste and the overflow outlet was as small as possible (maximum 300 mm) to maintain

low pore water pressure conditions. The inlet valves were then closed so that no further water was admitted and excess water was drained via the outlet port.

- gas was naturally allowed to accumulate in the sample. This displaced water from the sample which was expelled through the outflow outlet. The displaced water was collected in a container and the volume was measured (a less accurate estimate could also be made from the weight reduction shown by the load cells). Eventually (after one to two weeks) a threshold level of gas accumulation was attained with no further discharge of water or change in weight
- the drainable porosity in gas accumulated conditions was calculated by first deducting the total volume of water displaced during gas accumulation from the volume of water originally required to raise the sample from field capacity to saturated conditions (in the test conducted in nominally gas purged conditions). This drainable water volume was then divided by the total volume of the sample to give an average drainable porosity for the sample in gas accumulated conditions at low ( 0 to 20 kPa) pore water pressure

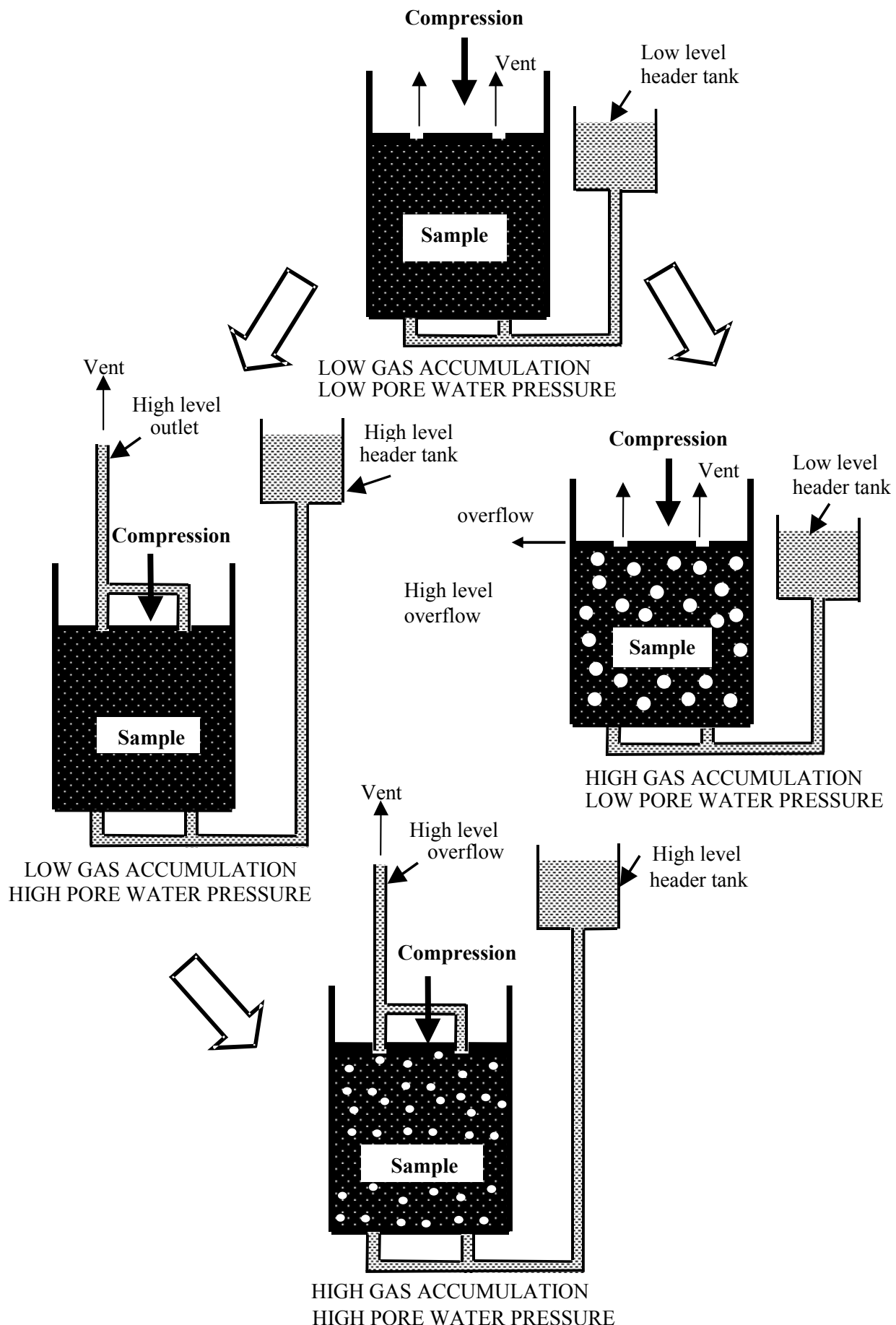


Figure 6.1 DN1 drainable porosity test configurations

Assessment of drainable porosity at higher pore water pressure was achieved by raising the outflow level (and therefore the head of water above the top of the sample) by several metres. The following procedure was used:

- gas was purged (as far as practically possible) from the sample by inducing a fast upward flow of water, preferably starting from drained conditions
- the top platen seals (section 3.3) were inflated to seal the top of the sample
- water was admitted into the sample until the free standing water level was visible in the pipework above the top platen. Load cell readings were noted
- the pore water pressure was increased by raising the water level several meters. The increase in load cell readings (indicating the increase in water content in the sample) were noted
- the drainable porosity in high pore water pressure conditions was calculated from the original volume of water required to raise the sample from field capacity to saturated conditions *plus* the additional volume of water in the sample under high pore water pressure (*less* any additional weight of water in the pipework during raising the pore water pressure)

The drainable porosity in gas accumulated conditions at high pore water was assessed using the same method as that used for low pore water pressure except the overflow was positioned at a much higher elevation.

### 6.3 Results and discussion

The average drainable porosity values obtained for the two samples are shown in Tables 6.1 and 6.2. These were deduced from the average gradient of the leachate level v. volume plot (these are shown in Appendix D, section D4). Some differences were usually evident between fill and drain plots but no consistent trends were evident – indicating systematic error / inconsistencies in the samples rather than hysteresis effects. No data are available at the higher stress stages due to the difficulty of obtaining consistent water levels and draining samples. The data for sample DN1 include the different effective drainable porosities measured using the methodology outlined in section 6.2 for different gas accumulated conditions and pore water pressures. These are also plotted in Figure 6.2

Table 6.1. Sample AG2 drainable porosity

Applied stress (kPa)	40	87	165	322	603
Drainable porosity	17.5%	11.5%	5%	1%	–

Table 6.2 Sample DN1 drainable porosity

Applied stress (kPa)	40	87	134	228	334	603
Drainable porosity in nominally saturated (gas purged) conditions at low pore water pressure (0 to 20 kPa)	15.0%	10.2%	6.8%	2.0%	–	–
Drainable porosity in gas accumulated conditions and low pore water pressure (0 to 20 kPa)	5.2%	6.9%	3.2%	0.9%	–	–
Drainable porosity in nominally saturated (gas purged) conditions at high pore water pressure (60 to 70 kPa)	–	18.6%	16.6%	13.6%	–	–
Drainable porosity in gas accumulated conditions and high pore water pressure (60 to 70 kPa)	–	11.5%	7.6%	4.6%	–	–

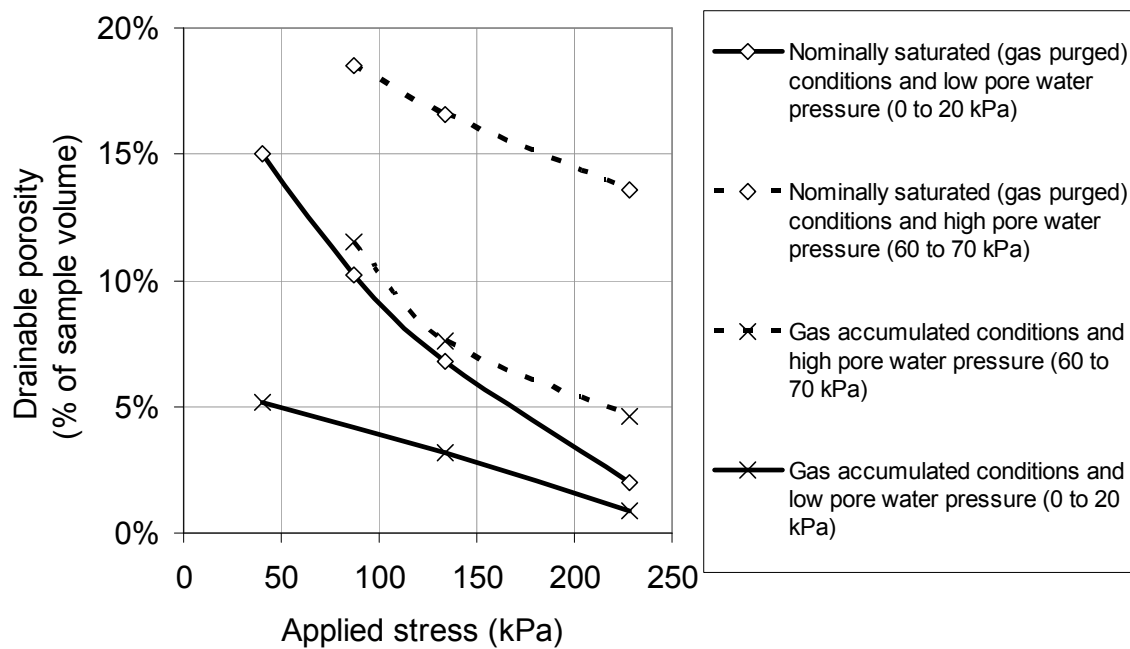


Figure 6.2. Comparison of drainable porosities for sample DN1 according to stress and gas conditions / pore water pressure

The influence of pore water pressure and gas accumulation on the drainable porosity of sample DN1 is evident in Table 6.2 and Figure 6.2. Gas accumulation reduced the drainable porosity to between 32 % and 66 % of that measured in nominally purged conditions. This was evident in both low pore water and high pore water conditions. For both conditions, the drainable porosity differences were greater at higher stresses possibly arising from increased gas entrapment within a more confined structure.

The implications of these findings in landfill design is that leachate levels in landfill monitoring wells could be elevated by gas accumulation. Estimates of leachate volumes in the saturated zones will be vastly over-estimated if based on drainable porosity data for nominally purged conditions. More accurate estimates will be obtained by using drainable porosity data in gas accumulated conditions at appropriate pore water pressures.

In both nominally saturated and gas accumulated conditions, large increases in drainable porosity were recorded when pore water pressure was increased. This is thought to be due to gas within the sample being compressed at the higher pressures allowing more water into the sample. Again this should not occur in truly saturated

conditions and the fact that it did indicates that gas remained in the sample after purging. It is likely that further increases in drainable porosity could have been attained if it had been possible to increase the high pore water pressure above the 60 to 70 kPa used (this is the maximum possible with the existing equipment). However saturated zones of most UK landfills are restricted to one metre (although there are exceptions). Pore water pressures are therefore usually low and so the data for low pore water pressure conditions will be of more practical use for most landfills.

The drainable porosity results for samples AG2 and DN1 are compared with those measured for three other samples tested by Beaven (2000). The DN1 data set for nominally saturated (gas purged) and low pore water pressure conditions is shown as this is the condition in which the other samples were tested. The stress values shown are average stress values according to the method by Beaven (2000) outlined in section 5.3.2. For comparative purposes the stress data for AG2 and DN1 have also been adjusted accordingly but, as discussed in section 5.3.2., these average values probably under-estimate the applied stress. With the exception of sample PV1, all drainable porosity data are very similar. This supports previous findings (Beaven, 2000) for UK household wastes that drainable porosity (and hydraulic conductivity) is mainly dependent on stress rather than waste type / pre-processing.

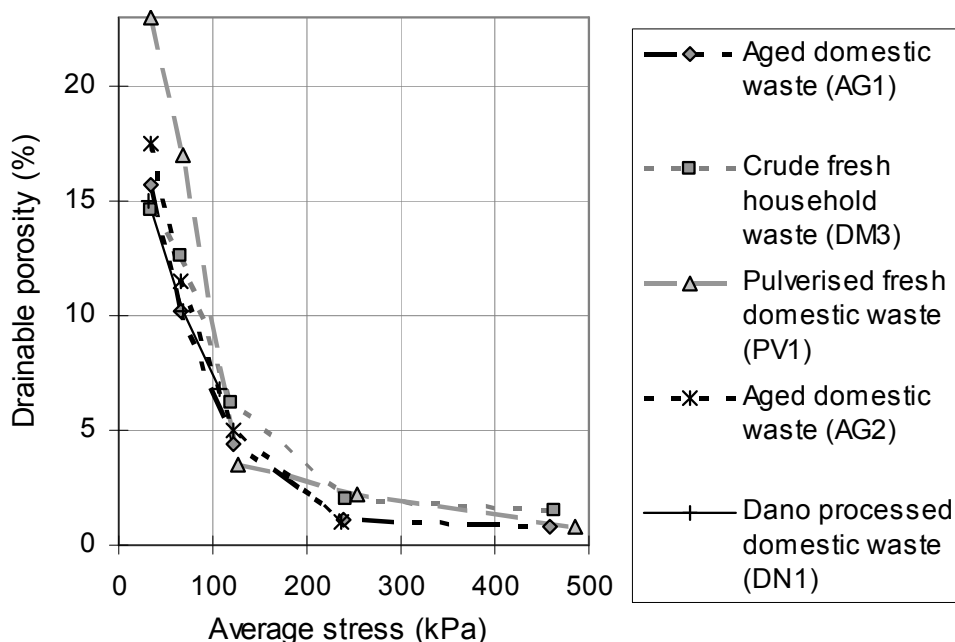


Figure 6.3 Comparison of AG2 and DN1 drainable porosities with other wastes (Beaven, 2000)

## 6.4 Summary

Drainable porosity is a useful parameter for assessing the leachate volumes within landfill saturated zones. The drainable porosity tests carried out on sample DN1 have demonstrated for the first time that drainable porosity can be significantly altered by pore water pressure and gas accumulation in the waste. The use of drainable porosity data for gas accumulated conditions and low pore water pressure is recommended for assessing leachate volumes in typical (shallow saturated zone) landfill conditions as previous data in nominally purged conditions is likely to over-estimate leachate volumes.

The drainable porosity results for sample AG2 and DN1 (for nominally saturated and low pore water pressure conditions) were similar to previously tested wastes - drainable porosity decreasing significantly with applied stress.

## 7. Vertical hydraulic conductivity

### 7.1 Introduction

In order to assess  $k_h:k_v$  ratios for the two samples being tested (chapter 8) it was necessary to first assess the vertical hydraulic conductivities at each compression stage. The methodology used for the vertical hydraulic conductivity tests is described in this chapter. This includes the procedure used to assess hydraulic conductivity in both nominally purged and gas accumulated conditions, and also different pore water pressures. This is original research that has not previously been attempted.

The results of the vertical hydraulic conductivity tests are shown in this chapter and compared with those from other research. Potential errors that may arise are evaluated and the possible effect of pore water pressure on the stress in the samples is considered. A summary of the hydraulic properties (including those evaluated in chapters 5 and 6) of the samples tested is shown at the end of the section

### 7.2 Vertical hydraulic conductivity methodology

A schematic view of the arrangement used for upward flow vertical hydraulic conductivity testing of a waste sample in the compression cell is shown in Figure 7.1. The inflatable seals on the top platen periphery were inflated to seal the gap between

the top platen and cylinder, sealing the sample within the cylinder and platens. A constant upward flow of leachate was established through the waste sample. Leachate was supplied from the header tanks to the inlet ports in the bottom platen by flexible hoses and distributed across the base of the sample by the bottom gravel layer.

Leachate in the header tanks was maintained at a constant level in order to maintain a consistent pressure and flow rate through the sample. Inlet flow rates were measured using in-line flow meters. Outflow from the top of the sample was taken from the outlet ports in the top platen via the gravel layer. Outlet flow rates were measured by timing the volume of leachate discharged into a graduated container.

Figure 7.1 also shows the routing of outflowing leachate through gas collection tanks as used on some DN1 vertical hydraulic conductivity tests. These are shown on the photograph in Figure 7.4. This configuration allowed gas entrained in the leachate to be separated and hence gas production rates to be monitored.

Open-ended piezometer tubes (usually 2 or 3 sets) were inserted into the waste sample to measure total heads throughout the depth of the sample. Vertical spacing between the piezometers ranged from 150 mm to 400 mm. Hydraulic gradients were calculated from the piezometer total head readings and the distances between them. Vertical hydraulic conductivities (both bulk average and intermediate values throughout the sample depth) were calculated according to the flow rate and hydraulic gradients using Darcy's law (equation 2.1). The method of obtaining an average reading for the sample is given in section 7.4.

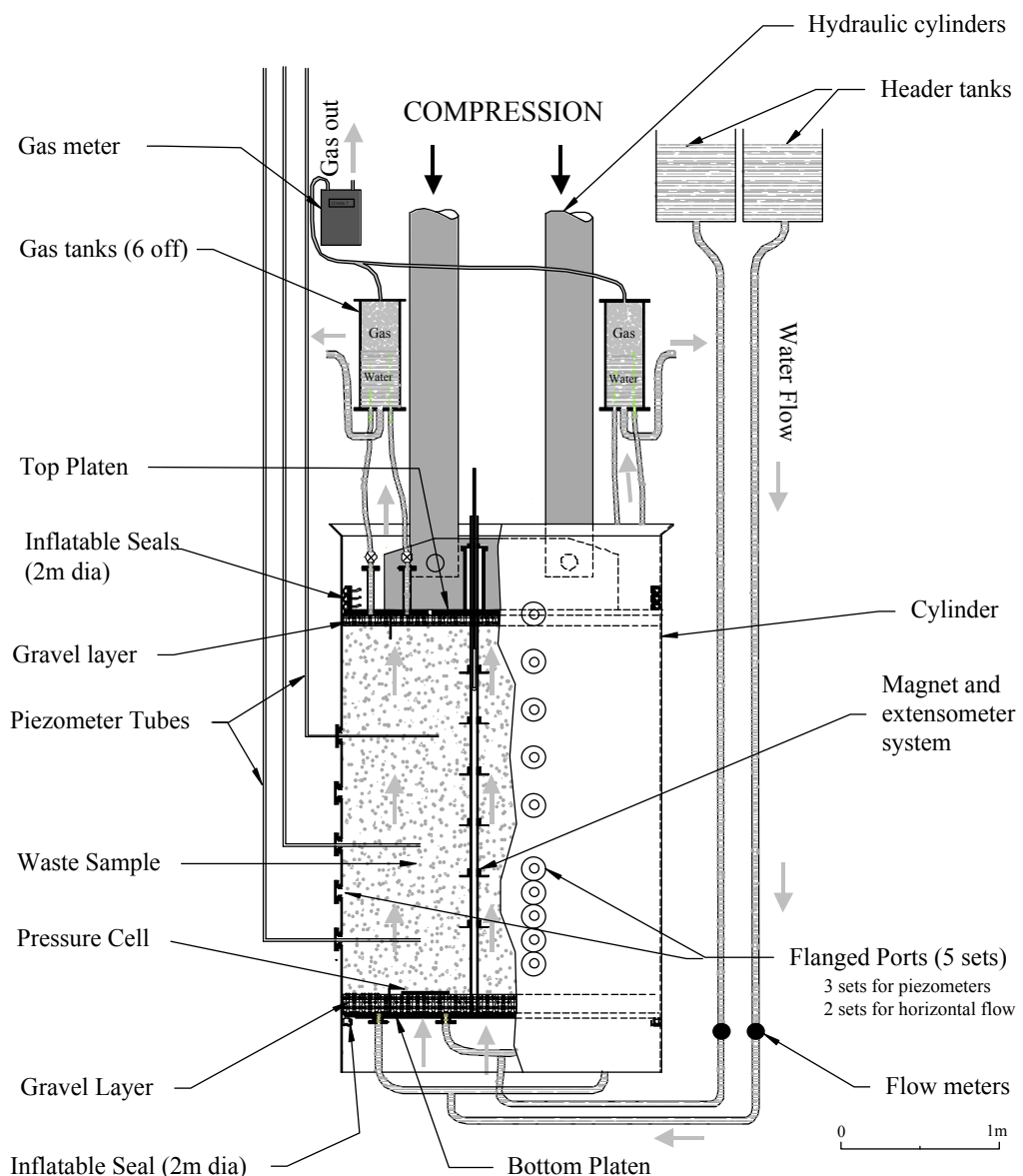


Figure 7.1 Test arrangement for vertical hydraulic conductivity assessment

In accordance with recommendations for similar but smaller scale constant head permeameter tests (e.g. Powrie, 1997), hydraulic conductivity tests were conducted at different flow rates. Flow rates were varied by changing the elevation of the inlet header tanks and outflow pipes. A schematic view of the possible configurations selected by switching valves is shown in Figure 7.2 and a photograph in Figure 7.3. These could be switched to create upward or downward flow providing that:

- the inlet elevation was above the outlet elevation; and
- the outlet elevation was above the top of the waste sample to ensure saturation (as nearly as possible) of the entire sample

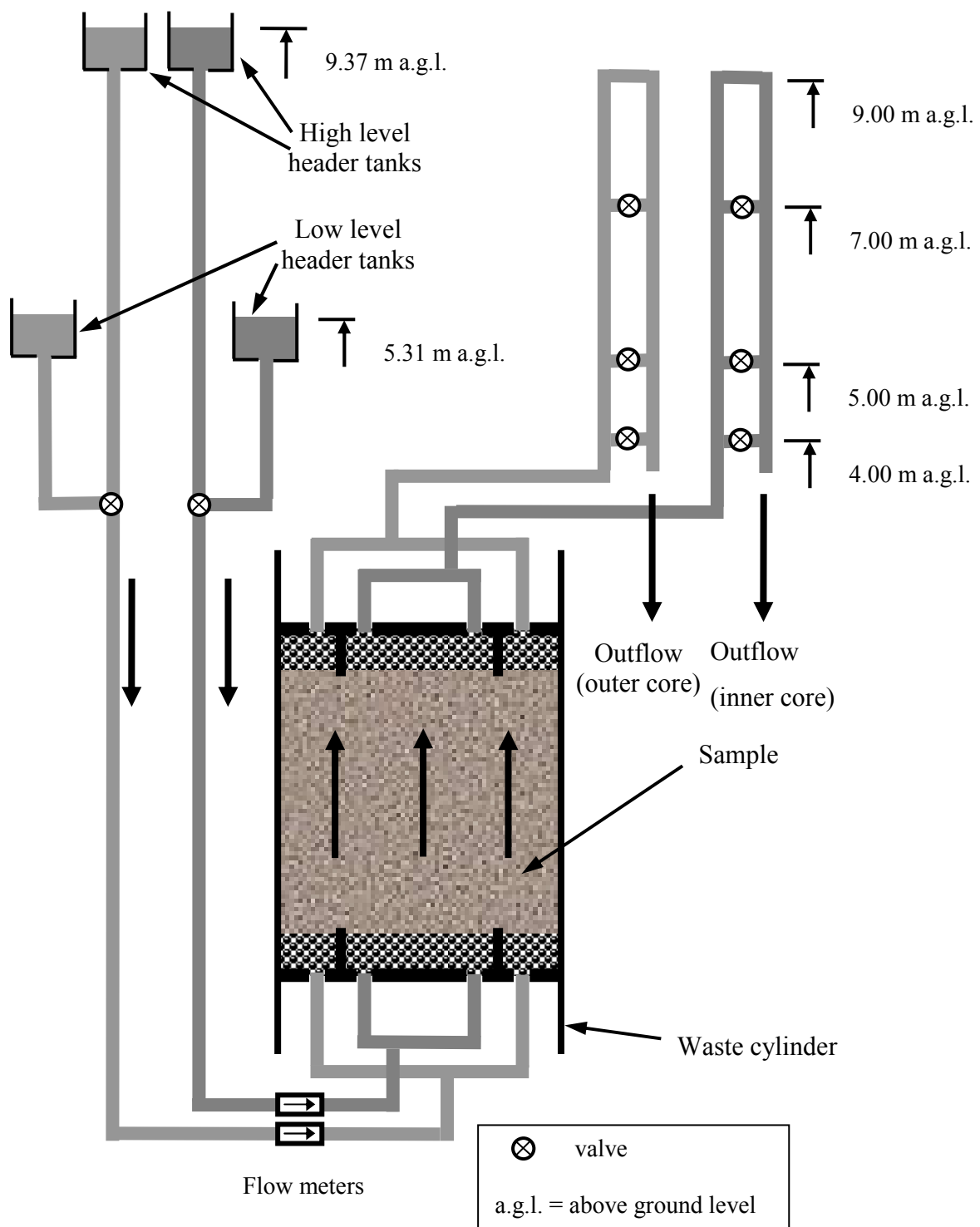


Figure 7.2 Inlet and outlet configurations for upward flow vertical hydraulic conductivity tests

The procedure adopted for tests at different pore water pressures (section 2.4.7) and gas accumulated conditions (section 2.4.6) were to:

1. purge gas from the sample by inducing a fast<sup>3</sup> upward flow of water, preferably commencing from drained conditions. Gas removal from samples of high hydraulic conductivity was apparent both visually (from gas bubbles in the outflow) and from the increase in load cell readings (assumed to be due to leachate displacing gas from pore spaces)
2. conduct hydraulic conductivity tests in purged conditions at both low (typically 30 to 40 kPa) and high pore water pressure (typically 60 to 70 kPa) by using different inlet and outlet elevations. During each test the weight of the sample was monitored to ensure a constant degree of saturation was maintained
3. create gas accumulated conditions by maintaining the flow through the sample for a number of days to allow gas to accumulate. Gas accumulation was evident by a decrease in load cell readings (presumed to be due to gas displacing leachate from pore spaces) and a decrease in flow rate through the sample. Eventually a threshold gas accumulation level was attained when no further reduction in load cell readings or flow rate was apparent
4. measure hydraulic conductivity in gas accumulated conditions. Again the sample weight was monitored as above
5. alter pore water pressure by changing inlet and/or outlet elevations. This may have produced some gas release and so a stabilisation period was again necessary to allow full gas accumulation
6. Measure hydraulic conductivity in gas accumulated conditions at new pore water pressure. Again sample weight was monitored as above

---

<sup>3</sup> Flow rate was maximised by using the highest available inlet head and lowest possible outlet head. Flow rates in the region of 100 l/m were achievable at low compression but were much lower at higher stresses due to the reduction in sample hydraulic conductivity

Downflow tests were also carried out at some compression stages. As for upward flow tests, the sample was sealed using the top platen inflatable seals and the same method was used to vary flow rates according to inlet and outlet flow rates.



Figure 7.3 The outlet valves and pipes mounted on the side of the compression cell

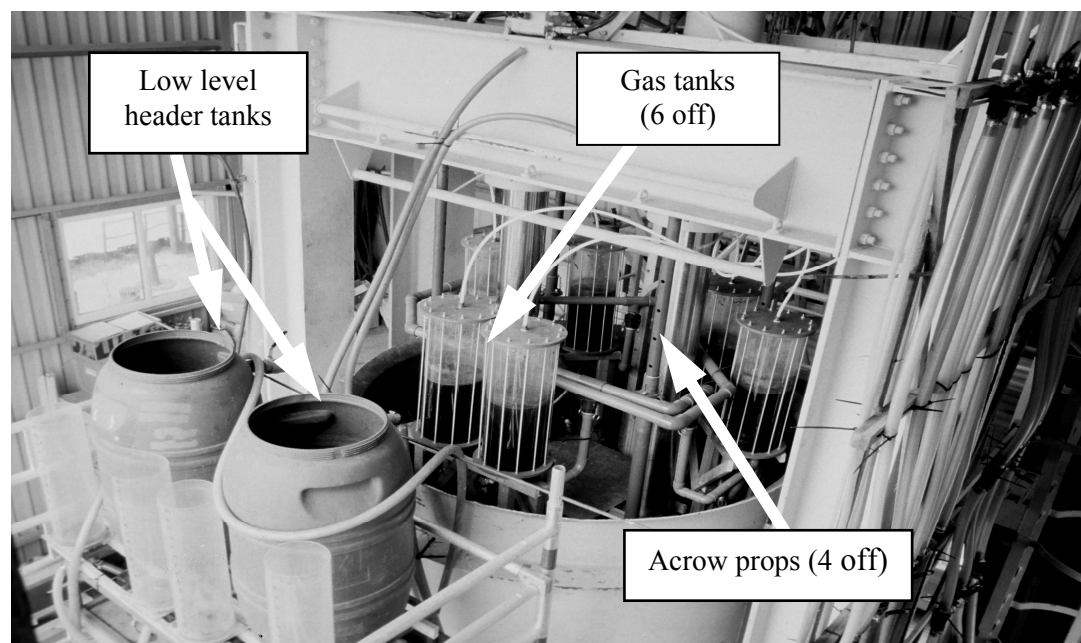


Figure 7.4 View of top of compression cell showing the gas tanks illustrated in Figure 7.1

### 7.3 Potential errors in hydraulic conductivity measurement

Potential systematic errors inherent in the hydraulic conductivity measurement consisted of:

- Flow measurement inaccuracies. The manufacturer's specified accuracy for the flow meters used to measure the inlet flow rates was within  $\pm 5\%$  for flow rates above 15 l/m. Outlet flow rates measurements (measured by timing a volumetric discharge into a graduated cylinder or bucket) were repeated to ensure that measured flow rates were consistent; acceptable repeatability being within 5 %. Generally, the difference between inlet and corresponding outlet flow rates did not exceed 5 % but greater differences could occur if steady state conditions had not been established. In such instances the test was run until the inflow and outflow rates were consistent to within  $\pm 5\%$ . Flow rates below 15 l/m were assessed on outflow measurement only and these were checked for consistency over periods of typically 30 minutes duration to ensure that flow through the sample had stabilised. In stable conditions the variation between measurements taken at such extended time intervals would not be expected to exceed 5 %. The above errors are not cumulative and so the overall accuracy for flow rate measurement is estimated to be within  $\pm 5\%$
- Errors in the estimation of hydraulic gradient. The method of measuring the hydraulic gradient using piezometers was the same as used by Beaven (2000). Errors were estimated to be within  $\pm 5\%$ .
- Peripheral flow. In hydraulic conductivity tests using small scale oedometers it is possible for preferential peripheral flow to occur between the sample and cylinder wall interface. The increased total flow rate may result in an overestimation of the hydraulic conductivity. Sidewall leakage can occur with very hard or stiff soils permeated at low stress but is rarely a problem for compressible soils subjected to compressive stresses of at least 50 kPa (Daniel, 1994) as lateral stresses caused by the vertical stress applied to the sample acts against the inner walls of the cell, minimising or preventing side-wall leakage (Shackelford, 1994) (Appendix A). In vertical hydraulic conductivity tests on samples AG2 and DN1, flow rates through

the inner and outer cores of the samples were measured independently (this was made possible by the dividing rings on the top and bottom platens described in section 5.2.1.). The flow rates could be affected by gas accumulation in the sample or slight differences in outlet pipe elevations but inner and outer flow rates were usually within 10 % of each other). This suggests that peripheral flow was not occurring, but an allowance of  $\pm 10\%$  is made based on the above inner / outer core flow rate variations.

The overall estimate for vertical hydraulic conductivity errors is within  $\pm 20\%$  based on flow rate errors of  $<\pm 5\%$ , hydraulic gradient errors of  $<\pm 5\%$  and a  $\pm 10\%$  allowance for peripheral flow.

In addition to systematic errors, the hydraulic conductivity results may also be affected by temperature and leachate properties (section 2.4.2). Sample and leachate temperatures were not recorded during the tests but subsequent measurements have shown that leachate temperatures are similar to ambient temperature (the compression cell and building are not insulated). Typical seasonal temperature variations of about 20°C could potentially result in differences in hydraulic conductivity measurements in excess of 50 % (Table 2.1 – assuming leachate exhibits similar changes with temperature as water). An approximate correction could be made to the reported values according to the time of year when the tests were undertaken (although the field operating temperature may also need to be considered for a given application). However, the main aim of this research is to compare vertical and horizontal hydraulic conductivities (expressed as a  $k_h : k_v$  ratio). As both sets of tests were undertaken at similar temperatures, it is not necessary to correct for temperature.

In section 2.4.2 it was also observed that the density and viscosity of leachates are usually higher than those of water, and this could result in differences in measured hydraulic conductivity values. Initially water was used to raise AG2 and DN1 from their initial water content to saturated conditions (section 6.2). However by the time the first hydraulic conductivity tests were carried out, the water had been passed through the sample several times and had effectively become leachate. No analyses were undertaken and so it is not known if leachate density and viscosity differed to that of water. However calculated  $k_h : k_v$  ratios are not likely to be affected as both

vertical and horizontal hydraulic conductivity tests were carried out using the same recirculated leachate.

## 7.4 Results

In the vertical hydraulic conductivity tests, some variation in head readings were evident between sets of piezometers (2 or 3 sets were usually used). This was expected to some extent in tests carried out on heterogeneous wastes (section 2.4.9), but it was also possible for readings to be affected by gas in the piezometers. To calculate the hydraulic conductivity between piezometers at two different elevations, the average value of the sets was usually taken, although on occasions some judgement was exercised if exceptional (erroneous) readings were evident.

The rationale for installing piezometers at several vertical positions (section 7.2) was to detect changes in hydraulic conductivity throughout sample depth that may have arisen from differences in sample density due to sample weight or frictional effects (section 5.3.2). These hydraulic conductivity values would need to be incorporated in the horizontal flow analyses (chapter 9). However as tests progressed it became apparent from the assessments discussed in section 5.3.2 and comparisons between intermediate hydraulic conductivities derived from both the upward and downward flow tests shown below (this was the first time that downflow tests were run in the compression cell), that there was no clear evidence of differential hydraulic conductivity with sample depth. Therefore a bulk average hydraulic conductivity value for each sample at each compression stage would suffice for the horizontal flow analyses.

The hydraulic conductivities for sample AG2 based on the average piezometer readings are shown in Figures 7.5 to 7.9. Data is shown for all but the extreme top and bottom of the waste (for example no data is shown between the base of the waste at 2053 mm a.g.l. and the lowest piezometer at 2220 mm a.g.l.) as hydraulic conductivity is difficult to calculate reliably over small distances from the gravel / waste interface. In some cases fairly large differences in hydraulic conductivity are evident throughout sample depth and between upward and downward flow results. The average hydraulic conductivity was estimated from these results based on the mathematical average and /

or a best approximation (for example the data in Figure 7.5 was reasonably straightforward to average as the upflow data was almost an inverse of the downflow data but in Figure 7.6 the downward flow test generally gave more consistent readings and so the average value is biased towards this).

By the time the DN1 tests were carried out it was evident that little purpose was served by attempting to assess hydraulic conductivities throughout the sample depth and the process was simplified for the DN1 data. The intermediate piezometer readings were not used and instead the overall (bulk) vertical hydraulic conductivity value was calculated at each compression stage using Darcy's law (equation 2.1), the hydraulic gradient ( $i$ ) being calculated from the difference between inlet and outlet head divided by total depth of the sample. Where more than one set of data was available (such as the upflow and downflow data), the average of the bulk values was normally used.

As tests for sample DN1 were conducted according to different gas accumulation and pore water pressure conditions, there are three or four sets of hydraulic conductivity data for each compression stage. Individual plots are therefore not shown but an example is shown in Figure 7.10 for tests conducted at an applied stress of 134 kPa in low gas accumulated conditions with minimum inlet and outlet pore water pressures.

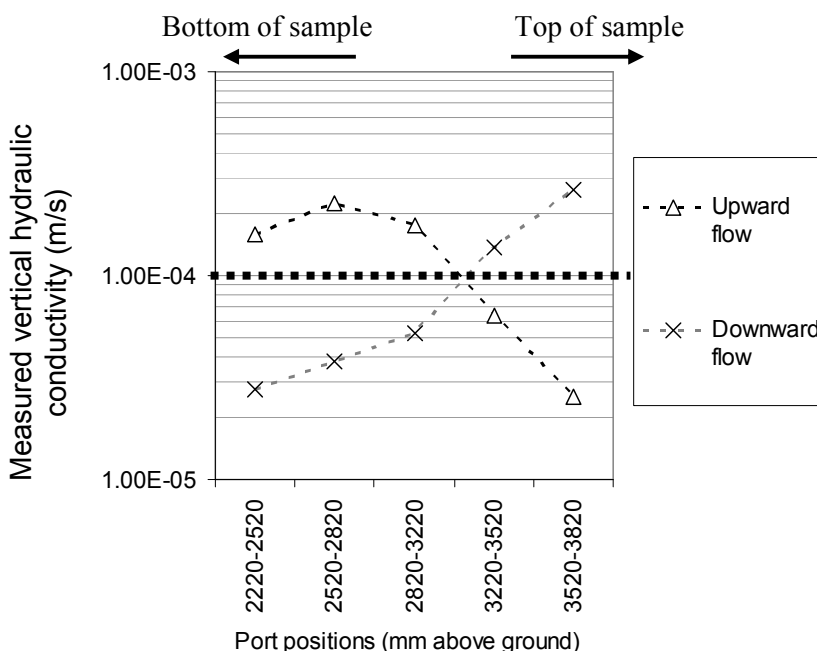


Figure 7.5 Vertical hydraulic conductivity with sample depth for sample AG2 at an applied stress of 40 kPa (dotted line shows estimated average hydraulic conductivity)

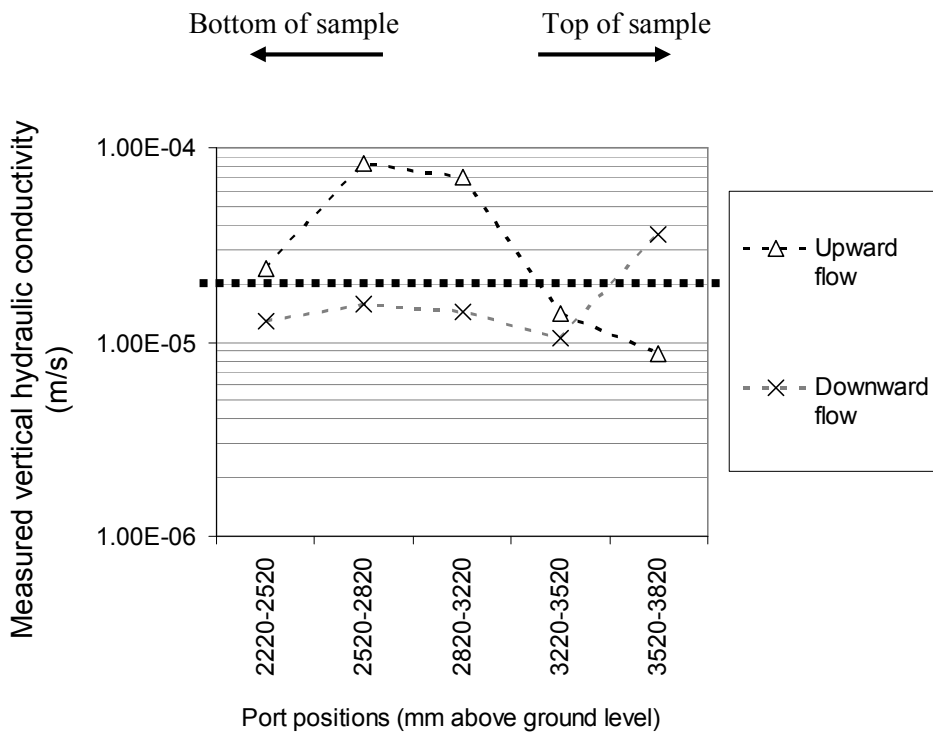


Figure 7.6 Vertical hydraulic conductivity with sample depth for sample AG2 at an applied stress of 87 kPa (dotted line shows estimated average hydraulic conductivity)

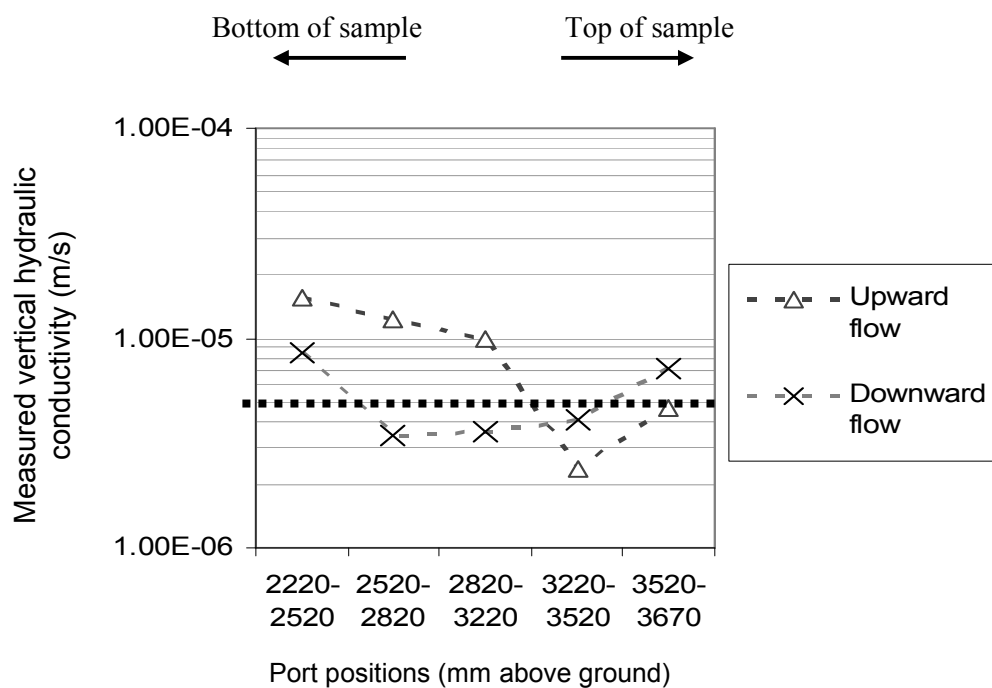


Figure 7.7 Vertical hydraulic conductivity with sample depth for sample AG2 at an applied stress of 165 kPa (dotted line shows estimated average hydraulic conductivity)

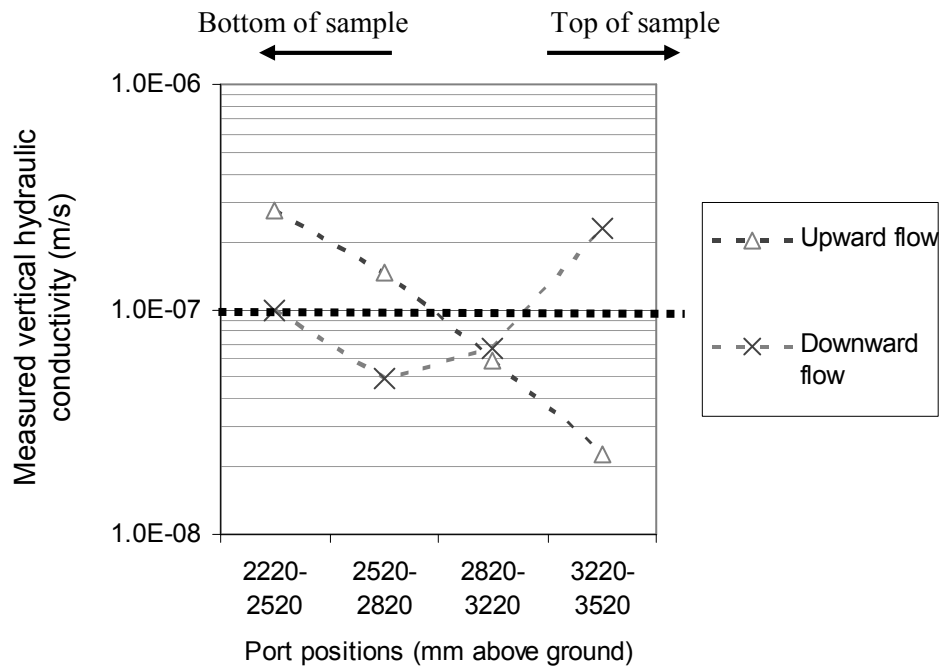


Figure 7.8 Vertical hydraulic conductivity with sample depth for sample AG2 at an applied stress of 322 kPa (dotted line shows estimated average hydraulic conductivity)

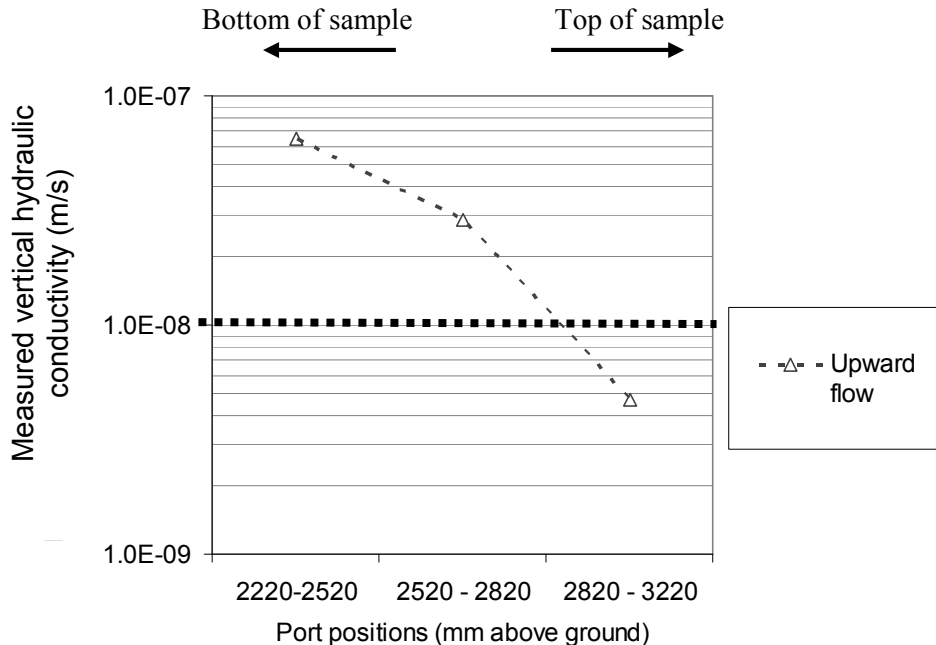


Figure 7.9 Vertical hydraulic conductivity with sample depth for sample AG2 at an applied stress of 603 kPa (dotted line shows estimated average hydraulic conductivity)

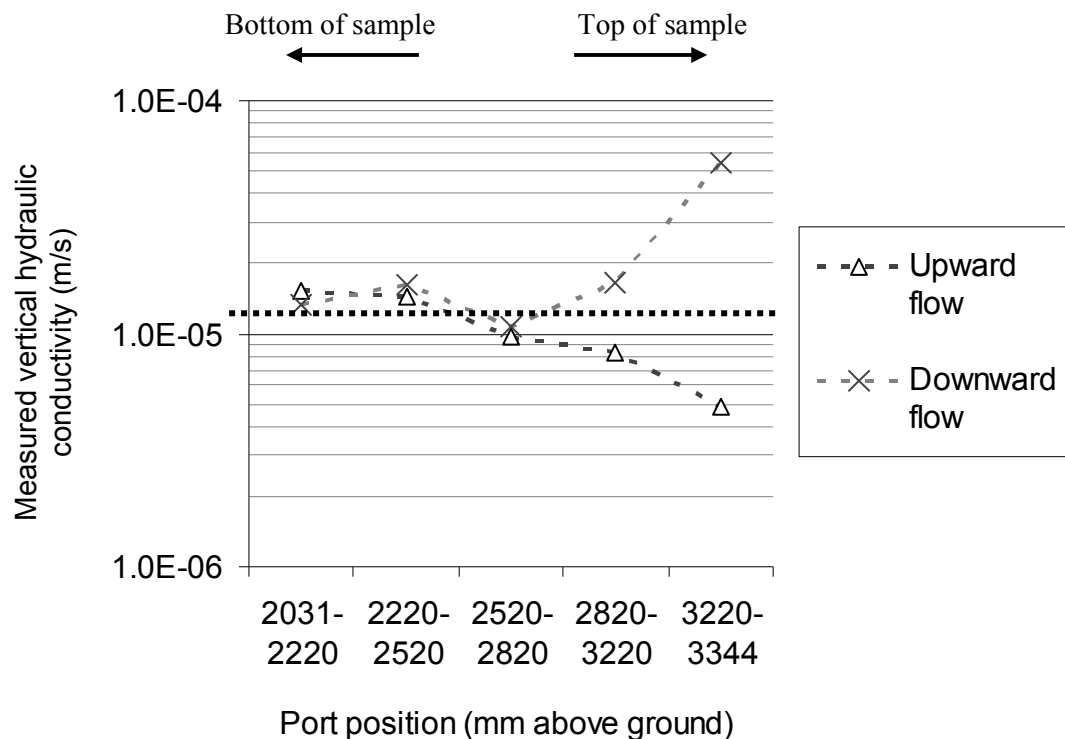


Figure 7.10. Vertical hydraulic conductivity with sample depth for sample DN1 at an applied stress of 134 kPa. Test conducted in low gas accumulated conditions with minimum inlet and outlet pore water pressures (the dotted line indicates the average estimated bulk vertical hydraulic conductivity value)

Average vertical hydraulic conductivity results for samples AG2 and DN1 are shown in Figures 7.11 and 7.12 and in the summary in Tables 7.1 and 7.2. The hydraulic conductivity values for the AG2 tests (Figure 7.11) were assessed in nominally gas purged conditions. Error bars are shown for applied stress values (section 5.3.2) but not for the relatively insignificant vertical hydraulic conductivity error range (section 7.3)

The sample DN1 results shown in Figure 7.12 are more comprehensive, showing the different hydraulic conductivity values obtained for different pore water pressures, and in purged and gas accumulated conditions (except at higher applied stresses due to difficulties in establishing flow through compressed samples). However gas purging was probably ineffective at the higher compression stages and all values at higher stresses are likely to have been reduced to some extent by gas accumulation. Again error bars are shown for the stress values as discussed in section 5.3.2 but for clarity the relatively insignificant hydraulic conductivity measurement errors (section 7.3) are

not shown. (n.b. for both sets of results it is possible that the actual stress could be anywhere within the range shown by the error bars on the x-axis. However the assessments in section 5.3.2 indicate that the actual stress is more likely to be at the top end of the possible stress range and so this is where the trend lines are shown).

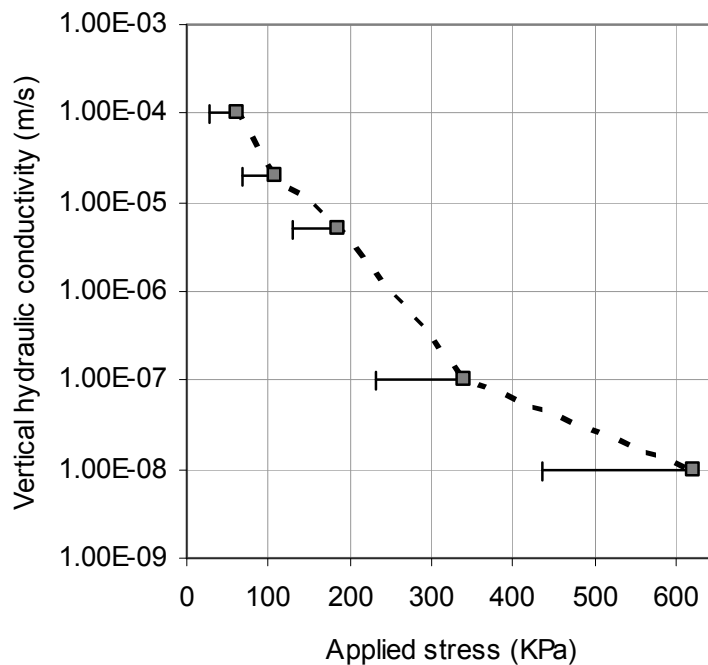


Figure 7.11 AG2 Vertical hydraulic conductivity

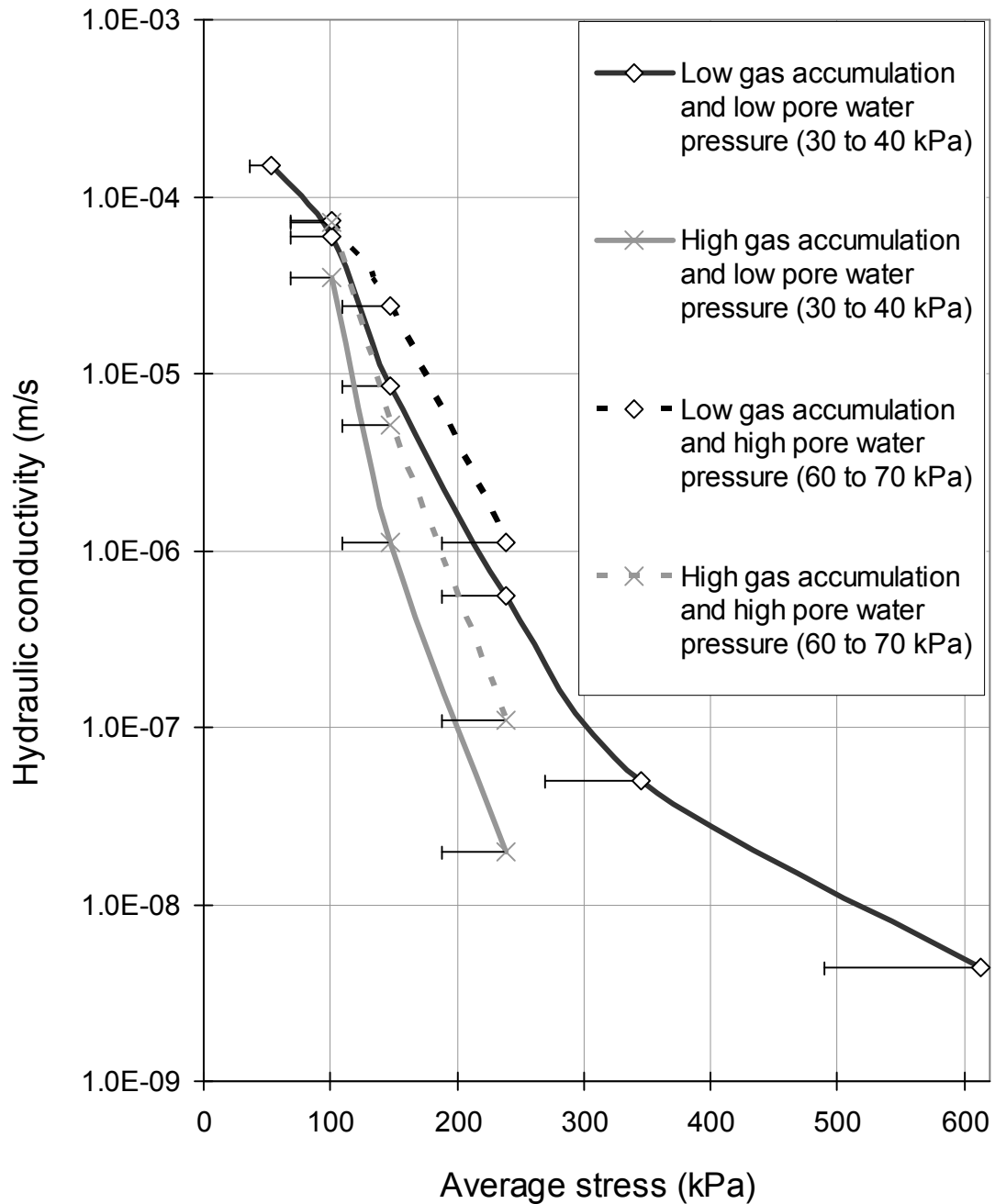


Figure 7.12 DN1 vertical hydraulic conductivity results

## 7.5 Discussion

### 7.5.1 Comparison of hydraulic conductivity results with previous research

Figure 7.13 shows the average vertical hydraulic conductivity values for samples AG2 and DN1 compared with those undertaken by Beaven (2000). The Beaven results are used as a comparison as these are the most comprehensive data sets available. As observed in section 2.4.4, stress is the main factor controlling hydraulic conductivity. Waste type appears to have some influence; for example the hydraulic conductivity of pulverised waste (PV1) in which large items would have been reduced in size, exhibits (as may generally be expected for samples of smaller particle size) lower hydraulic conductivities than crude unprocessed waste (DM3). At low stresses (up to 100 kPa) the hydraulic conductivity of samples AG2 and DN1 are similar to the Beaven data. At higher stresses, the hydraulic conductivity of both samples become significantly lower than those tested by Beaven, reducing to  $1 \times 10^{-8}$  m/s for sample AG2, and even less for sample DN1.

Published waste hydraulic conductivities reviewed by Oweis *et al.* (1990) (section 2.3) give little support for hydraulic conductivity as low as this (evaluations ranging from  $1.5 \times 10^{-6}$  to  $2 \times 10^{-4}$  m/s), and neither does the results of pumping tests by Burrows *et al.* (1997) for which hydraulic conductivities ranged from  $3.9 \times 10^{-7}$  and  $6.7 \times 10^{-5}$  m/s. However other data indicates that waste hydraulic conductivity can be much lower. A review of waste hydraulic conductivities by Jain *et al.* (2006) gave laboratory measurements as low between  $1 \times 10^{-8}$  m/s. Waste hydraulic conductivity values at the bottom of a landfill of  $1 \times 10^{-9}$  m/s were indicated by Bleiker *et al.* (1993).

The hydraulic conductivities of sample AG2 should be comparable with sample AG1 (obtained from the same landfill), and sample DN1 would be expected to be similar to processed wastes PV1. It will be observed from Figure 5.8 that densities were higher for AG2 than AG1, and DN1 higher than PV1. This is likely to have arisen from the prolonged (in comparison to the tests undertaken by Beaven) compression stages that AG2 and DN1 were subjected to and may account, at least in part, for the lower hydraulic conductivities attained. A further likely cause of low hydraulic conductivity

measurements is residual gas within the waste. This is particularly likely for sample DN1 as gas accumulation was allowed to take place at each compression stage. It is probable that residual gas remained after purging, particularly at reduced hydraulic conductivity at higher stresses (the ineffectiveness of an upward flow of water through a soil to remove trapped air was observed by Christiansen, 1944). Gas accumulation may also have affected sample AG2 as some gas activity from the sample was noted on occasions. This, coupled with the higher densities, appears to be a likely explanation for the low hydraulic conductivity values at high stress.

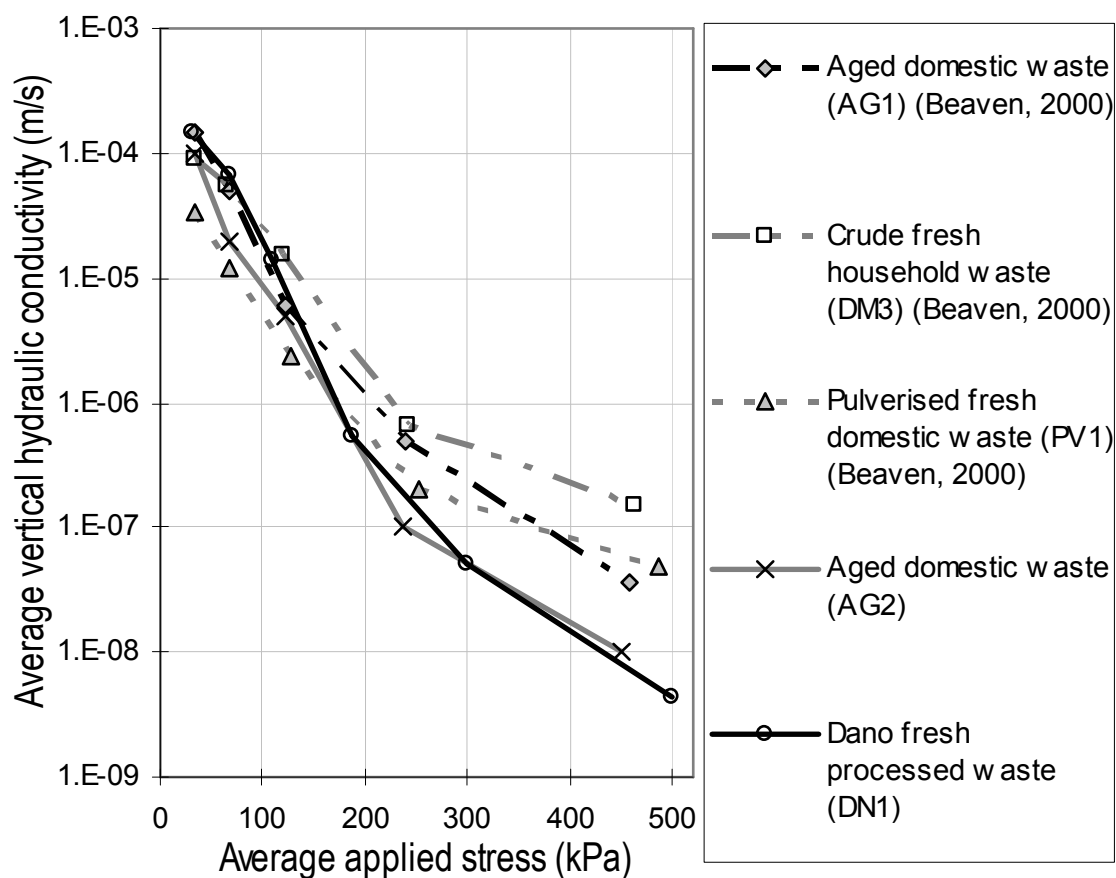


Figure 7.13. Hydraulic conductivity values measured for samples AG2 and DN1 compared with data from Beaven (2000). *n.b. to allow comparisons to be made, average stresses for all samples have been calculated using the same method to take into account the loss of transmitted stress arising from sidewall friction (Beaven, 2000, section 5.3.2). However the method used in this thesis (section 5.3.2) indicates that this overestimates the effects of sidewall friction*

### 7.5.2 The effect of pore water pressure on hydraulic conductivity

During hydraulic conductivity tests, the effective stress in the sample could potentially be reduced by high pore water pressure used in the tests. This is discussed in the appendices (Appendix E). It is concluded that as sample volume is held constant by the fixed position of the top platen (section 5.3.1), effective stress would remain unchanged. This requires qualification as small movements of the sample (usually not more than a few millimetres) were detected during the vertical flow tests by the magnetic extensometer system (section 5.2.1) indicating that some localised changes in effective stress occurred. Most movement occurred in the middle region of the sample at low applied stress (this was particularly evident in the high flow rate gas flushing which were not used to assess vertical hydraulic conductivity - the actual tests were run with as small a possible difference between inlet and outlet heads). This, as well as the possible compressive effect of pore water pressure on accumulated gas in the sample (section 7.4), may account for some of the differences in measured hydraulic conductivity with sample depth shown in Figures 7.5 to 7.10.

## 7.6 Summary of physical and hydraulic property results

Summaries of the results of the settlement, density, drainable porosity and vertical hydraulic conductivity tests are shown for the two samples in Tables 7.1 and 7.2. Dry density only is shown for AG2 as saturated and field capacity densities could not be calculated due to unreliable load cell data. Results for DN1 are much more comprehensive due to separate assessments being made in different pore water pressure and gas accumulated conditions.

Table 7.1. Summary of AG2 test results

Applied stress (kPa)	0	40	87	165	322	603
Minimum stress at base of sample (kPa)	-	28	68	131	232	435
Sample height (mm) drained	2329	2037	1818	1654	1491	1377
Sample height (mm) wet	-	1945	1778	1623	1480	1372
Dry density (t/m <sup>3</sup> )	0.58	0.69	0.75	0.83	0.91	0.98
Drainable porosity	-	17% to 18%	11% to 12%	4% to 6%	1%	-
Vertical hydraulic conductivity (m/s)	-	1.0x10 <sup>-4</sup>	2.0x10 <sup>-5</sup>	5.0x10 <sup>-6</sup>	1.0x10 <sup>-7</sup>	1.0x10 <sup>-8</sup>

Table 7.2 Summary of DN1 test results

Applied stress (kPa)	-	40	87	134	228	334	603
Minimum stress at base of sample (kPa)		22	66	107	177	270	490
Sample height (mm)	2239	1663	1437	1313	1120	1029	933
Water content (WC <sub>wet</sub> ) at field capacity (WC <sub>dry</sub> values shown in brackets)	-	38.5% (62.5%)	35.5% (55.0%)	32.8% (48.7%)	24.0% (31.6%)	20.8% (26.3%)	13.5% (15.6%)
<i>n.b. for full water content details see Table 6.3</i>							
Dry density (t/m <sup>3</sup> )	0.40	0.53	0.62	0.68	0.79	0.86	0.95
Density at field capacity (t/m <sup>3</sup> )	-	0.87	0.96	1.00	1.04	1.09	1.10
Density at low pore water pressure and nominally purged conditions	-	1.02	1.06	1.07	1.08	1.13	-
Drainable porosity in nominally purged conditions and low pore water pressure	-	15.0%	10.2%	6.8%	2.0%	-	-
Drainable porosity in gas accumulated conditions and low pore water pressure	-	5.2%	6.9%	3.2%	0.9%	-	-
Drainable porosity in nominally purged conditions and high pore water pressure	-	-	18.6%	16.6%	13.6%	-	-
Drainable porosity in gas accumulated conditions and high pore water pressure	-	-	11.5%	7.6%	4.6%	-	-
Vertical hydraulic conductivity (m/s) in nominally purged conditions and low pore water pressure	-	-	5.9x10 <sup>-5</sup>	1.2x10 <sup>-5</sup>	5.5x10 <sup>-7</sup>	-	-
Vertical hydraulic conductivity (m/s) in gas accumulated conditions and low pore water pressure	-	-	3.5x10 <sup>-5</sup>	1.5x10 <sup>-6</sup>	2.0x10 <sup>-8</sup>	5.0x10 <sup>-8</sup>	-
Vertical hydraulic conductivity (m/s) in nominally purged conditions and high pore water pressure	-	1.5x10 <sup>-4</sup>	7.3x10 <sup>-5</sup>	2.2x10 <sup>-5</sup>	1.1x10 <sup>-6</sup>	6.0x10 <sup>-8</sup>	4.4x10 <sup>-9</sup>
Vertical hydraulic conductivity (m/s) in gas accumulated conditions and high pore water pressure	-	-	3.1x10 <sup>-5</sup>	4.5x10 <sup>-6</sup>	1.1x10 <sup>-7</sup>	7.0x10 <sup>-8</sup>	-

## 7.7 Summary

Vertical hydraulic conductivity assessments were undertaken for both samples at compression stages with applied stress ranging from 40 kPa to 603 kPa. For sample DN1, hydraulic conductivity was also assessed in different gas accumulation and pore water pressure conditions. The results of this original research demonstrates that these conditions can significantly influence hydraulic conductivity.

The test results show variations in hydraulic conductivity throughout the depth of samples. These were averaged to give an overall bulk vertical hydraulic conductivity for each samples at each compression stage. Comparison of the hydraulic conductivity data for the two samples tested with those from other research shows that the hydraulic conductivities obtained were similar at lower stresses, but lower at higher stresses. Possible reasons for this are discussed.

An estimate for hydraulic conductivity errors of  $\pm 20\%$  has been made based on the evaluation of systematic errors present in the measurement of flow rates, hydraulic gradients and peripheral flow. Reported hydraulic conductivity values may also be affected by variations in temperature and possibly by leachate properties, but these effects will essentially cancel out for  $k_h : k_v$  assessments.

## 8. Horizontal hydraulic conductivity

### 8.1 Introduction

In this chapter a description is given of the procedure for assessing the horizontal hydraulic conductivity of the two waste samples AG2 and DN1 using the Pitsea compression cell (described in chapter 3). This includes the test methodology to induce a horizontal flow of leachate across the samples (section 8.2) and the numerical analysis method adopted (Groundwater Vistas in conjunction with MODFLOW) to assess the horizontal hydraulic conductivity from the horizontal flow rates obtained in the tests (section 8.3). A validation of the MODFLOW model is presented in section 8.4.

The main requirement of the research is met in the presentation of the  $k_h : k_v$  assessments for the two samples in section 8.5. This is the first time that this has been undertaken for unmodified samples subjected to a typical range of landfill overburden stresses. The implications of these findings are discussed (section 8.6). The accuracy of the results is examined, and possible ways of improving the test methodology are suggested (section 8.7).

## 8.2 Methodology to induce horizontal flow across samples

Figure 8.1 shows the general arrangement for a horizontal flow test in the Pitsea compression cell. The top platen seals were inflated during the test to prevent leakage of leachate through the gap between the top platen and cylinder (section 3.3).

Horizontal flow was induced across the sample between the two sets of diametrically opposite ports in the cylinder wall (section 3.4): inflow being through the set connected to the leachate supply tanks and outflow through the opposite set. All eleven sets of ports could be used when the sample was lightly compressed, but in later compression stages the sample height was reduced below the level of the upper sets and so these could not be used.

Each inlet port was connected to individual header tanks (section 3.5 and Figure 3.5) via flexible hose connections. These header tanks were connected to a common supply tank to maintain the same level of leachate in each tank and hence the same pressure head at each inlet port. Outlet pressure heads were governed by the elevation of the outlet inverted u-bends positioned at a common height below the elevation of the header tank water level in order to induce leachate flow across the sample. A more flexible arrangement was adopted for the later sample DN1 tests as used for the vertical hydraulic conductivity tests (section 7.2 , Figures 7.2 and 7.3). This allowed the outlet u-bend elevations to be controlled by switching valves to either 4.00, 5.00, 7.00 or 9.00 m above ground level (a.g.l.). This, in combination with two possible inlet pressure heads using either high or low level header tanks at elevations of 9.37 or 5.31 m a.g.l. respectively, extended the possible range of flow rates that could be used and permitted tests to be carried out at different pore water pressures (section 2.4.7). In all cases the outlet elevation had to be below that of the inlet (to induce horizontal flow) and also above the top of the sample (to maintain the sample in saturated conditions).

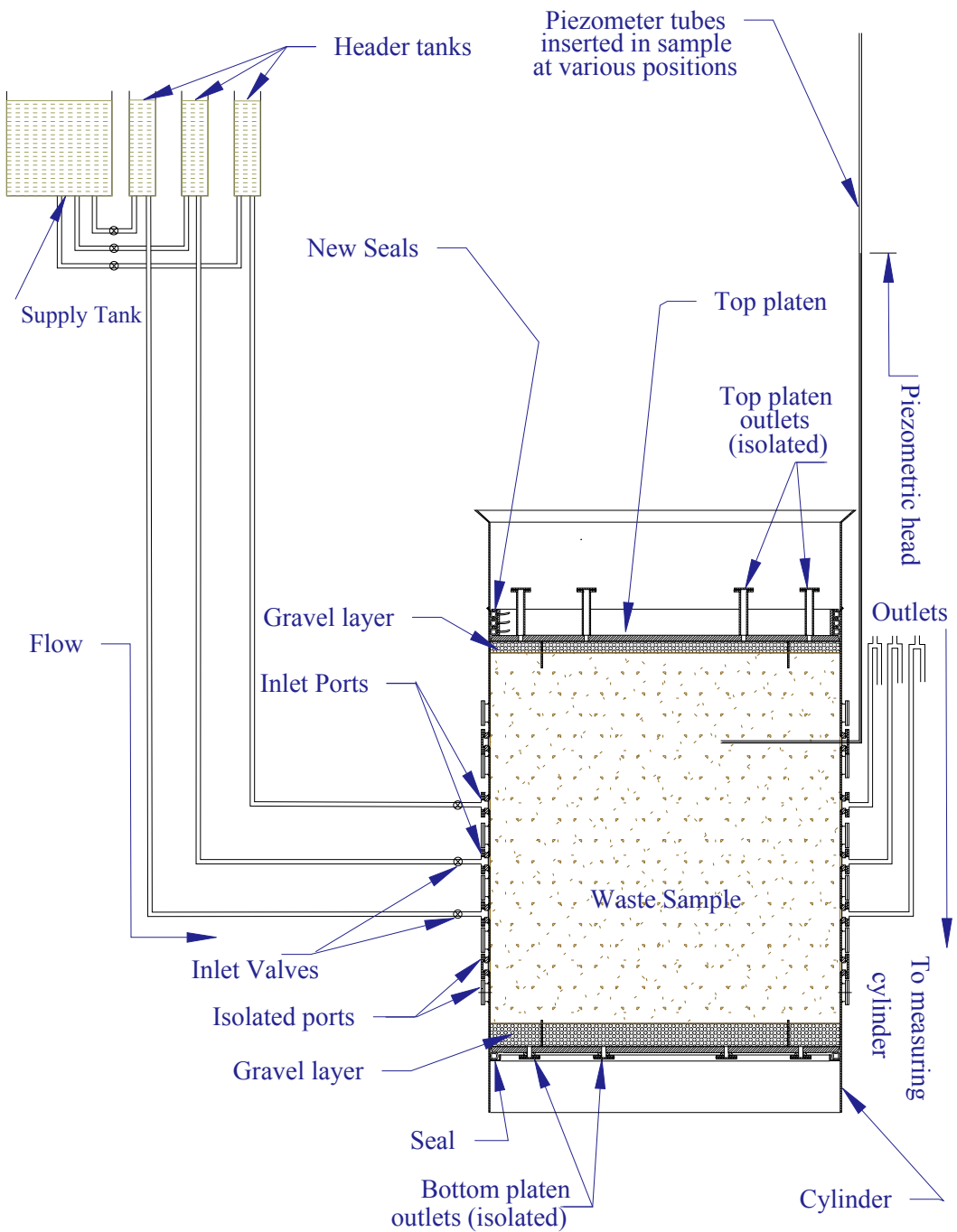


Figure 8.1 Arrangement of confined horizontal hydraulic conductivity test using three inlet and three outlet ports

Inlet flow rates through each horizontal flow port were measured by briefly shutting off the leachate supply to the relevant header tank, and timing the discharge of a measured volume of leachate from the tank. The leachate supply to the tank was then re-established. Outlet flow rates were measured by timing the discharge from each outlet pipe into a measuring cylinder. Inlet and outlet flow rates were compared to ensure steady state conditions had been achieved. At high applied stresses, inlet flow rates became too low to measure using the above method and only stabilised outflow rates were measured.

Pressure heads within the waste were measured using standpipes connected to open-ended piezometer tubes inserted into the sample through ports in the cylinder wall. These were positioned throughout the depth of the sample. In most tests three sets of piezometer tubes were used: one set with the end of the piezometer inserted near the centre of the sample (1 m from the cylinder wall), one set positioned in the vicinity of the inlets, and the other set near to the outlets (typically 30 cm to 50 cm from the cylinder wall). Later tests included piezometer tubes with ends positioned only a few centimetres from the inlets and outlets in an attempt to obtain in greater detail the pattern of head changes in these areas. Other piezometers were incorporated into the inlet pipework at the entry to the inlet ports to enable any head loss between the header tanks and inlet ports to be measured.

Several different tests were carried out at each applied stress using a variety of input and output port configurations. The configurations could be changed not only by varying the head of the inlet and/or outlet ports as described above, but also by changing the number of inlet and outlet ports. A few tests were run with outflow also allowed via the top and bottom gravel layers (which were maintained at the same head as the outlet ports). These are designated as ‘unconfined’ conditions. Normal tests with horizontal flow between the two sets of ports are referred to as ‘confined’.

Following the observations that vertical hydraulic conductivity was significantly affected by gas accumulation and pore water pressure (section 7.4), horizontal flow tests on sample DN1 were carried out in both ‘purged’ and gas accumulated conditions (this was not done on the aged sample AG2 which showed less signs of gas activity). Nominally purged conditions were attained by draining the sample and then inducing an upward

flow of leachate at a high flow rate. Gas accumulated conditions were usually attained by maintaining static saturated conditions for several days, with gas allowed to freely vent from the sample. Measurements of the volume of leachate displaced by gas accumulation and / or changes in sample weight according to load cell measurements were used to determine when gas accumulation had attained a threshold. Flow was then gradually established by opening the control valves in stages. This minimised gas displacement. The final stabilised flow rate was measured (*i.e.* when it was established that no further gas accumulation occurring). The process was carried out in both low and high pore water pressures by using the different header tank and outlet elevations described above. The above method, combined with the similar vertical hydraulic conductivity procedure, allowed separate  $k_h : k_v$  assessments to be made by comparing vertical and horizontal flow results according to gas accumulation and pore water pressure conditions.

### 8.3 Numerical analysis methodology

Inducing a horizontal flow of leachate across the compression cell cylinder (section 8.2) resulted in flow across a non-uniform cross sectional area. As a result the Darcy equation (2.1) used to calculate vertical hydraulic conductivity could not be directly applied to evaluate hydraulic conductivity in the horizontal direction. This situation was encountered by Agaki and Ishida (1994) for assessing the hydraulic conductivity of clays by inducing flow across a modified Shelby between with two diametrically opposite rows of holes (Appendix A, section A3). In this instance hydraulic conductivity was calculated according to the relationship:

$$k = \alpha (q / H) \quad (8.1)$$

where:

$H$  = inlet constant head

$q$  = rate of discharge

$\alpha$  = a constant

The constant  $\alpha$  was estimated to be 4. This was derived from different mathematical, numerical, electrical analogy and experimental assessments. However by the time the research for this thesis was undertaken, hydraulic conductivity across a non-uniform area could be assessed more simply by the use of numerical analyses. The horizontal flow arrangement used in the compression cell was modelled using Groundwater Vistas and the USGS groundwater flow model, MODFLOW (McDonald & Harbaugh, 1988). MODFLOW is a multi-layered numerical groundwater model simulating steady state or non-steady (transient) flow. Each layer comprises a number of rectangular cells that are designated with the appropriate hydrogeological properties. Flow in each layer is two-dimensional but layers are linked to create a three-dimensional representation of flow. Flow through the system is solved using a finite-difference approximation to the governing finite difference equations. Groundwater Vistas by Environmental Simulations Limited (version 1.99c) was used in conjunction with MODFLOW as a pre-processor to create MODFLOW data files and a post-processor for display and analysis of the MODFLOW output files.

MODFLOW was selected as this was a validated model which, by using multiple layers, could be used to give a 3D representation of the compression cell (validation of the compression cell representation is described in section 8.4.2). MODFLOW was suited to the saturated conditions of the tests undertaken, thus avoiding the complexity of models such as SEEP. Although designed for assessing groundwater flow over large areas, the same basic equations apply regardless of scale (there are no set units for distance or time) and MODFLOW should therefore be equally valid for small as well large scale applications.

The compression cell was represented in the MODFLOW model using up to 50 layers, each layer representing a vertical height of 5 cm (Figure 8.2). This allowed a maximum sample height of 2.5 m to be modelled (including gravel layers). The 5 cm layer height was convenient for representing most features of the compression cell; for example the 15 cm vertical spacing of the inlet and outlet ports equated to intervals of three layers. Where a feature did not coincide with the top and bottom of the standard 5 cm thick layer, the relevant layer was divided into two. Each layer consisted of a grid of  $52 \times 52$  cells. Each cell represented a  $4 \text{ cm} \times 4 \text{ cm}$  square to give the 2 metre diameter of the

cylinder (50 x 4 cm + two boundary layer condition cells). This grid size was also convenient for features such as the 20 cm offset between the columns of ports (section 3.4).

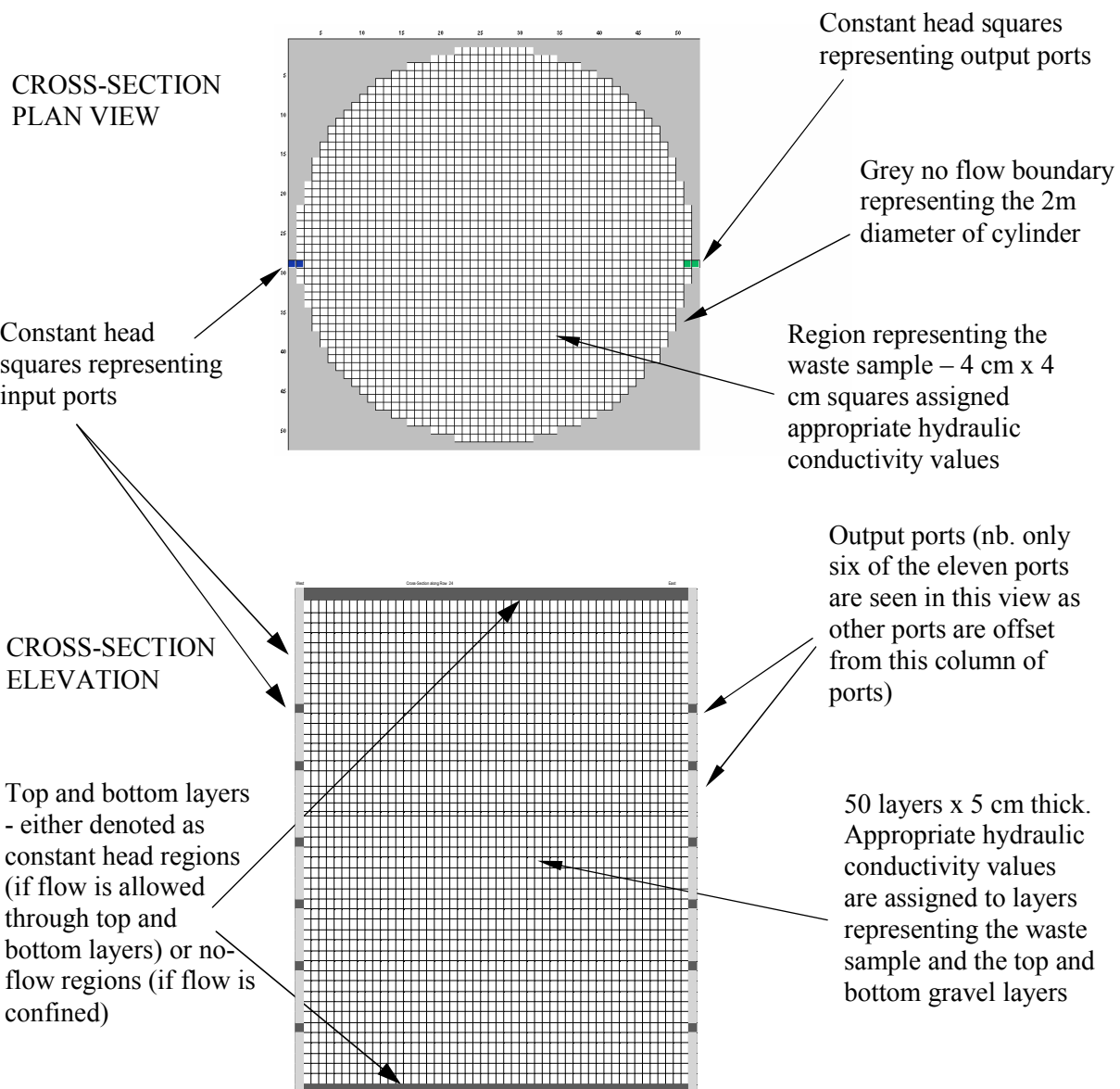


Figure 8.2 Grid representation of the compression cell using MODFLOW

The cylinder wall was represented in all layers by denoting cells lying on or outside the 2 m diameter of the cylinder as no-flow boundary cells, as were the layers representing the boundary of the top and bottom platen for confined (but not unconfined) tests. Cells representing the inlet and outlet ports were designated as constant head cells. Two cells (with a combined area of 4.00 cm<sup>2</sup>) were used to represent each inlet and outlet port (actual area of 4.07 cm<sup>2</sup>). The head at the inlet cells was set to that of the leachate level in the header tanks (centimetres above ground level, a.g.l.). The head at the outlet cells was set to the elevation of leachate in the inverted u-bend of the outlet pipes (cm a.g.l.). In unconfined tests, the cells in the layers representing the top and bottom outlets were designated as constant head cells.

The procedure for each  $k_h : k_v$  assessment was to run several numerical analyses under steady state flow conditions. Each cell in the active part of the model (representing the waste sample) was assigned a vertical and horizontal hydraulic conductivity value – the vertical hydraulic conductivity being the average value determined by vertical hydraulic conductivity tests (section 7.4). Cells representing the gravel layers were generally assigned an isotropic hydraulic conductivity value of 0.1 m/s (a range of 0.1 to 1 m/s is given for clean gravel in Powrie, 1997). Each analysis run used a different single horizontal hydraulic conductivity value that was typically between 4 times and 10 times the vertical hydraulic conductivity value as a first estimate. These produced a range of possible horizontal flow rates related to the horizontal hydraulic conductivity value used. The horizontal hydraulic conductivity of the sample was deduced by matching the flow rate from the analysis to that obtained in the test (this often entailed re-running analyses with a horizontal hydraulic conductivity value above or below the first estimate in order to attain a match with the actual flow rate).

A cross sectional view of a typical analysis showing the head contour pattern is given in Figure 8.3. Flow direction is not shown but would be perpendicular to the contours (the flow direction for each cell could be displayed but is too small to show in the figure). Total flow through the sample could be obtained either as a total for the whole model, or from the sum of flow rates shown for each individual input or output constant head square.

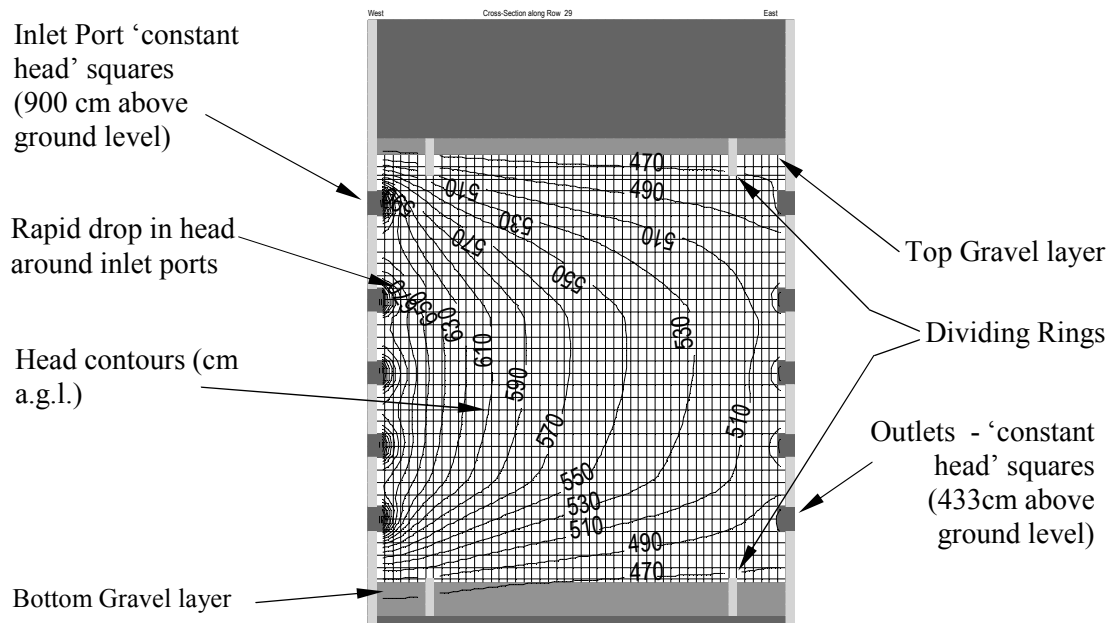


Figure 8.3 Cross sectional numerical analysis of an unconfined horizontal hydraulic conductivity test with 9 inlet and 9 outlet ports (only 5 seen on this view due to port offset) and outflow via the top and bottom of the sample

## 8.4 MODFLOW validation

Although MODFLOW is intended for groundwater applications possibly covering several kilometres, use of MODFLOW for small scale applications such as the compression cell tests described in this thesis should be valid as the same principles apply regardless of scale (the MODFLOW grid size is dimensionless). However some compromises were made in the depiction of the compression cell arrangement; for example the stepped representation of the compression cell walls and the use of squares to represent the round inlet and outlet port orifices. In order to validate this arrangement, two situations were represented. The first depicted one of the vertical flow hydraulic conductivity tests (section 8.4.1), for which the vertical flow rate given by MODFLOW could be compared with that measured in the test. For the second validation method, MODFLOW was used to represent a central drawdown well in the compression cell (section 8.4.2). For a given extraction rate, the drawdown of the phreatic surface obtained using MODFLOW were compared with those calculated using a standard mathematical model

### 8.4.1 Validation using simple vertical flow analysis

The hydraulic conductivity values obtained throughout the depth of waste sample DN1 in an upward flow vertical hydraulic conductivity test conducted at an applied stress of 134 kPa are shown in Table 8.1. The hydraulic conductivity values were calculated using Darcy's law (section 2.2) for a measured flow rate of 510 l/h. Some differences are apparent between the results given by the three sets of piezometers and an average value is shown in the right hand column.

Table 8.1 Hydraulic conductivity values obtained in a vertical hydraulic conductivity test for sample DN1 at an applied stress of 134 kPa.

Elevation (mm above ground level)	Hydraulic conductivity (m/s)			
	A Ports	B Ports	C Ports	Average
2031-2220	1.07E-05	1.74E-05	1.22E-05	1.34E-05
2220-2520	2.25E-05	1.33E-05	1.28E-05	1.62E-05
2520-2820	9.08E-06	1.00E-05	1.31E-05	1.07E-05
2820-3220	1.27E-05	1.73E-05	1.94E-05	1.65E-05
3220-3344	1.40E-04	1.26E-05	8.88E-06	5.37E-05

The test was represented using MODFLOW as described in section 8.3 using no-flow cells to represent the cell walls and top and bottom dividing rings. Horizontal flow ports were isolated during the test and the corresponding cells were changed to no-flow cells. Sample height and gravel layer thicknesses were represented by the appropriate number of layers; each layer representing a depth of 5 cm (some layers are divided to obtain the correct depths). The squares in the bottom layer were assigned a constant head value of 937 cm to represent the inlet head of 9.37 m above ground level (a.g.l.). The squares comprising the layer immediately above the top of the top gravel layer were given a constant head value of 502 cm to represent the outflow head of 5.02 m a.g.l. Layers representing the waste sample are assigned the appropriate average hydraulic conductivity values shown in Table 8.1.

In Figure 8.4 a cross-section of the analysis for the vertical flow test is shown. The total flow rate given by the analysis was 565 l/h. This is about 10% higher than the actual test result of 510 l/h. The cause of this difference is not readily apparent; the only reason immediately evident for there being low flow in the test would be a reduction in the inlet head arising from frictional loss in the inlet pipework. The piezometer readings in the test indicated that inlet head loss was negligible (less than 4 cm) and hence this was disregarded for the MODFLOW analysis. A head loss of about 40 cm would have been required to reduce the total flow rate of the MODFLOW simulation to that obtained in the test (reducing the inlet head in the analysis to 900 cm gave a flow rate of 516 l/h). Therefore the results of the vertical flow verification method indicate that the MODFLOW representation used gives approximately a 10% over-estimate of flow rates.

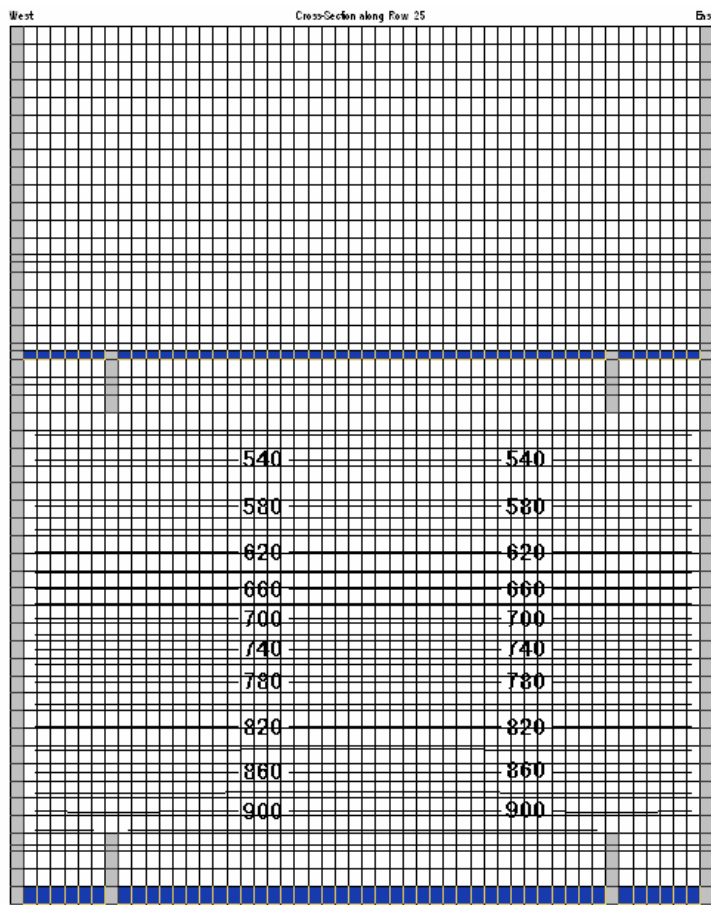


Figure 8.4 Section of vertical flow validation analysis

#### 8.4.2 Validation using well drawdown analysis

In this validation exercise, MODFLOW was used to represent a drawdown well in the centre of the compression cell. The compression cell arrangement was used as described in section 8.3 but in order to represent a confined aquifer of infinite extent the squares representing the cell walls were denoted as constant head squares (600 cm) and the top and bottom layers as no-flow boundaries. All cells within these boundaries were designated an arbitrary hydraulic conductivity value of  $1 \times 10^{-4}$  m/s. A central drawdown well of 10 cm diameter was added on all layers.

Two analyses were run: one for a pumping rate of 131 cm<sup>3</sup>/s and one at 1049 cm<sup>3</sup>/s. These pumping rates were selected to give a small (25 cm) and large (200 cm) drawdown over the sample depth of 250 cm and were calculated using the relationship:

$$Q = \frac{2 \pi H k \delta h}{\ln(R/r)} \quad (8.2)$$

where:

$Q$  = flow rate (cm<sup>3</sup>/s)

$H$  = depth of waste (250 cm)

$k$  = hydraulic conductivity (cm/s)

$\delta h$  = drawdown (cm)

$R$  = radius of cell (100 cm)

$r$  = radius of well (5 cm)

The plan view of the analyses are shown in Figures 8.5 and 8.6

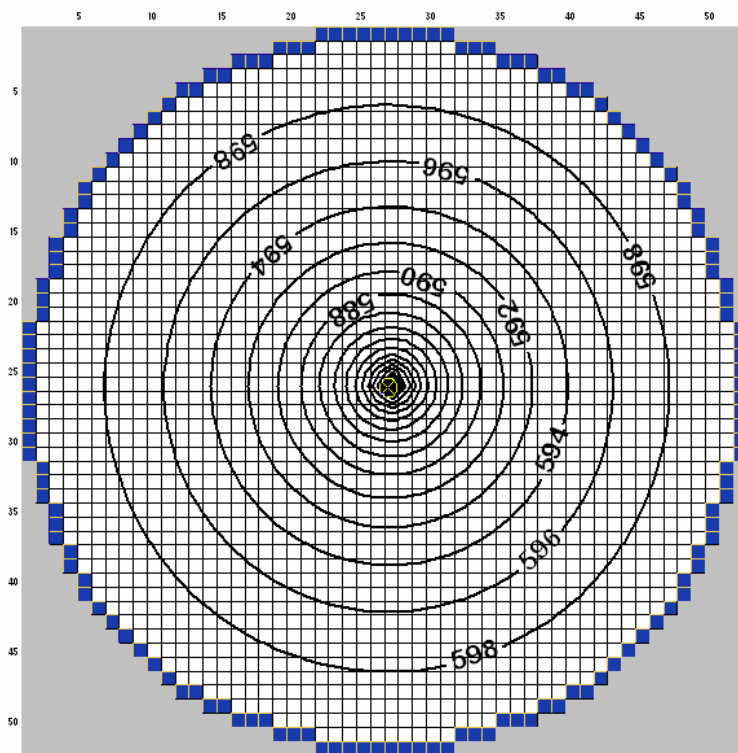


Figure 8.5 Drawdown validation test simulating central well in compression cell with a pumping rate of 131 cm<sup>3</sup>/s.

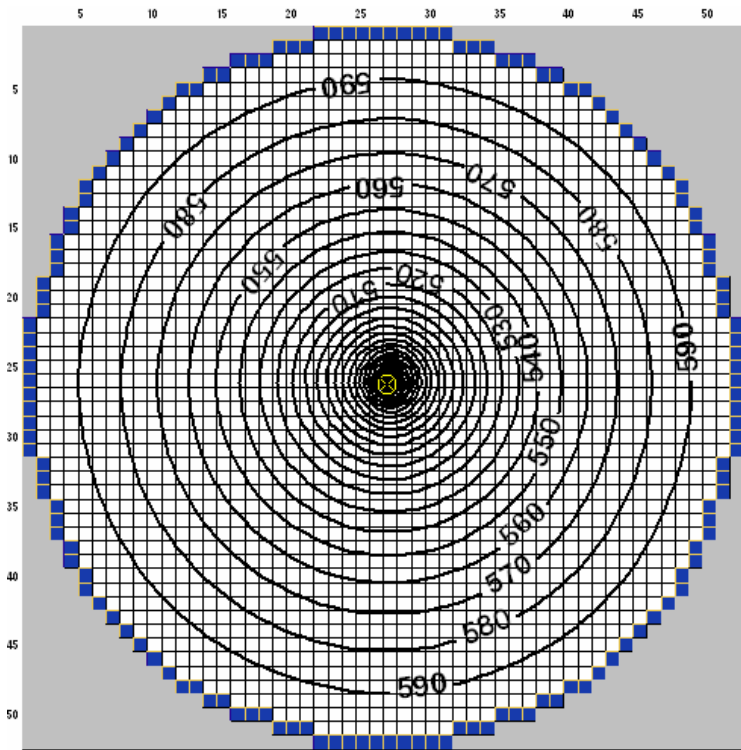


Figure 8.6 Drawdown validation test simulating central well in compression cell with a pumping rate of  $1049 \text{ cm}^3/\text{s}$

For both pumping rates the drawdown was calculated using equation 8.2 for several points between the centre and edge of the simulation. Comparisons were made with the drawdowns shown by the analyses and these are plotted in Figures 8.7 and 8.8.

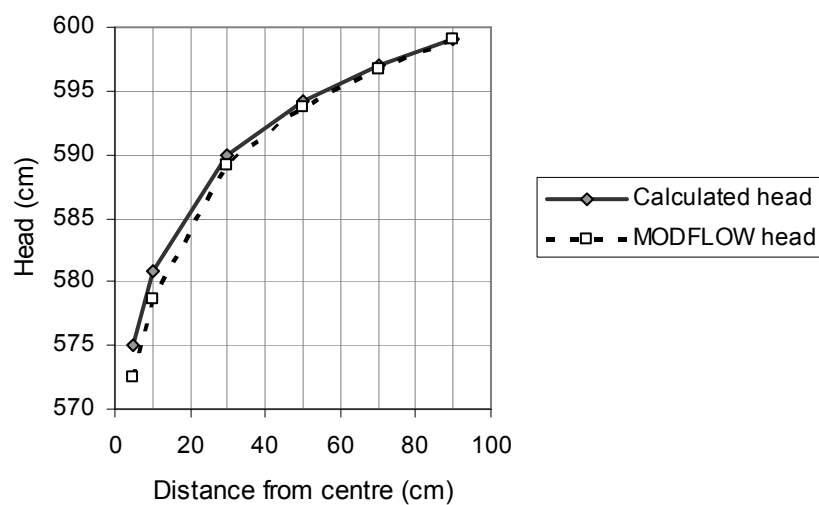


Figure 8.7 Comparison of MODFLOW and calculated drawdown for a pumping rate of  $131 \text{ cm}^3/\text{s}$ .

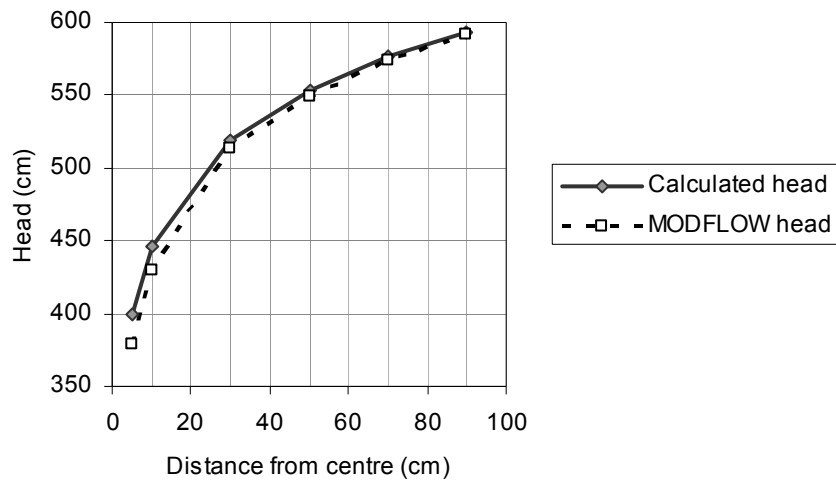


Figure 8.8 Comparison of MODFLOW and calculated drawdown for a pumping rate of  $1049 \text{ cm}^3/\text{s}$ .

Although the drawdowns in Figures 8.7 and 8.8 are similar, it is evident on both plots that those obtained using MODFLOW are marginally greater than the calculated drawdowns. To obtain a close match it was necessary to increase the flow rate used in the calculation by about 9 % (to 145 and 1150 l/h for the two examples respectively).

#### 8.4.3 Observations of the validation results

The validation process described above compared the results obtained from the MODFLOW representation of compression cell with calculated and test results. Both vertical flow (section 8.4.1) and essentially horizontal flow (section 8.4.2) were represented. The comparisons gave similar results but in both cases MODFLOW appeared to overestimate the flow rate for the given conditions by about 10%. The cause of this is not clear but would result in an underestimation of the horizontal hydraulic conductivity in the final  $k_h : k_v$  analysis. This apparent error has been included in Table 8.4 (list of potential causes of error in the  $k_h : k_v$  assessment process).

## 8.5 Results

The results of the horizontal flow tests are shown below in Tables 8.2 for sample AG2 and Table 8.3 for sample DN1. Details given indicate for each test:

- whether horizontal flow was confined (outlet via horizontal flow outlet ports only) or unconfined (outlet via horizontal flow ports and top and bottom platens)
- the head at the inlet and outlet ports (in centimetres above ground level) according to the elevation of the inlet header tanks and outlet overflow height. (actual heads at the ports may be affected by frictional losses in the pipework as discussed in Appendix F. Analyses corrected for this are indicated in the table)
- the number of horizontal inlet and outlet flow ports used
- the total horizontal flow rate
- the vertical hydraulic conductivity value (from the vertical hydraulic conductivity tests) used in the numerical analyses (Tables 7.1 and 7.2)
- the calculated  $k_h : k_v$  ratio
- the horizontal hydraulic conductivity according to the calculated  $k_h : k_v$  ratio

The vertical hydraulic conductivities and the calculated horizontal hydraulic conductivities for both samples are plotted in Figure 8.9. Separate hydraulic conductivities are shown for gas purged and gas accumulated conditions for sample DN1 where available. Results for low pore water pressure tests are not plotted for reasons of clarity and limited data. Hydraulic conductivity values are plotted against applied stress and no error bars are shown on the stress or hydraulic conductivity values for reasons of clarity. No horizontal hydraulic conductivity data is shown above an applied stress of 334 kPa as horizontal flow could not be reliably achieved at higher stresses.

Table 8.2 Summary of AG2 horizontal hydraulic conductivity tests

Test no.	Confined/ unconf'd	Inlet head (cm a.g.l.)	Outlet head (cm a.g.l.)	No. of inlet ports	No. of outlet ports	Flow rate (l/h)	Vertical hydraulic conductivity (m/s)	$k_h : k_v$ ratio	Calculated horizontal hydraulic cond. (m/s)
Average applied stress 87 kPa									
10	confined	900	460	9	9	666	$2.0 \times 10^{-5}$	4.8	$9.0 \times 10^{-5}$
12	confined	900	460	3	9	456	$2.0 \times 10^{-5}$	6.4	$1.3 \times 10^{-4}$
Average applied stress 165 kPa									
15	confined	900	460	9	9	10.2	$5.0 \times 10^{-6}$	1.6	$7.5 \times 10^{-6}$
Average applied stress 322 kPa									
23	unconf'd	900	460	3	3	6.0	$1.0 \times 10^{-7}$	14	$1.4 \times 10^{-6}$
24	unconf'd	900	460	1	1	1.7	$1.0 \times 10^{-7}$	9.2	$9.2 \times 10^{-7}$
25	conf'd	900	460	3	3	1.9	$1.0 \times 10^{-7}$	6.6	$6.6 \times 10^{-7}$
Average applied stress 603 kPa									
28	confined	900	460	3	3	0.2	$1.0 \times 10^{-8}$	9.0	$9.0 \times 10^{-8}$

Table 8.3 Summary of DN1 horizontal hydraulic conductivity tests

Test no.	Confined/ unconf'd	Inlet head (cm a.g.l)	Outlet head (cm a.g.l)	No. of inlet ports	No. of outlet ports	Flow rate (l/h)	Vertical hydraulic conductivity (m/s)	$k_h : k_v$ ratio	Calculated horizontal hydraulic conductivity (m/s)
Average applied stress 40 kPa									
37	confined	937+	400	4	4	3456	$1.5 \times 10^{-4}$	6.1	$9.2 \times 10^{-4}$
39	confined	937+	700	4	4	1614	$1.5 \times 10^{-4}$	6.3	$9.5 \times 10^{-4}$
40	confined	937	900	4	4	343	$1.5 \times 10^{-4}$	8.0	$1.2 \times 10^{-3}$
41	confined	533	500	4	4	306	$1.5 \times 10^{-4}$	8.0	$1.2 \times 10^{-3}$
42	confined	533	400	4	4	846	$1.5 \times 10^{-4}$	6.0	$9.0 \times 10^{-4}$
43	confined	937+	400	6	6	5424	$1.5 \times 10^{-4}$	6.5	$9.8 \times 10^{-4}$
Average applied stress 87 kPa									
56	confined	937	700	6	6	914	$7.3 \times 10^{-5}$	5.0	$3.7 \times 10^{-4}$
62*	unconf'd	937+	700	4	4	875	$3.1 \times 10^{-5}$	10.0	$3.1 \times 10^{-4}$
65*	unconf'd	937+	700	4	4	712	$3.1 \times 10^{-5}$	7.7	$2.4 \times 10^{-4}$
66*	unconf'd	533	500	4	4	87.6	$3.5 \times 10^{-5}$	6.0	$2.1 \times 10^{-4}$
67*	unconf'd	533	500	4	4	78.9	$3.5 \times 10^{-5}$	5.3	$1.9 \times 10^{-4}$
69*	confined	533	400	4	4	230	$3.5 \times 10^{-5}$	6.5	$2.3 \times 10^{-4}$
Average applied stress 134 kPa									
71*	confined	533	400	4	4	13.7	$1.5 \times 10^{-6}$	10.0	$1.5 \times 10^{-5}$
73	confined	937	700	4	4	274	$2.2 \times 10^{-5}$	7.5	$1.7 \times 10^{-4}$
77*	confined	937	700	4	4	31.2	$4.5 \times 10^{-6}$	4.5	$2.0 \times 10^{-5}$
79*	unconf'd	937	700	4	4	77.1	$4.5 \times 10^{-6}$	5.2	$2.3 \times 10^{-5}$
83	confined	937	900	4	4	27.5	$2.2 \times 10^{-5}$	4.3	$9.5 \times 10^{-5}$
Average applied stress 228 kPa									
90	confined	937	900	3	3	1.92	$1.1 \times 10^{-6}$	9.0	$9.9 \times 10^{-6}$
91	unconf'd	937	700	3	3	23.1	$1.1 \times 10^{-6}$	9.5	$1.1 \times 10^{-5}$
91a	unconf'd	937	700	4	4	33.6	$1.1 \times 10^{-6}$	11	$1.2 \times 10^{-5}$
Average applied stress 334 kPa									
97	confined	937	500	4	3	1.26	$5.0 \times 10^{-8}$	6.8	$4.8 \times 10^{-7}$
98	confined	937	700	4	3	0.88	$5.0 \times 10^{-8}$	12.3	$8.6 \times 10^{-7}$

\* = run in gas accumulated conditions

+ = adjustment for head loss in pipework included in analysis (Appendix F)

note: tests with inlet heads of 900 or 937 cm a.g.l. are referred to as high pore water pressure tests, those with 533 cm a.g.l. inlet heads are low pore water pressure tests. Vertical hydraulic conductivity values are shown for tests in comparative pore water pressure conditions (except sample DN1 at 40 kPa applied stress where all vertical flow tests were conducted in high pore water pressure conditions).

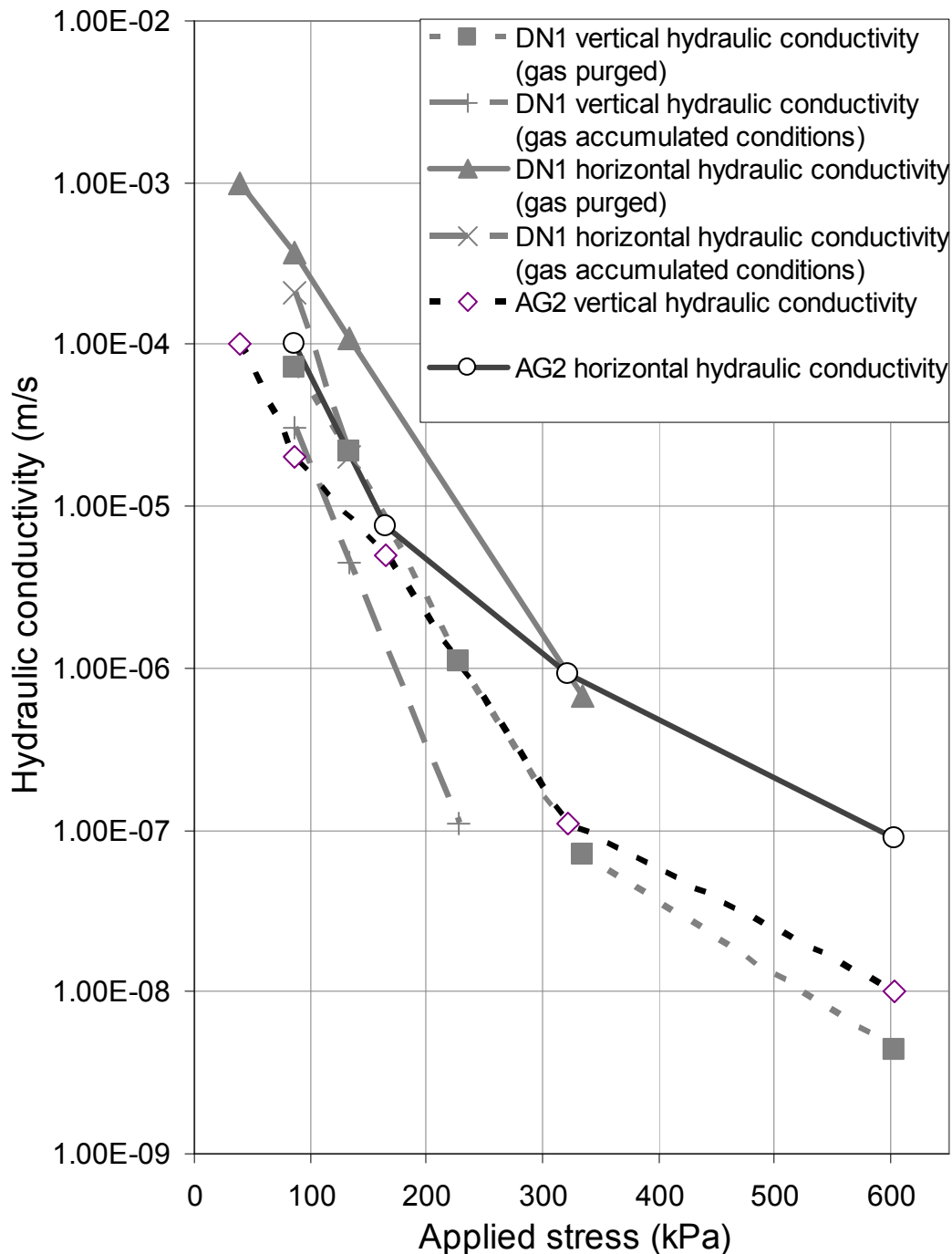


Figure 8.9 Comparison of vertical and horizontal hydraulic conductivity for sample AG2 and DN1

Figures 8.10 and 8.11 show the horizontal hydraulic conductivity results expressed as a ratio to the vertical hydraulic conductivity (as shown in Tables 8.2 and 8.3) for the two samples, plotted against applied stress. Error bars are shown for the  $k_h : k_v$  ratios as shown in section 8.6.3. In Figure 8.11 tests conducted in gas accumulated conditions are shown with white markers (these are limited to tests conducted at applied stresses of 87 and 134 kPa as no gas accumulation tests were conducted at 40 kPa and flow was too erratic in tests at higher stresses). Although both vertical and hydraulic conductivity were significantly lower in gas accumulated conditions than nominally purged conditions (Figure 8.9), the  $k_h : k_v$  ratios for both conditions are similar. This indicates that gas accumulation has no significant effect on  $k_h : k_v$  ratio.

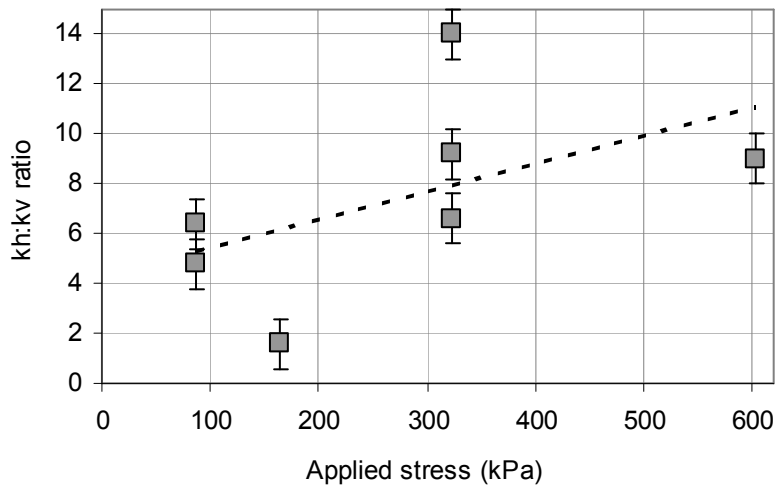


Figure 8.10  $k_h : k_v$  assessments for sample AG2

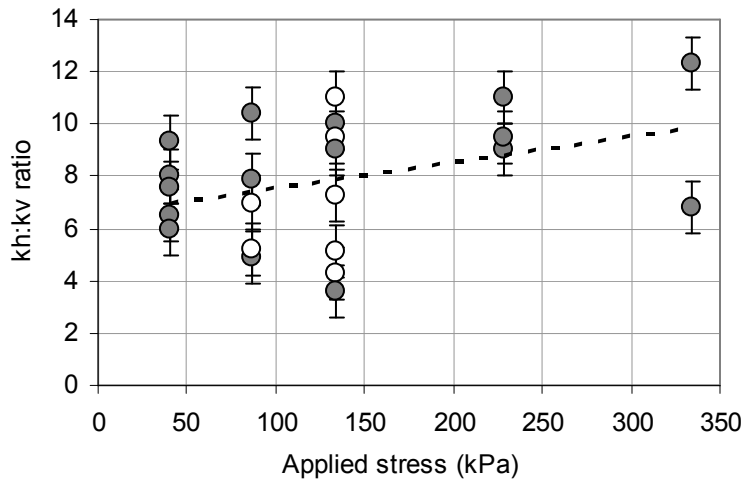


Figure 8.11.  $k_h:k_v$  assessments for sample DN1

(nb. unshaded markers indicate tests run in gas accumulated conditions)

Hydraulic conductivities at different pore water pressures are not shown as there are insufficient horizontal hydraulic conductivity data available. The limited data again indicates that  $k_h:k_v$  ratios are not affected by pore water pressure changes. For example, two tests (Tests 40 and 41 in Table 5.2) were conducted at different average pore water pressures (average about 20 kPa and 50 kPa respectively) in nominally purged conditions. The flow rate for each test was different but both flow rates equated to a  $k_h:k_v$  assessment of 8.0 when compared to the relevant vertical hydraulic conductivities measured in similar pore water pressures. At higher stresses the results between comparative tests were less consistent, and at an applied stress of 228 kPa large inconsistencies were evident (for example one test gave a  $k_h:k_v$  ratio of 22 in a low pore water pressure test and 9.5 in a higher pore water pressure test) and several test results (including this example) had to be discounted.

## 8.6 Discussion

### 8.6.1 Results overview

The  $k_h:k_v$  ratio plots (Figures 8.10 and 8.11) for the two waste samples tested indicate that landfilled wastes do exhibit intrinsic anisotropies. Horizontal hydraulic

conductivity is between five to ten times greater than vertical hydraulic conductivity. Several authors have previously anticipated that such anisotropy exists (section 2.5), but the research described in this thesis is the first to systematically demonstrate that this is so.

The results also demonstrate that:

***anisotropy increases with stress.***  $k_h:k_v$  ratios increase from about 5 to 7 at low stress to nearly 10 at high stress for both samples. The only other (limited) previous horizontal and vertical flow tests (Buchanan and Clark, 1997, 2001) concluded that anisotropy *decreased* with stress. The more comprehensive and representative tests undertaken in this thesis have demonstrated that this is not the case and instead supports the conceptual mechanism of preferential horizontal hydraulic conductivity developing further at higher stress as items become increasingly aligned to the horizontal plane and compressible components are deformed (section 2.5).

***$k_h:k_v$  ratios are unaffected by gas accumulation in the waste.*** As discussed in section 7.4 and 7.5, the research described in this thesis has demonstrated for the first time that the hydraulic conductivity of nominally saturated wastes can be significantly affected by gas accumulation in the waste. A further finding of this research is that both vertical and horizontal hydraulic conductivities appear to be affected to a similar degree (Fig 8.9) and so  $k_h:k_v$  ratios are essentially unaffected by gas accumulation (Figure 8.11)

### 8.6.2 Application of results

The findings of this research may be applied to leachate management in both conventional landfills and future sustainable designs. The findings should be particularly beneficial in modelling leachate and contaminant movement in landfills as previously isotropic conditions, or an arbitrary  $k_h:k_v$  ratio, would have been assumed. Two examples mentioned in section 2.5 that use assumed  $k_h:k_v$  ratios are the

modelling of landfill leachate movement by McCreanor and Reinhart (2000) and analyses of leachate pumping wells by Rowe and Nadarajah (1996). The results may also be relevant to flushing contaminants from wastes based on the principle of flushing bioreactor landfills (DoE, 1995, IWM, 1998). Horizontal flow will potentially be greater than vertical flow and so it may be beneficial to induce horizontal flushing particularly in wastes of low hydraulic conductivity.

A basic example of the application of the findings is given in Appendix G for the control of landfill leachate levels by vertical pumping wells. By using the above  $k_h : k_v$  ratios rather than assumed isotropic values, it is found that the number of wells required to maintain given conditions is significantly less. Typically the number of wells required would only be about 10 % to 25 % of the number based on isotropic conditions. This potentially represents a substantial cost saving to the landfill operator.

In applying the results some caution should be exercised as the findings may not be applicable in all circumstances. Particularly it should be appreciated that the  $k_h : k_v$  ratios obtained are for wastes only and do not take into account other landfill features such as boreholes or the inclusion of daily cover layers cases. These may drastically alter flow paths within a waste body. The type of waste type also needs to be considered. The similarity of anisotropy assessments for both fresh processed and aged wastes suggest that values remain essentially unchanged throughout the decomposition process. However  $k_h : k_v$  values of wastes with a different physical structure such as highly processed MBP wastes or unprocessed wastes may be different, as may commercial, industrial or agricultural wastes. It may also be necessary to consider the way that the waste was originally deposited. The method used for loading the samples for this research is considered to be reasonably representative of normal tipping procedure (section 5.2.2). However deposition methods may vary and this could alter the structure, and hence anisotropic flow, through the waste. The stress exerted by on-site compaction plant may also need to be considered.

### 8.6.3 Accuracy of results

The anticipated potential errors for the method used are summarised in Table 8.4. This essentially consists of systematic errors in flow rate measurements combined with the possible errors highlighted by the validation process. Possible errors arising from the numerical analyses were fairly insignificant ( $\pm 0.5\%$ ) and can be disregarded. The effects of permeant temperature and differences between the viscosity and density of water and leachate are effectively cancelled out for the  $k_h : k_v$  assessments as both vertical and horizontal hydraulic conductivity tests were carried out at essentially the same temperature and using the same leachate (although correction may need to be considered for the hydraulic conductivity values stated in Tables 8.2 and 8.3).

These give a total flow rate error range of  $+10\% / -20\%$ . According to the sensitivity plots in Appendix H, this could produce an uncertainty in the  $k_h : k_v$  assessments of about  $+1 / -2$  (*i.e.* the possible range for a test giving a  $k_h : k_v$  ratio of 10 would be  $k_h : k_v$  ratios from 8 to 11).

The variations between the  $k_h : k_v$  ratios of individual tests carried out at the same compression stage for each sample, shown in Figures 8.10 and 8.11, are much greater than this. This is perhaps not surprising considering that the  $k_h : k_v$  ratios are obtained by comparing vertical and horizontal hydraulic conductivities. Both can be significantly influenced by gas accumulation and pore water pressure. The difficulty of establishing the same conditions for both sets of tests will inevitably result in some differences between vertical and horizontal measurements.

Table 8.4. List of potential causes of error in the  $k_h : k_v$  assessment process

Cause of error	Estimated error
Inaccuracies in flow rate measurement (Appendix F )	$\pm 10 \%$ .
Head loss (Appendix F)	0 (corrected)
MODFLOW analyses (Appendix I)	$\pm 0.5 \%$ (negligible)
MODFLOW overestimate of flow rate (section 8.4.3)	- 10 %
Temperature (section 2.4.2, 7.3, 8.6.3)	Compensated
Leachate density / viscosity (section 2.4.2, 7.3, 8.6.3)	Compensated
<b>TOTAL</b>	<b>+ 10 % / -20 %</b>

## 8.7 Recommendations

Although the modified compression cell fulfilled several important test criteria, some shortcomings of the design were apparent during testing. These, and possible remedies to them, are discussed in this section.

### 8.7.1 Suggested improvements to the compression cell design

Perhaps the most serious criticism of the compression cell design was the use of relatively small horizontal flow inlet and outlet ports (the size of the ports being limited in order not to weaken the cylinder – section 3.4). As detailed in Appendix J, flow appeared to have been affected by variations in waste permeability in the vicinity of the ports. Although the effect on flow is assumed to be averaged by the use of several ports in each test it may have been beneficial to conduct two sets of tests for each horizontal flow configuration, reversing the flow in the second test. This would have allowed the flow characteristics of each port to have been investigated but would have required more complex pipework and extended test times.

If further horizontal flow tests were to be carried out in the Pitsea compression cell, it would be worth considering abandoning the horizontal flow ports and replacing them with a pair of larger orifices set diametrically opposite each other in the cylinder wall

(Figure 8.12). Flow through the larger horizontal area would be less susceptible to localised variations in waste hydraulic conductivity. During compression, the orifices in the cylinder would have to be blanked off with a solid curved panel to prevent waste being squeezed out. This could remain in place during vertical hydraulic conductivity tests but removed for the horizontal flow tests. A mesh panel may have to be fitted during the horizontal flow tests to prevent the waste collapsing or being washed out in this area. Suitable strengthening of the cylinder would be required.

A further modification would be to fit gas venting pipes through the top platen to prevent gas build up in the upper regions of the sample during horizontal flow tests. This could potentially reduce flow or divert it through the lower regions of the sample.

The results of some tests had to be excluded from the final  $k_h$ : $k_v$  assessments as exceptionally high flows were evident through the lower ports (Appendix J). It is assumed that leachate flow was short-circuiting from the bottom inlet port, across the bottom gravel layer to the bottom outlet port. This highlights a fundamental problem in the design of bi-planar flow test equipment – how to prevent the distribution layer necessary for flow in one of the planes affecting flow in tests conducted in the other plane. In the compression cell design the use of small ports for the horizontal flow would have been unlikely to affect vertical flow, but it appears that the gravel layers for the vertical flow may have allowed horizontal flow to short circuit in some tests. The above proposed orifice would not be positioned as low as the previous lower ports and this may be sufficient to prevent short circuiting. The path length between inlets and gravel layers could be increased further by confining the top and bottom gravel layer to the area within the dividing ring (Figure 8.12). Consequently gravel could not be used as the distribution medium as its low compressibility would prevent compression of the outer ring of waste. Tyre shreds would probably be suitable, being highly permeable and exhibiting similar compression under load as wastes (Benson *et al.*, 2002, Hudson *et al.*, 2003, 2004). A disadvantage with this arrangement is that installation of samples would be more complicated. Furthermore a component of horizontal flow would be introduced in the vertical hydraulic conductivity test and so numerical analyses, rather than straightforward application of equation 2.1, would be required to determine vertical hydraulic conductivity.

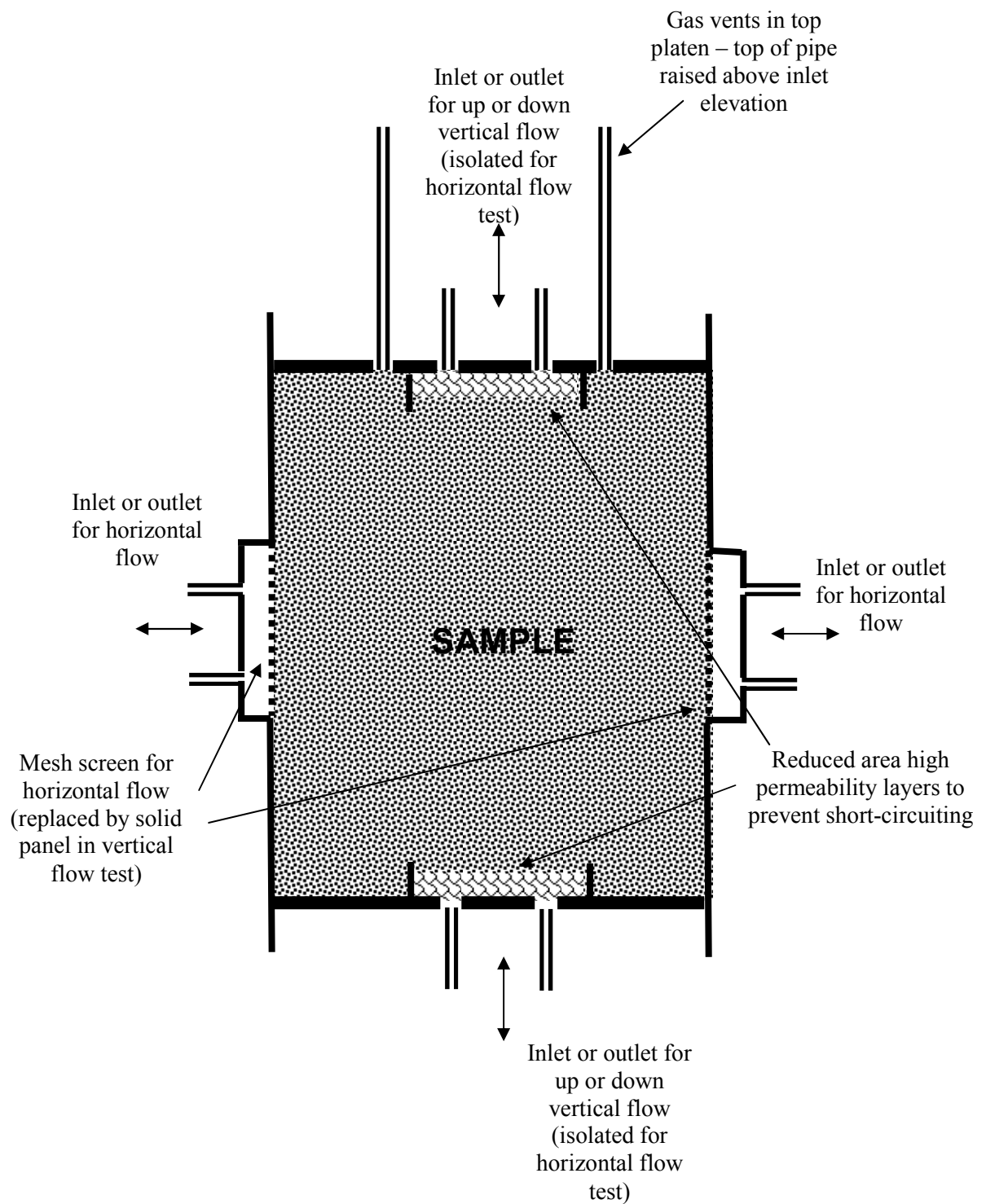


Figure 8.12 Suggested modifications to the Pitsea compression cell for improved horizontal and vertical hydraulic conductivity tests

An alternative method of preventing horizontal flow across the bottom high permeability layers would be to add vertical baffle plates to the bottom platen (Figure 8.13). In effect the top platen already has baffle plates across its diameter (Figure 8.14) and this may be why short-circuiting was not evident across the top gravel layer. A suggested pattern for the bottom platen is shown in Figure 8.13 showing two baffle plates across the existing dividing ring. These would protrude into the samples as shown in Figure 8.15, directing any flow across the bottom gravel layer upwards and back into the waste sample.

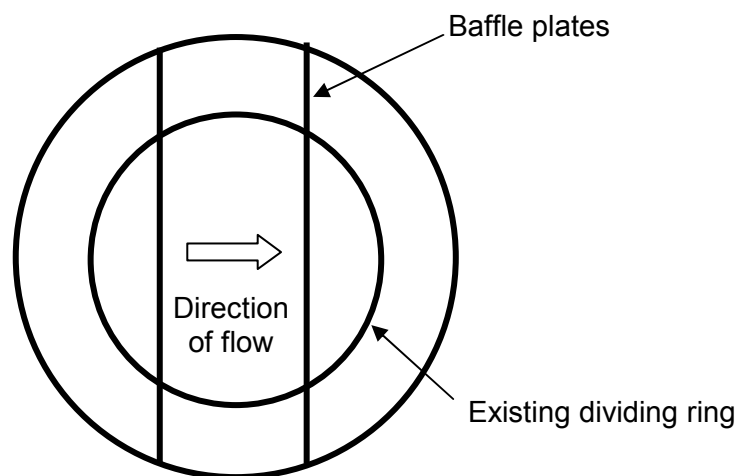


Figure 8.13 Sketch of suggested baffle plate arrangement on bottom platen to prevent short-circuiting via high permeability layer (view from above)



Figure 8.14 Compression cell bottom platen (in fully extended eject position) showing top surface normally covered by the bottom gravel layer. The dividing ring protrudes through the gravel layer into the waste sample

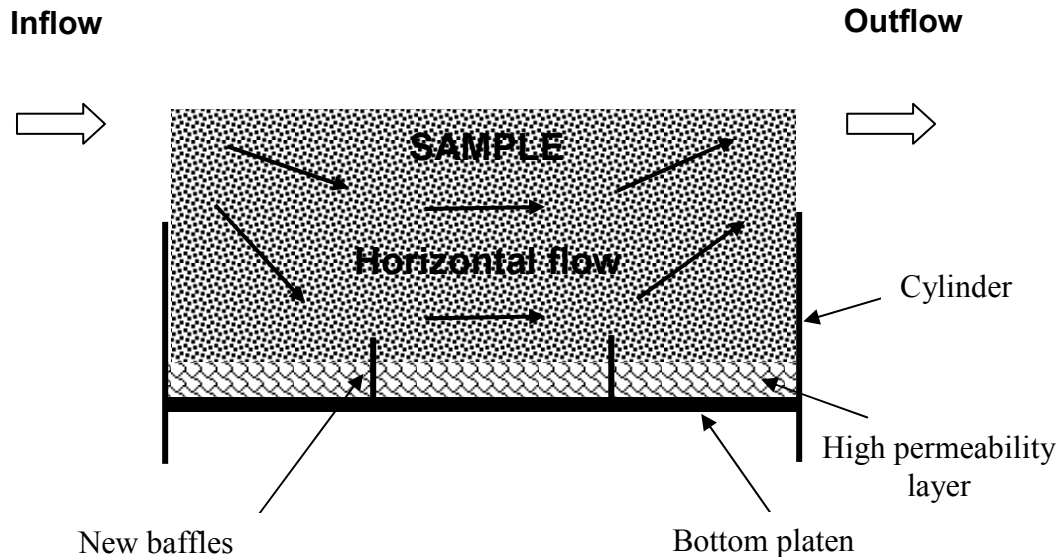


Figure 8.15. Cross section of lower portion of suggested modified arrangement showing baffle plates

### 8.7.2 Alternative methods of obtaining waste samples

In section 2.4.10 it was questioned whether the structure of waste samples were realistically replicated by the loading process described in section 5.2. Of particular concern was the preservation of the structure of the aged waste sample AG2 (section 5.2.2).

An alternative approach may be the use of a large-scale sampling tube as used by Rosqvist (1999). A 1.93 m diameter x 2 m high steel tube was alternately excavated and driven into landfill waste. Top and bottom plates were then welded in place and the assembly lifted out. When installed in the laboratory the cylinder then served as the test column (no compression applied).

In effect this method is essentially a large scale version of a Shelby tube and piston sampler (section 2.4.10). The same advantages and disadvantages are apparent: the

structure and fabric structure of the sample is retained but there may be a degree of deformation or smearing at the edges. Gouging of the tube walls during sampling, which is a possible source of short-circuit flow for Shelby tube tests is probably not a problem on this scale. The approach may have been possible for this research but the requirement to conduct tests at several stresses adds further complications. Possible solutions would be to use the sampling cylinder within the compression cell framework or extract and transfer the sample from the sampling cylinder to the compression cell cylinder.

### 8.7.3 Alternative laboratory testing design

A potentially simpler alternative laboratory design to that of the compression cell would be a rectangular permeameter. Figure 8.16 shows the basis of a rectangular design used for measuring horizontal but not vertical hydraulic conductivity of wastes (TU Braunschweig, Germany - unpublished). The waste sample is contained within a rectangular box and compressive stress is applied by a piston acting on the top plate. Horizontal flow is induced through the sample by the head difference between the inlet and outlet compartments. Flow is not strictly through a uniform cross sectional area of the sample, but providing the difference between inlet and outlet head is small, this and the small vertical flow component is fairly insignificant. Darcy's law can therefore be applied directly to calculate horizontal hydraulic conductivity. Due to the low hydraulic gradient, tests are limited to samples of medium to high hydraulic conductivity. The low pore water pressure test conditions will be representative of very shallow leachate depths only.

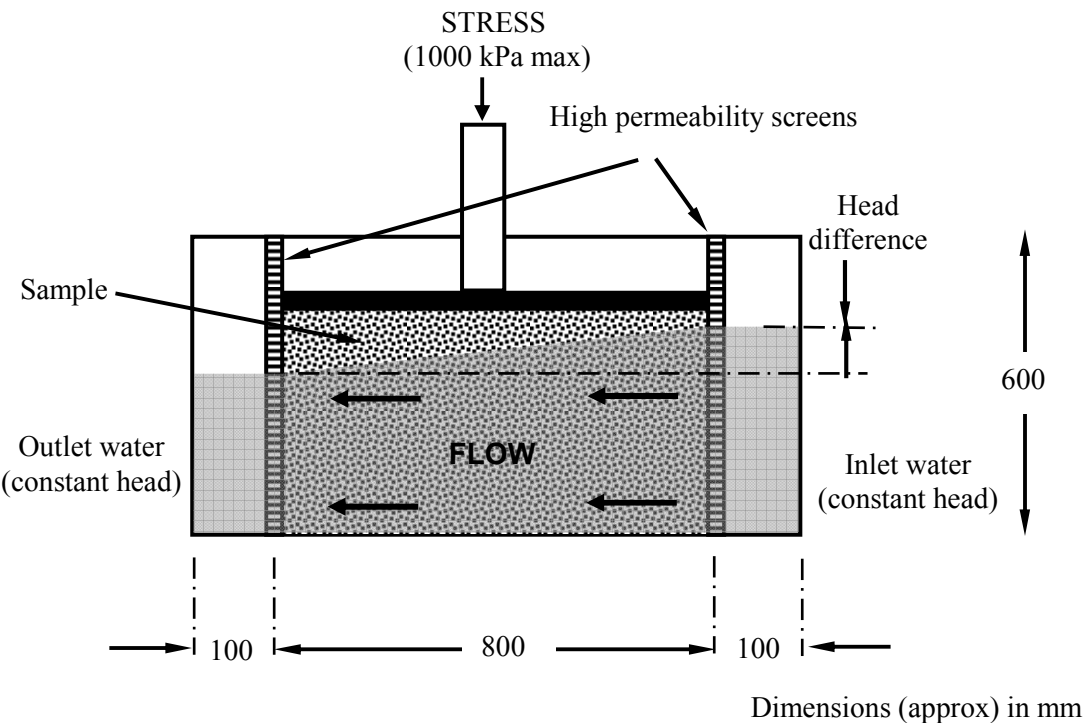


Figure 8.16 Side view of horizontal flow permeameter (TU Braunschweig – unpublished)

The basic design could be modified to measure vertical flow as well as horizontal flow (Figure 8.17). This would require inlet holes on the base and top platen. During the vertical flow test, flow through the vertical screens (for horizontal flow) would have to be prevented to avoid the risk of short circuiting. It may be possible to have interchangeable screens and solid panels to achieve the required configurations. Alternatively it may be possible to insert flexible but impermeable packing behind the screens as required. Baffles as described in section 8.7.1 could be fitted to the top and bottom plates to prevent short circuiting across the top and bottom of the sample during horizontal flow tests.

A sealing arrangement such as that shown in Figure 8.17 would allow hydraulic conductivity tests to be conducted at higher pore water pressure representative of deeper saturated zones. Essentially the design then becomes a square version of the Pitsea compression cell, but with a different sealing arrangement. It has the advantage of full inlet and outlet areas for flow in both planes (providing short circuiting can be satisfactorily prevented in tests in each plane) with a uniform cross sectional area of

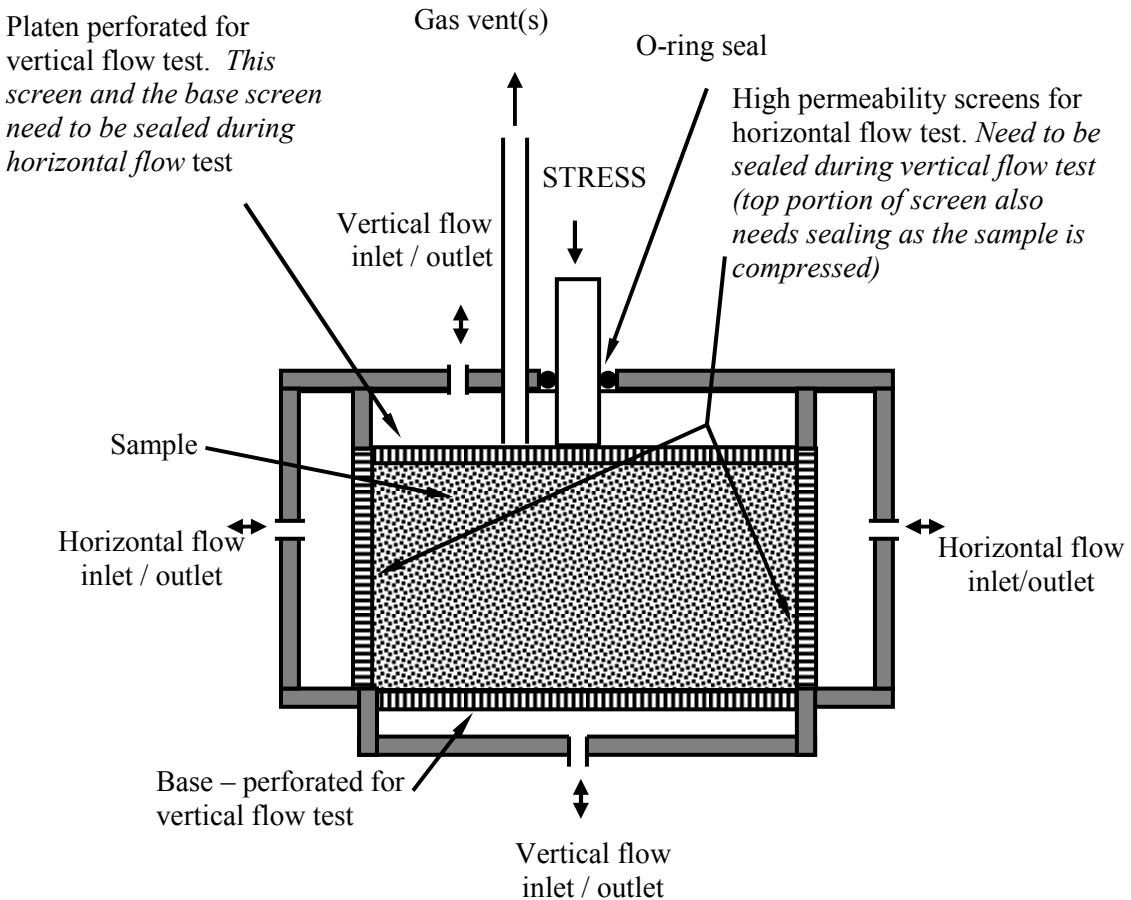


Figure 8.17 Outline of suggested design of rectangular section permeameter for measurement of vertical and horizontal hydraulic conductivity in wastes

the sample for both vertical and horizontal flow. There is neither any enforced vertical component to horizontal flow (as is present with the compression cell inlet and outlet port arrangement) nor any horizontal element to the vertical flow. Darcy's law could be applied directly to flow in both directions and so numerical modelling would not be required as it is for flow across a cylinder. Venting would be required at the top of the sample to release excess gas.

However sample packing in a square/rectangular receptacle is more problematic than in a round one, and the design may be more prone to frictional losses during compression. Access to the sample would be more restrictive than the compression cell arrangement, requiring removal of both the top cover and the top platen screen.

## 8.8 Summary

Horizontal hydraulic conductivity tests were carried out on samples AG2 and DN1 in the Pitsea compression cell. A horizontal flow of leachate was induced across the samples and flow rates were measured. A variety of test configurations were used using different numbers of ports. Both ‘confined’ (outflow via horizontal flow ports only) and ‘unconfined’ (outflow through horizontal flow ports and top and bottom of the sample) tests were carried out. Tests on sample DN1 were run in both gas purged and gas accumulated conditions, and at different pore water pressures and flow rates by altering inlet and outlet head configurations.

Groundwater Vistas and the USGS groundwater flow model, MODFLOW was used to assess horizontal hydraulic conductivity of each sample at each compression stage using horizontal flow rates obtained in tests in conjunction with previously determined vertical hydraulic conductivity values. The results showed that horizontal hydraulic conductivity was greater than vertical hydraulic conductivity with  $k_h : k_v$  ratios of both samples being between 5 and 10. This is the first time that such anisotropic flow has been systematically demonstrated for landfill wastes. Further findings of the test results are that  $k_h : k_v$  ratios tend to increase with stress but are unaffected by gas accumulation and possibly different pore water pressures.

The findings are highly significant for the modelling of leachate management and contaminant movement within landfill wastes for which isotropic conditions or an arbitrary anisotropic value previously have had to be assumed.

## 9. Summary and conclusion

The aim of the research described in this thesis has been to evaluate the hydraulic conductivity of two different household waste samples in both horizontal and vertical planes for a range of applied stresses. This has not been previously undertaken on unmodified waste samples subjected to typical landfill overburden stresses.

The findings of this research for the two samples tested are:

- that horizontal hydraulic conductivity was between five to ten times greater than vertical hydraulic conductivity
- that  $k_h : k_v$  ratios tended to increase slightly at higher stresses ( $k_h : k_v$  ratios of 5 to 7 are typical at stresses of 100 kPa or less, increasing to about 10 at stresses above 300 kPa)
- that  $k_h : k_v$  ratios are unaffected by gas accumulation and probably pore water pressure in the waste

These findings confirm the notion expressed by several authors that hydraulic conductivity of landfill waste will be higher in the horizontal plane due to the predominantly horizontal orientation of waste constituents arising from overburden stress. This has not previously been proven. Previous research has been limited to tests on a fines-only waste fraction under limited stress (Buchanan & Clark, 1997,

2001) for which a  $k_h : k_v$  ratio of less than 2 was measured. The findings of the research in this thesis demonstrate that unmodified (*i.e.* coarse items not removed) waste samples of representative size exhibit much higher  $k_h : k_v$  ratios.

The trend of increasing  $k_h : k_v$  ratios with an increase in stress indicated by the research also supports the conceptual mechanism that as stress increases, items tend to become increasingly flattened or aligned to the horizontal plane (section 2.5, Landva and Clark, 1990, Bendz and Flyhammar, 1999). In contrast the tests undertaken by Buchanan & Clark (1997, 2001) indicated that  $k_h : k_v$  ratio *decreased* with waste density.

The similarity of results for two waste samples of differing particle size distribution, pre-processing and age suggests that similar anisotropy may be present in most domestic landfill wastes, but not necessarily highly pre-processed or source-specific wastes.

Much experience was gained during the testing period and recommendations for improving methods for assessing the hydraulic conductivity of wastes are given in section 8.7. A particularly notable finding encountered during the tests was that waste hydraulic conductivities were significantly affected by gas accumulation and pore water pressure (section 7.4). This has lead to further research by the University of Southampton (as yet unpublished) on the relationship between hydraulic conductivity, gas accumulation and pore water pressure. Similarly the research has shown for the first time that that drainable porosity is significantly altered by pore water pressure and gas accumulation in the waste (section 6.3). The use of this data should allow more accurate assessments to be made of leachate volumes in landfill saturated zones.

The findings of this research are applicable to the management of leachate in both conventional landfills (eg. Rowe and Nadarajah, 1996, Beaven, 2000) and future sustainable designs (DoE, 1995, IWM, 1998). They are particularly beneficial to the modelling of leachate and contaminant movement in landfills for which previously

isotropic conditions, or an arbitrary  $k_h : k_v$  ratio, would have been assumed (e.g. McCreanor and Reinhart 2000). In such applications it has to be appreciated that:

- the findings are concerned only with the inherent anisotropy of wastes and do not include the effects of layers of other materials within the waste body such as low permeability daily cover, or highly permeable trenches or boreholes. It is likely that landfills with such features will exhibit very different, possibly localised, anisotropic values
- the findings apply only to nominally saturated wastes. Leachate flow in unsaturated zones would be expected to be much lower and predominantly influenced by gravity. Vertical hydraulic conductivity would be expected to be higher than horizontal hydraulic conductivity
- the findings may not be applicable to all types of wastes

The research undertaken has provided original and comprehensive evaluations of waste hydraulic conductivities in both vertical and horizontal planes at an acceptable cost. It has confirmed the concept of waste anisotropy based on field observations and has provided valuable data needed for the modelling of leachate transport in landfills. An understanding of the influence of gas accumulation and pore water pressure on hydraulic conductivity has been gained during testing and this has resulted in the development of new techniques and further original research.

## Appendix A. Laboratory methods of testing hydraulic conductivity

### A1 Test arrangements

#### Constant head test

The requirements for a constant head test are outlined in British Standards 1377 part 5 (1990), and the main features are illustrated in Figure A1. A flow of water (or other liquid) is passed through the sample at a constant flow rate ( $Q$ ) maintained by the constant inlet and outlet heads. De-aired water should be used to ensure saturation is maintained during the test (Craig, 1983). The sample (saturated under vacuum to ensure maximum saturation – section 2.4.6) is enclosed in a ring or tube (of cross sectional area  $A$ ) sandwiched between porous discs or gravel layers (the different types of ring/tube permeameters are described in section A2). The permeability of these layers must be significantly higher than the sample in order to minimise head loss and to give an even distribution of water across (and therefore one-dimensional water flow through) the sample (Daniel, 1994). The hydraulic gradient ( $i$ ) induced across the sample is determined from the head difference ( $\Delta h$ ) indicated by the manometers inserted into the sample at a known distance ( $L$ ) apart ( $i = \Delta h/L$ ). Intermediate manometer points are recommended to ensure that the hydraulic gradient through the sample is uniform (Barnes, 2000). When steady state conditions have been established (*i.e.* constant flow rate and constant head difference), Darcy's law may be applied directly to obtain the hydraulic conductivity ( $k$ ):

$$k = \frac{Q}{Ai} \tag{A1.1}$$

The calculated value of  $k$  should be corrected for the effect of temperature if the test is not conducted at the normally accepted temperature of 20°C (Barnes, 2000).

Temperature correction values were shown in Table 2.1 in section 2.4.2.

It is recommended that separate upward and downward flow tests are conducted, and also tests run at different flow rates (by altering the difference between the inlet and outlet heads – but see note on limitations below) (Powrie, 1997). Tests should also be carried out on samples compacted at a range of densities as hydraulic conductivity can vary according to density. Hydraulic conductivity can then be plotted against density or void ratio in order to interpolate the *in situ* value from field density (Barnes, 2000).

Limitations of constant head tests are:

- hydraulic conductivity is only measured in one direction (vertical) which is unlikely in the field (Barnes, 2000). Consequently the results may not be a reliable indicator of flow through anisotropic soils (section 2.5)
- the hydraulic conductivity measurements may be affected in tests using high flow rates (and associated larger hydraulic gradients). This can arise from loosening of the packing of the sample in upward flow tests, or compaction during downward flow tests. A head not exceeding more than half of the sample length is recommended (Fetter, 1988)
- peripheral flow may occur between the sample and cylinder wall especially if the sample shrinks due to interaction with the permeant (a double-ringed permeameter can be used to indicate if peripheral flow is present – see section A2 and Figure 4)
- full saturation of the sample is difficult to achieve and this may affect the measured hydraulic conductivity (section 2.4.6)
- tests are limited to higher permeability samples between  $1 \times 10^{-5}$  and  $1 \times 10^{-2}$  m/s - typically clean sands and gravels with less than 10% fines (Barnes, 2000, Sarsby, 2000, BS1377: part 5, 1990). Low flow rates associated with low permeability samples are difficult to measure accurately – one potential source of error being evaporative losses from the measuring cylinder for collecting the outflow water

- undisturbed samples of coarse grained materials are difficult to obtain (consequently the main use of the test is for assessing the drainage properties of fill material) (Sarsby, 2000)
- The inside diameter of commercially available constant head apparatus is 75 mm or 114 mm. This is not a problem for assessing remoulded soils for use as filters or drainage materials, but is insufficient to replicate features of the macrostructure (such as fissures, bedding, laminations or root holes) which affect the overall hydraulic conductivity value (section 2.5)

*Falling head test*

The arrangement of a laboratory falling head test is shown in Figure A2. The test was designed to enable accurate measurement of low flow rates associated with soils of low to intermediate permeability, such as silts and clays. The samples are contained within a cylinder – the sample being loaded either directly from a sample tube, or using the sampling tube as a cylinder. Soils of very low permeability may be sealed inside the cylinder to prevent seepage along the sides of the specimen, although this is unlikely to occur if the sample swells during the test.

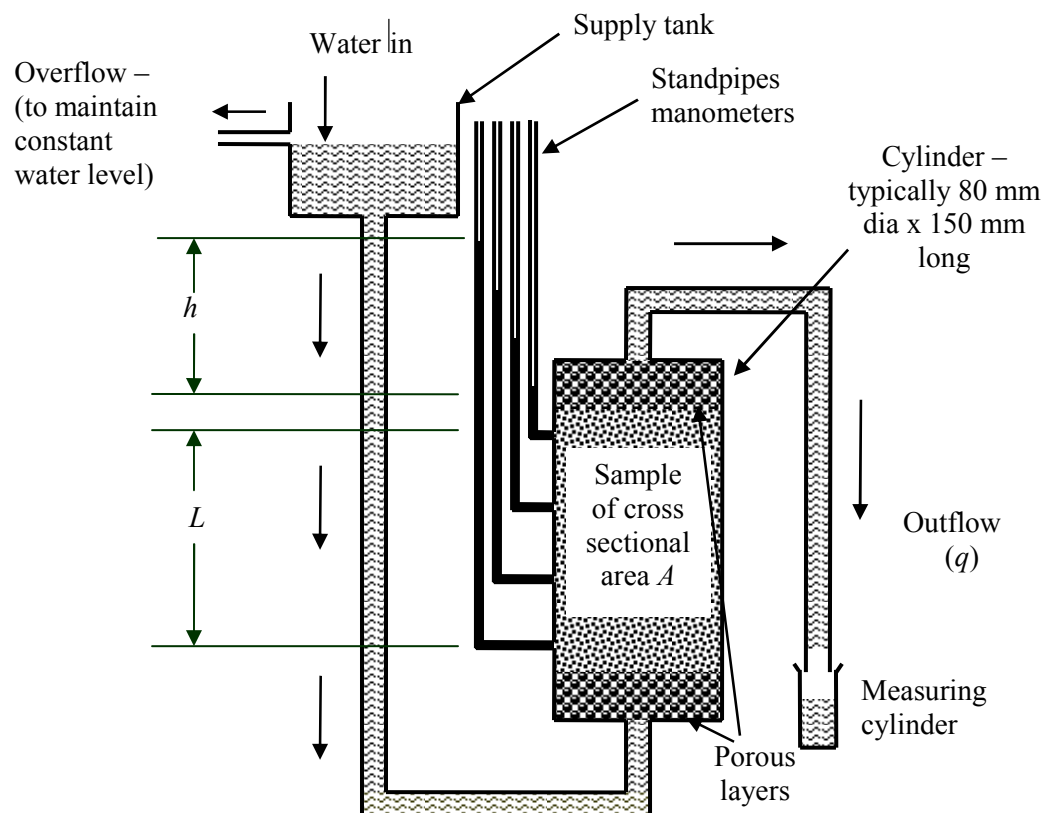


Figure A1. Constant head permeameter (upward flow)

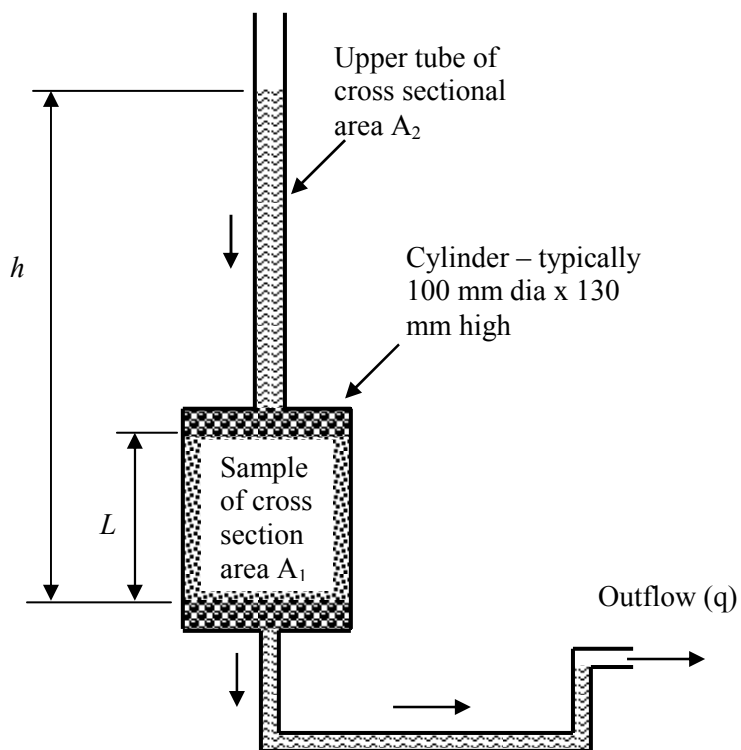


Figure A2 Falling head permeameter

Water flows from a standpipe of cross-sectional area  $A_2$  and through the sample contained within the tube of designated cross-sectional area  $A_1$ . The fall in water level in the standpipe is timed ( $T$ ) from a starting height ( $h_1$ ) to final height ( $h_2$ ). The bore diameter of the standpipe relative to that of the sample diameter depends on the material being tested – for coarse materials similar diameters are usually suitable. For lower flow rates typical of tests with low permeability samples, a smaller standpipe diameter, possibly about  $1/10^{\text{th}}$  that of the sample diameter, is required to obtain a reasonable timed head change (Freeze and Cherry, 1979). Hydraulic conductivity ( $k$ ) is given by:

$$k = (A_2 L/A_1 T) \ln(h_1/h_2) \quad (\text{A1.2})$$

(Freeze and Cherry, 1979, Oweis and Khera, 1990, Powrie, 1997)

The same precautions to ensure a high degree of saturation of the sample outlined for the constant head test apply to the falling head test. The falling head arrangement does not however allow the use of a pressurised pore fluid. Therefore full saturation of the sample, particularly of fine-grained soils, cannot be guaranteed (Oweis and Khera, 1990, Sarsby, 2000). It is recommended that a series of tests are run using different  $h_1$  and  $h_2$  or  $A_1$  and  $A_2$  values (Craig, 1983). Inconsistent results may indicate the presence of air, or swelling or contraction of the sample (Sarsby, 2000).

In the method described above the pressure at the outlet is constant and may be described as a ‘falling-headwater, constant-tailwater-pressure test’. This is a convenient method for testing soils with hydraulic conductivities greater than  $1 \times 10^{-5}$  m/s. An alternative arrangement for soils of lower hydraulic conductivity is the ‘falling-headwater, rising-tailwater-pressure test’. Effluent water rises in a standpipe rather than that used in the constant-tailwater-pressure method of draining into a receptacle. The calculation used to determine hydraulic conductivity is slightly different (Daniel, 1994).

In general the equipment used for variable-head tests is simpler than that used for constant-head tests, but the hydraulic conductivity calculations are more complicated.

The main disadvantages of the falling head test arise from the reduction of the inlet pressure head during the test. Any head losses in the equipment will not be constant during the test and therefore cannot be simply taken into account as they can with the constant head arrangement. Head reduction occurring during the test may result in the expansion of air present in the sample or the release of dissolved gas from the permeant. The resultant increased volume of air in the void spaces of the sample may restrict water flow and reduce hydraulic conductivity (section 2.4.6). It is also possible that some test samples may change volume as the pressure head changes, again affecting hydraulic conductivity. A further scenario with flexible wall cells is that the reduction in pore water pressure may alter the effective stress (section A2), and again result in a change in hydraulic conductivity of the sample during the test. This is particularly a problem for highly compressible materials. (Daniel, 1994, Sarsby, 2000).

#### Constant rate of flow

An alternative arrangement is to induce a constant permeant flow through the sample by pumping at a controlled rate and measuring the induced pressure difference across the sample using a transducer. The advantage of this method compared with constant-head and falling-head methods is that steady state conditions are attained quickly (providing the test sample is saturated) and therefore the time taken to perform the test is minimised. For example, expected testing time for samples with a hydraulic conductivity between  $1 \times 10^{-6}$  m/s and  $1 \times 10^{-7}$  m/s would be a few hours compared to a few weeks for constant head or falling head methods (Olsen *et al.*, 1994). Hydraulic gradients are lower unless high flow rates are used. The chief disadvantages are additional complexity and higher equipment costs (Daniel, 1994, Olsen *et al.*, 1994). If this method is used on flexible wall permeameters (section A2), the confining pressure must be higher than the pore water pressure to prevent the sample expanding.

## A2 Laboratory equipment for assessing hydraulic conductivity

### -single plane flow

#### Introduction

In this section different types of permeameters are described. These can be broadly divided into rigid wall or flexible wall designs. Rigid wall permeameters are simpler and less expensive than flexible wall permeameters but are more prone to permeant leakage between the sample and the permeameter walls during tests (referred to as peripheral flow / leakage or sidewall flow / leakage). If this is not prevented or assessed (as described later in this section), the apparent flow rate ( $q$ ) through the sample will produce an over-estimation of hydraulic conductivity. Another shortcoming of most rigid walled permeameters is that high back-pressures cannot be applied to saturate the sample (as used in flexible walled permeameters) and this can result in hydraulic conductivity being under-estimated (section 2.4.6). A high back pressure cannot be used as this will reduce the effective stress of the sample unless the permeameter is of a design that permits vertical stresses to be applied to the sample during testing to reproduce *in situ* stresses. A reduction in effective stress may result in hydraulic fracturing of the sample (the formation of fractures or channels in the sample), side-wall leakage and expansion of the permeameter may occur. This can result in a several fold increase in measured hydraulic conductivity (Daniel, 1994, Shackelford, 1994).

#### Rigid wall permeameters

The most basic type of permeameter uses a sampling tube with top and bottom caps attached. For undisturbed samples a thin walled Shelby sampling tube (section 2.4.10) can be used as the permeameter cylinder. However the use of these tubes for soils (other than for soils that are easy to sample) is not recommended as the shearing action along the sidewall during sampling may remould the soil. Additionally, hard particles may damage the thin walled tubes during insertion, possibly resulting in gouges on the

sample leading to sidewall leakage during tests (Daniel, 1994). For compacted samples a Proctor mould fitted with top and bottom caps may be used as a permeameter (Figure A3). These are frequently referred to as compaction mould permeameters. A typical standard commercially available size of a compaction mould permeameters is 101.6 mm diameter x 116.5 mm high (ELE, 1999).

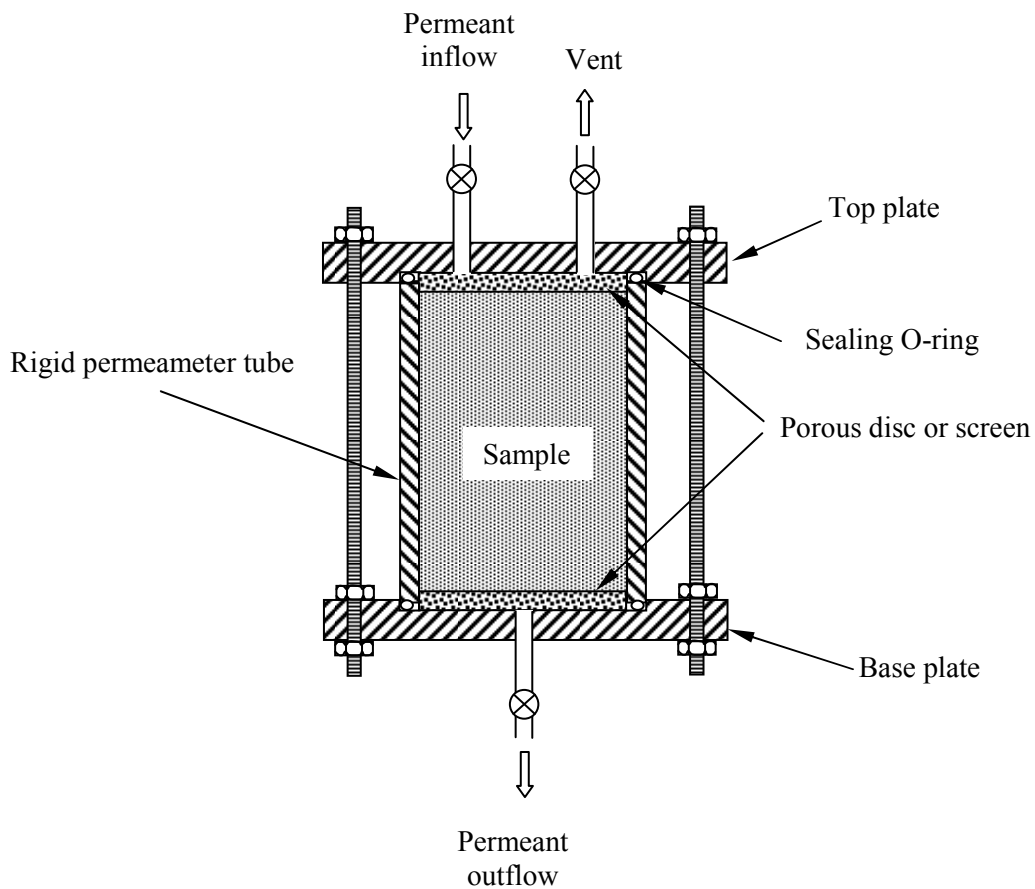


Figure A3. Cross section of a rigid walled compaction (Proctor) mould wall permeameter (it is also possible to operate this design of permeameter with upward permeant flow)

During hydraulic conductivity testing permeant flow through the sample may be upward (assists with achieving saturation of the samples) or downward, providing high permeability layers are installed above and below the sample to distribute the inflow. Normally porous discs are used for lower permeability samples, or screens for coarse sands or gravel samples.

The basic design gives no provision for expansion of swelling samples, simulation of *in situ* stress, assessment of peripheral flow or measurement of horizontal hydraulic conductivity. Swell rings can be added to some permeameters to accommodate samples that swell during testing (Figure A4). Excessive swelling may necessitate trimming of the sample prior to final hydraulic conductivity assessment. Testing is usually limited to upward flow only due to the difficulties of using a porous layer on top of the sample.

In permeameters equipped with a loading piston (as shown on Figure A5) vertical stress can be applied to the sample to replicate *in situ* stress. This, as mentioned above, allows the use of back-pressure. It is also useful for the testing of swelling samples as it allows a controlled amount of swelling rather than full resistance to swelling in the basic arrangement shown in Figure A3, or conditions of low / no resistance that may occur if swell rings are used. During loading, transmitted stress may be reduced with sample depth due to friction between the sample and the cylinder wall. Samples may become preferentially compressed in the upper regions. To minimise this it is recommended that the length to diameter ratio of the permeameter is low. A ratio of 0.25 or less is recommended (compared to a typical ratio of 1 for a compaction mould permeameter and between 1 to 2 for a sampling tube permeameter) (Daniel, 1994).

As mentioned above, peripheral flow between the sample and the permeameter wall during testing will result in overestimation of hydraulic conductivity. A double (Figure A4) or triple ringed permeameter can be used to assess if this is occurring. Rings fixed to the base plate and protruding into the sample are used to divide the base area of the sample. During tests, flow rates through the individual regions of the sample should be proportional to the area of each region. It is usual for the double ringed configuration to be divided into equal inner and outer areas. With this arrangement equal inner and outer flow rates would be expected if no peripheral flow was present. A higher proportion of flow from the outermost region would be indicative of peripheral flow.

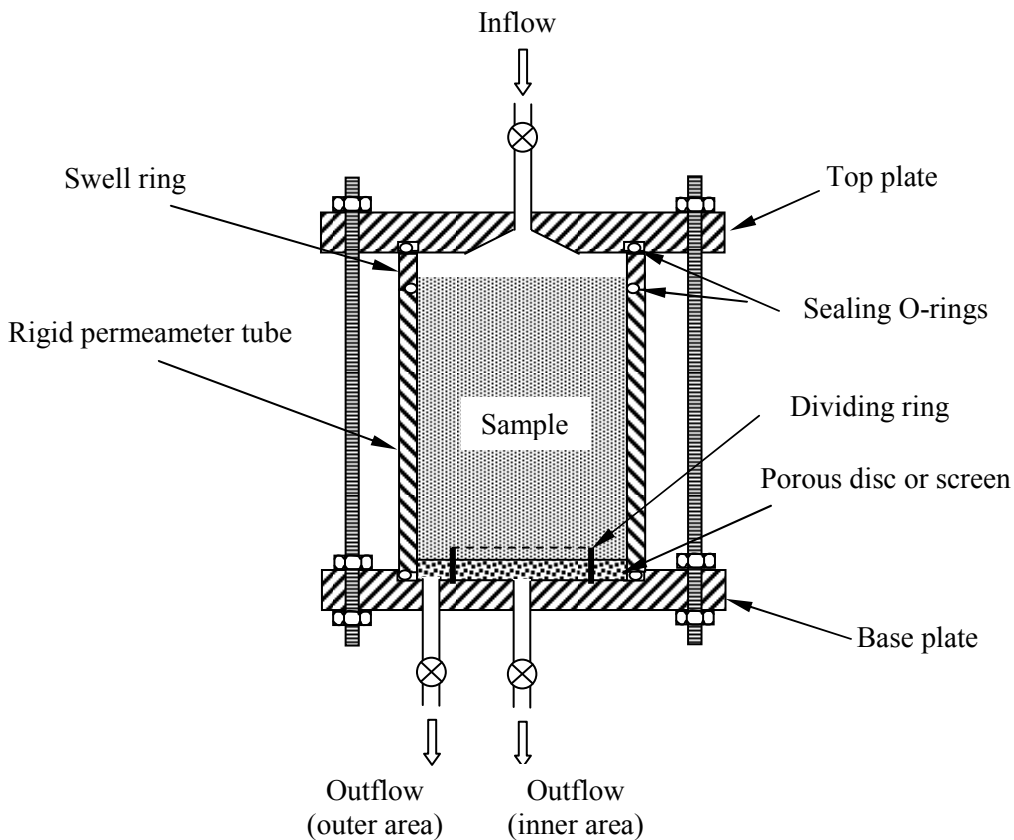


Figure A4. Double-ringed permeameter for detecting sidewall flow (with swell ring)

The use of dividing rings allows the presence of sidewall leakage to be detected but does not prevent it. An oversize permeameter can be used to prevent leakage by surrounding the sample with an annular seal (typically bentonite). Although good results can be obtained, the forming and checking the performance of the seal is very time consuming and is not recommended for general use (Daniel, 1994).

The consolidation cell permeameter (or consolidometer or oedometer cell) is illustrated in Figure A5. This is mounted in a loading frame to allow vertical stress to be applied to the sample to represent a range of different stress conditions. The test sample is contained within a ring. Typical sample diameters are 40 mm to 100 mm and a height of up to 100 mm (Oweis and Khera, 1990). The ring can be fixed to the base (*fixed-ring* type), or a gap can exist between the bottom of the ring and the base (*floating-ring* type). Friction between the sample and ring is less in the floating ring arrangement (Freeze and Cherry, 1979).

Hydraulic conductivity can be calculated either:

- i) from the rate of consolidation arising from incremental loadings to the sample – this is not a recommended method as the theory makes use of a series of assumptions that do not accurately fit actual soil/clay behaviour (Tavenas *et al.*, 1983) and hydraulic conductivity may be under-estimated by 50% due to the effects of secondary consolidation (Daniel, 1994)
- ii) by permeating the sample directly. After air is flushed out of the sample (the high back pressure saturation method cannot be used - Tavenas *et al.*, 1983), a falling head is applied through the base of the sample. The outlet head is maintained at a constant overflow level. If additional pressure is not used in the inlet head (as is sometimes necessary for low permeability samples to reduce the time of the test and therefore errors due to evaporation) the hydraulic conductivity is calculated using the equation shown in section A1 for the falling head test

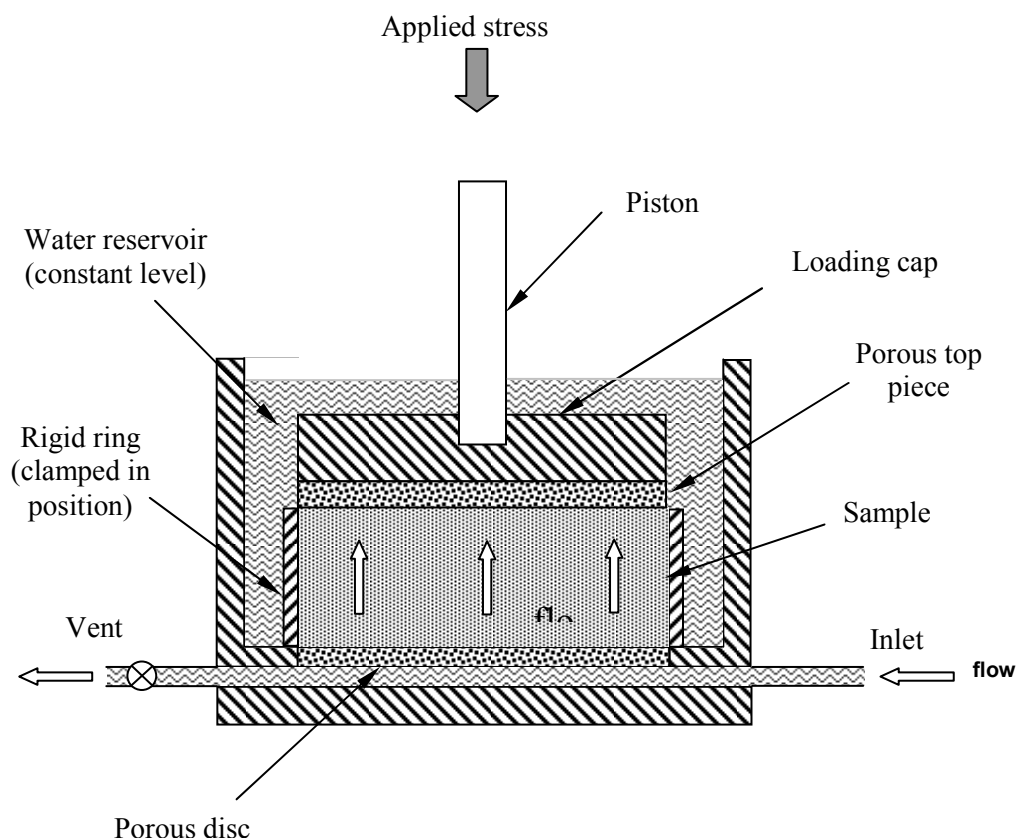


Figure A5. Consolidation-cell permeameter (oedometer) – fixed ring type (Daniel, 1994)

An advantage of the consolidation permeameter is that both equipment and procedure is simple, allowing tests to be conducted fairly rapidly at different vertically applied stresses (Tavenas *et al.*, 1983, Shackelford, 1994). Additionally the vertical stress applied to the sample results in a lateral stress within the sample which acts against the inner walls of the cell, minimising or preventing side-wall leakage (Shackelford, 1994). However the consolidation permeameter is only suitable for clayey soils that contain no gravel or coarse sand and its use has declined in favour of more versatile types of permeameter (Daniel, 1994).

#### *Flexible wall permeameters / triaxial cells*

Although flexible wall permeameters are more complicated and costly than rigid wall permeameters, they have a principal advantage that peripheral flow between the sample and membrane wall is virtually eliminated during hydraulic conductivity testing (Daniel, 1994). Samples are contained within a flexible membrane and subjected to an all-round stress by pressurised water (Figure A6). This arrangement is even suitable for testing stiff materials (such as sandstones and shales) and samples with irregular surfaces that cannot be properly trimmed to exact diameters for mounting in rigid walled equipment. Vertical stress may additionally be applied in a triaxial cell (flexible wall permeameter is a general term which does not necessarily include vertical stress – Shackelford, 1994).

Samples for flexible wall permeameters typically measure 70mm or 100mm diameter, consisting either of compacted soil or extrusions from a field boring. These are sandwiched between porous discs and enclosed in a thin rubber membrane (neoprene or a teflon layer can be used if liquids that degrade rubber are to be used in the test) sealed to the top and bottom caps using o-rings. When the sample is installed in the permeameter it is surrounded by pressurised fluid (usually water), subjecting the sample to an all-round isotropic pressure known as the confining or cell pressure. Additional vertical stress can be applied to the sample by a ram acting on the top cap. This simulates typical field conditions for which axial (vertical) stress is usually greater than radial (horizontal) stress (Powrie, 1997). Hydraulic conductivity tests may be carried out on the sample at a range of stresses. Permeant flow is via the flow

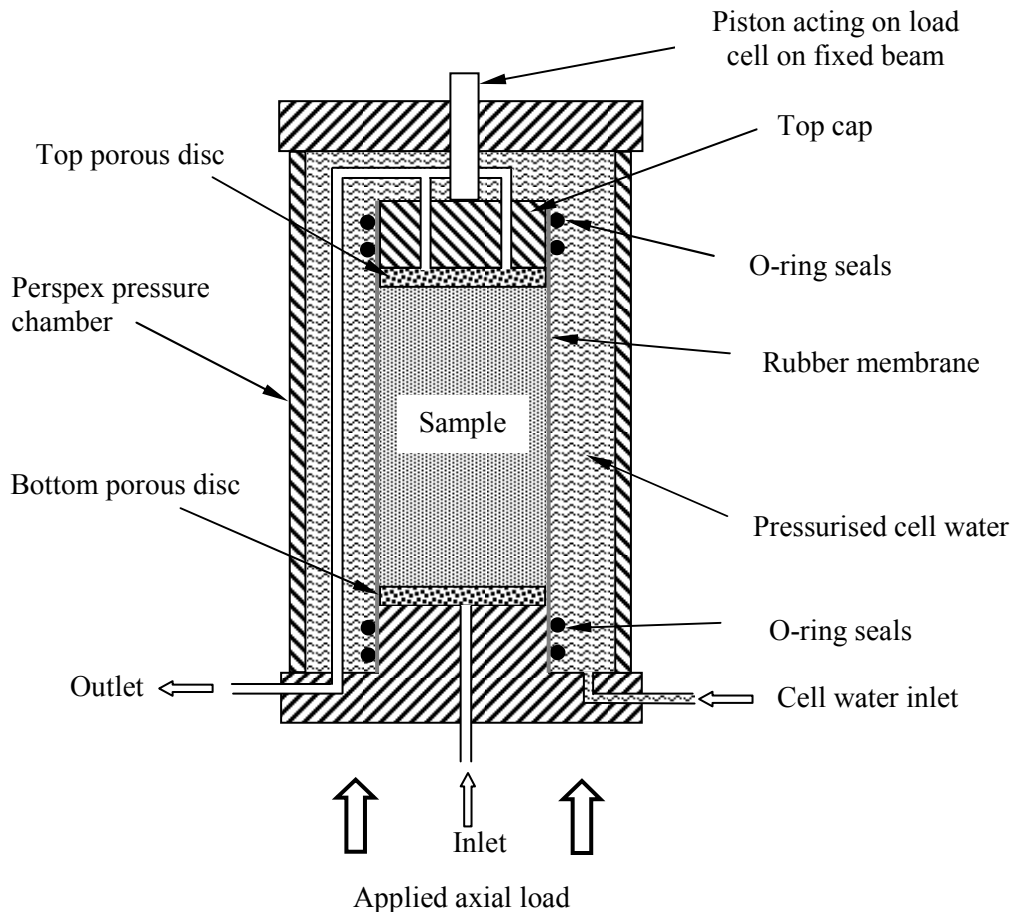


Figure A6. Schematic view of a flexible wall permeameter

lines to the top and bottom caps and high permeability layers at the top and bottom of the sample. Constant head tests are normally conducted, but variable head tests can also be carried out (Tavenas *et al.*, 1983).

Prior to testing, samples are usually subjected to back-pressure (typically between 200 kPa and 500 kPa) by applying pressurised water through the flow lines to the top and bottom caps. The pressure (which may be introduced in several incremental stages over several days) ensures full saturation of the sample as air bubbles in the sample are compressed or dissolved<sup>4</sup> into the pore water. This method of saturating samples is much quicker than using de-aired water. Therefore test times using flexible wall

<sup>4</sup> the amount of air that can be dissolved in water increases linearly with pressure (Henry's law)

permeameters are generally less than those for fixed wall permeameters which cannot use back-pressure. Saturation of the sample can be checked using the B coefficient:

$$B = \frac{\text{change in pore water pressure in the sample } (\Delta u)}{\text{change in confining pressure } (\Delta \sigma)} \quad (A1.3)$$

Prior to conducting hydraulic conductivity tests, it is recommended that a B-value of 0.95 is attained (Oweis and Khera 1990, BS 1377 part 6: 1990). However the B-value indicates different saturation ratios ( $S_r$ ) for materials of different stiffness. For completely saturated hard soils and rocks the B coefficient will exceed 1.0 (Daniel, 1994), for a stiff clay the 0.95 B-value may indicate a  $S_r$  of 99.9% but only 96% for a soft clay (Black and Lee, 1973 *cited in Powrie 1997*). A value of 0.90 is considered satisfactory for some clays if attained for three consecutive pressure increase stages. If air is present, the volume of water admitted at each stage will be greater than the volumetric swell of the sample, and so it is recommended that water admitted and the dimensional changes of the sample are recorded at each stage (BS1377 part 6: 1990).

To reduce testing time hydraulic gradients (the decrease in total head divided by distance over which head decrease occurs – section 2.2) as high as 200 (Day and Daniel, 1985) and possibly 500 (Oweis and Khera, 1990) are used. The hydraulic gradient can be altered for different tests by increasing the headwater pressure or decreasing the outlet (tailwater) pressure. However the headwater pressure must be kept below the confining pressure and tailwater pressure must not be decreased to levels that result in release of air from the permeant into the sample. High hydraulic gradients may result in a higher effective stress at the outlet end of the sample causing differential consolidation and hydraulic conductivity of compressible samples. They may result either in opening of void pathways by erosion, or migration of particles which may block pathways, and can therefore result in either an overestimation or underestimation of hydraulic conductivity (Oweis and Khera, 1990). ASTM D 5084 recommends maximum hydraulic gradients of 30 for soils with a hydraulic conductivity less than  $1 \times 10^{-9}$  m/s (Shackelford, 1994). A further consequence of a higher effective stress at the outlet end may be deformation of the sample. As the sample is contained within a flexible membrane, the differential effective stress

throughout sample depth may result in the sample being slightly tapered towards the top. In this case the outlet area would be smaller than the inlet area. Flow through the sample is therefore two dimensional, rather than one dimensional as expressed by Darcy's law. The use of Darcy's law to calculate hydraulic conductivity of samples using flexible wall permeameters may therefore be regarded as an approximation. The potential error will be greater for higher effective stress differentials and compressible samples (Shackelford, 1994).

Flexible wall permeameters are suitable for testing most soils with hydraulic conductivities ranging from  $1 \times 10^{-2}$  m/s to  $1 \times 10^{-8}$  m/s (ELE, 1999). Although peripheral flow between the sample and membrane wall is virtually eliminated, leakage may occur through the seals at the top and bottom of the sample. This, particularly when testing low permeability samples, can result in significant errors in measured hydraulic conductivity (Oweis and Khera, 1990). Other potential sources of leakage are in fittings and by osmosis and diffusion through the rubber membrane. Leakage from external fittings can be eliminated by enclosing them in a back-pressure chamber. Leakage from internal fittings can be reduced by careful construction and tightening, and use of a viscous cell fluid. Osmosis and diffusion through the membrane can be reduced by using a double membrane separated by foil and a film of silicone grease (Tavenas *et al.*, 1983).

Other errors in measured flow rate may occur by water uptake by the membrane during the test. To avoid this, the membrane should be saturated before mounting. (Tavenas *et al.*, 1983).

A limitation of the flexible wall permeameter is that testing at very low stress is not feasible as confining pressures below this are insufficient to prevent sidewall leakage. A minimum confining pressure of 14 kPa is stipulated by Daniel (1994), although in tests undertaken by Tavenas *et al.* (1983) a pressure of 25 kPa was required. It was recommended that the magnitude of the stress required to prevent sidewall leakage should be determined for the sample size and the characteristics of the membrane to be used. The need for a minimum confining pressure limits the minimum *in situ* depth that can be represented in flexible wall permeameter tests.

Flexible wall permeameter / triaxial cell have also been adapted to investigate permeability characteristics in unsaturated conditions (Fredlund and Rahardjo, 1993, Hung *et al.*, 1998). A Two-phase, High-Pressure Triaxial Apparatus has been devised by Ranjith (2004) in which both fluid and gas can be introduced through the test sample. The ratio of fluid and gas can be controlled allowing the relative permeability characteristics to be assessed according to the degree of saturation. As observed in section 2.4.6, it may be argued that the affects of two-phase flow should be considered when testing wastes as the presence of landfill gas in the waste matrix and leachate will affect hydraulic conductivity.

### A3 Laboratory equipment for assessing hydraulic conductivity

- bi-planar flow

#### *Rowe Cell / Hydraulic cell*

A limitation to the test arrangements described so far is that they are designed to measure hydraulic conductivity in the vertical direction (i.e. in the plane parallel to overburden stress). Horizontal hydraulic conductivity measurements can be performed on some soils by installing samples in test equipment orientated to induce flow along the natural horizontal plane of the sample (Bouwer, 1978, Agaki and Ishida, 1994), but in most standard equipment the major stress cannot then be applied perpendicular to the natural horizontal plane. The Rowe cell (also referred to as a hydraulic consolidation cell – Barnes, 2000, BS 1377: part 6, 1990) was developed by Rowe and Barden (1966) for the purpose of carrying out consolidation tests, but hydraulic conductivity can also be assessed in both vertical and horizontal directions using constant head type tests. Tests are conducted under the relevant vertical stress without introducing an all round stress (as in the triaxial cell permeameter). The resulting induced lateral stress is more representative of field situations (Whitlow 1983, Sarsby 2000). The Rowe cell is suitable for testing soils of low to intermediate permeability. Comparatively large specimens can be tested – 250 mm diameter and 100 mm thick are considered to be sufficiently representative (Barnes, 2000).

Diagrams of the general arrangement for the vertical and horizontal tests are shown in Figures A7 a) and b) respectively. The original design is shown in which the vertical stress is applied to the sample by pressurised water acting on a flexible rubber diaphragm. The membrane has a bellow arrangement that allows movement as the sample compresses. Vertical movement of the sample is registered by a dial-gauge or displacement transducer. The purpose of the rigid disc underlying the flexible rubber membrane is to apply a planar pressure to the sample (known as equal strain loading). Alternatively the disc can be removed to give a uniformly distributed pressure to the surface of the sample (free strain loading).

A variant of the Rowe cell is shown in Figure A8. A platen with an o-ring seal on the periphery is used instead of a flexible rubber diaphragm and rigid disc. As the platen is rigid, the sample can only be subjected to equal strain loading. An advantage of this simpler design is that the platen movement is potentially less restricted than the diaphragm arrangement, allowing highly compressible samples to be tested.

Prior to the tests the system should be checked for leaks. Air should be flushed from the system using de-aerated tap water and then replaced by fresh de-aerated water for the tests. Porous materials such as plastics, sintered bronze discs and sand need to be de-aired by boiling in distilled water and stored in de-aerated water before use. Further precautions are needed to ensure that the sample, pressure lines and gauges are fully saturated. This is achieved by applying alternate increases (typically 50 kPa for the first two stages then 100 kPa increases thereafter) in diaphragm and pore water pressure until air in the samples' void spaces are absorbed into solution. The steady state pore water pressure is measured at each stage to allow the saturation ratios ( $S_r$ ) to be calculated (eqn. A1.3). A saturation ratio ( $S_r$ ) of 0.95 is considered acceptable, although as noted above it may not be possible to attain this for all materials.

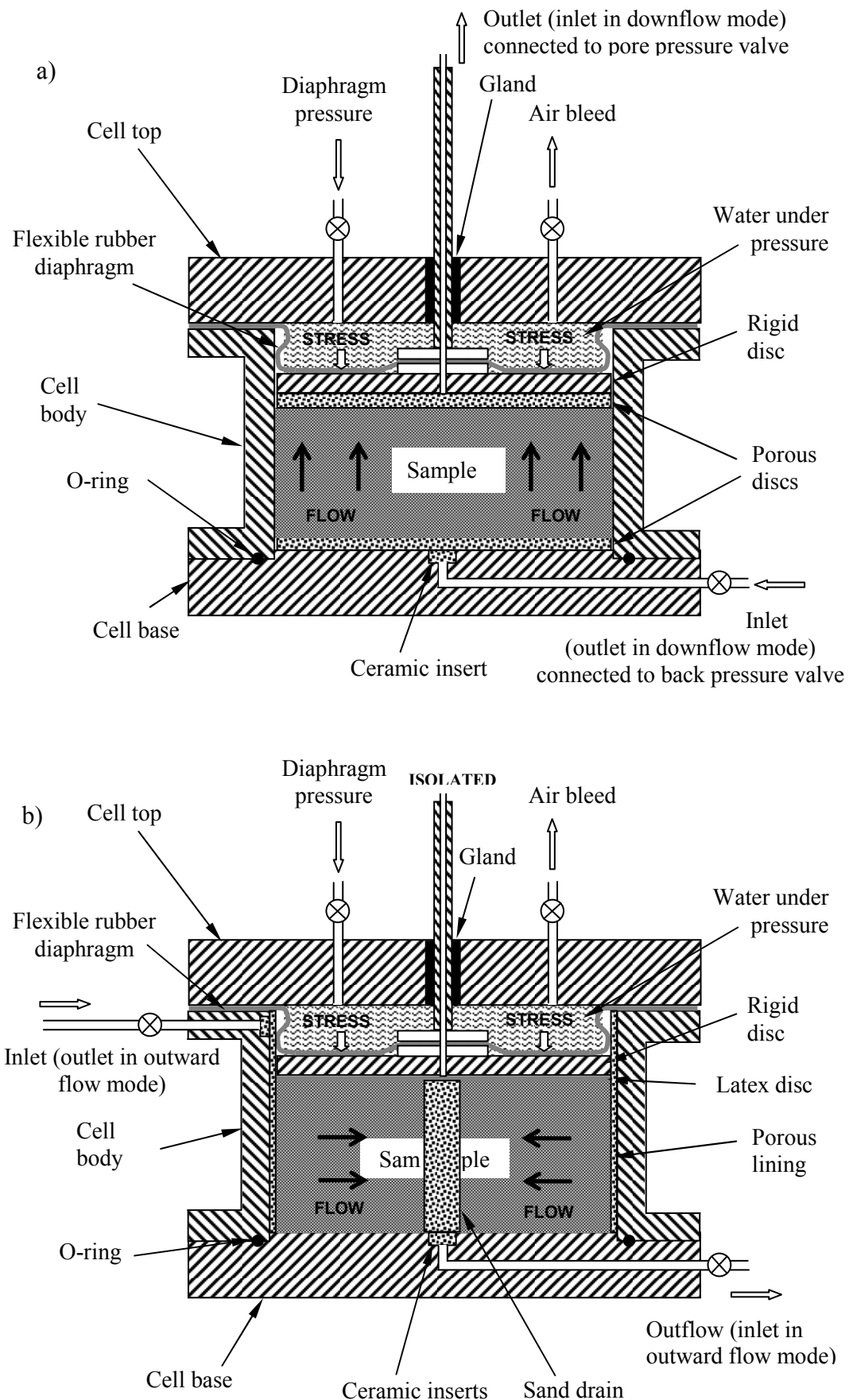


Fig A7. Rowe cell configured for a) vertical hydraulic conductivity measurement and b) horizontal hydraulic conductivity measurement

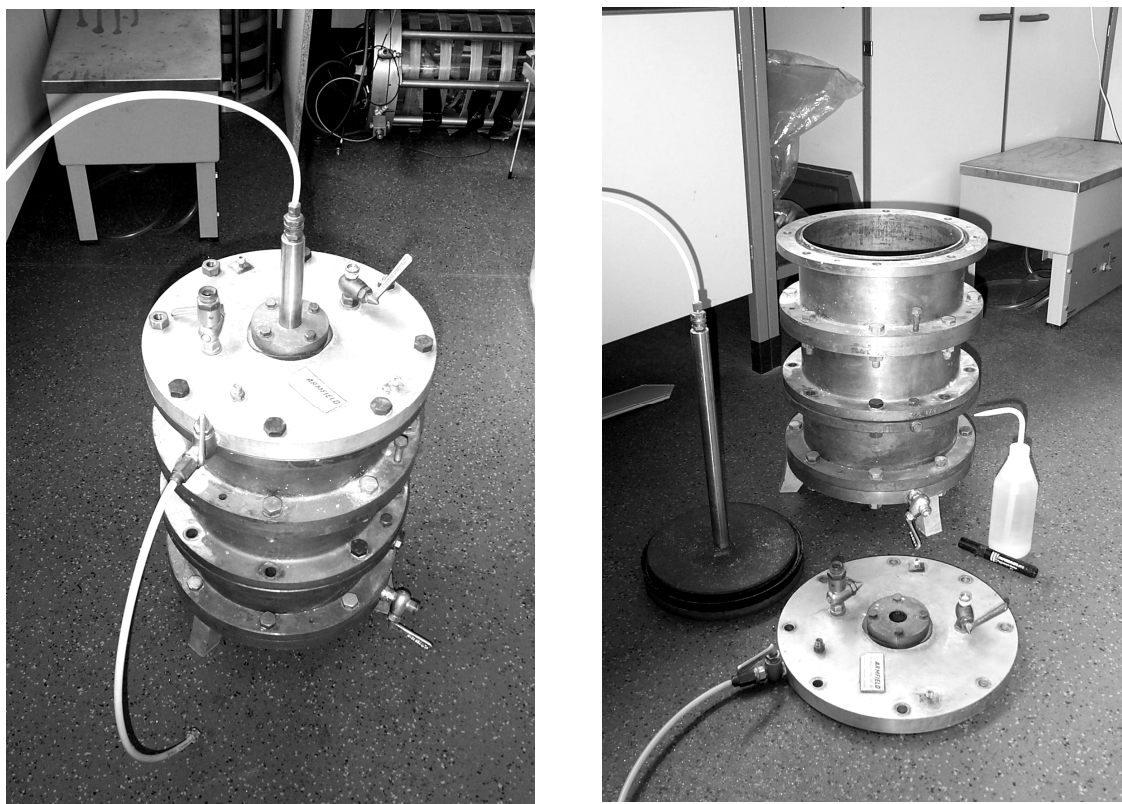


Figure A8. Rowe cell design using o-ring seal in top plate assembled (left) and disassembled (right)

Vertical hydraulic conductivity (Figure A7a) can be assessed at different effective pressures using either upward or downward flow. Tests are conducted under the influence of back pressure to prevent air or gas bubbles coming out of solution and affecting results. Flow is induced by the inlet pressure being greater than the outlet pressure, but inlet pressures must be less than the applied stress. The required head difference may be only be a few centimetres for silty and sandy soils, but may need to be up to 2 m to obtain measurable flow through clay samples (Barnes, 2000). In such cases where high ( $I = 20$  or more) hydraulic gradients are required, the gradient should be increased carefully and the flow rate observed to avoid / detect the onset of piping or internal erosion of the sample. Flow rates should be kept below 20 ml/minute to prevent head loss in the system, although head losses for high flow rates can be determined during calibration of the equipment (Barnes, 2000). The test is essentially the same as the constant head test (section A1.1) and the same calculation for vertical hydraulic conductivity ( $k_v$ ) is used:

$$k_v = \frac{q}{Ai} = \frac{ql\gamma_w}{A(p_1 - p_2)} R_T \quad (A1.4)$$

where:

$k_v$  is vertical hydraulic conductivity (m/s)

$A$  is the cross sectional area of the sample in the horizontal plane ( $m^2$ )

$q$  is the steady state flow rate ( $m^3/s$ )

$i$  is the hydraulic gradient

$l$  is the flowpath length (*i.e.* the sample depth)

$p_1$  is the inlet back pressure

$p_2$  is the outlet back pressure

$\gamma_w$  is the unit weight of permeating fluid

$R_T$  is the temperature correction factor (section 2.4.2)

(Barnes, 2000)

In the horizontal hydraulic conductivity test vertical flow is prevented and a permeable central core (usually sand but sintered bronze can be used) and porous peripheral layer (1.5 mm thick porous plastic – BS1377: part 6, 1990) are added (Figure A7b). Either can be used as inlet or drain to permit tests to be conducted either with flow radially outwards from the core to the peripheral drain, or with flow from the periphery to the core.

The expression for determining horizontal hydraulic conductivity ( $k_h$ ) is:

$$k_h = 0.26 \frac{q}{H \cdot \Delta p} \log_e \left( \frac{D}{d} \right) \times 10^{-4} \text{ m/s} \quad (\text{A1.5})$$

where:

$q$  is measured flow rate (ml/m)

$\Delta p$  = pressure difference (kPa) =  $p_1 - p_2$

$D$  = the diameter of the sample (mm)

$d$  = diameter of central drain well (mm)

$H$  = height of sample (mm)

(Head, 1986)

Care must be taken with the construction of the sand core. This can be drilled into the sample, but smearing can affect the results. The recommended ratio of sand drain to sample diameter is 1:20 or less (Barnes, 2000)

A potential problem is that the core could restrict sample compression. This is obviously not a problem if full compression of the sample under the applied stress has occurred prior to testing, but could be a significant problem with compressible samples subject to changes in effective stress. Alternatives are to use compressible materials such as rubber crumb as the core material or to allow vertical movement on the central core as shown in the design in Figure A9.

One drawback to the method is that vertical and horizontal tests cannot be performed without disturbing or replacing the sample between the two tests. This is a potential source of error when assessing the  $k_h : k_v$  ratios of a soil as even in the testing of homogeneous soils, 'identical' soil samples are likely to exhibit a range of hydraulic conductivity values by a factor of 2 or 3 (Sarsby, 2000).

*Modified Oedometer*

Al-Tabbaa and Wood (1987) modified an oedometer to conduct both horizontal and vertical hydraulic conductivity testing of kaolin samples (Figure A9). The test method was similar to that used for the Rowe cell (above). For inducing horizontal flow a permeable peripheral layer and central ceramic core were added and a head difference introduced to induce horizontal flow radially from the core to the perimeter. Vertical stress was applied to the sample via a piston acting on top of the sample. The design differed to the Rowe cell in so far as the central core was designed to move downwards as the sample was compressed, thus not restricting sample compression (assuming that friction between the core and o-rings, and the core and the sample was low in comparison to the applied stress). It is possible that the movement of the core could have resulted in smearing of the sample but this was not taken into account in the hydraulic conductivity calculations.

It will be noted that vertical flow tests cannot be conducted with the core in place as flow would be through the core rather than the sample. It is therefore necessary, as in the Rowe cell design, to disturb or replace the sample between vertical and horizontal flow tests.

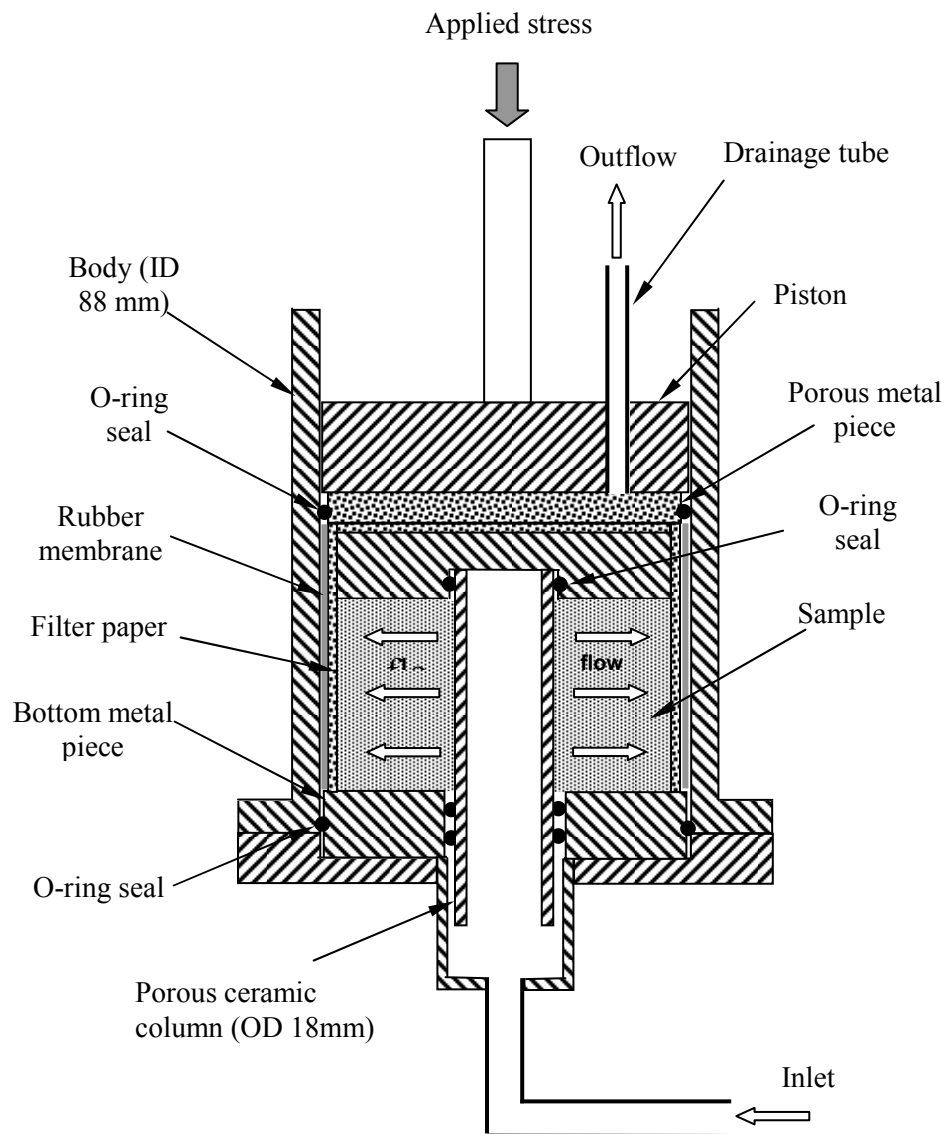


Figure A9. Modified oedometer for horizontal hydraulic conductivity testing of kaolin samples. (Al-Tabbaa and Wood, 1987)

Modified Shelby tube

Agaki and Ishida (1994) conducted a series of horizontal hydraulic conductivity tests on clays by inducing horizontal flow across a thin-walled Shelby sampling tube. Samples were taken by pushing the tubes into the soil stratum using a piston sampler. The tubes measured 75 mm diameter x 1000 mm long with two sets of diametrically opposite rows of holes in the tube wall (1 mm dia x 2.5 mm spacings) along the length of the tube (holes rather than slits were used for ease of manufacture). The ends of the tube were sealed and constant head hydraulic conductivity tests undertaken by inducing a flow across the sample via the diametrically opposite holes. Tests were run at different pore water pressures.

Hydraulic conductivity ( $k$ ) was calculated according to the relationship:

$$k = \alpha (q / H)$$

where: (A1.6)

$H$  = inlet constant head

$q$  = rate of discharge

$\alpha$  = a constant

(the constant  $\alpha$  was estimated to be approximately 4 derived from different mathematical, numerical, electrical analogy and experimental assessments).

## Appendix B. Determination of horizontal flow port sizes

At the design stage the size and number of ports required were based on an estimation of the likely range of flow rates that would occur for wastes under the applied stresses to be used. Darcy's law could not be directly applied as flow across the sample would be forced to diverge on entry and converge in the outlet region. Instead numerical analyses were used - USGS' three dimensional groundwater flow model, MODFLOW (McDonald & Harbaugh, 1988) in conjunction with the pre and post processor package, Groundwater Vistas. The setup and configuration of MODFLOW is described in chapter 8. This was used to estimate horizontal flow rates for the various options of:

- different number of ports (1, 5 and 9 pairs) and spacings
- a range of vertical hydraulic conductivities (from  $1 \times 10^{-4}$  to  $1 \times 10^{-9}$  m/s) anticipated for a range of wastes at applied stresses ranging from 40 kPa to 603 kPa
- alternate port diameters of 42mm (standard port main bore diameter) or 72mm (standard port main bore diameter effectively enlarged by countersink on the inside on cylinder wall – a port cross section is shown in Figure 5.1)
- two possible test conditions of 1) confined or 2) unconfined top and bottom boundaries (in confined conditions the outlet is restricted to the outlet ports only but in unconfined conditions water is allowed to flow out through the top and bottom of the waste as well as outlet ports)
- A range of  $k_h : k_v$  ratios from 1 to 100 – it was anticipated that waste  $k_h : k_v$  ratios would be somewhere in this range

Tables B1 to B4 summarise the flow rates for the computer analyses for the possible port arrangements of a set of single ports, a set of 5 ports (Table B4 only) and a set of 9 ports (the number of available horizontal flow ports would be restricted as the samples were compressed). Flow rates are shown for 72 mm diameter ports and 42 mm

diameter for a range of waste hydraulic conductivities and  $k_h : k_v$  ratios. For multiple ports, the flow rate shown is the sum of all the individual input flow rates. The input and output heads were designated 600 cm and 100 cm above ground level respectively<sup>5</sup>. Pressure heads at the centre of the waste body are also shown as it was hoped that pressure heads within the waste could be used as a complementary indicator of the  $k_h : k_v$  ratio. For the ‘confined’ tests in particular, the ‘head at centre’ values were insufficiently sensitive to  $k_h : k_v$  ratios to be used as such.

Table B1. Flow rates (litres/hr) for single 72 mm diameter ports [*42 mm dia in brackets*].

No outflow via top and bottom of waste

$K_v$ (m/s)	$K_H = K_v$	$K_H = K_v \times 5$	$K_H = K_v \times 10$	$K_H = K_v \times 100$
$1 \times 10^{-4}$	60 [27]	262 [111]	460 [200]	3700 [1600]
$1 \times 10^{-5}$	6.0 [2.7]	26.2 [11.1]	46 [20]	370 [160]
$1 \times 10^{-6}$	0.6 [0.27]	2.62 [1.11]	4.6 [2.0]	37.0 [16]
$1 \times 10^{-7}$	0.06 [0.027]	0.26 [0.11]	0.46 [0.2]	3.7 [1.6]
<b>Head at centre</b> (cm)	348 [315]	340 [325]	348 [329]	350 [345]

Table B2 Flow rates (litres/hr) for single 72 mm diameter ports [*42 mm dia in brackets*]. Outflow via ports and top and bottom of waste

$K_v$ (m/s)	$K_H = K_v \times 5$	$K_H = K_v \times 10$	$K_H = K_v \times 100$
$1 \times 10^{-4}$	500 [200]	900 [370]	5700 [2600]
$1 \times 10^{-5}$	50 [20]	90 [37]	570 [260]
$1 \times 10^{-6}$	5.0 [2.0]	9.0 [3.7]	57 [26]
$1 \times 10^{-7}$	0.5 [0.2]	0.9 [0.37]	5.7 [2.6]
<b>% of I/P flow to O/P ports</b>	1.6	3.8	30
<b>Head at centre</b> (cm)	115 [105]	125 [110]	222 [170]

<sup>5</sup> the actual inlet and outlet heads used later in tests were higher than this but the values used were acceptable as flow rates are a function of the *difference* between inlet and outlet heads. A similar 500

Table B3 Flow rates (litres/hr) for 9 off x 72 mm ports with 140mm spacing [9 off x 42 mm dia. 140mm spacing in brackets]. No outflow via top and bottom of waste

$K_v$ (m/s)	$K_H = K_v$	$K_H = K_v \times 10$	$K_H = K_v \times 40$
$1 \times 10^{-4}$	450 [191]	3600 [1700]	13500 [5887]
$1 \times 10^{-5}$	45.0 [19.1]	360 [170]	1350 [589]
$1 \times 10^{-6}$	4.5 [1.9]	36 [1.7]	135 [58.9]
$1 \times 10^{-7}$	0.45 [0.19]	3.6 [1.7]	13.5 [5.9]
<b>Head at centre (cm)</b>	350 [346]	350 [340]	350 [349]

Table B4. Flow rates (litres/hr) for 9 off 72 mm ports with 140mm spacing with outflow also through top and bottom of waste  
[9 off 42mm dia. 140mm spacing in brackets]  
5 x 72 mm dia. 280 mm spacing denoted by \*

$K_v$ (cm/s)	$K_H = K_v \times 2$	$K_H = K_v \times 5$	$K_H = K_v \times 10$	$K_H = K_v \times 20$	$K_H = K_v \times 40$
$1 \times 10^{-4}$	1673	3665	6480 [3040] 4200*	11241	23000 [11300] 15000*
$1 \times 10^{-5}$	167.3	366.5	648 [304] 420*	1124	2300 [1130] 1500*
$1 \times 10^{-6}$	16.7	36.7	64.8 [30.4] 42*	112.4	230 [113] 150*
$1 \times 10^{-7}$	1.7	3.7	6.5 [3.0] 4.2*	11.2	23 [11.3] 15*
<b>% of I/P to O/P</b>	1.7	6.5	14 [8] 7.4*	25.6	45 [27.5] 30.6*
<b>Head at centre (cm)</b>	125	160	200 [151] 165*	247	302 [244] 264*

cm head difference was initially used in the tests

The analyses indicated that flow rates could vary considerably depending on:

- the number of inlet and outlet ports
- whether flow was allowed out of the top and bottom of the sample
- the hydraulic conductivity of the waste
- the  $k_h : k_v$  ratio

For example, a rate of 0.06 l/h was estimated for flow from a single input to a single output port through waste of low permeability ( $k_v$  and  $k_h = 1 \times 10^{-7}$  m/s) – Table B1. In comparison, a total flow rate in excess of 2000 l/h was indicated for a high permeability waste ( $k_v = 1 \times 10^{-5}$  m/s and  $k_h = 40 \times k_v$ ) multiple inlet/outlet port arrangement with outflow also through the top and bottom of the sample – Table B4. Excessively high flow rates would be difficult to manage and could wash material from the sample out of the outlet ports. Head losses of several centimetres could arise from frictional losses in the pipework for flow rates of several hundred litres an hour through each port (Figure F1). Conversely low flow rates (below 1 l/h) would be difficult to measure with any accuracy. The low flow rates were more of a concern as high flow rates could be controlled to some degree by reducing inlet head height. As a result it was evident that it was necessary to have as many large (72 mm) diameter ports as possible, with an isolating valve on each port to allow the inlet/outlet configuration to be changed as required.

## Appendix C. Relationship between hydraulic ram pressure and applied stress

Sample compression was controlled by the hydraulic pressure in the rams acting on the top platen. The total force (F) applied to the sample is given by:

$$F = P_1 \cdot A_1 + F_{plat} + F_{topgl} + F_{oil} \quad (C1.1)$$

where:

$F$  = total applied force (kN)

$P_1$  = hydraulic pressure in rams (kPa)

*(as indicated on pressure gauge in bar, 1 bar = 100 kPa)*

$A_1$  = cross sectional area of both hydraulic rams

$$= 2 \pi (0.125)^2 = 0.0982 \text{ m}^2$$

$F_{plat}$  = weight of cylinders and top platen (28.85 kN)

$F_{topgl}$  = weight of top gravel layer (kN)

$F_{oil}$  = weight of oil in rams (kN)

The weight of the top gravel layer ( $F_{topgl}$ ) was between 300 and 350 kg for the two samples tested. This equates to a stress of approximately only 1 kPa (stress = load /area =  $325 \text{ kg} \times 9.81 \text{ m/s} / 3.14 \text{ m}^2 = 1.01 \text{ kPa}$ ) and so is usually disregarded. The weight of the oil in the hydraulic rams is dependent on the length that the rams are extended as shown in Figure C1. Even at full ram extension, the weight of the oil is only 150 kg. This additional weight only represents a maximum additional stress of approximately 0.5 kPa and so is again disregarded for practical purposes.

The stress applied ( $P_2$ ) to the sample is given by:

$$P_2 = F / A_2$$

where:

$$(C1.2)$$

$F$  = total applied force (kN)

$A_2$  = area of top platen ( $m^2$ ) =  $\pi$  (as diameter is 2 m)

The maximum operating pressure is 190 bar (19,000 kPa). This (disregarding  $F_{topgl}$  and  $F_{oil}$ ) gives a maximum applied stress of:

$$P_2 = \frac{(19,000 \times 0.0982) + 28.85}{\pi}$$

$$= 603 \text{ kPa}$$

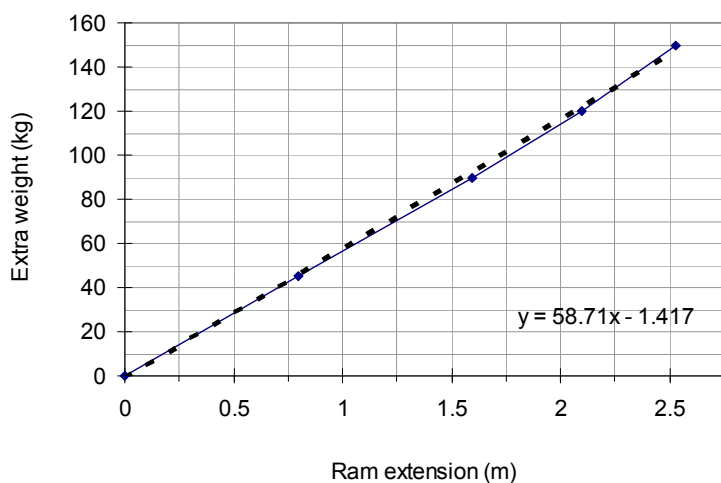


Figure C1. Additional weight of oil (recorded by load cells) with extension of top platen rams

## **Appendix D. Assessment of stress transmission losses arising from friction between the waste sample and cylinder wall**

### **D1. Measurement of stress transmission loss using pressure cells**

Total earth pressure cells were installed in the samples (section 5.5) to directly measure stress transmitted to the base and intermediate depths of the sample. Although the pressure cells gave consistent readings in response to changes in pore water pressure (maximum recorded errors of about 1 % at pore water pressures up to 73 kPa), response to applied stress was inconsistent and it was not possible to deduce stress transmission losses from the data obtained.

### **D2 Use of strings inserted in the sample**

Lengths of string were inserted into the sample AG2 at various elevations via ports in the cylinder wall as shown in Figure D1. During compression measurements were made of the length that each string was pulled into the waste by downward movement of the sample. The data obtained from this method were inconsistent and are not shown in this thesis.

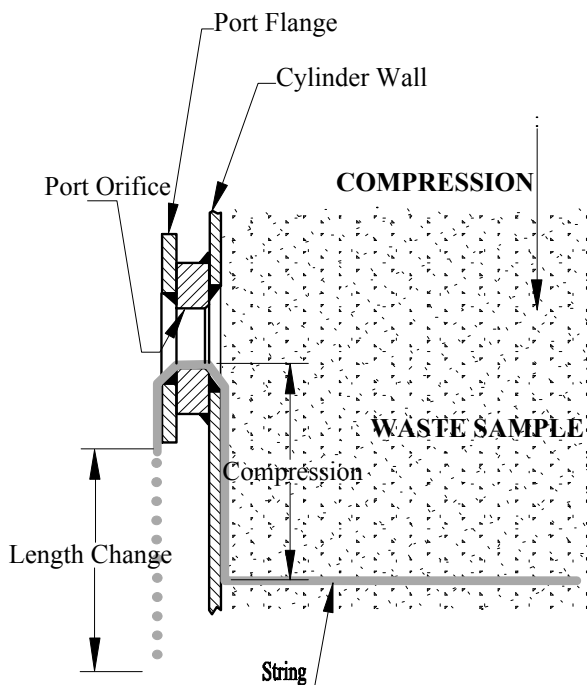


Figure D1 Cross-section of differential compression measurement string method used on sample AG2

### D3. Use of magnetic extensometer

An alternative approach to that described in section D2 to assess stress transmission losses in sample DN1 was to measure the settlement throughout the depth of a sample during compression using a magnetic extensometer manufactured by Soil Instruments. A vertical plastic tube (Figure 5.1) was installed throughout the depth of the sample with ring magnets (consisting of three equispaced magnets set in a plastic ring) located at various vertical positions on the tube (shown on Figures 5.5). During compression of the sample, the change in the position of the magnets was detected using a probe inserted into the tube. The probe consisted of reed switches enclosed in a metal weight. In the vicinity of a ring magnet the contacts on the reed switches closed completing a circuit containing a light and buzzer. With careful use, measurements with a repeatability of less than 1 mm could be attained.

The displacements of the magnets during the first five compression stages of sample DN1 are shown in Figures D2 a) to e). Problems with tube distortion were encountered at the higher compression stages and no data for the final compression stage (603 kPa applied stress) are available. Data for the 228 kPa applied stress compression stage (Figure D2 d) were taken before compression was complete. Beyond this stage, the extensometer was trapped in the distorted plastic tube necessitating adjustment of the tube and magnet positions (hence loss of data) in order to release it. Detection of the lower magnet positions was not possible at the 334 kPa applied stress stage as the extensometer would not pass through the damaged area in the lower part of the tube. However at this stage a number of additional 'phantom' magnets were detected which are shown as additional points on Figure D2 e). The extra readings were originally presumed to be caused by metal items in the waste sample. Subsequently it has been discovered that the plastic housing rings can be brittle and could have broken at higher stress. It is probable that the extra signals came from fragments containing one of the three magnets originally held together in the ring.

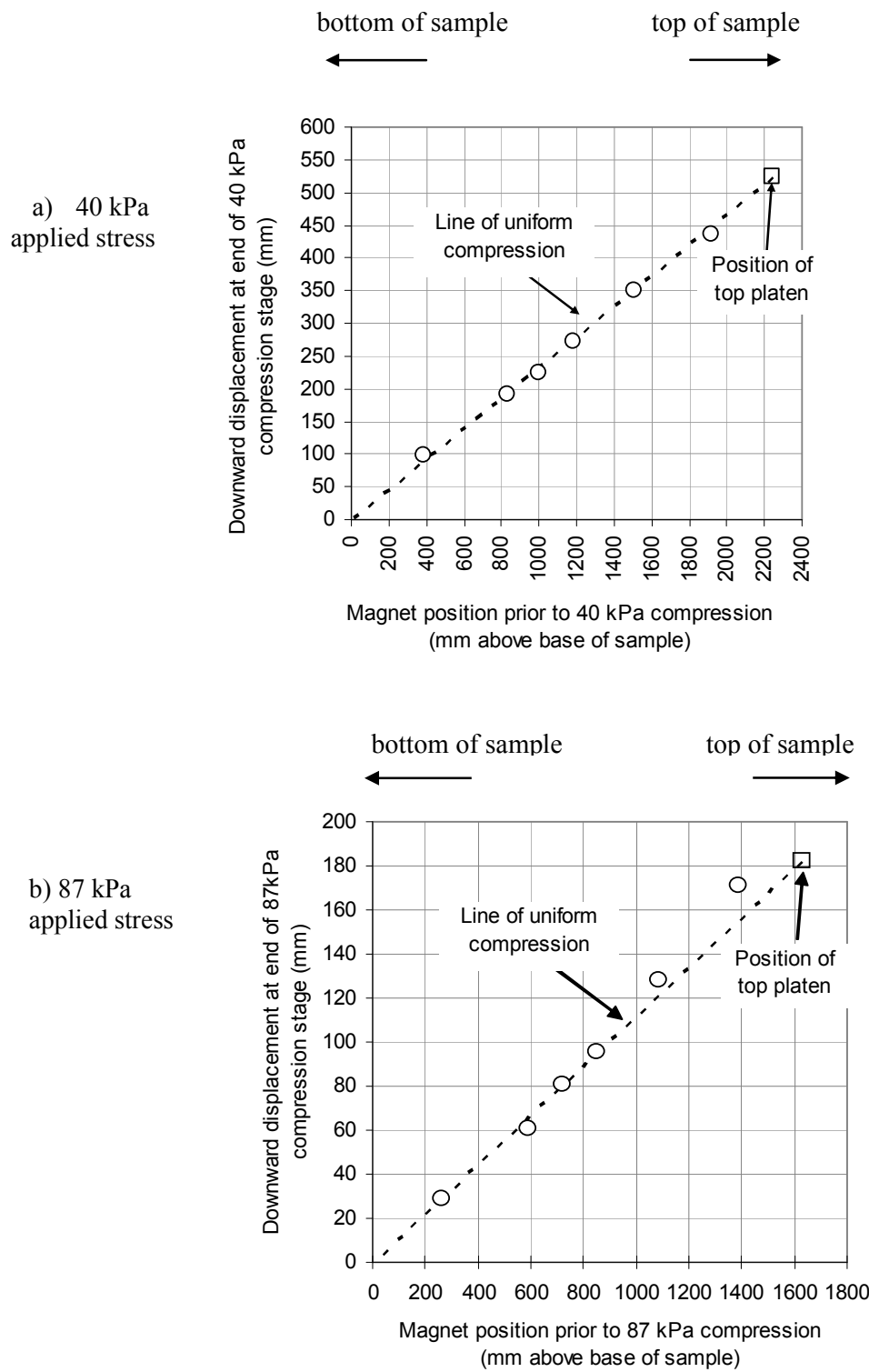


Figure D2 a) and b). Displacement of magnets in sample DN1 at 40 kPa and 87 kPa applied stress

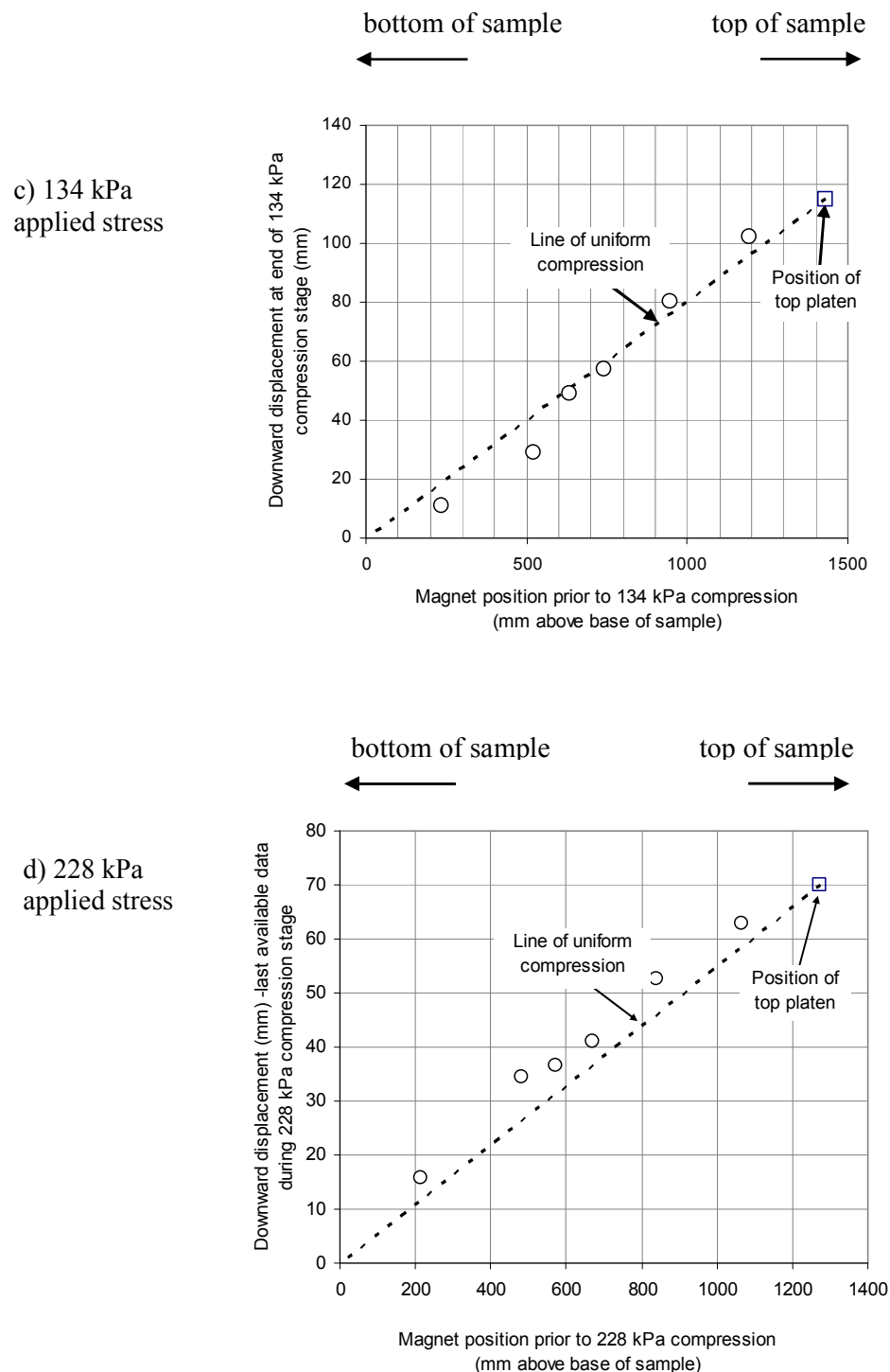


Figure D2 c) & d). Displacement of magnets in sample DN1 at 134 kPa and 228 kPa applied stress

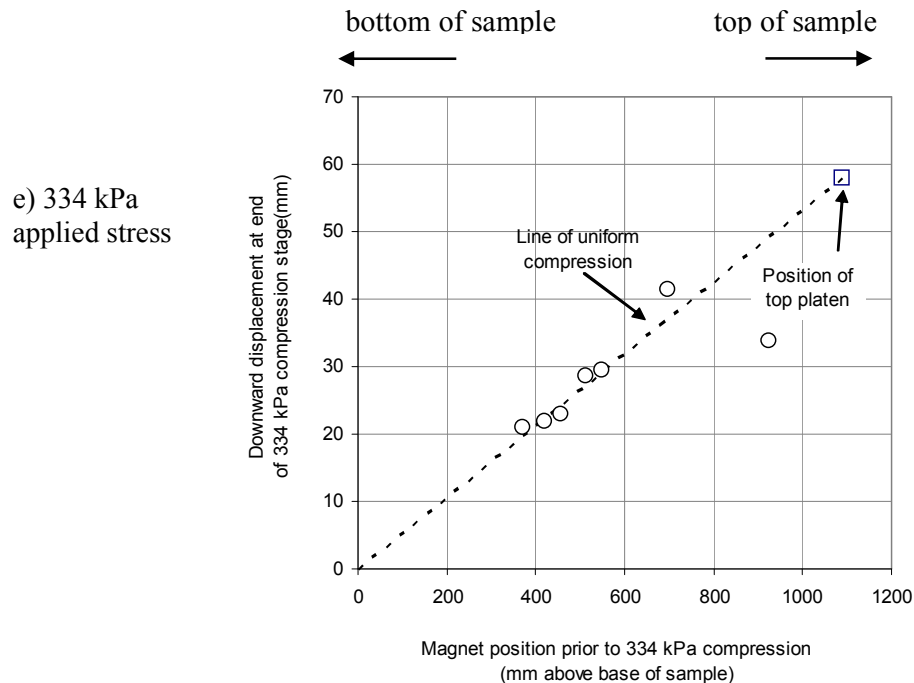


Figure D2 e) Displacement of magnets in sample DN1 at 334 kPa applied stress

In Figures D a) to e), the co-ordinates of each point on the graphs represent the vertical displacement of each of the six magnets after each compression stage. Also shown is the theoretical line of uniform compression throughout the sample according to the downward displacement of the top platen during compression; uniform compression throughout sample depth should result in all points representing the magnet positions lying directly on the line of uniform compression. This is more or less the case in Figure D2 a) for the first compression stage at 40 kPa effective stress. Data at subsequent compression stages shown in Figures D2 b) to e) are less reliable. In several instances the measured displacement of the magnets exceeds that indicated by the line of uniform compression. This should not have arisen and the cause is not clear. Preferential compression should result in a below average displacement of the magnets and the points representing the magnets would lie below the line of uniform compression.

In general the data in Figures D2 a) to e) show no consistent under-reading. This indicates that there is no significant differential settlement of the sample, although this cannot be stated unreservedly due to the inconsistencies in some of the data.

#### D4 Use of drainable porosity data to determine density variations with sample depth

The method for measuring drainable porosity was described in section 6.2, but essentially after the completion of each compression stage, leachate or water was either added in stages to raise a sample from field capacity to saturated condition, or drained in stages from a saturated sample to field capacity condition. For either situation, the amount of leachate / water added or drained can be plotted against the change in leachate / water level for which the drainable porosity at each compression stage is determined. These plots are shown for sample AG2 in Figures D3 and sample DN1 in Figures D4. Due to the sensitivity of drainable porosity to waste density, variations in the drainable porosity may be evident in accordance with density changes throughout sample depths. A straight line plot would be indicative of uniform porosity and therefore uniform density throughout sample depth. The presence of sidewall friction during compression would result in decreasing density with sample depth and an increase in the gradient of the line towards the top of the sample. In the absence of sidewall friction, increasing sample density with sample depth may occur from the weight of the sample. This should produce an increase in gradient of drainable porosity plots at the base rather than the top of the sample, although this is only likely to be noticeable in the initial compression stages as stress due to sample weight is negligible compared to applied stress at higher compression.

The plots of water level against the volume added shown in Figures D3 and D4 generally exhibit straight line relationships. Some inconsistencies are apparent between the individual points of the drainable porosity data, particularly where gas has caused water level rises or stabilised readings have been difficult to achieve. No data are available at the highest stress stages due to problems in obtaining consistent water levels and difficulties in draining samples.

The straight line plots indicate reasonably uniform densities throughout the depth of the samples at all compression stages. However it cannot be stated with certainty that stress is unaffected by friction between the sample and cylinder wall as it is possible that density variations are hidden by the inconsistencies between individual readings.

Although the drainable porosity data is insufficiently accurate to definitely determine the presence or absence of density variations throughout sample depth, it is possible to use the drainable porosity plots to estimate the maximum probable transmission losses. It is known from compression cell tests on shredded tyres for which preferential compression was evident (Hudson *et al.*, 2003) that a 2 % difference in a drainable porosity plot (for example a drainable porosity value of 8 % at the top of the sample and 10 % at the bottom) is readily identifiable amongst variations between individual points on the plot. This has been applied to the AG2 and DN1 data below to estimate the maximum likely loss of stress at the base of the samples

In Figure D5 the average drainable porosities for sample AG2 at each compression stage (obtained from the gradients shown in Figure D3) are plotted against the applied stress. Also shown is the curve representing a drainable porosity 2 % higher than the average value throughout the applied stress range. This is the maximum likely drainable porosity at the base of the sample on the basis that differences greater than 2 % would have been evident from the drainable porosity plots. At each compression stage the upper curve has been used to determine the minimum stress likely at the base of the sample for each compression stage.

No reliable drainable porosity data were available at higher stresses. In Figure D7 the revised minimum stress values have been extrapolated to estimate the minimum stress at the base of the sample at an applied stress of 603 kPa. The process is repeated for sample DN1 (Figures D6 and D8). For both samples the stress loss calculated using the drainable porosity data is much less than the maximum theoretical loss (50% or more – section 5.3.2).

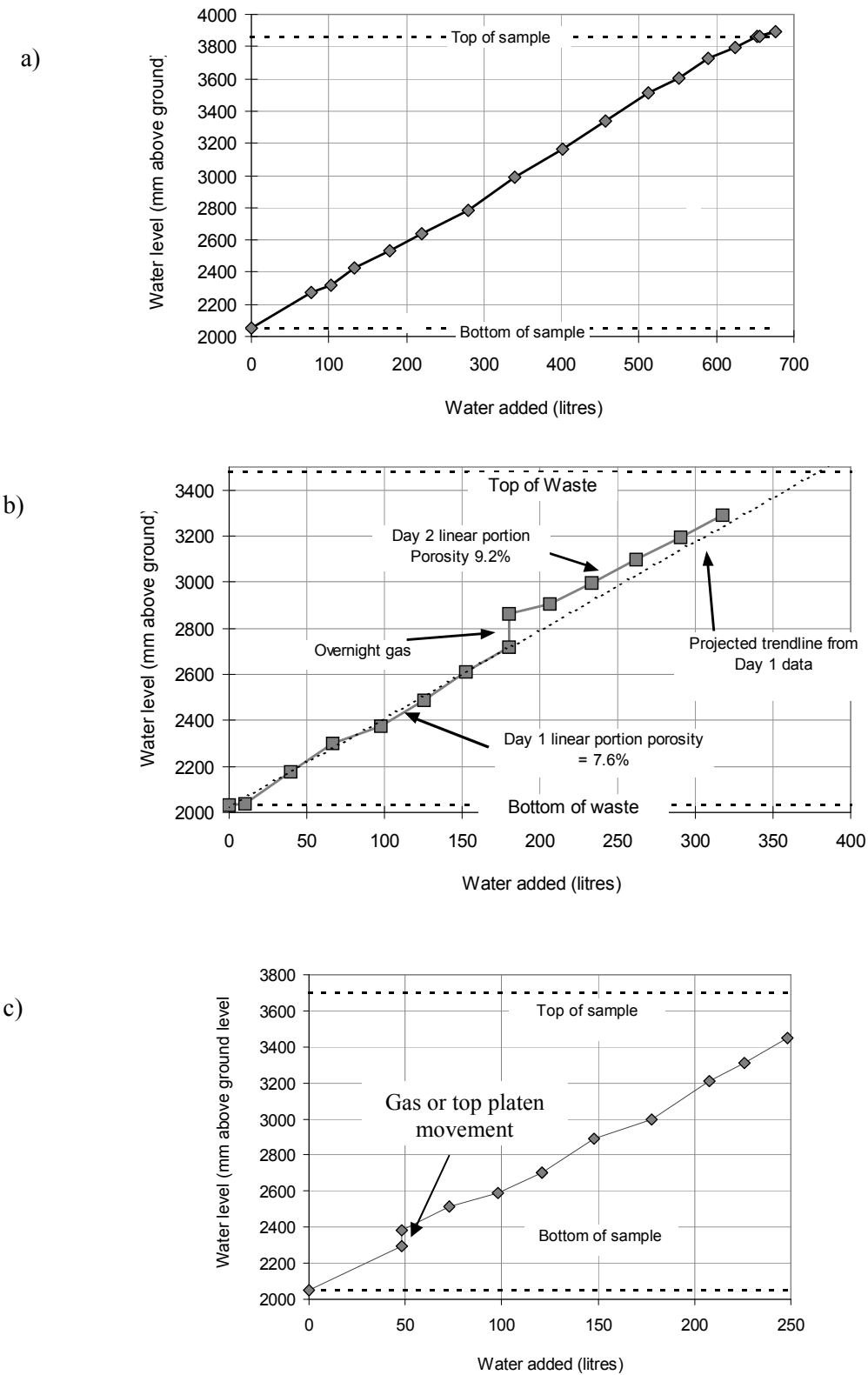


Figure D3 Drainable porosity plots for sample AG2 at applied stresses of a) 40 kPa, b) 87 kPa and c) 165 kPa.

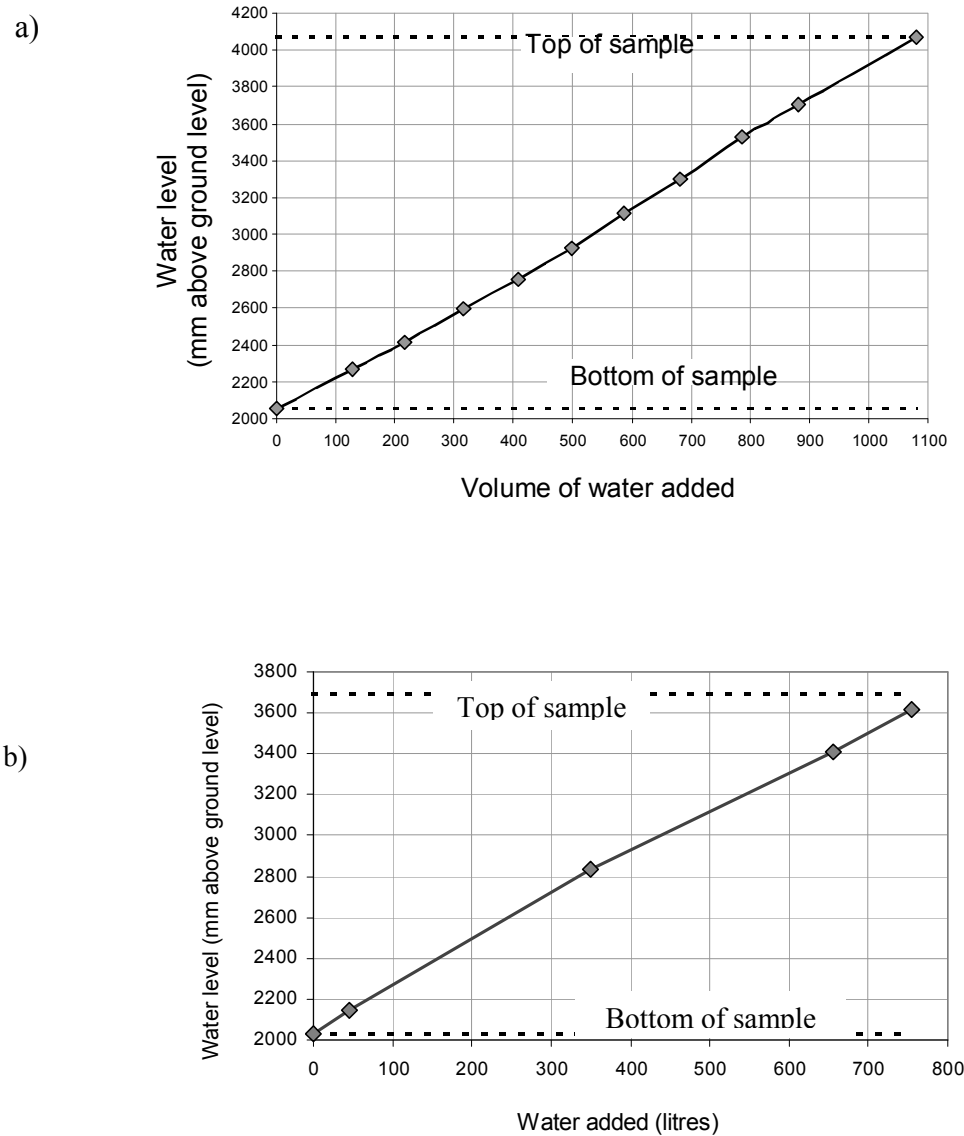


Figure D4 a) and b). Drainable porosity plots for sample DN1 at applied stresses of a) 40 kPa, b) 87 kPa

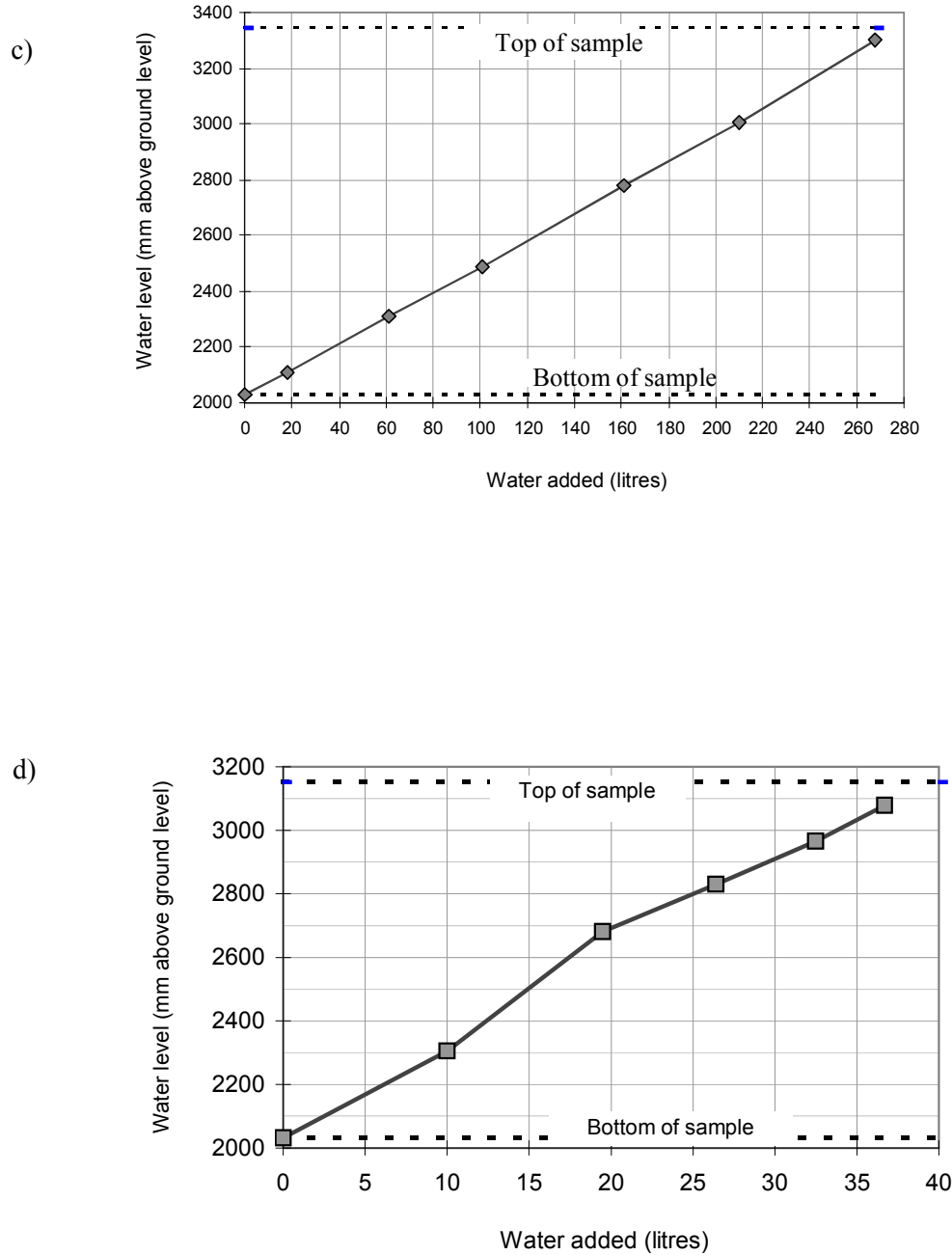


Figure D4 c) and d). Drainable porosity plots for sample DN1 at applied stresses of c) 134 kPa and d) 228 kPa

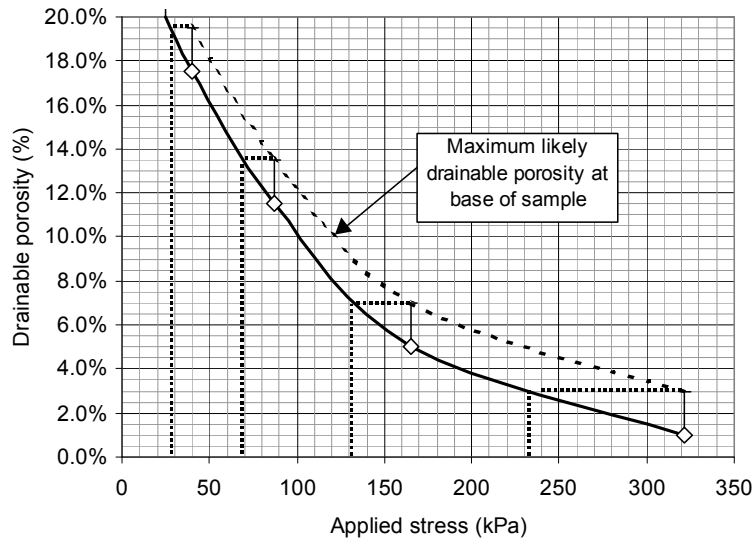


Figure D5. Drainable porosity plots for sample AG2 showing estimated minimum stress at base of the sample for each compression stage (based on maximum 2 % variation in drainable porosity gradients)

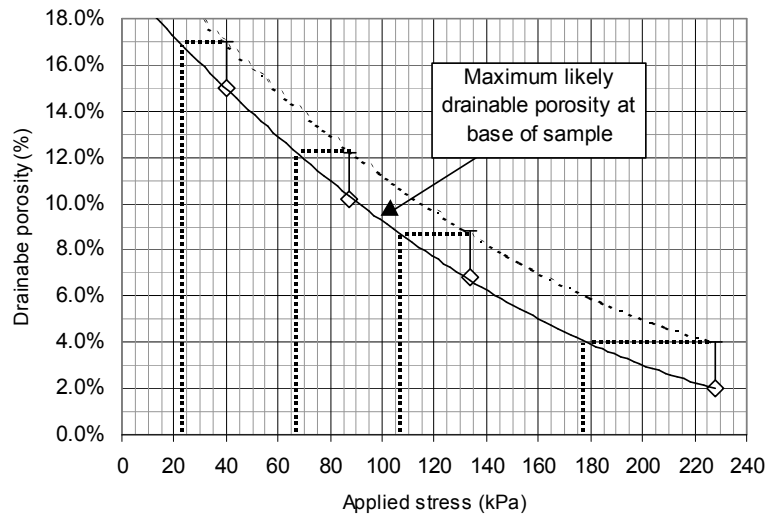


Figure D6. Drainable porosity plots for sample DN1 showing estimated minimum stress at base of the sample for each compression stage (based on maximum 2 % variation in drainable porosity gradients)

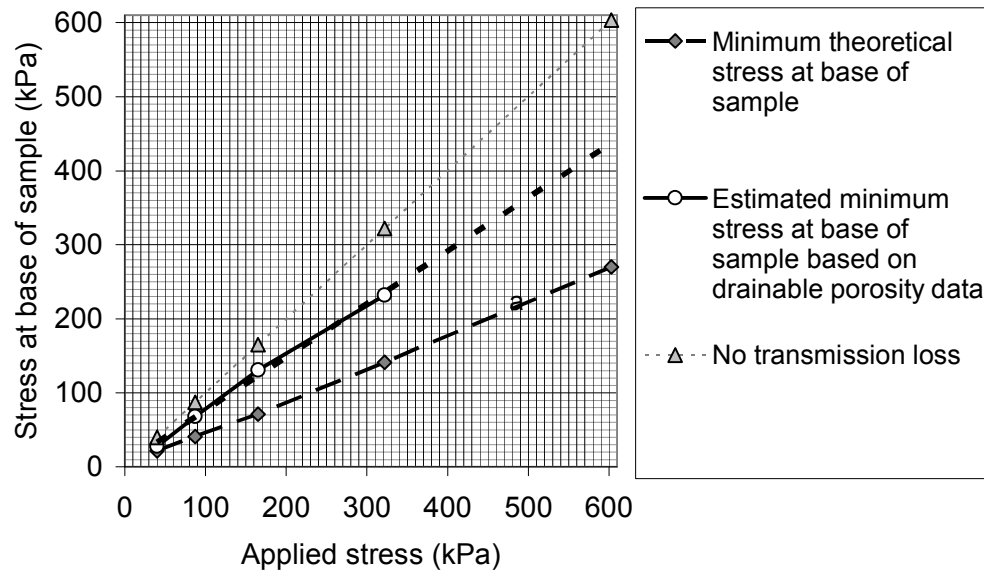


Figure D7 Plot of theoretical maximum and estimated transmission losses at base of sample AG2 based on drainable porosity data

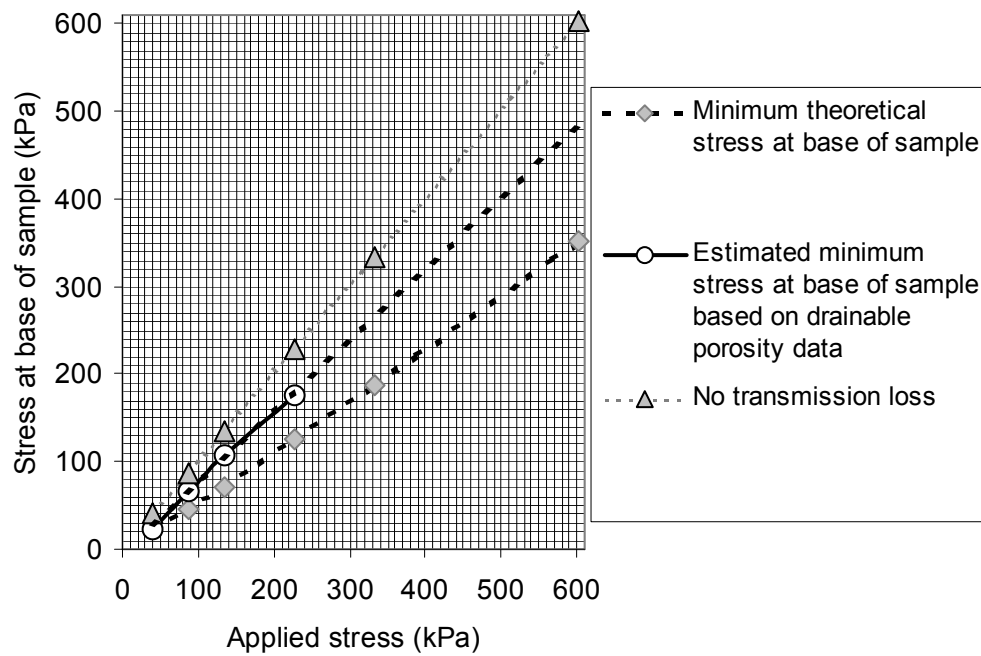


Figure D8. Plot of theoretical maximum and estimated transmission losses at base of sample DN1 based on drainable porosity data

## Appendix E. Effective stress

The introduction of leachate into the sample for the drainable porosity and hydraulic conductivity tests following completion of each compression stage would have produced a change in pore water pressure in the samples, and hence a change in effective stress. The relationship between effective stress, applied stress and pore water pressure is given by:

$$\text{Effective stress } (\sigma') = \text{total normal stress } (\sigma) - \text{pore water pressure } (u)$$

(Terzaghi, 1936)

In unsaturated conditions the applied stress would have been borne by the waste structure but when the sample was saturated the applied stress would be carried by both the waste structure and the pore water pressure of the leachate. Effective stress would be the component of the applied stress taken by the waste structure.

It is the effective stress, rather than normal total stress, that controls the volume and strength of the soil (Powrie, 1997). In triaxial cell tests on soils, changes in pore water pressure (back-pressure) can be compensated by altering the vertical or confining stress to maintain the effective stress. This was not done on tests in the compression cell and it would appear that the applied stress values should be corrected to the effective stress value in presentation of the results. There is however some question as to whether the principle of effective stress can be applied to landfill wastes as although it gives a close approximation of the effective stress in most saturated soils, it does not produce valid results for concrete, some rocks and compressible materials (Skempton, 1960, Craig, 1983, Powrie, 1997, Barnes, 2000). As waste is compressible and is unlikely to be fully saturated (section 2.4.6), it is uncertain if the principle of effective stress will be valid. Expressions relating effective stress with the saturation ratio in unsaturated soils have been proposed but are not totally satisfactory (Skempton, 1960, Powrie, 1997). Sarsby (2000) observed that soils with air bubbles in the soil are usually assumed to have a negligible effect on effective stress calculations

if the saturation is 90% or more. It is possible that the waste samples tested may have been sufficiently saturated in nominally gas purged conditions but not when gas had been allowed to accumulate. However until this is demonstrated, it is assumed that the effective stress relationship is applicable to wastes.

If it is accepted for the present that landfill wastes conform to the principle of effective stress, it is evident that significant changes in effective stress could have occurred according to changes in pore water pressure during hydraulic conductivity tests. This would have particularly occurred at the first compression stages where pore water pressures were of a similar order or even higher than the applied stress. In such circumstances the effective stress would be much lower than the applied stress, or even negative if pore water pressure was greater than applied stress. As volume is controlled by effective stress (Mitchell, 1976) it would be expected that a reduction in effective stress in the sample following the introduction of pore water at high pressure would have resulted in the sample expanding (compression cell tests have demonstrated that waste samples will rebound to some extent when applied stress is reduced). In the case of the pore water pressure being greater than the applied stress the sample may be expected to become fluidised or even pushed out of the cylinder. None of this occurred as sample expansion was essentially prevented by the fixed position of the top platen (section 5.3.1) during the hydraulic conductivity tests (a slight movement of the top platen was evident during some tests, presumably due to 'slack' in the Acrow props, but this amounted to maximum changes in sample volume of about only 0.1%). As sample volume essentially remained unchanged when pore water pressure was increased it is concluded that effective stress in the sample was not altered. In these strain controlled rather than stress controlled conditions, it can be assumed (as was by Beaven, 2000) that effective stress in the sample is the applied stress (with the addition of stress arising from the weight of the sample less frictional losses as discussed in section 5.3.2). This assumes that the forces within the sample remain 'locked in' by fixing the top platen position prior to removal of the applied stress (section 5.3.1). This is probably a safe assumption for typical test periods of days or a few weeks. However this could be a problem for extended tests in fresh or recent wastes which would normally undergo long-term consolidation (Watts *et al.* 2001, 2002, 2006, Sarsby, 2000). It would be expected that the 'locked in' stress would decrease with time. Eventually, possibly after several months or years, the

sample may decompose to such an extent that it would no longer be in contact with the top platen.

In the compression cell arrangement used it would appear that pore water pressures were transmitted via the hydraulic rams and / or Acrow prop supports to the compression cell framework. Attempts were made to detect changes in stress in the Acrow props according to changes in pore water pressure by inserting load cells between the base of the Acrow props and the top platen. Increases in stress were recorded but were not consistent and so are not presented in this thesis. It is possible that not all the stress was transmitted through the Acrow props. Some stress may have been taken by the top platen seals and the hydraulic cylinders.

The general conclusion that applied stress remains unaffected by pore water pressure may however require further qualification due to the effect of uneven distribution of pore water pressure in the sample during tests. Differences in pore water pressure between the top and bottom of the sample were inevitable during hydraulic conductivity tests and these could be significant if there was several meters difference in elevation between the inlet header tank and outlet U-bend elevations. Figure E1 shows typical inlet and outlet pore water pressures that could be present for the a) upward flow and b) downward flow arrangements

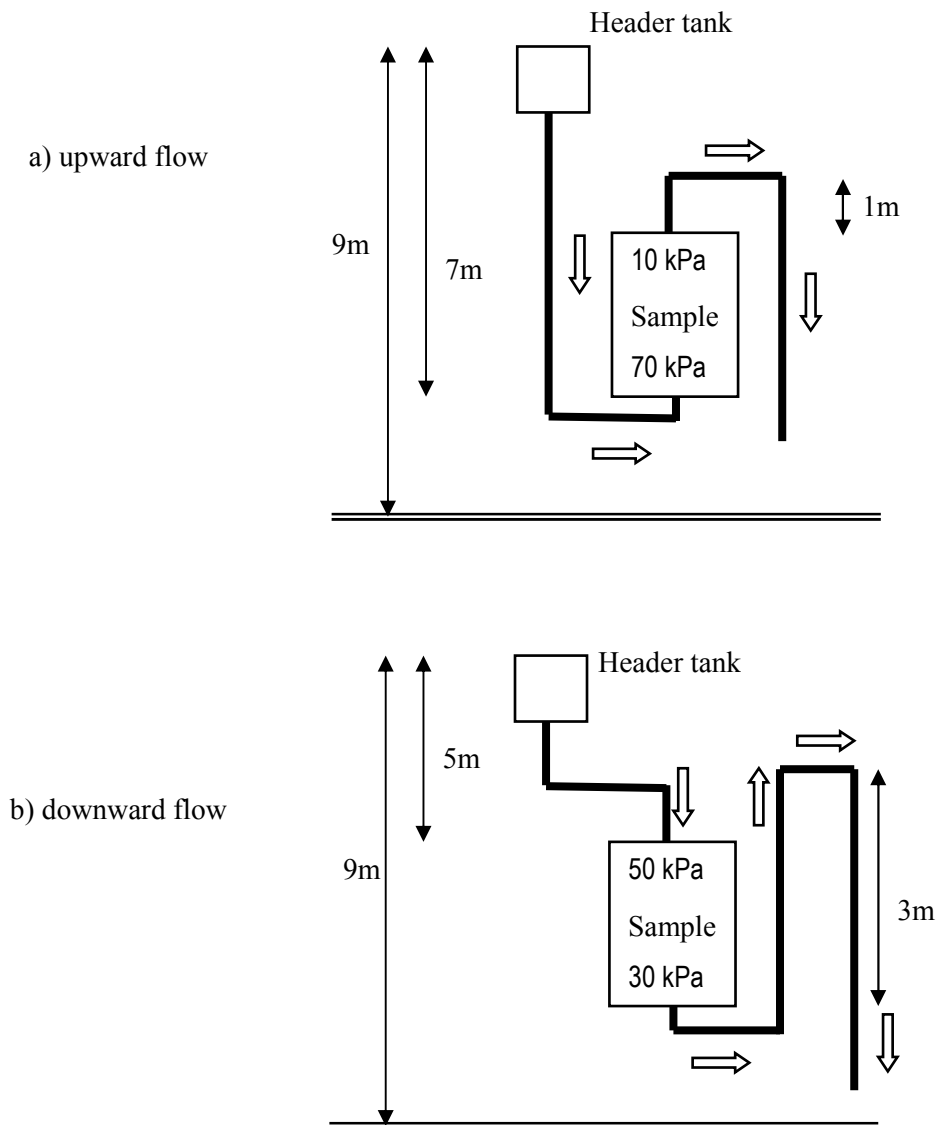


Figure E1. Diagram of typical inlet and outlet pore water pressure for upward and downward flow vertical hydraulic conductivity tests

In established test conditions, variations in hydraulic conductivity throughout the sample depth could be determined from the head readings shown by the piezometer tubes installed at different elevations in the sample. Sometimes these indicated that hydraulic conductivity was higher in areas of high pore water pressure (typically in the vicinity of the inlet) and lower in areas of reduced pore water pressure (towards the outlet region). An example is shown in Figure E2 (sample DN1 at an applied stress of 134 kPa) which shows the different hydraulic conductivity values obtained throughout sample depth for upward and downward flow tests.

Upflow tests using a high (70 kPa) pore water pressures inlet and low outlet pressure (15 kPa) produced approximately an order of magnitude decrease in hydraulic conductivity from the bottom to the top of the sample. The result of reducing the inlet pore water pressure (from about 70 kPa to about 30 kPa) can also be seen on Figure E2. The hydraulic conductivity remained unchanged in the middle to upper region of the sample but reduced significantly at the base of the waste, producing a more uniform hydraulic conductivity throughout sample depth. In the downward flow test the reverse trend is again apparent with hydraulic conductivity being greatest at the top of the sample where the pore water pressure was highest (55 kPa). In accordance with the lower pore water pressure differential in this test the hydraulic conductivity are more consistent throughout sample depth than the upward flow test with a large pore water pressure differential.

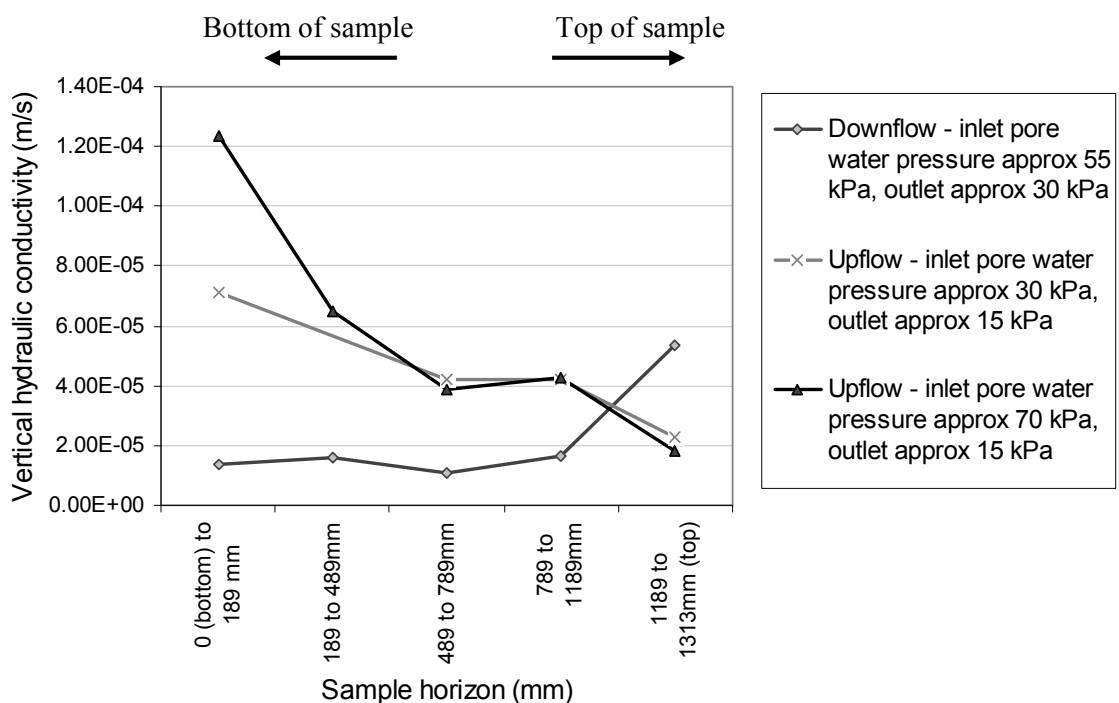


Figure E2. Variations in vertical hydraulic conductivity assessments with sample depth for sample DN1 at an applied stress of 134 kPa

The cause of the elevated hydraulic conductivities in high pore water pressure areas may be due to compression of accumulated gas in high pore water pressure areas but it could also be due to changes in effective stress in high pore water pressure areas.

Although the total volume and therefore bulk density of the sample remained unchanged, the magnetic extensometer readings for sample DN1 showed that the vertical flow of leachate used in the hydraulic conductivity tests could cause movement within the waste. Generally these showed a slight upward shift of the middle portion of the sample during upward flow tests (the magnets positioned at the top and bottom of the sample hardly moved in any circumstances), and a downward shift during downflow tests. Most movement occurred during hydraulic conductivity tests with high flow rates. Magnet movements of up to 15 mm (approx 6% of total sample height) were initially recorded at the first compression stage but this reduced on re-compression and subsequent compression stages to maximum movements of about 3% of sample height.

It follows that some changes in density and therefore localised effective stress occurred during these tests. Figure E generally shows the highest hydraulic conductivity to be at the inlet regions (*i.e.* bottom of the sample during upflow test and top of the sample for downflow tests). As most magnet movement was in the middle of the sample it would tend to suggest, at least in this case, that the higher hydraulic conductivities were due to elevated pore water pressure. However not all hydraulic conductivity plots show the same trends and so changes in density due to localised changes in effective stress cannot be ruled out.

## Appendix F. Potential head loss in horizontal hydraulic conductivity assessments

### Reduction in flow due to falling head in header tanks

As the method for assessing horizontal hydraulic conductivity was based on the total horizontal flow rate through the sample, the accuracy was directly dependent on the accuracy of flow rate measurements during tests. Some systematic error between inlet and outlet flow rates was expected due to the small reduction in head that occurred after the supply to the header tank was shut off during inlet flow measurements. Generally, inlet and outlet flow rates were within 10 % of each other and it is therefore estimated that the overall flow rate was determined within  $\pm 10\%$ .

Horizontal flow measurement in tests run with only small differences between inlet and outlet heads could have incurred fairly large errors for just a few centimetre reduction in inlet head during inlet flow rate measurement. However the uncorrected results for the tests affected (tests 40, 41, 66, 83 and 90 in Table 8.3) do not exhibit unduly low  $k_h : k_v$  ratios compared to respective tests using larger inlet/outlet head differences. It is possible that the delay in the system response (particularly the outlet flow rates) to the drop in inlet head meant that errors were not as great as expected.

### Effect of frictional loss in pipework on flowrate

Another possible source of error was frictional losses in the pipework between the flowing leachate and the internal wall of the pipe. The main effect of this would be to reduce the pressure head at the inlet ports and consequently lower flow rates. The head losses needed to be known in order to adjust the analysis to the test conditions. Figure F1 shows the head losses calculated for the inlet pipes (25.4 mm inside diameter plastic pipe with a typical length of 7 m) for a range of flow rates through the pipes. This shows that losses increase at higher flow rates. In the vast majority of

tests, flow rates were too low (at medium to higher compression stages flow rates through each port were generally less and often much less than 100 l/h) for head loss to make any practical difference to the results. However in exceptional conditions (low compression coupled with a large difference between inlet and outlet heads) flow rates could be as high as 1000 l/h through each port. Figure F1 indicates that in this situation head losses would be about 12 cm. Comparative numerical analyses run with and without this head loss produced flow rate differences of about 5%. This could lead to the overestimation of horizontal hydraulic conductivity by about 0.5 times (for example a test results giving a  $k_h : k_v$  ratio 5.0 without head losses taken into account would produce a  $k_h : k_v$  ratio to 5.5 if head loss was included). To avoid this additional error, the input heads in numerical analyses were reduced. The tests requiring this correction are shown in Table 8.3.

No corrections have been undertaken for frictional losses in the outlet pipework as the losses in the short length of outlet pipe are fairly inconsequential.

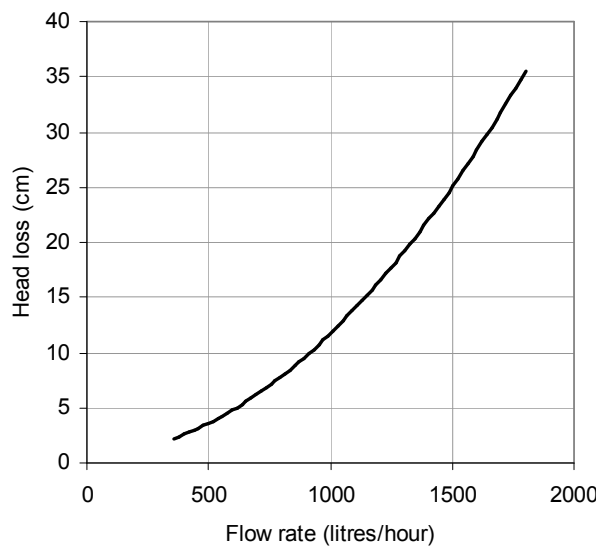


Figure F1. Relationship between inlet flow rate and head loss (for a 7 m length of 25.4 mm ID plastic pipe)

## Appendix G. Application of results to pumping of vertical wells

In this section, the findings of the research are applied to calculations for determining the spacing between vertical drainage wells for maintaining landfill leachate levels. Although inefficient in comparison with basal drainage systems, vertical drainage wells are often the only option for retrospective installation in landfills built without adequate drainage systems.

The spacing required between wells comes from the radius of capture (or influence) ( $r_v$ ) the wells calculated using the following parameters (shown on Figure G1):

- the hydraulic conductivity of the waste ( $k$ )
- the recharge rate ( $v$ )
- the bore size of the well ( $r_w$ )
- the maximum leachate head on the base ( $H$ )
- the head in the well ( $h_w$ )

In the following two examples well spacings based on isotropic conditions are compared with spacings using the horizontal hydraulic conductivity values obtained from the research in this thesis. The spacings were calculated by the use of a spreadsheet by Beaven (2000) based on standard well calculations (Bouwer, 1978).

Both examples use hydraulic conductivity values obtained in tests at an applied stress of 134 kPa – this is approximately equivalent to a waste depth of 13 m (based on an average waste density of 1 t/m<sup>3</sup>). The radius of the well ( $r_w$ ) used in the calculations was 0.15 m.

In the first example conventional landfill conditions are considered. A low recharge rate ( $v$ ) of 50mm/annum has been used to represent an efficient clay cap. A maximum permissible head ( $H$ ) of 5 metres has been assumed with full drawdown in the wells (*ie.*  $h_w = 0$ ). In unconfined conditions the pore water pressure in the saturated zone would be between 0 and 50 kPa. Hydraulic conductivity values approximately

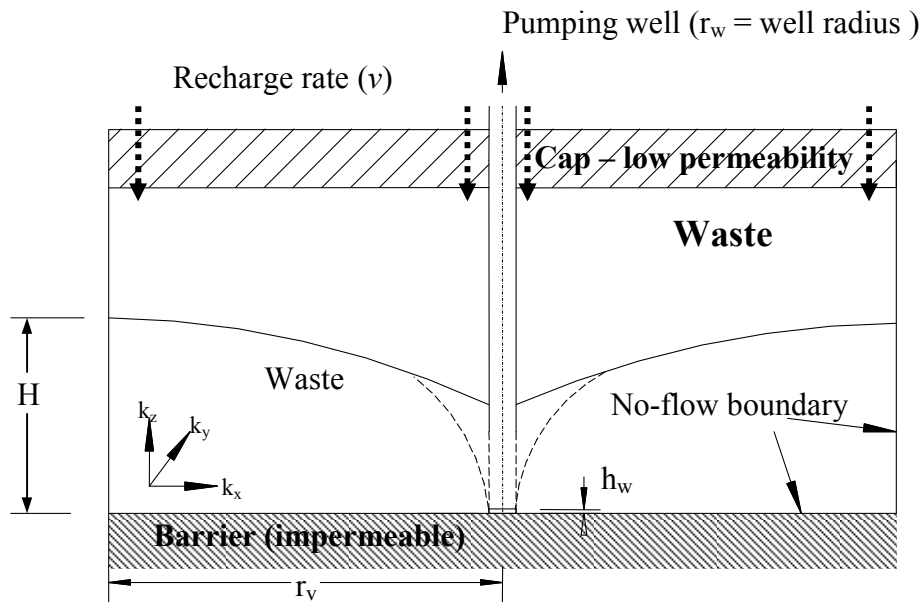


Figure G1 Vertical drainage well pumping arrangement (from Beaven, 2000)

corresponding with these conditions have been used in the calculations (the pore water pressure in the tests was between 30 and 40 kPa representing an average saturated zone depth of 3 to 4 m). These hydraulic conductivity values,  $1.5 \times 10^{-6}$  m/s for vertical hydraulic conductivity and  $1.5 \times 10^{-5}$  m/s for horizontal hydraulic conductivity (Table 9.2) were evaluated in gas accumulated conditions which would be expected in all but totally inert waste. Figure G2 shows a) the grid spacings of the vertical wells based on isotropic conditions *ie.*  $k_h : k_v = 1$  and b) the revised grid spacings using  $k_h : k_v = 10$  as determined in the horizontal flow tests for the above conditions. The grid spacings are the approximate spacings of wells in a block centred grid that would be required to achieve the leachate head specified on the x-axis of Figure G2.

Figure G2 shows that for the specified conditions above, well spacings calculated using the revised horizontal hydraulic conductivity values are much larger than those obtained using the previously assumed isotropic values. For example for a maximum permissible head (H) of 1 m, a grid spacing of 76 m would be required in comparison with 26 m for isotropic conditions.

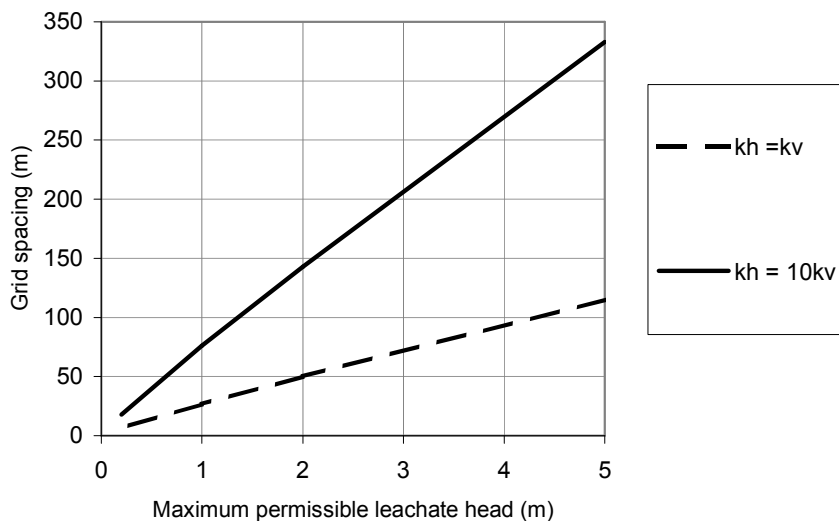


Figure G2 Vertical well spacings for isotropic and anisotropic conditions ( $k_h : k_v = 10$ ) for a waste depth of 13 m, recharge of 50mm/ annum and  $h_w = 0$  m

In the second example a possible scenario for flushing pollutants from wastes (Chapter 1) is examined. Saturated conditions are assumed in order to flush pollutants from waste of several metres depth. Correspondingly, hydraulic conductivity values used are those for high pore water pressure (60 to 70 kPa<sup>6</sup>) and gas accumulated conditions. Gas accumulated conditions are likely to become established unless the wastes are totally inert and it is unlikely that gas will be removed by flushing leachates from the waste as flow rates would be very low – a flushing rate of about 3 metres/ annum is envisaged for site of 30 m depth (IWM, 1998). The hydraulic conductivity values used were  $4.5 \times 10^{-6}$  m/s for vertical hydraulic conductivity and  $2.2 \times 10^{-5}$  m/s for horizontal hydraulic conductivity (Table 8.3). These values were again obtained for an applied stress of 134 kPa representing waste at a depth of about 13 metres. A well radius ( $r_w$ ) of 0.15 m was specified. A maximum possible recharge rate of 500 mm/ annum (average UK rainfall) is used to represent unimpeded rainfall entry through the top surface of the landfill. If leachate is to be extracted (for recirculation or treatment) by pumping from vertical wells, the pumping rate would have to be sufficient to prevent the piezometric surface exceeding the height of the waste. However the drawdown in the pumped vertical wells should be small to prevent the possibility of large unsaturated zones in the waste. A drawdown of 3 m was used in

<sup>6</sup> For the example shown with saturated depths of 10m to 11m, the pore water pressures would be higher (100 to 110 kPa in unconfined conditions). Hydraulic conductivity data is not available for these pore water pressures and the values used may be marginally low

this example (*ie.*  $h_w = 10$  m), although it may be possible to use a much smaller value than this. Figure G3 compares the vertical well spacings required according to both isotropic and anisotropic conditions.

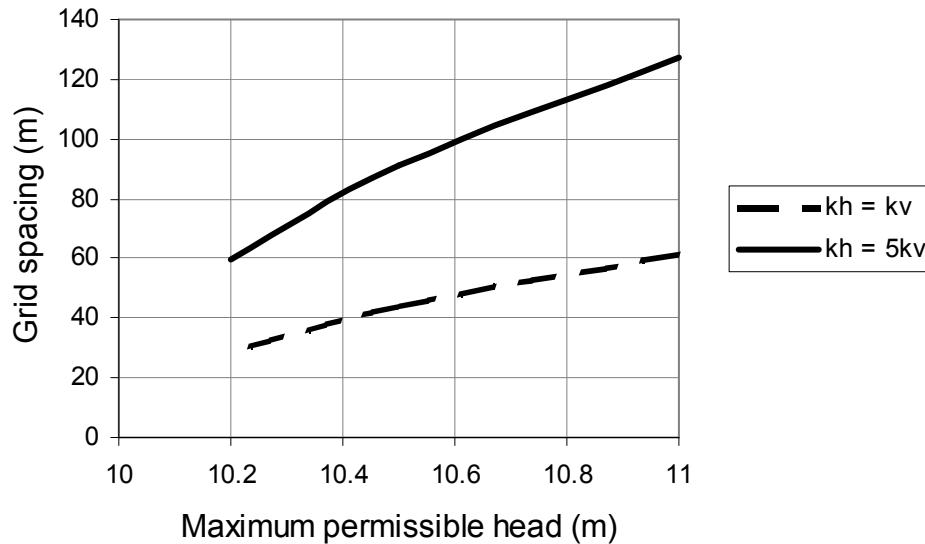


Figure G3 Vertical well spacings for isotropic and anisotropic ( $k_h : k_v = 5$ ) conditions for a waste depth of 13 m, recharge of 500mm/annum and  $h_w = 10$  m

For the above scenario Figure G3 shows the grid spacing for the vertical wells based on the revised horizontal hydraulic conductivity values to be about twice that calculated for isotropic conditions.

In summary, the application of revised horizontal hydraulic conductivity values obtained in this research indicates that spacings of vertical wells in both conventional and flushing landfills could be much further apart (by a factor of 2 to 3) than would have been envisaged using isotropic hydraulic conductivity values based on previous laboratory tests. Although the analyses are simplified to some extent (for example average pore water pressures and hydraulic conductivities are assumed – as is the absence of other features such as low permeability layers within the waste body that may influence horizontal flow) and clogging and other well efficiency issues would need to be examined, the revised spacings indicate that the number of wells required would only be about 10 % to 25 % of the number based on isotropic conditions. This represents a substantial cost saving.

## Appendix H. Sensitivity of numerical analyses

### H1 Introduction

The two parameters measured during horizontal hydraulic conductivity tests were flow rates across the sample and head at various positions within the sample. It was necessary to assess the sensitivity of the  $k_h : k_v$  ratios deduced using the numerical analyses to potential errors in these measurements. The sensitivity of the numerical analysis method to errors in horizontal flow rates is discussed in section H2 and to head measurements in section H3.

### H2 Sensitivity of horizontal flow rates

In Table 8.4 the total error in the  $k_h : k_v$  assessment process was estimated to be within +10 % / -20%. The possible effect of the potential error on the derived  $k_h : k_v$  ratios are assessed for a number of examples shown below that represent waste samples at different applied stresses and test configurations. For each of these conditions, the calculated flow rate has been plotted against the  $k_h : k_v$  ratio used in the numerical analyses to assess the sensitivity of the method in different test conditions.

Three examples are used to represent different confined (no outflow through top and bottom of the waste) test conditions:

Example 1: This uses a high vertical hydraulic conductivity of  $1.5 \times 10^{-4}$  m/s typical of a waste sample at low compression. Flow is through four inlet and four outlet ports responding to a moderate inlet / outlet head difference of 237 cm.

Example 2: A lower hydraulic conductivity value of  $2 \times 10^{-5}$  m/s is used in this example but total flow is less restricted by the test configuration than example 1 as nine inlet ports and nine outlet horizontal flow ports are used combined with a greater inlet / outlet head difference of 440 cm.

Example 3: This example exhibits reduced flow due to the low vertical hydraulic conductivity value of  $5 \times 10^{-6}$  m/s (representing a waste at high applied stress) and flow restricted by the use of only four inlet and four outlet ports with a moderate inlet / outlet head difference of 237 cm as in example 1.

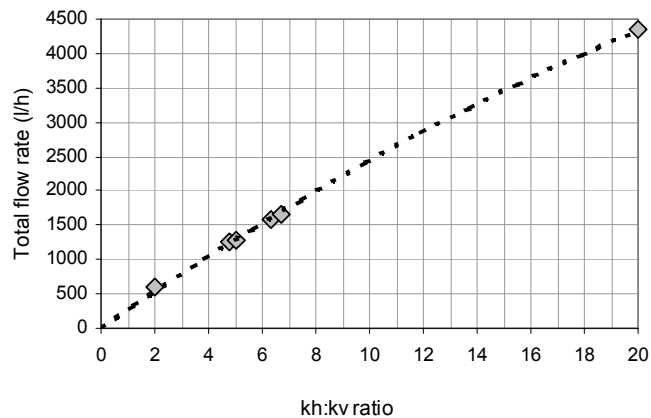
Unconfined conditions are represented by:

Example 4: The same high vertical hydraulic conductivity of  $1.5 \times 10^{-4}$  m/s is used as in example 1; typical of a waste sample at low applied stress. A low difference in pressure head of 133 cm was used between the four horizontal flow inlet ports and the outlets via the top and bottom gravel layer and four horizontal flow outlet ports

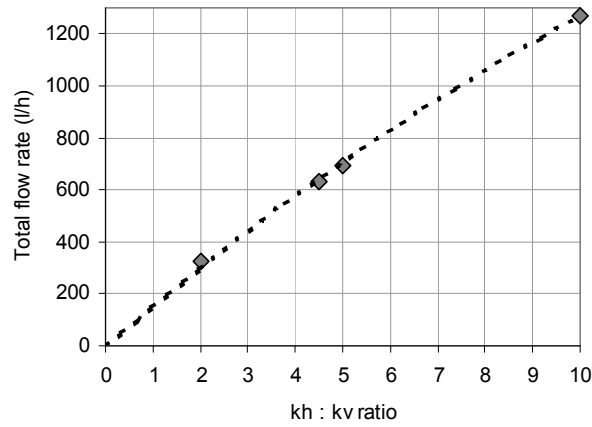
Example 5: This uses a low vertical hydraulic conductivity of  $1 \times 10^{-6}$  m/s typical of a waste sample at high applied stress. A difference in head of 237 cm was used between the three horizontal flow inlet ports and the outlets via the top and bottom gravel layer and three outlet horizontal flow ports

Figure H1 shows the horizontal flow rates for the three above confined examples indicated by the numerical analyses for different  $k_h : k_v$  ratios. Figure H2 shows the flow rates for the unconfined examples. In all examples significant variations in flow rates are evident depending on the  $k_h : k_v$  ratio used. The slight curve on the plots indicates marginally higher sensitivity at lower  $k_h : k_v$  ratios, but in general there is approximately a 10 % difference between calculated flow rates per unit change in  $k_h : k_v$  ratio (for example between  $k_h : k_v = 9$  and  $k_h : k_v = 10$ ). The allowance for up to +10 % / -20 % total error means that the accuracy of most  $k_h : k_v$  assessments would be within about + 1 / -2 (ie. a calculated  $k_h : k_v$  ratio of 10 could be a minimum of 8 and a maximum of 11).

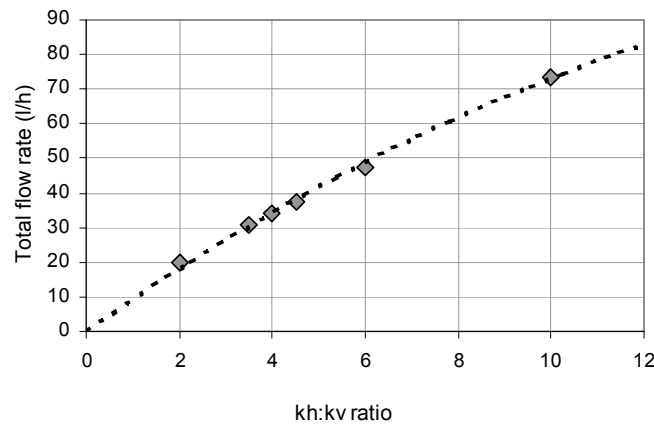
Example 1



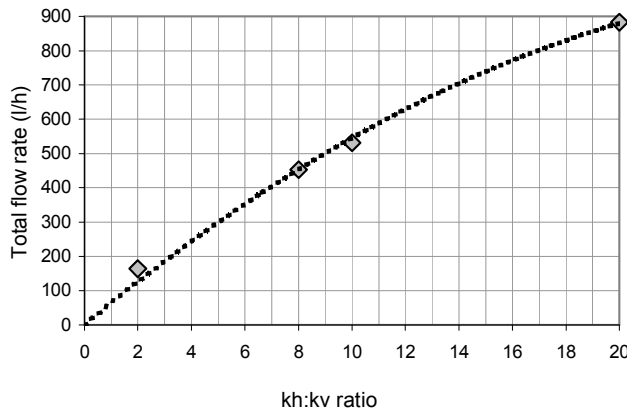
Example 2



Example 3

Figure H1. Examples of changes in flow rate according to different  $k_h : k_v$  ratios used in numerical analyses

## Example 4



## Example 5

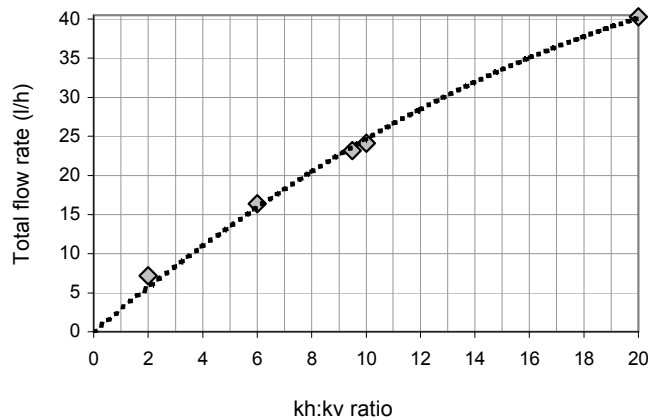


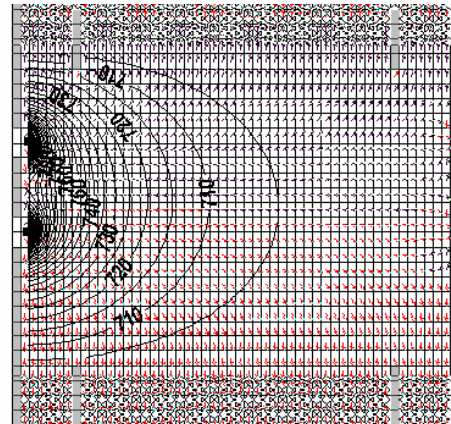
Figure H2 Examples of changes in flow rate in unconfined tests according to different  $k_h : k_v$  ratios used in numerical analyses

## H3 Sensitivity to pressure head distribution

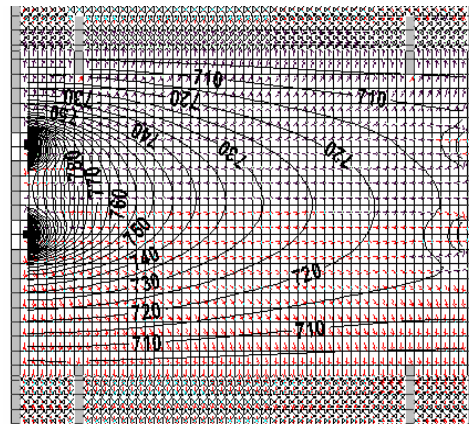
Varying the horizontal hydraulic conductivity value in the numerical analyses also resulted in changes in the pattern of head distribution in the sample. The changes were barely perceptible in confined tests configurations but were more apparent for unconfined arrangements. An example is shown in Figure H3 showing cross-sections for the different  $k_h : k_v$  ratios of 2, 9.5 and 20. The respective pressure heads in the

centre of the sample were approximately 705, 730 and 750 cm a.g.l. This would have been a possible secondary method of  $k_h : k_v$  assessment had the piezometer method of measuring pressure heads being more accurate. In tests the measured heads could vary significantly (several tens of centimetres) to those indicated by the numerical analyses and it was clear that  $k_h : k_v$  assessment would have to be based on flow rates alone.

$k_h : k_v$  ratio = 2  
total flow rate = 7.3 l/h



$k_h : k_v$  ratio = 9.5  
total flow rate = 23.2 l/h



$k_h : k_v$  ratio = 20  
total flow rate = 40.3 l/h

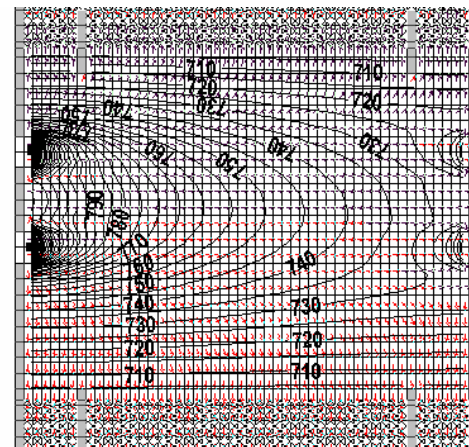


Figure H3 Numerical analyses cross-sections for  $k_h : k_v$  ratios of 2, 9.5 and 20 showing changes in pressure head

## Appendix I. Numerical analyses accuracy

The mass balance error (the difference between the calculated inlet and outlet flow rates) was displayed by Groundwater Vistas for each analysis. Generally a lower mass balance error could be achieved by specifying a low (more accurate) convergence value. This increased the number of calculation steps (iterations) and the calculation time. A convergence value of 0.005 cm was usually sufficient to obtain a mass balance error below 0.1% which was insignificant in comparison to test flow rate accuracies

Problems with numerical stability and unacceptably large mass balance errors occurred in analyses of tests conducted at higher applied stress. The cause of the problem appeared to be the large difference in hydraulic conductivity between the layers representing the gravel and those representing the waste. This could not be overcome by specifying a lower convergence value and had to be resolved by running the numerical analyses in a number of stages. In the first stage, the hydraulic conductivity of the layers representing the gravel layers was reduced to a value similar to the waste and stable results were obtained. The gravel layer hydraulic conductivity values were then increased and the analysis re-run using the head change file from the initial analysis. In many cases the process had to be repeated a number of times using small increases in the gravel layer hydraulic conductivity to obtain an acceptable mass balance error of less than 0.5%. In some cases the difference in hydraulic conductivity between the waste and gravel was so great that it was not possible to obtain stable results. In such cases a lower final gravel layer hydraulic conductivity had to be accepted, and consequently it was necessary to examine the effect this had on the calculated flow rate through the sample. Figure I1 shows cross-sections of an analysis using a high gravel hydraulic conductivity of 10 m/s (left) and a normal value 0.1 m/s (right). The head distribution (cm above ground level) is

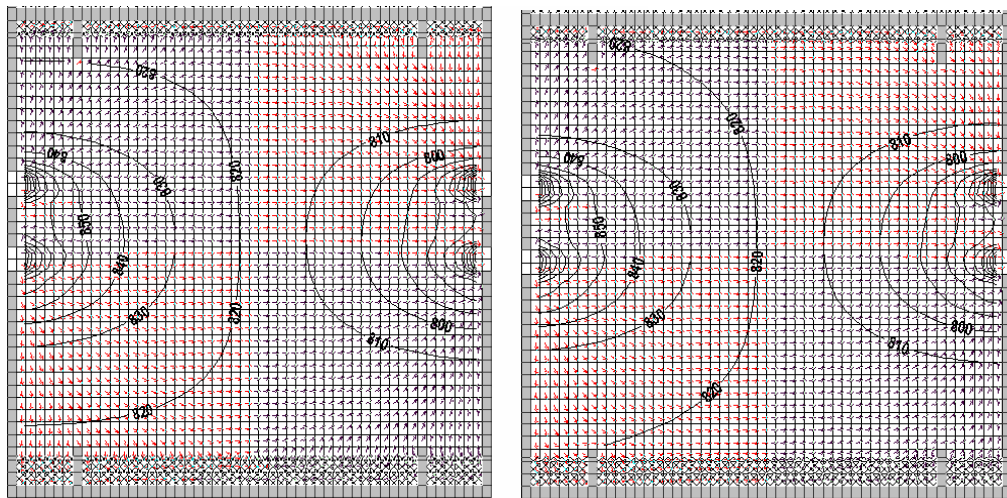


Figure I1. Comparison of numerical analyses cross-sections using a gravel hydraulic conductivity of 10m/s (left) and 0.1 m/s (right)

almost identical and total flow rate was practically unchanged at 1931.9 l/h and 1930.7 l/h respectively (0.1% difference). The above example represents a waste at a low applied stress (below 100 kPa). Similar results were obtained for examples at higher applied stresses. This demonstrated that it was not necessary to use precise hydraulic conductivity values for gravel layers throughout the range of applied stress used in tests.

The cumulative mass balance and gravel layer error would be insignificant (< 0.5 %) for most analyses. For analyses using lower gravel hydraulic conductivity and less accurate mass balances, the error is estimated to be within  $\pm 2\%$ .

## **Appendix J. Anomalous flow rates in horizontal hydraulic conductivity tests**

### **Introduction**

Unexpected flow patterns occurred in several horizontal hydraulic conductivity tests, differing significantly to that shown by the numerical analyses. These are discussed in the following sections.

#### **J1. High flow rates through some ports**

In some AG2 tests carried out at the first two compression stages it was found that exceptionally high flow rates occurred through some of the horizontal flow ports. This was attributed to a siphoning effect in the pipework between the header tank and outlet. This only happened when the pipework was at or near full capacity and did not occur at lower flow rates typical of tests conducted after the second compression stage. The problem was addressed in the later tests on sample DN1 by incorporating a breather pipe in the outlet pipework. This allowed air to be drawn in, presumably breaking the siphoning effect.

The results from tests affected by siphoning were not used in the final horizontal hydraulic conductivity assessments as use of header tank and outlet pipe elevations as inlet and outlet values in the numerical analyses was probably invalidated by a lowering of pressure heads at ports affected by siphoning. As actual pressure heads at the ports were not measured at this stage the results had to be disregarded. This applied to all AG2 tests at the first compression stage (40 kPa applied stress) and some at the second compression stage (87 kPa applied stress).

## J2 High flow rates through bottom ports

In some tests exceptionally high flow rates occurred through the lowest ports. The flow rate through the bottom inlet and outlet ports could represent more than 70 % of the total horizontal flow, in contrast to 10 % to 30 % indicated by the numerical analyses (depending on the number of ports used). Closing these lower ports during a test often transferred the high flow rate to the ports immediately above. It appeared that flow via the lower ports was short-circuiting across the bottom gravel layer. However in most tests the distance between the bottom ports and bottom gravel layer was similar to that between the upper ports and upper gravel layer. Short circuiting would therefore also be expected to occur across the upper gravel layer, but the absence of high flow rates through the upper ports indicated that this was not so.

Three possible explanations for the presence of high flow rates occurring only at the bottom of the sample are:

i) any gas within the sample may have tended to accumulate towards the top of the sample (there being no means of escape in confined conditions), restricting flow in the upper portions of the sample.

ii) the pore water pressure would be greater at the bottom of the sample and this may have partly compressed any gas present in the lower portion

of the sample, increasing hydraulic conductivity (and therefore flow) in the lower region. The pore water pressure differential between the top and bottom of the sample would have only been about 10 to 20 kPa, but tests on the interaction of pore water pressure and gas (Hudson *et al.*, 1999, 2000) have shown that hydraulic conductivity can be affected by fairly minor changes in pore water pressure

iii) partition plates added (for other purposes) to the underside of the top platen prior to the start of the DN1 tests (Figure J1) protruded through the top gravel

layer and into the sample may have acted as baffle plates preventing horizontal flow across the gravel layer. This principle is discussed further in section 11.2.2. In contrast short circuit flow across the bottom gravel layer (and top gravel layer in the AG2 tests) would have been unimpeded in the zone outside the dividing ring.



Figure J1. Underside of top platen showing extra plates added to the inner/outer dividing ring

The precise cause of high flow rates across the bottom of the sample is not known, and could be a combination of the above possible explanations. The results from tests exhibiting high flow rates through the lower ports were disregarded as they were not in accordance with the flow patterns of the numerical analyses.

### J3 Erratic flow

Erratic flow was only evident in tests carried out on sample DN1 in gas accumulated conditions at applied stresses of 228 kPa and above. For example during a horizontal flow test at an applied stress of 228 kPa, the total flow rate from four outlet<sup>7</sup> ports varied from 0.1 l/h to 0.8 l/h (readings averaged over 30 minutes). Horizontal hydraulic conductivity assessments using the maximum and minimum of these rates gave an unacceptably large range of possible  $k_h : k_v$  ratios between 3.0 and 34.0. As it

---

<sup>7</sup> at these compression stages flow rates were too low for inlet flow rates to be measured

was not possible to obtain reasonable  $k_h : k_v$  assessments, results from tests with erratic flow had to be discounted.

The erratic flow was almost certainly caused by gas accumulation and gas movement in the sample affecting the leachate flow, possibly exacerbated by the concentration of flow through a small area in the port regions. Similar erratic flow in the vertical direction was noted in subsequent compression cell tests in gas accumulated conditions with the vertical flow divided into smaller areas.

#### J4 Different flow rates through each port

Besides the problem of high flow rates via the bottom ports apparent in some horizontal flow tests as discussed above in section J2, it was noted that flow rates through some ports could be several times higher than through others. The numerical analyses showed only minor differences between flow rates for each of the ports.

The differences appeared to be greater at higher applied stresses. Three examples for sample DN1 are shown in Figures J2 to J4:

- example 1 (Figure J2) was conducted at low stress (applied stress 40 kPa) in nominally gas purged conditions
- example 2 (Figure J3) was run at a higher stress (applied stress 134 kPa) in nominally gas purged conditions
- example 3 (Figure J4) used the same test arrangement as the second example, but was run in gas accumulated conditions.

In each figure the measured and calculated flow rates (both total flow and flow for each port) are shown.

At low applied stress (Figure J2) the measured individual flow rates for each port vary by a factor of up to two. This variation is typical of tests conducted at low stress and is greater than that shown by the numerical analyses (about 10 %).

At higher stress (Figure J3) individual flow rates varied from 9.6 l/h (E2820) to 150 l/h (D2370)<sup>8</sup> - a variation of a factor of 15 times. This is much greater than the two times variation typical of tests at low stress.

Figure J4 shows the flow rates obtained with the same arrangement and stress as that in Figure J3, but in gas accumulated conditions. Gas accumulation reduced the total horizontal flow through the sample to only 11.3 % of that in nominally gas purged conditions. Gas accumulation also appears to have altered the pattern of flow. For example 76 % of the measured inflow was via the lowest port used (D2370) compared to 28 % indicated by the numerical analysis and 50 % measured in the gas purged test shown in Figure J3 - but outflow via the opposite port (E2370) at 17 % of the total flow is much lower than that of the gas purged test (50 % of total flow). The difference between the maximum and minimum flow rates through individual ports is about 18 fold. This is only slightly more than the test in non-gas accumulated conditions (15 times difference), and so although gas accumulation affected flow rates and flow patterns through the waste, it did not appear to significantly exacerbate the differences between flow rates through individual ports.

---

<sup>8</sup> 'D' indicates inlet ports and 'E' outlet ports. The accompanying number refers to the elevation of the port above ground level (a.g.l.) in millimetres – hence D2370 is an inlet port 2370mm a.g.l

TEST 39: Sample DN1 at 40 kPa applied stress.

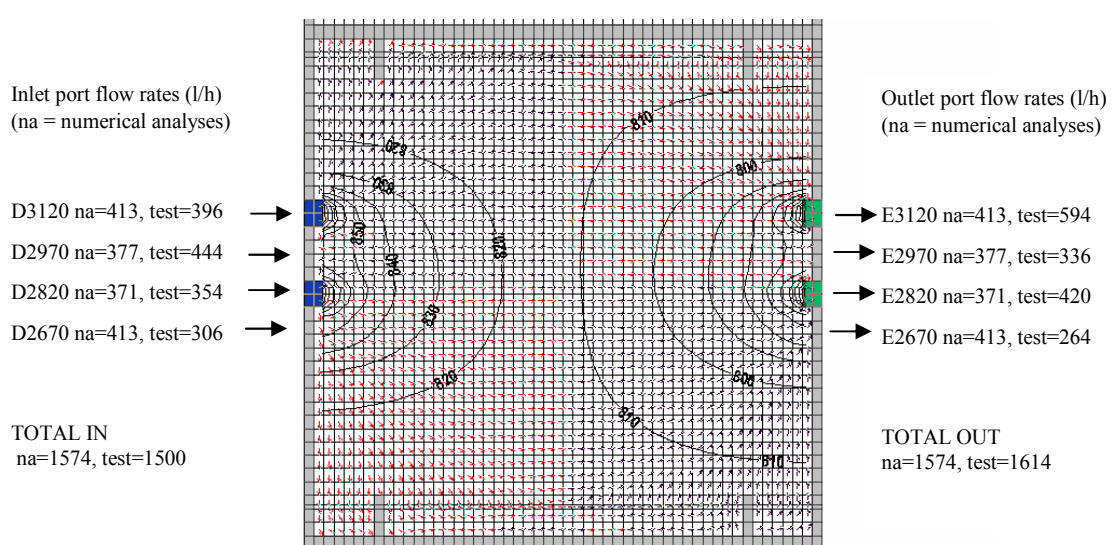
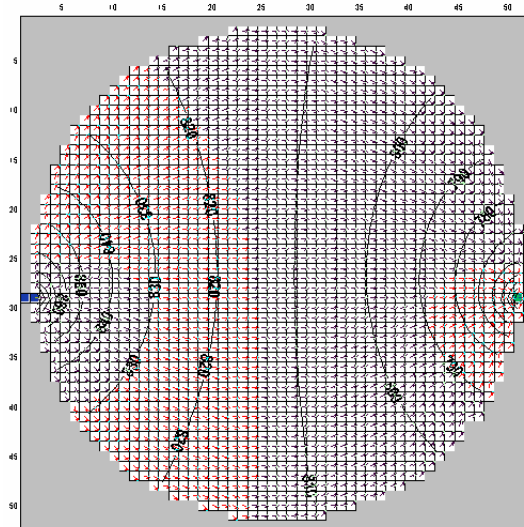
(10DNx6.3\_4x937\_4x700hl)

4 inlets, 4 outlets

Inlet head = 937cm a.g.l, outlet head = 700 cm a.g.l

Vertical hydraulic conductivity =  $1.5 \times 10^{-4}$  m/s $k_h : k_v = 6.3$  (horizontal hydraulic conductivity =  $9.45^{-4}$  m/s)

Section at 2820mm a.g.l.



*nb. some inlet and outlet ports are not apparent on the cross section due to the offset arrangement of the ports*

Figure J2 Plan (top) and elevation (bottom) of MODFLOW cross sections for Test 39

## TEST 73: Sample DN1 at 134 kPa applied stress.

(40DNx7.2\_4x937\_4x700hplg)

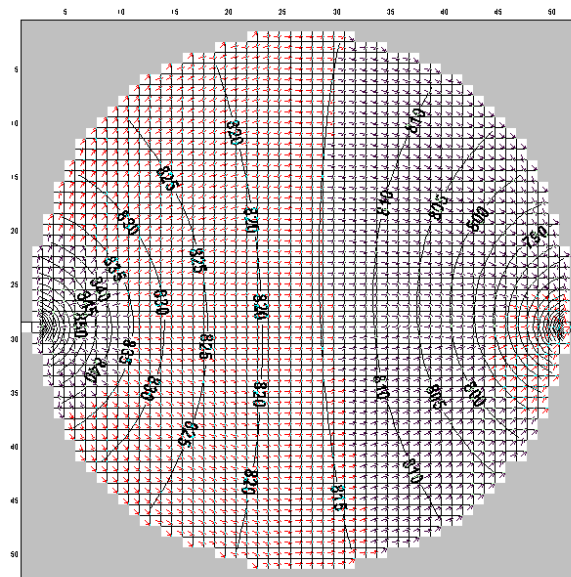
4 inlets, 4 outlets

Inlet head = 937cm a.g.l, outlet head = 700 cm a.g.l

Vertical hydraulic conductivity =  $2.2 \times 10^{-5}$  m/s (high pore water pressure / low gas accumulation )

$k_h : k_v = 7.2$  (horizontal hydraulic conductivity =  $1.6 \times 10^{-4}$  m/s)

section at 2820mm a.g.l



Inlet port flow rates (l/h)  
(na = numerical analyses)

D2970 na=68.2, test=44.4 →

D2820 na=62.3, test=53.4 →

D2670 na=66.1, test=21.6 →

D2370 na=74.9, test=150 →

TOTAL IN  
na=271.5, test=269.4

Outlet port flow rates (l/h)  
(na = numerical analyses)

→ E2970 na=69.8, test=52.8

→ E2820 na=66.0, test=9.6

→ E2520 na=66.5, test=79.8

→ E2370 na=68.9, test=132

TOTAL OUT  
na=271.4, test=274.2

*nb. some inlet and outlet ports are not apparent on the cross section due to the offset arrangement of the ports*

Figure J3. Plan (top) and elevation (bottom) of MODFLOW cross sections for Test 73



TEST 77: Sample DN1 at 134 kPa applied stress.

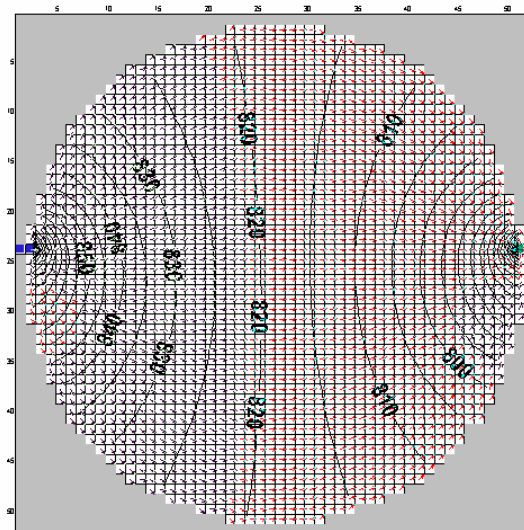
(40DNx3.5\_4x937\_4x700hphlg)

4 inlets, 4 outlets

Inlet head = 937cm a.g.l, outlet head = 700 cm a.g.l

Vertical hydraulic conductivity =  $4.5 \times 10^{-6}$  m/s (high pore water pressure / low gas accumulation ) $k_h, k_v = 3.5$  (horizontal hydraulic conductivity =  $1.6 \times 10^{-5}$  m/s)

section at 2820mm a.g.l

Inlet port flow rates (l/h)  
(na = numerical analyses)

D2970 na=7.8, test=3.0



D2820 na=7.1, test=2.1



D2670 na=7.4, test=1.5



D2370 na=8.5, test=21.3

TOTAL IN  
na=30.7, test=27.9Outlet port flow rates (l/h)  
(na = numerical analyses)

→ E2970 na=7.9, test=9.6

→ E2820 na=6.9, test=1.2

→ E2520 na=7.5, test=15.0

→ E2370 na=7.9, test=5.4

TOTAL OUT  
na=30.7, test=31.2*nb. some inlet and outlet ports are not apparent on the cross section due to the offset arrangement of the ports*

Figure J4. Plan (top) and elevation (bottom) of MODFLOW cross sections for Test 77

It is considered that the differences in flow rates may have been caused by variations in sample permeability in the immediate vicinity of each port - this being a shortcoming of the compression cell design with relatively small inlet and outlet areas. This heterogeneity was not replicated in the numerical analyses as an average vertical hydraulic conductivity value was assigned throughout, hence similar flow rates were indicated for each port. The use of several ports in the horizontal flow tests should have helped to average out the effect of waste heterogeneity on flow through each port (the numerical analysis assessment being based on the total flow rate through all the ports), but it may be the cause of some of the variations in the results shown in chapter 8.

## Summary

All tests exhibited greater differences in flow rates through each of the horizontal flow ports to that shown by the respective numerical analysis. The differences were greater at higher stress. These differences were averaged in the numerical analyses by using total flow rate for several ports.

Additionally several tests exhibited extremely high flows through certain ports. These appear to have been caused by siphoning or short-circuiting via the bottom gravel layer. In some tests gas accumulation caused large fluctuations in total flow rates. The results of the tests affected have not been used in the  $k_h : k_v$  assessments shown in chapter 8.

## **Appendix K**

### **Details of test results**

<b>TEST 10. 9<sup>th</sup> July 1998</b> <b>AG2 87 kPa. Confined. 9 inlets / 9 outlets .</b> <b>Inlet head 9.00 m a.g.l. Outlet head 4.60m a.g.l.</b>					
Port elevation (mm above ground level)	Input flow rate (l/min)	Outlet flow rate (l/min)	'A' heads mm above ground level (piezometer depth in brackets)	'B' heads mm above ground level (piezometer depth in brackets)	'C' heads mm above ground level (piezometer depth in brackets)
3820 (top)	-	-	6660 (15cm)	6590(25cm)	6500 (28cm)
3670	0.9	0.5			
3520	1.2	0.1	6830 (90cm)	6660 (18cm)	6280 (29cm)
3295	1.0	1.7			
3220	-	-	6900 (15cm)	6450 (17cm)	5890
3120	0.7	1.8			
2970	1.4	0.5			
2820	1.3	0.7	6970 (87cm)	6320 (23cm)	5850 (27cm)
2670	1.7	1.4	(40cm)	6390 (15cm)	
2520	1.4	1.7	7290 (15cm)	6220 (15cm)	5840
2370	0.9	2.8	(27cm)	6190 (20cm)	
2220 (bottom)	-	-	6070 (90cm)	5970 (22cm)	5980 (36cm)
<b>TOTAL</b>	<b>10.5</b>	<b>11.1</b>			
<u><b>Notes</b></u> <ul style="list-style-type: none"> <li>• Readings taken 20 to 50 minutes after starting</li> <li>• More uniform flow rates – although higher outflow at base. Reduction in outlet (c) heads towards bottom of waste (siphoning / short-circuiting?)</li> <li>• Compared with test 8, 18% reduction in ports = 50% approx reduction in flow</li> </ul>					

<b>TEST 12. 9<sup>th</sup> July 1998</b> <b>AG2 87 kPa. Confined. 3 inlets / 9 outlets .</b> <b>Inlet head 9.00 m a.g.l. Outlet head 4.60m a.g.l.</b>					
<b>Port elevation (mm above ground level)</b>	<b>Input flow rate (l/min)</b>	<b>Outlet flow rate (l/min)</b>	<b>'A' heads (mm above ground level)</b>	<b>'B' heads (mm above ground level)</b>	<b>'C' heads (mm above ground level)</b>
3820 (top)	-	-	6140	6140	6060
3670	-	0.6			
3520	-	0.1	6360	6190	5960
3295	-	1.1			
3220	-	-	6640	6150	5670
3120	1.3	1.3			
2970	2.3	0.3			
2820	3.0	0.5	6670	6080	5670
2670	-	0.9		6140	
2520	-	1.2	7150	5980	5670
2370	-	3.6		5970	
2220 (bottom)	-	-	5850	5790	5780
<b>TOTAL</b>	<b>6.6*</b>	<b>9.4*</b>			

**Notes**

- Readings started approx 18 minutes after test started – discrepancy between inlet and outlet readings may be due to flow not being established (outlet readings taken first). Later measurements gave 7.4 l/min inflow, 7.6 l/min outflow
- Higher flow at base still evident and reduction in outlet (c) heads towards bottom of waste (siphoning / short-circuiting?)  
see *Test 10 for piezometer depths*

<b>TEST 15. 2nd September 1998</b> <b>AG2 165 kPa. Confined. 9 inlets / 9 outlets .</b> <b>Inlet head 9.00 m a.g.l. Outlet head 4.60m a.g.l.</b>					
Port elevation (mm above ground level)	Input flow rate (l/min)	Outlet flow rate (l/min)	'A' heads (mm above ground level)	'B' heads (mm above ground level)	'C' heads (mm above ground level)
3820 (top)	-	-			
3670	-	0.28			
3520	0.47	0.16			
3295	0.18	drip			
3220	-	-			
3120	0.06	0.09			
2970	0.16	0.15			
2820	0.14	drip			
2670	0.01	0.15			
2520	0.44	0.23			
2370	0.23	0.61			
2220 (bottom)	0.08	-			
<b>TOTAL</b>	<b>1.77</b>	<b>1.67+drips</b>			
<b><u>Notes</u></b>					
<ul style="list-style-type: none"> <li>• Possibly affected by gas – saturated tests since 19/8</li> <li>• head in top gravel layer = 6.53m. Increased if D3670 opened (= short circuit?)</li> </ul>					

<b>TEST 23. 30<sup>th</sup> November 1998</b> <b>AG2 322 kPa unconfined 3 input/ 3 outlets .</b> <b>Inlet head 9.00 m a.g.l. Horizontal ports outlet head 4.60m a.g.l.</b> <b>Top gravel layer 4.12m a.g.l</b> <b>Bottom gravel layer 4.12m a.g.l</b>					
<b>Port elevation (mm above ground level)</b>	<b>Input flow rate (l/min)</b>	<b>Outlet flow rate (l/min)</b>	<b>'A' heads (mm above ground level)</b>	<b>'B' heads (mm above ground level)</b>	<b>'C' heads (mm above ground level)</b>
3820 (top)	-	-			
3670	-	-			
3520	-	-	4410	4440	4440
3295	-	-			
3220	-	-	6350	5310	4710 gassy
3120	0.070	drip			
2970		-			
2820	0.013	drip	6350	5690	4835 gassy
2670	-	-	6010	5400	
2520	0.033	drip	5420	4920	4440
2370	-	-	5150	4850	
2220 (bottom)	-	-	4590	4385	4390
Top inner gravel		0.034			
Top outer gravel		0			
Bottom inner gravel	-	0			
Bottom outer gravel	-	0.056			
<b>TOTAL</b>	<b>0.116</b>	<b>0.090+drips</b>			
<b>Notes</b>					
<ul style="list-style-type: none"> <li>• Readings taken after 5 hrs running – earlier flow rates higher (input 0.217 l/h, output 0.117 l/h) <ul style="list-style-type: none"> <li>• Gas present</li> </ul> </li> <li>• No flow from top outer and bottom inner gravel. Siphoning not suspected (flow too low and not indicated by piezometer readings. Air locks? Slight difference in outlet elevations?)</li> </ul>					

<b>TEST 24. 2<sup>nd</sup> December 1998</b> <b>AG2 322 kPa unconfined 1 input/ 1 outlets .</b> <b>Inlet head 9.00 m a.g.l. Horizontal ports outlet head 4.60m a.g.l.</b> <b>Top gravel layer 4.12m a.g.l</b> <b>Bottom gravel layer 4.12m a.g.l</b>					
Port elevation (mm above ground level)	Input flow rate (l/min)	Outlet flow rate (l/min)	'A' heads (mm above ground level)	'B' heads (mm above ground level)	'C' heads (mm above ground level)
3820 (top)	-	-			
3670	-	-			
3520	-	-	4440	4390	4390
3295	-	-			
3220	-	-	5190	4760	4570
3120	-	-			
2970	-	-			
2820	0.032	0	5410	5040	4410 gassy
2670	-	-	5190	4910	
2520	-	-	4730	-	4620 v.gassy
2370	-	-	4650	4575	
2220 (bottom)	-	-	4490	4400	4480
Top inner gravel	-	0.017			
Top outer gravel	-	0.001			
Bottom inner gravel	-	0.013			
Bottom outer gravel	-	0			
<b>TOTAL</b>	<b>0.032</b>	<b>0.031</b>			
<b>Notes</b>					
<ul style="list-style-type: none"> <li>• Input = output on all occasions. Leak problems on Test 23 fixed.</li> <li>• Top and bottom pipes adjusted – now no flow from bottom outer gravel. <ul style="list-style-type: none"> <li>• Gas present</li> <li>• Reduction to one inlet = significant pressure reductions</li> </ul> </li> </ul>					

<p style="text-align: center;"><b>TEST 25. 7<sup>th</sup> to 16th December 1998</b></p> <p style="text-align: center;"><b>AG2 322 kPa confined 3 inputs/ 3 outlets .</b></p> <p style="text-align: center;"><b>Inlet head 9.00 m a.g.l. Horizontal ports outlet head 4.60m a.g.l.</b></p> <p style="text-align: center;"><b>Fluoroscein tracer test</b></p>					
<b>Port elevation (mm above ground level)</b>	<b>Input flow rate (l/min)</b>	<b>Outlet flow rate (l/min)</b>	<b>'A' heads (mm above ground level)</b>	<b>'B' heads (mm above ground level)</b>	<b>'C' heads (mm above ground level)</b>
3820 (top)	-	-			
3670	-	-			
3520	-	-	7810	7810	7805
3295	-	-			
3220	-	-	7920	7650	7500
3120	0.017	0.007			
2970	-	-			
2820	0.003	0.002	7715	7510	6985
2670	-	-	7640	7410	
2520	0.013	0.020	7520	7260	6980
2370	-	-	7420	7265	
2220 (bottom)	-	-	7265	7190	7180
<b>TOTAL</b>	<b>0.033</b>	<b>0.029</b>			
<b>Notes</b>					
<ul style="list-style-type: none"> <li>• Above readings taken 8<sup>th</sup> Dec. Load cells indicated further gas accumulation as test progressed. (at least 110 litres). Output reduced to 0.018 l/m by end of test</li> </ul>					

<b>TEST 28. 26th January 1999</b> <b>AG2 603 kPa confined 3 input/ 3 outlet</b> <b>Inlet head 9.00 m a.g.l. Horizontal ports outlet head 4.60m a.g.l.</b>					
<b>Port elevation (mm above ground level)</b>	<b>Input flow rate (l/min)</b>	<b>Outlet flow rate (l/min)</b>	<b>'A' heads (mm above ground level)</b>	<b>'B' heads (mm above ground level)</b>	<b>'C' heads (mm above ground level)</b>
3820 (top)	-	-			
3670	-	-			
3520	-	-			
3295	-	-			
3220	-	-	7230		
3120	-	-			
2970	0.0008	0.0005			
2820	0.0017	0.0025	7830	7410	
2670	0.0017	0.0003			
2520	-	-	7460	7320	
2370	-	-			
2220 (bottom)	-	-	7230	7250	
<b>TOTAL</b>	<b>0.0042</b>	<b>0.0033</b>			
<b>Notes</b>					
<ul style="list-style-type: none"> <li>• Probably gas accumulated conditions – saturated since 11<sup>th</sup> Jan</li> </ul>					

<p style="text-align: center;"><b>TEST 37 15th September 1999</b></p> <p style="text-align: center;"><b>DN1 40 kPa confined 4 input/ 4 outlet</b></p> <p style="text-align: center;"><b>Inlet head 9.37, outlet head 4.00m a.g.l.</b></p> <p style="text-align: center;"><b>Using framework with BREATHER PIPES</b></p>								
<b>Port elevation (mm above ground level)</b>	<b>Input flow rate (l/h)</b>	<b>Outlet flow rate (l/h)</b>	<b>'A' heads 45cm deep* (mm above ground level)</b>	<b>'B' heads 95cm deep (mm above ground level)</b>	<b>'C' heads 45cm deep (mm above ground level)</b>			
3820 (top)	-	-						
3670	-	-						
3520	-	-	6200	5940	5930			
3295	-	-						
3220	-	-	6330	5990	5690			
3120	900	not recorded						
2970	948	not recorded						
2820	840	not recorded	6260	6005	5610			
2670	768	not recorded	6180					
2520	-	-	6040	6020	5810			
2370	-	-	6010					
2220 (bottom)	-	-	5960	5935	5920			
<b>TOTAL</b>	<b>3456</b>	output not recorded	Others (depths into waste in brackets) D3120(IH)=7780, D3120(30cm)=6880 D2670(5cm)=8390, D2820(10cm)=7980 D2970(IH)=8630, D3295 (50cm)=6320 E2670OH=4100, E2820(30cm)=5550 E3120(OH)=4420, E2970(OH)=4240 E2820(OH)=4320, E2670(15cm)=5430 Bot grav inner=5932, outer=5930					
<b>Notes</b>								
<ul style="list-style-type: none"> <li>• May be affected by gas</li> <li>• Input flow rates v.consistent</li> <li>• Input head losses respectively measured at tanks 35cm, 36.5cm, 32cm , 18cm.</li> <li>• Much higher head loss recorded at input by D2970 and D3120 (additional loss in hoses)           <ul style="list-style-type: none"> <li>• A2670 55cm deep, A2370 70cm deep orientated towards D ports               <ul style="list-style-type: none"> <li>• <math>k_h, k_v</math> assessment = x6.1</li> </ul> </li> </ul> </li> </ul>								

<p style="text-align: center;"><b>TEST 39 23rd September 1999</b></p> <p style="text-align: center;"><b>DN1 40 kPa confined 4 input/ 4 outlet</b></p> <p style="text-align: center;"><b>Inlet head 9.37, outlet head 7.00m a.g.l.</b></p> <p style="text-align: center;"><b>Repeat of test 36</b></p>								
<b>Port elevation (mm above ground level)</b>	<b>Input flow rate (l/h)</b>	<b>Outlet flow rate (l/h)</b>	<b>'A' heads 45cm deep* (mm above ground level)</b>	<b>'B' heads 95cm deep (mm above ground level)</b>	<b>'C' heads 45cm deep (mm above ground level)</b>			
3820 (top)	-	-						
3670	-	-						
3520	-	-	7690	7640	7580			
3295	-	-						
3220	-	-	7750	7610	7500			
3120	396	594						
2970	444	336						
2820	354	420	7730	7600	7450			
2670	306	264	7680					
2520	-	-	7630	7590	7520			
2370	-	-	7610					
2220 (bottom)	-	-	7590	7570	7570			
<b>TOTAL</b>	<b>1500</b>	<b>1614</b>	Others (depths into waste in brackets) D3120(IH)=9250, D3120(30cm)=7490 D2670(5cm)=8860, D2820(10cm)=8730 D2970(IH)=9200, D3295 (50cm)=7740 E2670OH=7010, E2820(30cm)=7430 E3120(OH)=7100, E2970(OH)=7000 E2820(OH)=7020, E2670(15cm)=7380 Bot grav inner=7565, outer=7563					
<b>Notes</b>								
<ul style="list-style-type: none"> <li>• Higher flow rates (approx 22%) than Test 36 but LC's indicate 55 litres /less gas in Test 36.           <ul style="list-style-type: none"> <li>• Input/output flow rates consistent (max variation x2.25)</li> </ul> </li> <li>• Input head losses respectively measured at tanks 80mm, 110mm, 80mm, 50mm.</li> <li>• Higher head loss recorded at input by D3120 and D2970 (additional loss in hoses)           <ul style="list-style-type: none"> <li>• Most head change within 30cm depth of input and output               <ul style="list-style-type: none"> <li>• <math>k_h, k_v</math> assessment = x6.3</li> </ul> </li> </ul> </li> </ul>								
* A2670 55cm deep, A2370 70cm deep orientated towards D ports								

<p style="text-align: center;"><b>TEST 40 23<sup>rd</sup> September 1999</b></p> <p style="text-align: center;"><b>DN1 40 kPa confined 4 input/ 4 outlet</b></p> <p style="text-align: center;"><b>Inlet head 9.37, outlet head 9.00m a.g.l.</b></p> <p style="text-align: center;"><b>Repeat of Test 35 (but with 4 inlets instead of 3) and Test 33</b></p>					
<b>Port elevation (mm above ground level)</b>	<b>Input flow rate (l/h)</b>	<b>Outlet flow rate (l/h)</b>	<b>'A' heads 45cm deep* (mm above ground level)</b>	<b>'B' heads 95cm deep (mm above ground level)</b>	<b>'C' heads 45cm deep (mm above ground level)</b>
3820 (top)	-	-			
3670	-	-			
3520	-	-	9040	9040	9010
3295	-	-			
3220	-	-	9045	9030	9010
3120	66	202			
2970	108	49			
2820	50	40	9005	9020	9010
2670	56	52	9005		
2520	-	-	9030	9040	9010
2370	-	-	9030		
2220 (bottom)	-	-	9030	9050	9010
<b>TOTAL</b>	<b>280</b>	<b>343</b>	Others (depths into waste in brackets) D3120(IH)=9360, D3120(30cm)=9090 D2670(5cm)=9200, D2820(10cm)=9240 D2970(IH)=9360, D3295 (50cm)=9055 E2670OH=8955, E2820(30cm)=9020 E3120(OH)=8990, E2970(OH)=8920 E2820(OH)=8950, E2670(15cm)=9020 Bot grav inner=9025, outer=9020		

**Notes**

- Not a good match between input and output – fully stabilised? nb. also run as Test 33 (flow rate about 280 l/h)
  - May be affected by gas
- Input flow rates. not as consistent as earlier tests (x5 variation)
  - Practically no input head loss
- Proportionally higher flow rates than Test 35 (as test 39 and 36)– settlement?
  - Some output heads under-reading (minimum should be 9000)
    - $k_h : k_v$  assessment = 8.0 (300 l/h)
  - \* A2670 55cm deep, A2370 70cm deep orientated towards D ports

<p style="text-align: center;"><b>TEST 41 23<sup>rd</sup> September 1999</b></p> <p style="text-align: center;"><b>DN1 40 kPa confined 4 input/ 4 outlet</b></p> <p style="text-align: center;"><b>Inlet head 5.33, outlet head 5.00m a.g.l.</b></p> <p style="text-align: center;"><b>First low pore water pressure test</b></p>								
<b>Port elevation (mm above ground level)</b>	<b>Input flow rate (l/h)</b>	<b>Outlet flow rate (l/h)</b>	<b>'A' heads 45cm deep* (mm above ground level)</b>	<b>'B' heads 95cm deep (mm above ground level)</b>	<b>'C' heads 45cm deep (mm above ground level)</b>			
3820 (top)	-	-						
3670	-	-						
3520	-	-	5150	5095	5110			
3295	-	-						
3220	-	-	5110	5095	5085			
3120	78	102						
2970	72	60						
2820	24	78	5125	5095	5050			
2670	84	64	5130					
2520	-	-	5110	5095	5105			
2370	-	-	5105					
2220 (bottom)	-	-	5100	5095	5100			
<b>TOTAL</b>	<b>258</b>	<b>306</b>	Others (depths into waste in brackets) D3120(IH)=5330, D3120(30cm)=5155 D2670(5cm)=5300, D2820(10cm)=5180 D2970(IH)=5320, D3295 (50cm)=5120 E2670OH=4995, E2820(30cm)=5050 E3120(OH)=5185, E2970(OH)=5000 E2820(OH)=5015, E2670(15cm)=5035 Bot grav inner=5090, outer=5090					
<b>Notes</b>								
<ul style="list-style-type: none"> <li>• Some flow rate variation (upto x 4.25)           <ul style="list-style-type: none"> <li>• Minimal input head loss</li> <li>• Some output head discrepancies</li> <li>• <math>k_h : k_v</math> assessment = 8.0 (300 l/h)</li> </ul> </li> </ul>								
* A2670 55cm deep, A2370 70cm deep orientated towards D ports								

<p style="text-align: center;"><b>TEST 42 23<sup>nd</sup> September 1999</b></p> <p style="text-align: center;"><b>DN1 40 kPa confined 4 input/ 4 outlet</b></p> <p style="text-align: center;"><b>Inlet head 5.33, outlet head 4.00m a.g.l.</b></p> <p style="text-align: center;"><b>Low pore water pressure test</b></p>								
<b>Port elevation (mm above ground level)</b>	<b>Input flow rate (l/h)</b>	<b>Outlet flow rate (l/h)</b>	<b>'A' heads 45cm deep*</b> (mm above ground level)	<b>'B' heads 95cm deep (mm above ground level)</b>	<b>'C' heads 45cm deep (mm above ground level)</b>			
3820 (top)	-	-						
3670	-	-						
3520	-	-	4505		4320			
3295	-	-						
3220	-	-	4445	nr	4245			
3120	186	307						
2970	216	161						
2820	144	228	4430	nr	4230			
2670	180	150	4430					
2520	-	-	4410	nr	4340			
2370	-	-	4400					
2220 (bottom)	-	-	4395	nr	4370			
<b>TOTAL</b>	<b>726</b>	<b>846</b>	Others (depths into waste in brackets) D3120(IH)=5325, D3120(30cm)=4570 D2670(5cm)=5250, D2820(10cm)=5015 D2970(IH)=5305, D3295 (50cm)=4430 E2670(OH)=4010, E2820(30cm)=4220 E3120(OH)=4020, E2970(OH)=4010 E2820(OH)=4020, E2670(15cm)=4200 Bot grav inner=nr, outer=nr					
<b>Notes</b>								
<ul style="list-style-type: none"> <li>• Not a good match between input and output – fully stabilised?</li> <li>• Gas released when output head lowered to 400 but probably still affected by gas           <ul style="list-style-type: none"> <li>• Input flow rates fairly consistent (x2.1 variation)</li> <li>• Some input head loss</li> <li>• <math>k_h, k_v</math> assessment = 6.0 (846 l/h)</li> </ul> </li> </ul>								
* A2670 55cm deep, A2370 70cm deep orientated towards D ports								

<p style="text-align: center;"><b>TEST 43 27<sup>th</sup> September 1999</b></p> <p style="text-align: center;"><b>DN1 40 kPa confined 6 input/ 6 outlet</b></p> <p style="text-align: center;"><b>Inlet head 9.37, outlet head 4.00m a.g.l.</b></p>					
<b>Port elevation (mm above ground level)</b>	<b>Input flow rate (l/h)</b>	<b>Outlet flow rate (l/h)</b>	<b>'A' heads 45cm deep* (mm above ground level)</b>	<b>'B' heads 95cm deep (mm above ground level)</b>	<b>'C' heads 45cm deep (mm above ground level)</b>
3820 (top)	-	-			
3670	-	-			
3520	-	-	6990	6340	6470
3295	1056	564			
3220	-	-	7060	6440	6110
3120	912	1368			
2970	834	894			
2820	828	936	6830	6490	5910
2670	810	468	6850		
2520	780	1194	6550	6530	5990
2370	-	-	6450		
2220 (bottom)	-	-	6350	6820	6290
<b>TOTAL</b>	<b>5220</b>	<b>5424</b>	Others (depths into waste in brackets) D3120(IH)=8815, D3120(30cm)=7430 D2670(5cm)=8870, D2820(10cm)=8030 D2970(IH)=8780, D3295 (50cm)=nr E2670OH=4060, E2820(30cm)=5835 E3120(OH)=4440-4500, E2970(OH)=4290 E2820(OH)=4320, E2670(15cm)=5625 Bot grav inner=6307, outer=6301		
<b>Notes</b>					
<ul style="list-style-type: none"> <li>• Gas released from top platen prior to measurements being taken. Gas accumulation probably quite low due to high flow           <ul style="list-style-type: none"> <li>• Input flow rates fairly consistent (x2.9 variation)</li> </ul> </li> <li>• Input head loss not recorded – about 60cm according to piezometer readings           <ul style="list-style-type: none"> <li>• Flow rate proportional to Test 37, 4in/4out (<math>3456 \times 6/4 = 5184 \text{ l/h}</math>)</li> <li>• Output heads too high (should be 4000)</li> </ul> </li> <li>• A2670 55cm deep, A2370 70cm deep orientated towards D ports           <ul style="list-style-type: none"> <li>• <math>k_h \cdot k_v</math> assessment = x6.5</li> </ul> </li> </ul>					

<p style="text-align: center;"><b>TEST 56 18<sup>th</sup> November 1999</b></p> <p style="text-align: center;"><b>DN1 87 kPa confined 6 input/ 6 outlet</b></p> <p style="text-align: center;"><b>Inlet head 9.37, outlet head 7.00m a.g.l.</b></p>								
<b>Port elevation (mm above ground level)</b>	<b>Input flow rate (l/h)</b>	<b>Outlet flow rate (l/h)</b>	<b>'A' heads (mm above ground level) depths in brackets</b>	<b>'B' heads (mm above ground level) depths in brackets</b>	<b>'C' heads (mm above ground level) depths in brackets</b>			
3820 (top)	-	-						
3670	-	-						
3520	-	-	-					
3295	-	-						
3220	-	-	7670 (35cm)	7540 (90cm)	7610 (40cm)			
3120	55	84						
2970	173	166						
2820	70	103	7895 (50cm)	7750 (80cm)	7460 (40cm)			
2670	74	-	8065(35cm*)					
2520	-	146	7945 (30cm)	7910 (90cm)	7380 (40cm)			
2370	196	175	7370(35cm*)					
2220 (bottom)	360	240	7720 (45cm)	7655 (90cm)	7385 (50cm)			
<b>TOTAL</b>	<b>928</b>	<b>914</b>	Others (depths into waste in brackets) D3120(IH)=9360, D3120(18cm)=8105 D2670(5cm)=9260, D2820(10cm)=8285, D2970(IH)=9340, D2520 (40cm)=7335 E2820(30cm)=7255, E3120(OH)=7010, E2970(OH)=7030, E2820(OH)=7025, E2670(15cm)=7285, Bot grav =7650					
<b>Notes</b>								
<ul style="list-style-type: none"> <li>• Inlet head drops: 3120=0cm (1cm at inlet), 2970=1cm(3cm at inlet), 2820=0cm, 2670=0cm, 2370=2cm, 2220=4cm           <ul style="list-style-type: none"> <li>• High 2220 input flow rates (input x5.1 variation)</li> <li>• Output flow rates fairly consistent (x2.9 variation)</li> </ul> </li> <li>• Flow rates 13.5% higher than Test 53 – in accordance with preferential compression           <ul style="list-style-type: none"> <li>• <math>k_h : k_v</math> assessment = 5.0</li> </ul> </li> </ul>								
* A2670 A2370 piezometers orientated towards D ports								

<p style="text-align: center;"><b>TEST 62 7<sup>th</sup> December 1999</b></p> <p style="text-align: center;"><b>DN1 87 kPa unconfined 4 input/ 4 outlet + gravel layers</b></p> <p style="text-align: center;"><b>Inlet head 9.37, outlet head 7.00m a.g.l.</b></p> <p style="text-align: center;"><b>HIGH GAS ACCUMULATED CONDITIONS</b></p>								
<b>Port elevation (mm above ground level)</b>	<b>Input flow rate (l/h)</b>	<b>Outlet flow rate (l/h)</b>	<b>'A' heads (mm above ground level) depths in brackets</b>	<b>'B' heads (mm above ground level) depths in brackets</b>	<b>'C' heads (mm above ground level) depths in brackets</b>			
3820 (top)	-	-						
3670	-	-						
3520	-	-	-					
3295	-	-						
3220	-	-	7180 (35cm)	7130 (90cm)	7090(40cm)			
3120	-	-						
2970	202.2	31.2						
2820	82.2	31.8	7420 (50cm)	7720 (80cm)	7135(40cm)			
2670	104.4	-	7540(35cm*)					
2520	-	20.4	7360 (30cm)	7280 (90cm)	7100 (40cm)			
2370	400.2	33.0	7610(35cm*)					
2220 (bottom)		-	7090 (45cm)	7030 (90cm)	7050 (50cm)			
Top gravel		295.2 (33%)						
Bottom gravel		463.6 (53%)						
<b>TOTAL</b>	<b>789.0</b>	<b>875.2</b>	Others (depths into waste in brackets) D3120(IH)=7640(low), D3120(18cm)=7475 D2670(5cm)=9320, D2820(10cm)=7885, D2970(IH)=9340, D2520 (40cm)=7740 E2820(30cm)=7000, E3120(OH)=7060, E2970(OH)=7020, E2820(OH)=7000, E2670(15cm)=7080, Bot grav =7000					
<b>Notes</b>								
<ul style="list-style-type: none"> <li>• Gas accumulated conditions – left to gas for 7 days.</li> <li>• Input head loss D2970=2.5cm(3cm at inlet), D2820=1cm,D2670=2cm,D2370=6cm           <ul style="list-style-type: none"> <li>• Output flow rates fairly consistent (x1.6 variation)               <ul style="list-style-type: none"> <li>• High inlet flow through 2370</li> </ul> </li> <li>• Higher % of flow to bottom gravel layer than Test 61</li> </ul> </li> </ul>								
* A2670 A2370 piezometers orientated towards D ports								

<p style="text-align: center;"><b>TEST 65 7<sup>th</sup> December 1999</b></p> <p style="text-align: center;"><b>DN1 87 kPa unconfined 4 input/ 4 outlet + gravel layers</b></p> <p style="text-align: center;"><b>Inlet head 9.37, outlet head 7.00m a.g.l.</b></p> <p style="text-align: center;"><b>REPEAT OF TEST 62 after attempted FLUSHING OF ACCUMULATED GAS</b></p>								
<b>Port elevation</b> (mm above ground level)	<b>Input flow rate</b> (l/h)	<b>Outlet flow rate</b> (l/h)	<b>'A' heads</b> (mm above ground level) depths in brackets	<b>'B' heads</b> (mm above ground level) depths in brackets	<b>'C' heads</b> (mm above ground level) depths in brackets			
3820 (top)	-	-						
3670	-	-						
3520	-	-						
3295	-	-						
3220	-	-						
3120	-	-	7125	7080	7050			
2970	nr	31.8						
2820	nr	24.0	7340	7220	7075			
2670	nr	-	7440					
2520	-	16.2	7270	7205	7060			
2370	nr	31.8	7470					
2220 (bottom)	-	-	7080	7030	7040			
Top gravel		223.2 (31%)						
Bottom gravel		385.2 (54%)						
<b>TOTAL</b>	not recorded	<b>712.2</b>	Others (depths into waste in brackets) D3120(IH)=7580(low), D3120(18cm)=7400 D2670(5cm)=9350, D2820(10cm)=7805, D2970(IH)=9340, D2520 (40cm)=9540, E2820(30cm)=7040, E3120(OH)=7030, E2970(OH)=7050, E2820(OH)=7020, E2670(15cm)=7040, Bot grav =4042					
<b>Notes</b>								
<ul style="list-style-type: none"> <li>Flow rates reduced by 23% compared with Test 62 (all readings decreased except E2970 – slight increase) <ul style="list-style-type: none"> <li>Load cells indicate 25 litres less gas than Test 62</li> </ul> </li> </ul>								
* A2670 A2370 piezometers orientated towards D ports								

<b>TEST 66 16<sup>th</sup> December 1999</b> <b>DN1 87 kPa unconfined 4 input/ 4 outlet + gravel layers</b> <b>Inlet head 5.33, outlet head 5.00m a.g.l.</b>								
<b>Port elevation</b> (mm above ground level)	<b>Input flow rate</b> (l/h)	<b>Outlet flow rate</b> (l/h)	<b>'A'</b> heads (mm above ground level) depths in brackets	<b>'B'</b> heads (mm above ground level) depths in brackets	<b>'C'</b> heads (mm above ground level) depths in brackets			
3820 (top)	-	-						
3670	-	-						
3520	-	-						
3295	-	-						
3220	-	-						
3120	-	-	5015	5000	nr			
2970	16.8	1.8						
2820	7.8	2.4	5105	5050	nr			
2670	7.2	-	5105					
2520	-	0	5045	5030	nr			
2370	45.8	13.2	5100					
2220 (bottom)	-	-	5020	5005	nr			
Top gravel		25.8 (29.5%)						
Bottom gravel		44.4 (50.7%)						
<b>TOTAL</b>	<b>77.6</b>	<b>87.6</b>	Others (depths into waste in brackets) D3120(IH)=5120, D3120(18cm)=5100 D2670(5cm)=blocked, D2820(10cm)=5190, D2970(IH)=5340, D2520 (40cm)=5145, E2820(30cm)=nr, E3120(OH)=nr, E2970(OH)=nr, E2820(OH)=nr, E2670(15cm)=nr, Bot grav =4990					
<b>Notes</b>								
<ul style="list-style-type: none"> <li>Gas situation uncertain – had been left for 9 days in saturated conditions. Heads lowered for test and a lot of gas released. Test repeated (Test 67) PROBABLY gas accumulated conditions</li> <li>Flow rates taken 1 hour after starting test – checked 30 mins later – same rates</li> </ul> <p>* A2670 A2370 piezometers orientated towards D ports</p>								

<p style="text-align: center;"><b>TEST 67 23rd December 1999</b></p> <p style="text-align: center;"><b>DN1 87 kPa unconfined 4 input/ 4 outlet + gravel layers</b></p> <p style="text-align: center;"><b>Inlet head 5.33, outlet head 5.00m a.g.l.</b></p> <p style="text-align: center;"><b>REPEAT OF TEST 66</b></p>								
<b>Port elevation (mm above ground level)</b>	<b>Input flow rate (l/h)</b>	<b>Outlet flow rate (l/h)</b>	<b>'A' heads (mm above ground level) depths in brackets</b>	<b>'B' heads (mm above ground level) depths in brackets</b>	<b>'C' heads (mm above ground level) depths in brackets</b>			
3820 (top)	-	-						
3670	-	-						
3520	-	-						
3295	-	-						
3220	-	-						
3120	-	-	5015	4990	4995			
2970	nr	0.3						
2820	nr	1.2	5130	5060	5005			
2670	nr	-	5145					
2520	-	0	5060	5060	5015			
2370	nr	9.6	5120					
2220 (bottom)	-	-	5015	4995	5000			
Top gravel		21.0 (26.6%)						
Bottom gravel		46.8 (59.3%)						
<b>TOTAL</b>	-	<b>78.9</b>	Others (depths into waste in brackets) D3120(IH)=5150, D3120(18cm)=5110 D2670(5cm)=5315, D2820(10cm)=5195, D2970(IH)=5330, D2520 (40cm)=5150, E2820(30cm)=5020, E3120(OH)=4990, E2970(OH)=4990, E2820(OH)=4990, E2670(15cm)=5020, Bot grav =4995					
<b>Notes</b>								
<ul style="list-style-type: none"> <li>• Test re-started from saturated conditions (4m a.g.l. outlets?)</li> <li>• Flow rate slightly reduced compared to Test 66. Load cells indicate 20 litres more gas</li> <li>• Increase in bottom gravel layer flow rate, decrease in top gravel layer</li> </ul> <p style="text-align: center;">* A2670 A2370 piezometers orientated towards D ports</p>								

<b>TEST 69 16<sup>th</sup> December 1999</b> <b>DN1 87 kPa confined 4 input/ 4 outlet</b> <b>Inlet head 5.33, outlet head 4.00m a.g.l.</b>								
<b>Port elevation</b> (mm above ground level)	<b>Input flow rate</b> (l/h)	<b>Outlet flow rate</b> (l/h)	<b>'A'</b> heads (mm above ground level) depths in brackets	<b>'B'</b> heads (mm above ground level) depths in brackets	<b>'C'</b> heads (mm above ground level) depths in brackets			
3820 (top)	-	-						
3670	-	-						
3520	-	-						
3295	-	-						
3220	-	-						
3120	-	-	4585	4240	4275			
2970	45.0	43.2						
2820	20.4	36.0	4570	4405	4200			
2670	25.8	-	4620					
2520	-	37.2	4450	4445	4220			
2370	108.0	114.0	4540					
2220 (bottom)	-	-	4295	4445	4225			
<b>TOTAL</b>	<b>199.2</b>	<b>230.4</b>	Others (depths into waste in brackets) D3120(IH)=4710, D3120(18cm)=4620 D2670(5cm)=5325, D2820(10cm)=4810, D2970(IH)=5330, D2520 (40cm)=4595, E2820(30cm)=4115, E3120(OH)=4110, E2970(OH)=4010, E2820(OH)=4000, E2670(15cm)=4115, Bot grav =nr					
<b>Notes</b>								
<ul style="list-style-type: none"> <li>• Gas situation uncertain – probably gas accumulated conditions</li> <li>• High flow through bottom ports – upper ports restricted by gas?</li> </ul>								
* A2670 A2370 piezometers orientated towards D ports								

<p style="text-align: center;"><b>TEST 71. 22<sup>nd</sup> June 2000</b></p> <p style="text-align: center;"><b>DN1 134 kPa confined 4 input/ 4 outlet</b></p> <p style="text-align: center;"><b>Inlet head 5.33, outlet head 4.00m a.g.l.</b></p> <p style="text-align: center;"><b>GAS ACCUMULATED CONDITIONS – 12 days running</b></p>								
<b>Port elevation</b> (mm above ground level)	<b>Input flow rate</b> (l/h)	<b>Outlet flow rate</b> (l/h)	<b>'A'</b> heads (mm above ground level) depths in brackets	<b>'B'</b> heads (mm above ground level) depths in brackets	<b>'C'</b> heads (mm above ground level) depths in brackets			
3820 (top)	-	-						
3670	-	-						
3520	-	-						
3295	-	-						
3220	-	-	4430 (30cm)	4070 (80cm)	4060 (60cm)			
3120	-	-						
2970	2.4	4.68						
2820	2.1	0.18	4710 (50cm)	4310 (85cm)	4095 (30cm)			
2670	1.8	-	4800 (30cm)					
2520	-	2.16	4460 (40cm)	4470 (50cm)	4130 (40cm)			
2370	7.2	6.72	5165 (35cm)					
2220 (bottom)	-	-	4155 (35cm)	4135 (70cm)	4250 (40cm)			
<b>TOTAL</b>	<b>13.5</b>	<b>13.74</b>	Others (depths into waste in brackets) D3120(IH)=4000 low, D2670(IH)=5325, D2820(12cm)=5040, D2970(IH)=5320, D2520 (18cm)=4935, E2820(20cm)=4040, E3120(OH)=4000-4010, E2970(OH)=4000-4010, E2820(OH)=4000-4010					
<b>Notes</b>								
<ul style="list-style-type: none"> <li>• x 13 decrease compared to Test 70 due to gas accumulated conditions – load cells indicate 300 litres of gas           <ul style="list-style-type: none"> <li>• Generally better flow variations (x26 or x3.7 if E2820 ignored) ADD TO TEXT!!!!               <ul style="list-style-type: none"> <li>• Some piezometer readings lower than Test 70</li> <li>• Output flow rate checked twice – minor variations</li> </ul> </li> </ul> </li> </ul>								
* A2670 A2370 piezometers orientated towards D ports								

<b>TEST 73. 23<sup>rd</sup> June 2000</b> <b>DN1 134 kPa confined 4 input/ 4 outlet</b> <b>Inlet head 9.37, outlet head 7.00m a.g.l.</b>								
<b>GAS PURGED CONDITIONS</b>								
Port elevation (mm above ground level)	Input flow rate (l/h)	Outlet flow rate (l/h)	'A' heads (mm above ground level) depths in brackets	'B' heads (mm above ground level) depths in brackets	'C' heads (mm above ground level) depths in brackets			
3820 (top)	-	-						
3670	-	-						
3520	-	-						
3295	-	-						
3220	-	-	7660 (30cm)	7420 (80cm)	7575 (60cm)			
3120	-	-						
2970	44.4	52.8						
2820	53.4	9.6	7805 (50cm)	7330 (85cm)	7480 (30cm)			
2670	21.6	-	8030 (30cm)					
2520	-	79.8	7680 (40cm)	7415 (50cm)	7610 (40cm)			
2370	150.0	132.0	8780 (35cm)					
2220 (bottom)	-	-	7500 (35cm)	7475 (70cm)	7630 (40cm)			
<b>TOTAL</b>	<b>269.4</b>	<b>274.2</b>	Others (depths into waste in brackets) D3120(IH)=8670 low, D2670(IH)=9350, D2820(12cm)=8610, D2970(IH)=9360, D2520 (18cm)=8500, E2820(20cm)=nr, E3120(OH)=nr, E2970(OH)=nr, E2820(OH)=nr					
<b>Notes</b>								
<ul style="list-style-type: none"> <li>• Should be purged –directly followed Test 72</li> <li>• Flow variations for individual ports (x15.6 or x7 if E2820 ignored) <ul style="list-style-type: none"> <li>• Piezometer readings indicate rapid head loss at input</li> <li>• Output readings checked twice – minor variations</li> </ul> </li> </ul>								
* A2670 A2370 piezometers orientated towards D ports								

<p style="text-align: center;"><b>TEST 77. 4th July 2000</b></p> <p style="text-align: center;"><b>DN1 134 kPa confined 4 input/ 4 outlet</b></p> <p style="text-align: center;"><b>Inlet head 9.37, outlet head 7.00m a.g.l.</b></p> <p style="text-align: center;"><b>FULL GAS ACCUMULATED CONDITIONS</b></p>								
<b>Port elevation (mm above ground level)</b>	<b>Input flow rate (l/h)</b>	<b>Outlet flow rate (l/h)</b>	<b>'A' heads (mm above ground level) depths in brackets</b>	<b>'B' heads (mm above ground level) depths in brackets</b>	<b>'C' heads (mm above ground level) depths in brackets</b>			
3820 (top)	-	-						
3670	-	-						
3520	-	-						
3295	-	-						
3220	-	-	7400 (30cm)	7285 (80cm)	7300 (60cm)			
3120	-	-						
2970	3.0	9.6						
2820	2.1	1.2	7760 (50cm)	7510 (85cm)	7190 (30cm)			
2670	1.5	-	8240 (30cm)					
2520	-	15.0	7850 (40cm)	7395 (50cm)	7200 (40cm)			
2370	21.3	5.4	9145 (35cm)					
2220 (bottom)	-	-	7505 (35cm)	7560 (70cm)	7320 (40cm)			
<b>TOTAL</b>	<b>27.9</b>	<b>31.2</b>	Others (depths into waste in brackets) D3120(IH)=nr, D2670(IH)=9370, D2820(12cm)=8430, D2970(IH)=9370, D2520 (18cm)=8985, E2820(20cm)=7100, E3120(OH)=7640 approx (gassing), E2970(OH)=7010, E2820(OH)=7030					
<b>Notes</b>								
<ul style="list-style-type: none"> <li>• Similar flow rate variations in full gas accumulated conditions x14.2 (x15.5 variation for Test 74 and x15.6 for Test 73)</li> <li>• Load cells indicate 45 litres of gas since Test 74 and 320 litres since Test 73</li> <li>• Flow rate reduced by 66% since Test 74 and a total x8.8 reduction from gas purged conditions in Test 73</li> <li>• As with Test 74, B piezometer readings higher (0.8m to 1.0m approx) – others vary * A2670 A2370 piezometers orientated towards D ports</li> </ul>								

TEST 79. 4 <sup>th</sup> July 2000								
DN1 134 kPa unconfined 4 input/ 4 outlet + top and bottom gravel layer								
Inlet head 9.37, outlet head 7.00m a.g.l.								
FULL GAS ACCUMULATED CONDITIONS								
Port elevation (mm above ground level)	Input flow rate (l/h)	Outlet flow rate (l/h)	'A' heads (mm above ground level) depths in brackets	'B' heads (mm above ground level) depths in brackets	'C' heads (mm above ground level) depths in brackets			
3820 (top)	-	-						
3670	-	-						
3520	-	-						
3295	-	-						
3220	-	-	7020 (30cm)	7050 (80cm)	7050 (60cm)			
3120	-	-						
2970	23.5	2.3						
2820	11.0	0	7390 (50cm)	7255 (85cm)	7065 (30cm)			
2670	7.0	-	7760 (30cm)					
2520	-	2.4	7445 (40cm)	7060 (50cm)	7040 (40cm)			
2370	30.0	1.0	9000 (35cm)					
2220 (bottom)	-	-	7160 (35cm)	7223 (70cm)	7050 (40cm)			
Top gravel		39.6 (51%)						
Bottom gravel		31.8 (41.3%)						
<b>TOTAL</b>	<b>71.5</b>	<b>77.1</b>	Others (depths into waste in brackets) D3120(IH)=nr, D2670(IH)=9380, D2820(12cm)=7990, D2970(IH)=9370, D2520 (18cm)=8620, E2820(20cm)=7035, E3120(OH)=7010, E2970(OH)=7010, E2820(OH)=7010					
<b>Notes</b>								
<ul style="list-style-type: none"> <li>Much higher flow rate with top and bottom gravel open (x 2.5 increase on Test 77)</li> </ul>								
* A2670 A2370 piezometers orientated towards D ports								

<b>TEST 83. 5<sup>th</sup> July 2000</b> <b>DN1 134 kPa confined 4 input/ 4 outlet</b> <b>Inlet head 9.37, outlet head 9.00m a.g.l.</b>					
<b>GAS PURGED CONDITIONS</b>					
<b>Port elevation (mm above ground level)</b>	<b>Input flow rate (l/h)</b>	<b>Outlet flow rate (l/h)</b>	<b>'A' heads (mm above ground level) depths in brackets</b>	<b>'B' heads (mm above ground level) depths in brackets</b>	<b>'C' heads (mm above ground level) depths in brackets</b>
3820 (top)	-	-			
3670	-	-			
3520	-	-			
3295	-	-			
3220	-	-	nr (30cm)	nr (80cm)	nr (60cm)
3120	-	-			
2970	nr	0.7			
2820	nr	4.0	nr (50cm)	nr (85cm)	nr (30cm)
2670	nr	-	nr (30cm)		
2520	-	14.6	nr (40cm)	nr (50cm)	nr (40cm)
2370	nr	8.2	nr (35cm)		
2220 (bottom)	-	-	nr (35cm)	nr (70cm)	nr (40cm)
<b>TOTAL</b>	<b>nr</b>	<b>27.5</b>			
<b>Notes</b>					
<ul style="list-style-type: none"> <li>• No equivalent test run in gas accumulated conditions</li> <li>• High flow from E2520, not E2370 as in Test 82 <ul style="list-style-type: none"> <li>• Flow variation x20.8</li> </ul> </li> </ul>					
* A2670 A2370 piezometers orientated towards D ports					

<b>TEST 90. 23rd<sup>nd</sup> November 2000</b> <b>DN1 228 kPa confined 3 input/ 3 outlet</b> <b>Inlet head 9.37, outlet head 9.00m a.g.l.</b> <b>LOW GAS ACCUMULATED CONDITIONS</b>					
<b>Port elevation (mm above ground level)</b>	<b>Input flow rate (l/h)</b>	<b>Outlet flow rate (l/h)</b>	<b>'A' heads (mm above ground level) (30 to 50 cm depth)</b>	<b>'B' heads (mm above ground level) (80cm to 100 cm depth)</b>	<b>'C' heads (mm above ground level) (30 to 50 cm depth)</b>
3820 (top)	-	-	-	-	-
3670	-	-	-	-	-
3520	-	-	-	-	-
3295	-	-	-	-	-
3220	-	-	-	-	-
3120	-	-	-	-	-
2970	-	-	-	-	-
2820	nr	0.33	-	-	-
2670	nr	0.21	-	-	-
2520	nr	1.38	-	-	-
2370	nr	-	-	-	-
2220 (bottom)	-	-	-	-	-
<b>TOTAL</b>	<b>nr</b>	<b>1.92</b>			
<b>Notes</b>					
<ul style="list-style-type: none"> <li>• High flow rate from 2520 (72%)</li> </ul>					

<b>TEST 91. 23rd<sup>nd</sup> November 2000</b> <b>DN1 228 kPa unconfined 3 input/ 3 outlet + top and bottom</b> <b>Inlet head 9.37, outlet head 7.00m a.g.l.</b> <b>LOW GAS ACCUMULATED CONDITIONS</b>								
<b>Port elevation (mm above ground level)</b>	<b>Input flow rate (l/h)</b>	<b>Outlet flow rate (l/h)</b>	<b>'A' heads (mm above ground level) (30 to 50 cm depth)</b>	<b>'B' heads (mm above ground level) (80cm to 100 cm depth)</b>	<b>'C' heads (mm above ground level) (30 to 50 cm depth)</b>			
3820 (top)	-	-	-	-	-			
3670	-	-	-	-	-			
3520	-	-	-	-	-			
3295	-	-	-	-	-			
3220	-	-	-	-	-			
3120	-	-	-	-	-			
2970	-	-	-	-	-			
2820	nr	0.38	7540	7000	7020			
2670	nr	0.86	nr	-	-			
2520	nr	0.58	7175	7000	7060			
2370	-	-	nr	-	-			
2220 (bottom)	-	-	7020	7065	7060			
Top gravel layer		10.5 (45.5%)						
Bottom gravel layer		10.8 (46.8%)	7005					
<b>TOTAL</b>	<b>nr</b>	<b>23.1</b>						
<b>Notes</b>								
<ul style="list-style-type: none"> <li>• Test run after drain and refill + 1 day</li> <li>• Load cell readings indicate 220 litres more water (ie. less gas) than Test 87</li> <li>• Total flow rate between x4 and 10.5 that measured in gas accumulated conditions <ul style="list-style-type: none"> <li>• Outlet port flow rates consistent</li> </ul> </li> <li>• Test run 1 day earlier but with bottom outer ring off BUT SAME FLOW RATE <ul style="list-style-type: none"> <li>• Numerical analyses = 13% horizontal flow (actual = 7.8%)</li> </ul> </li> </ul>								

<p style="text-align: center;"><b>TEST 97. 7th December 2001</b></p> <p style="text-align: center;"><b>DN1 322 kPa confined 4 input/ 3 outlet</b></p> <p style="text-align: center;"><b>Inlet head 9.37, outlet head 5.00m a.g.l.</b></p> <p style="text-align: center;"><b>LOW GAS ACCUMULATED CONDITIONS</b></p>					
<b>Port elevation (mm above ground level)</b>	<b>Input flow rate (l/h)</b>	<b>Outlet flow rate (l/h)</b>	<b>'A' heads (mm above ground level) (30 to 50 cm depth)</b>	<b>'B' heads (mm above ground level) (80cm to 100 cm depth)</b>	<b>'C' heads (mm above ground level) (30 to 50 cm depth)</b>
3820 (top)	-	-	-	-	-
3670	-	-	-	-	-
3520	-	-	-	-	-
3295	-	-	-	-	-
3220	-	-	-	-	-
3120	-	-	-	-	-
2970	-	-	-	-	-
2820	nr	0.54	-	-	-
2670	nr	0.06	-	-	-
2520	nr	0.66	-	-	-
2370	nr	-	-	-	-
2220 (bottom)	-	-	-	-	-
<b>TOTAL</b>	<b>nr</b>	<b>1.26</b>			
<b>Notes</b>					
<ul style="list-style-type: none"> <li>• x4 reduction in flow rate by closing E2370</li> <li>• flow more or less distributed between top and bottom outlet ports</li> </ul>					

<b>TEST 98. 10th December 2001</b> <b>DN1 322 kPa confined 4 input/ 3 outlet</b> <b>Inlet head 9.37, outlet head 7.00m a.g.l.</b> <b>LOW GAS ACCUMULATED CONDITIONS</b>					
Port elevation (mm above ground level)	Input flow rate (l/h)	Outlet flow rate (l/h)	'A' heads (mm above ground level) (30 to 50 cm depth)	'B' heads (mm above ground level) (80cm to 100 cm depth)	'C' heads (mm above ground level) (30 to 50 cm depth)
3820 (top)	-	-	-	-	-
3670	-	-	-	-	-
3520	-	-	-	-	-
3295	-	-	-	-	-
3220	-	-	-	-	-
3120	-	-	-	-	-
2970	-	-	-	-	-
2820	nr	0.18	-	-	-
2670	nr	0.10	-	-	-
2520	nr	0.60	-	-	-
2370	nr	-	-	-	-
2220 (bottom)	-	-	-	-	-
<b>TOTAL</b>	<b>nr</b>	<b>0.88</b>			
<b>Notes</b>					
<ul style="list-style-type: none"> <li>• unlike Test 97, most flow 68% through bottom outlet port</li> </ul>					

## REFERENCES

Agaki T. and Ishida T. (1994). Horizontal mass permeability of a clay stratum. *Developments in Geotechnical Engineering*, Balasubramaniam *et al.*(eds.), Balkema, Rotterdam, 1994. ISBN 90 5410 522 4

Akroyd T.N.W. (1957). Laboratory testing in Soil Engineering. *Geotechnical Monograph No.1*. 1957

Al-Tabbaa A. and Wood D.M. (1987). Some measurements of the permeability of kaolin. *Geotechnique* 37, no 4., pp499-503

ASTM 1142 (1994). *Hydraulic Conductivity and Waste Contaminant Transport in Soil*. American Society for Testing and Materials. Philadelphia, 1994

ASTM D 2434 – 68 (2000). Standard test method for permeability of granular soils (constant head). American Society for Testing and Materials. 1968 (Reapproved 2000)

Barnes G.E. (2000). *Soil Mechanics: Principles and Practice*. MacMillan Press Ltd. ISBN 0-333-77776-X

Barry D.L., Summersgill I.M., Gregory R.G. and Hellawell E. (2001). *Remedial engineering for landfill sites*. CIRIA C557 London 2001 ISBN 0 86017 557 X

Beaven R.P. (1996). Evaluation of geotechnical and hydrogeological properties of wastes. In *Engineering geology and waste disposal*. Bentley S.P.(ed.) Geological Society Engineering Geology Special Publication no. 11, pp57-65

Beaven R.P. (2000). The hydrogeological and geotechnical properties of household waste in relation to sustainable landfilling. PhD dissertation. January 2000. Queen Mary and Westfield College, University of London. 388pp

Beavis F.C. (1985). *Engineering Geology*. Blackwell Scientific Publications 1985

Bell F.G. (1992). *Engineering Properties of Soils and Rocks*. Butterworth Heinemann 1992

Bendz, D. and Flyhammar P. (1999). Channel flow and its effects on long-term leaching of heavy metals in msw landfills in *Proceedings of the 7<sup>th</sup> International Sardinia Landfill Conference*, S.Margherita Dipula, Cagliari, Italy. Vol II pp43-50

Bendz D., Singh V.P. and Berndtsson R. (1997). The flow regime in landfills – implications for modelling in *Proceedings of the 6<sup>th</sup> International Sardinia Landfill Conference*, S.Margherita Dipula, Cagliari, Italy. Vol II pp97-108

Benson, A., Warith, M., Evgin, E. and Moore, R. (2002). Suitability of shredded tires for use in landfill leachate collection systems. *Ground and Water: Theory to Practice; Proceedings of the 55<sup>th</sup> Canadian Geotechnical and 3<sup>rd</sup> Joint IAH-CNC and CGS Groundwater Speciality Conferences*, Niagara Falls, Ontario, October 20-23, 2002. pp565-572

Black D.K. and Lee K.L. (1973). Saturating laboratory samples by back pressure. *Proceedings of the American Society of Civil Engineers: Journal of the Soil Mechanics and Foundations Division*, SM1, January, pp75-93

Bleiker D. E., McBean E. and Farquahar G. (1993). Refuse Sampling and Permeability Testing at the Brock West and Keele Valley Landfills in *Proceedings of the Sixteenth International Waste Conference - Madison USA 1993*

Blight G.E. (1996). Lateral spreading of soluble salts in a municipal landfill. *Environmental Geotechnics*, Balkema, Rotterdam

Boltze U. and de Freitas M.H.(1997). Monitoring gas emissions from landfill sites. *Waste Management & Research* **15**, pp463-476

Bouwer H. (1970). Ground water recharge design for renovating waste water. *Journal of the Sanitary Engineering Division, Proceedings of the American Society of Civil Engineers*, vol 96, 1970, pp59 -74

Bouwer H. (1978). *Groundwater hydrology*. McGraw-Hill. ISBN 0-07-006715-5

Bouwer H. and Rice R.C. (1967). Modified tube diameters for the double-ring tube apparatus. *Soil Sci. Soc. Am. Proc.* Vol 31, 1967, pp437-439

Bowles J.E. (1979). *Physical and Geotechnical Properties of Soils*. McGraw-Hill 1979

Boynton S.S. and Daniel D.E. (1985). Hydraulic conductivity tests on a compacted clay. *Journal of Geotechnical Engineering, ASCE* Vol III, no 4., pp465-478

BS1377 (1990). Methods of test for civil engineering purposes. British Standards Institution 1990

Buchanan D. and Clark C. (1997). The Impact of Waste Processing on the Hydraulic Behaviour of Landfilled Wastes. *Designing and Managing Sustainable Landfill*, IBC 1997

Buchanan D. and Clark C. (2001). Hydraulic characteristics of wet-pulverised municipal waste. *J.CIWEM*. **15**. pp14-20. March 2001

Burrows M.R., Joseph J.B. and Mather J.D. (1997). The Hydrogeological Properties of in-situ Landfilled Waste. *Proceedings of the 6th International Sardinia Landfill Conference*, S.Margherita Dipula, Cagliari, Italy. Vol II, pp77-83

Campbell D. (1989). Landfill gas migration, effect and control, in Sanitary Landfilling: Process, Technology and Environmental Impact (eds. T.H.Christensen, R. Cossu and R.Stegmann), Academic Press, London, pp1-28

Campbell D. J. V. (1995). Landfill Bioreactor Design and Operation - International Perspectives. EPA seminar - Landfill Bioreactor Design and Operation, March 1995, Wilmington DE(USA)

Cartwright K. and Hensel B.R. (1995). Hydrogeology – basic principles, in Geotechnical Practice for Waste Disposal (ed. D.E.Daniel), Chapman & Hall, 1995 ISBN 0 412 35170 6

Cedergren, H. (1989). Seepage, drainage and flow nets. Wiley, New York. 3<sup>rd</sup> ed., 1989

Cernuschi and Giugliano (1996). Emission and Dispersion Modelling of Landfill Gas. Landfilling of Waste: Biogas. (eds T.H. Christensen, R.Cossu and R. Stegmann) E&FN Spon, London. pp215-234. ISBN 0 419 19400

Chen T. and Chynoweth D. P. (1995). Hydraulic Conductivity of Compacted Municipal Solid Waste in Biosource Technology, 51 (1995) pp205-212, Elsevier Science Ltd, 1995

Christensen T.H. (1997). Attenuation of landfill leachate pollutants in aquifers. Documents of IBC UK conference 1997

Christiansen J.E. (1944). Effect of entrapped air upon the permeability of soils. Soil Science. Vol 58. pp355-365

Craig, R.F. (1983). Soil Mechanics. 3<sup>rd</sup> edition. Von Nostrand Reinhold, 1983

Crawford J.F. and Smith P.G. (1985). Landfill Technology. Butterworths, 1985. ISBN 0 408 01407 5

Danhamer H., Dach J., Obermann I., Jager J. and Ostrowski M.W. (1999) Simulation of Emissions from Landfills containing MBP Waste. Proceedings of the 7th International Sardinia Landfill Conference, S.Margherita Dipula, Cagliari, Italy. Vol I, pp519-532.

Daniel D. E. (1994). State-of-the- Art: Laboratory Hydraulic Conductivity Tests for Saturated Soils. Hydraulic Conductivity and Waste Contaminant Transport in Soil, ASTM STP 1142. David E.Daniel and Stephen J.Trautwein, Eds., American Society for Testing and Materials. Philadelphia, 1994.

Daniel D.E., Anderson D.C. and Boynton S.S. (1985). Fixed-wall versus flexible wall permeameters. Hydraulic barriers in soil and rock, ASTM STP 874. A.I.Johnson, R.K.Fobel, N.J.Cavalli and C.B.Petterson, Eds., American Society for Testing and Materials, Philadelphia, pp107-126

Day S.R. and Daniel D.E. (1985). Hydraulic conductivity of two prototype clay liners. Journal of Geotechnical Engineering, vol III, no.8, ASCE, August 1985

DoE (1995). Landfill design, construction and operational practice. Waste Management Paper 26B. HMSO London

ELE International Limited (1999). Construction materials testing equipment 10<sup>th</sup> edition

Fetter C.W. (1988). Applied Hydrology 2<sup>nd</sup> edition. Merrill Publishing Co., 1988

Figueroa R.A. and Stegmann R. (1996). Landfill gas migration through landfill liners. Landfilling of Waste: Biogas (eds T.H. Christensen, R.Cossu and R. Stegmann) E&FN Spon, London, pp669-682 ISBN 0 419 19400 2

Fredlund D.G. and Rahardjo H. (1993). Soil mechanics for unsaturated soils. John Wiley and Sons Inc. New York

Freeze R. A. and Cherry J. A. (1979). Groundwater. Prentice-Hall 1979

Giardi, M. (1997). Hydraulic behaviour of waste: observations from pumping tests. Proceedings Sardinia 97, Sixth International Landfill Symposium, II, pp63-72

Hillel D. (1980). Fundamentals of Soil Physics. Academic Press 1980

Hudson A.P., Beaven R.P. and Powrie W. (1999). Measurement of the Horizontal Hydraulic Conductivity of Household Waste in a Large Scale Compression Cell. In Proceedings of the 7th International Sardinia Landfill Conference, S.Margherita Dipula, Cagliari, Italy. Vol III, pp461-468

Hudson A.P., Beaven R.P. and Powrie W. (2000). Current research into the hydrogeological properties of household waste using a large scale compression cell . In Proceedings of the Waste 2000 Conference, Stratford-upon-Avon, Warwickshire, UK. pp227-237

Hudson A.P., Beaven R.P. and Powrie W. (2001). Interaction of water and gas in saturated household waste in a large scale compression cell. Proceedings of the 8<sup>th</sup> International Sardinia Landfill Conference, S.Margherita Dipula, Cagliari, Italy. Vol III pp585-594

Hudson A.P., Beaven R.P. and Powrie W. (2002). Interaction of water and gas in saturated household waste in a large scale compression cell. In Proceedings of the Waste 2002 Conference, Stratford-upon-Avon, Warwickshire, UK. pp702-712

Hudson A.P., Beaven R.P. and Powrie W. (2003). Bulk compressibility and hydraulic conductivity of used tyres for landfill drainage applications. Proceedings of the 9<sup>th</sup> International Sardinia Landfill Conference, S.Margherita Dipula, Cagliari, Italy. CD only.

Hudson A.P., Beaven R.P. and Powrie W. (2004). Evaluation of the hydraulic and compressive properties of landfill tyre drainage layers. In Proceedings of the Waste 2004 Conference, Stratford-upon-Avon, Warwickshire, UK. pp625-632

Hung S., Fredlund D.G. and Barbour S.L. (1998). Measurement of the coefficient of permeability for a deformable unsaturated soil using a triaxial permeameter. Canadian Geotechnical Journal, vol 35. pp426-432 1998

IWM - Institute of Wastes Management (1998). The Role and Operation of the flushing bioreactor. IWM Sustainable Landfill Working Group

Jain P., Powell J., Townsend P.E. and Reinhart D.R. (2006). Estimating the hydraulic conductivity of landfilled municipal solid waste using the borehole permeameter test. Journal of Environmental Engineering. ASCE June 2006. pp645-652

Jessberger H.L. and Kockel R. (1991). Mechanical properties of waste materials. Ciclo di Conferenze di geotechnical di Torino. Torino, Italy

Kjeldsen P. (1996). Landfill gas migration in soil. Landfilling of Waste: Biogas. (eds T.H. Christensen, R.Cossu and R. Stegmann) E&FN Spon, London. pp 87-132 ISBN 0 419 19400 2

Lancellotta R. (1995). Geotechnical Engineering. A.A.Balkema, Netherlands. 1995

Landva A. O. and Clarke J. I., Geotechnics of Waste Fill. In Geotechnics of Waste Fill - Theory and Practice, ASTM STP1070, 1990

Lofy R.J (1996) Zones of vacuum influence surrounding gas extraction wells. Landfilling of Waste: Biogas. (eds T.H. Christensen, R.Cossu and R. Stegmann) E&FN Spon, London. pp319-394. ISBN 0 419 19400

Maasland M. (1957). Soil Anisotropy and Land Drainage in Drainage of Agricultural Lands, (ed. J.N.Luthin), American Society of Agronomy monograph no 7. 1957 pp216-287

McCreanor P.T. and Reinhart D.R. (2000). Mathematical modeling of leachate routing in a leachate re-circulating landfill. In Water Research, Vol 34, Issue 4, March 2000. pp1285-1295

McDonald, M.G. and Harbaugh A.W. (1988). A modular three-dimensional finite-difference ground-water flow model, USGS TWRI Chapter 6-A1

Mitchell J.K.(1976). Fundamentals of Soil Behaviour, John Wiley & Sons, Inc 1976

Mitchell J.K., Hooper D.N. and Campanella R.G. (1965). Permeability of compacted clay. ASCE, Journal of Soil Mechanics and Foundations Division, **91**, no. S4, Part 1, pp 41-46

Motherwell Bridge Envirotec (1998) *DANO Composting and Recycling Systems*

Nikolova R., Powrie W., Humphreys P. and Smallman D.J. (2001). Performance of leachate drainage systems. Proceedings of the 8<sup>th</sup> International Sardinia Landfill Conference, S.Margherita Dipula, Cagliari, Italy. Vol III. pp103-112

Olsen H.W., Willden A.T., Kiusalaas N.J., Nelson K.R. and Poeter E.P. (1994). Volume-controlled hydrologic property measurements in triaxial systems. Hydraulic Conductivity and Waste Contaminant Transport in Soil. ASTM STP 1142, 1994

Oweis I.S. and Khera R.P. (1990). *Geotechnology of Waste Management*. Butterworths 1990

Oweis I.S., Smith D.A., Ellwood R.B. and Greene D.S. (1990). Hydraulic characteristics of municipal refuse in Journal of Geotechnical Engineering, Vol 116, no 4. April 1990, 539-553

Powrie W. (1997). Soil Mechanics, Concepts and Applications, E & FN Spon 1997

Powrie W. and Beaven R.P. (1999). The Hydraulic Properties of Waste and their Implications for Liquid Flow in Landfills. Proceedings of the Institution of Civil Engineers, Geotechnical Engineering, October 1999

Price M. (1985). Introducing Groundwater, George Allen & Unwin 1985

Ranjith P.G. (2004). Recent advances in triaxial facilities for soil and rock testing. The Electronic Journal of Geotechnical Engineering, Vol 9, B, 2004

Rowe P.W., and Barden L. (1966). A new consolidation cell. *Geotechnique* **16** (2) 1966

Rowe R.K. and Nadarajah P. (1996). Estimating leachate drawdown due to pumping wells in landfills. *Can. Geotech. J.* **33**: 1-10. 1996

Rosqvist H. (1999). Solute transport through preferential flow paths in landfills. Proceedings of the 7<sup>th</sup> International Sardinia Landfill Conference, S.Margherita Dipula, Cagliari, Italy. Vol II pp51-60

Sarsby R. (2000). Environmental Geotechnics. Thomas Telford 2000

Shackelford C.D.(1994). Waste-soil interactions that alter hydraulic conductivity. Hydraulic conductivity and waste contaminant transport in soil. ASTM STP 1142. David E. Daniel and Stephen J. Trautwein, Eds., American Society for Testing and Materials, Philadelphia, 1994. pp111-168

Sills G.C., Wheeler S.J., Thomas S.D. and Gardner T.N. (1991). Behaviour of offshore soils containing gas bubbles. *Geotechnique* **41**, no 2. pp227-241

Skempton A.W. (1960). Effective stress in soil, concrete and rocks. Proceedings of the Conference on Pore Pressure and Suction in Soils, pp4-16, Butterworths, London

Smith G.N. (1974). Elements of soil mechanics for civil and mining engineers. The Pitman Press, Bath. 1974

Smith R.M. and Browning D.R. (1942). Persistent water-unsaturation of natural soil in relation to various soil and plant factors. *Soil Sci. Soc. Amer. Proc.* **7**, pp114-119

Stephens D.B. (1994). Hydraulic assessment of unsaturated soils. Hydraulic conductivity and waste contaminant transport in soil. ASTM STP 1142. David E.Daniel and Stephen J.Trautwein, Eds., American Society for Testing and Materials. Philadelphia, 1994

Talsma T. (1960). Measurement of soil anisotropy with piezometers. *Journal of Soil Science*, vol.11, no. 1, 1960. pp159-171

Tavenas F., Leblond J.P and Leroueil S. (1983). The permeability of natural soft clays. Part 1: Methods of laboratory measurement. *Journal of Can. Geotech.* **20**, pp629-644 1983

TU (Technical University) of Braunschweig, Leichtweiss-Institute for Hydraulic Engineering

Terzaghi K. (1936). The shearing resistance of saturated soils. *Proceedings of the First International Conference on Soil Mechanics*, 1. pp54-56

Trautwein S.J. and Boutwell G.P.(1994). In situ hydraulic conductivity tests for compacted clay liners and caps. In Hydraulic conductivity and waste contaminant transport in soil. ASTM STP 1142 David E. Daniel and Stephen J. Trautwein, Eds., American Society for Testing and Materials, Philadelphia, 1994

Vesilind P.A., Worrell W. and Reinhart D. (2002). Solid Waste Engineering. Brooks/Cole. ISBN 0-534-37814-5

Warith M.A., Evgin E. and Benson P.A.S. (2004). Suitability of shredded tires for use in landfill leachate collection systems. *Waste Management* **24** (2004) pp 967-979

Watkins D.C. (1997). Engineering controls on the rates of leachate seepage through mineral liners. In *Designing and Managing a Sustainable Landfill*, IBC 1997

Watts K.S., Fisher A.R.J. and Lewicki R.A. (2001). A large-scale instrumented test of the behaviour of newly placed domestic waste. In *Proceedings of the 8<sup>th</sup> International Sardinia Landfill Conference*, S.Margherita Dipula, Cagliari, Italy. Vol II pp105-114

Watts K.S., Charles J.A. and Blake N.J.R. (2002). Settlement of landfills: Measurements and their significance. In *Proceedings of the Waste 2002 Conference*, Stratford-upon-Avon, Warwickshire, UK. pp673-682

Watts K.S., Charles J.A. and Skinner H.D. (2006). Predicting long-term settlement of landfills. In *Proceedings of the Waste 2006 Conference*, Stratford-upon-Avon, Warwickshire, UK. pp537-548

Weeks E. P. (1969). Determining the ratio of horizontal to vertical permeability by aquifer test analysis. *Water Resources Research*. Vol 5, no. 1, February 1969

Whitlow R. (1983). *Basic Soil Mechanics*. Construction press. 1983

Wood D.M. (1990). *Soil behaviour and critical state soil mechanics*. Cambridge University Press, 1990. ISBN 0-521-33782-8

Wittmann S.G. (1985). Landfill gas migration: early warning signs, monitoring techniques and migration control systems. In *Proceedings 23<sup>rd</sup> Annual International Seminar, Equipment, Services and Systems show*, 27-29th August, Denver, Colorado GRDCA, Silver Spring, MD, USA. pp317-328

Yong R.N. (1986). Selected leaching effects on some mechanical properties of sensitive clay, in *Int. Symp. on Environmental Geology*, Vol 1. pp349-362

Zeiss C. and Major W. (1992). Moisture flow through municipal solid waste: patterns and characteristics. *J. Environmental Systems*, vol 22(3), 1992-93. pp211-231

Zimmie T.F., Doynow J.S. and Wardell J.T. (1981). Permeability testing of soils for hazardous waste disposal sites. In *Proc. of the tenth ICSMFE*, Stockholm, Vol 2. pp.403-406